RTO-MP-18
AC/323(AVT)TP/8

RTO-MP-18

NORTH ATLANTIC TREATY ORGANIZATION

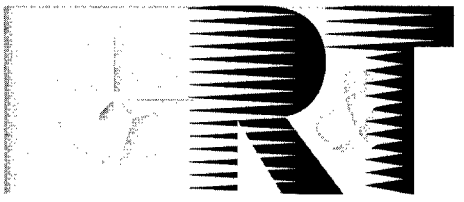

RESEARCH AND TECHNOLOGY ORGANIZATION
BP 25, 7 RUE ANCELLE, F-92201 NEUILLY-SUR-SEINE CEDEX, FRANCE

RTO MEETING PROCEEDINGS 18

Fatigue in the Presence of Corrosion

(Fatigue sous corrosion)

Papers presented at the Workshop of the RTO Applied Vehicle Technology (AVT) Panel (organised by the former AGARD Structures and Materials Panel) held in Corfu, Greece, 7-9 October 1998.

DISTRIBUTION STATEMENT A
Approved for public release;
Distribution Unlimited

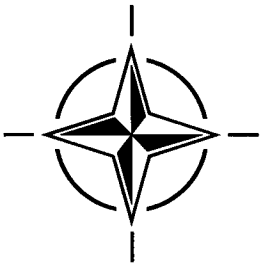

Published March 1999

Distribution and Availability on Back Cover

RTO-MP-18
AC/323(AVT)TP/8

NORTH ATLANTIC TREATY ORGANIZATION

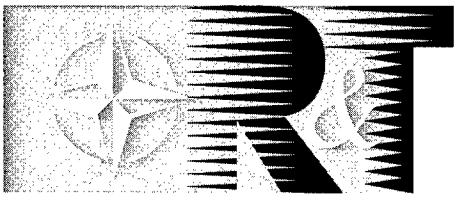

RESEARCH AND TECHNOLOGY ORGANIZATION
BP 25, 7 RUE ANCELLE, F-92201 NEUILLY-SUR-SEINE CEDEX, FRANCE

RTO MEETING PROCEEDINGS 18

Fatigue in the Presence of Corrosion

(Fatigue sous corrosion)

Papers presented at the Workshop of the RTO Applied Vehicle Technology (AVT) Panel (organised by the former AGARD Structures and Materials Panel) held in Corfu, Greece, 7-8 October 1998.

19990308 162

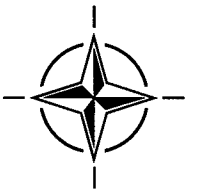

DTIC QUALITY INSPECTED 1

AQF99-06-1130

The Research and Technology Organization (RTO) of NATO

RTO is the single focus in NATO for Defence Research and Technology activities. Its mission is to conduct and promote cooperative research and information exchange. The objective is to support the development and effective use of national defence research and technology and to meet the military needs of the Alliance, to maintain a technological lead, and to provide advice to NATO and national decision makers. The RTO performs its mission with the support of an extensive network of national experts. It also ensures effective coordination with other NATO bodies involved in R&T activities.

RTO reports both to the Military Committee of NATO and to the Conference of National Armament Directors. It comprises a Research and Technology Board (RTB) as the highest level of national representation and the Research and Technology Agency (RTA), a dedicated staff with its headquarters in Neuilly, near Paris, France. In order to facilitate contacts with the military users and other NATO activities, a small part of the RTA staff is located in NATO Headquarters in Brussels. The Brussels staff also coordinates RTO's cooperation with nations in Middle and Eastern Europe, to which RTO attaches particular importance especially as working together in the field of research is one of the more promising areas of initial cooperation.

The total spectrum of R&T activities is covered by 6 Panels, dealing with:

- SAS Studies, Analysis and Simulation
- SCI Systems Concepts and Integration
- SET Sensors and Electronics Technology
- IST Information Systems Technology
- AVT Applied Vehicle Technology
- HFM Human Factors and Medicine

These Panels are made up of national representatives as well as generally recognised 'world class' scientists. The Panels also provide a communication link to military users and other NATO bodies. RTO's scientific and technological work is carried out by Technical Teams, created for specific activities and with a specific duration. Such Technical Teams can organise workshops, symposia, field trials, lecture series and training courses. An important function of these Technical Teams is to ensure the continuity of the expert networks.

RTO builds upon earlier cooperation in defence research and technology as set-up under the Advisory Group for Aerospace Research and Development (AGARD) and the Defence Research Group (DRG). AGARD and the DRG share common roots in that they were both established at the initiative of Dr Theodore von Kármán, a leading aerospace scientist, who early on recognised the importance of scientific support for the Allied Armed Forces. RTO is capitalising on these common roots in order to provide the Alliance and the NATO nations with a strong scientific and technological basis that will guarantee a solid base for the future.

The content of this publication has been reproduced
directly from material supplied by RTO or the authors.

Printed on recycled paper

Published March 1999

Copyright © RTO/NATO 1999
All Rights Reserved

ISBN 92-837-1011-8

Printed by Canada Communication Group Inc.
(A St. Joseph Corporation Company)
45 Sacré-Cœur Blvd., Hull (Québec), Canada K1A 0S7

Fatigue in the Presence of Corrosion

(RTO MP-18)

Executive Summary

The NATO Applied Vehicle Technology Panel organized a workshop with the title "Fatigue in the Presence of Corrosion" held 7-8 of October in Corfu, Greece. There were 18 papers given on this subject followed by a round table discussion and conclusions. The papers selected represented eight countries. Canada contributed two, Germany one, Greece two, Italy two, Netherlands one, United Kingdom two and the United States seven papers.

The papers were primarily oriented towards the airplane corrosion problem although the content of many of the papers could well apply to land or sea vehicles. The attendance at the workshop, which exceeded seventy, consisted of specialists in the fields of aircraft design, airline operation, and aircraft maintenance. This mix of interests contributed to considerable discussion of the individual papers.

The stated objectives of the workshop were

- to promote general discussion on the viability of the current approaches to addressing corrosion-fatigue interactions,
- to exchange technical and life cycle management experiences related to cost effective and safe approaches to fleet management and repair of corrosion, and,
- to identify potential areas for coordinated and prioritized collaborative activities amongst the NATO nations.

The workshop met these objectives. The scope of the papers given provided the attendees with a remarkably good insight on the issues associated with the corrosion problem.

Some of the workshop papers discussed the significance of corrosion-fatigue as a safety issue or an economic issue. There is ample data to support the contention that it is definitely an economic issue. There is also ample data to support the contention that it has not been a significant safety problem. However, the problem is certainly a potential safety concern if maintenance does not perform their task diligently. The economic issue alone is sufficient to motivate the support of research and development that can reduce the maintenance burden. This research will also reduce the threat of catastrophic failure from the corrosion damage.

The workshop identified many questions about corrosion that must be resolved in order to implement effective life cycle management practices. One question is the ability of nondestructive inspections to detect corrosion adequately. The word adequately refers to (1) the detection of what is today referred to hidden corrosion and (2) the quantification of corrosion pitting and thinning such that corrosion management becomes viable. It would be supportive for maintenance to have the capabilities of nondestructive inspections quantified by means of probability of detection for corrosion in the same manner that one is able to quantify the ability of nondestructive inspection for crack detection.

A second question is on the need for institutionalizing the corrosion management process. Currently, there are no strong linkages between the structural engineer and the corrosion engineer. The structural engineer sizes the components of the aircraft based on strength, durability, damage tolerance, and stiffness requirements. There is no formal approach for combining the effects of corrosion with fatigue in a maintenance program. This type of program should start with the designer working for the original equipment manufacturer and be a part of the policy of the systems (or program) manager. It should be passed down to the depots performing the major maintenance and finally to the base and squadron level

for the implementation in the field. One virtue of this approach is that all elements of the maintenance chain are completely aware of criticality of corrosion found in operational aircraft. Another virtue is that this effort should reduce the cost burden through prevention at the design level.

Another question is on the return on investment from the use of corrosion prediction methods. Considerable effort has been expended on tool development for the prediction of corrosion damage in the future from the observance of the current state of corrosion. The return on investment of this effort should be examined carefully. Most structural components are designed to zero static margins. This has been the accepted policy for both military and commercial aircraft for many years. Consequently, they are unable to withstand any thinning without causing the static margins to become negative. When the nondestructive inspection process indicates that corrosion is present, it may be that at that time the margins have become negative indicating that remedial actions are required. In such a case, the use of predictive capability would not be justified.

Another question is whether the testing that is being performed today provides the proper data for the corrosion-fatigue problem. There is a need to establish the corrosion fatigue data for the commonly used materials in aircraft. The paper by B. Schmidt-Brandecker highlighted the need for a test approach involving corrosion fatigue for material selection.

A final question is on the current capability of corrosion prevention compounds and their potential uses in the future. Questions such as (1) should they be an integral part of airworthiness, (2) should there be increased process control on parts that are non-inspectable, and (3) is there a need for process qualification? Item number (3) refers to issues such as long-term breakdown of the compounds, technician training, and performance standards for durability, assurance of sufficient coverage through nondestructive inspection.

It is recommended that the questions above be the subject of a focussed workshop or working group.

Fatigue sous corrosion

(RTO MP-18)

Synthèse

La Commission des technologies appliquées aux véhicules a organisé un atelier sur « La fatigue sous corrosion » du 7 au 8 octobre à Corfou en Grèce. En tout, 18 communications ont été présentées, suivie d'une table ronde et de conclusions. Huit pays étaient représentés. Deux communications ont été présentées par le Canada, une par l'Allemagne, deux par la Grèce, deux par l'Italie, une par les Pays-Bas, deux par le Royaume-Uni et sept par les Etats-Unis.

Les communications ont traité essentiellement du problème de la corrosion des aéronefs, mais les technologies citées auraient pu, dans beaucoup de cas, s'appliquer aux véhicules terrestres ou maritimes. Plus de soixante-dix personnes ont participé à l'atelier, dont la plupart étaient des spécialistes dans le domaine de la conception aéronautique, de l'exploitation des lignes aériennes et de la maintenance des aéronefs. Cette rencontre a été à l'origine de discussions soutenues.

L'atelier avait pour objectifs :

- faciliter une discussion générale sur la viabilité des approches actuelles du problème des interactions corrosion-fatigue,
- permettre de confronter les expériences sur la gestion technique et sur le cycle de vie, en vue de l'élaboration d'approches sûres et rentables de la gestion des flottes d'avions et de la réparation de la corrosion,
- identifier les domaines possibles d'activités coordonnées, hiérarchisées et conjointes entre les pays membres de l'OTAN.

L'atelier a atteint ces objectifs. Le champ d'activités couvert a donné aux participants un très bon aperçu des problèmes de la corrosion.

Certaines présentations ont abordé la corrosion sur le plan économique, ainsi que sur celui de la sécurité. Beaucoup d'éléments permettent d'affirmer qu'il s'agit bien d'une question économique. En même temps, suffisamment de données existent pour soutenir l'affirmation que la corrosion n'a jamais posé de problèmes de sécurité. Cependant, la sécurité pourrait être mise en cause en cas de défaillance du personnel de maintenance. Cet aspect économique est suffisamment important pour justifier, à lui seul, une aide en matière de Recherche et Développement pour diminuer la maintenance. Ces recherches permettront de réduire le risque d'une défaillance catastrophique occasionnée par la corrosion.

L'atelier a fait ressortir le besoin de définir des procédures efficaces de gestion du cycle de vie. L'une des questions posées concerne l'efficacité de la détection de la corrosion par le biais des inspections non-destructives. Le terme définit de façon acceptable (1) la détection du phénomène communément appelé « la corrosion cachée » et (2) la quantification des piqûres de corrosion et de l'amincissement de façon à permettre la gestion de la corrosion. Il serait souhaitable pour le personnel de maintenance que les performances des inspections non-destructives soient quantifiées en ce qui concerne la probabilité de détection de la corrosion, de la même façon que pour la détection des fissures par les méthodes non-destructives.

Une deuxième question concerne l'intérêt de l'homologation du processus de gestion de la corrosion. A l'heure actuelle, il n'existe aucun lien formel entre l'ingénieur des structures et le spécialiste en

corrosion. L'ingénieur responsable de la conception des structures décide des dimensions des éléments structuraux en fonction de la résistance demandée, de la solidité, de la tolérance à l'endommagement, et des normes de rigidité. Il n'existe aucune procédure normalisée permettant de tenir compte à la fois des effets de la corrosion et de ceux de la fatigue dans un programme de maintenance. Ce type de programme doit faire partie de la politique du gestionnaire systèmes (ou programmes) dans une situation où le concepteur travaille pour l'équipementier. Il doit être transmis au dépôts qui réalisent les grands travaux de maintenance et enfin aux bases aériennes au niveau des escadrons pour application opérationnelle. L'un des avantages de cette approche est que tous les éléments de la chaîne de maintenance sont pleinement conscients du niveau de risque représenté par l'éventuelle corrosion des avions en service. La diminution des coûts par l'intervention au stade de la conception représente un avantage supplémentaire.

Une troisième question concerne la rentabilité des investissements liés aux méthodes de prévision de la corrosion. Des efforts considérables ont été consacrés au développement d'outils de prévision des dégâts de corrosion, basé sur l'observation de l'état actuel de la pièce en question. La rentabilité de cette opération doit être suivie de près. Les marges statiques de conception de la plupart des composants structuraux sont de zéro. Ces marges font partie de la politique préconisée pour les avions civils et militaires depuis de nombreuses années. Par conséquent, tout amincissement de ces composants aurait pour effet de placer les marges statiques en négatif. Lorsque les résultats des inspections non destructives indiquent une trace de corrosion, les marges peuvent être négatives et entraîner des mesures correctives. L'emploi de moyens de prévision ne serait pas justifié dans un tel cas.

Une quatrième question concerne l'adéquation des résultats des essais actuellement en cours vis à vis du problème de corrosion sous fatigue. Il faut recueillir des données sur le phénomène de corrosion-fatigue pour les matériaux les plus communément utilisés dans l'industrie aéronautique. Au cours de sa communication, M. B. Schmidt-Brandecker a insisté sur une approche des procédures d'essais qui comprenne la fatigue sous corrosion, aux fins du choix des matériaux.

Une dernière question concerne les possibilités actuelles des composés utilisés pour la prévention de la corrosion, et leurs applications potentielles. En fait, un certain nombre de questions restent posées à cet égard, comme par exemple: (1) est-ce qu'ils devraient faire partie intégrante du domaine de l'aptitude au vol ? (2) est-ce qu'il faut augmenter le nombre de contrôles en cours de fabrication pour les pièces qui ne sont pas contrôlables autrement ? (3) faut-il instaurer des processus de qualification ? Le point (3) concerne des questions comme la décomposition à terme des composés, la formation des techniciens, les normes de performance en matière de longévité, et l'assurance d'une couverture suffisante lors des inspections non destructives.

Il serait souhaitable que ces questions fassent l'objet d'un atelier spécifique ou d'études d'un groupe de travail.

Contents

† Paper not available at time of printing.

Preface

Corrosion and fatigue are two factors that affect the life cycle costs and the airworthiness of the NATO aircraft fleets, particularly those in the "aging" category. Corrosion and fatigue have independently been the subject of substantial research and developmental work. More recently, because of the increased concern related to the extended use of airframes, there is an increased requirement to more fully understand the synergistic interactions between corrosion and fatigue. High costs and decreased availability because of expensive repairs and increased down time are characteristic of the situation.

The NATO fleet is aging in both real time and in accrued fatigue damage. Corrosion and fatigue, independently, are high cost maintenance items and both can affect airworthiness. There is also a synergistic relationship between these two phenomena that must be understood before cost effective and airworthy approaches to design and corrosion prevention can be defined. In addition, there is substantial work in progress in NATO countries that could be accelerated by a sharing of experience. There is a strong potential for coordinated and prioritized collaborative activities amongst the NATO nations.

Previous NATO-AGARD activities have provided significant advances in understanding the corrosion and fatigue phenomena independently. To address their synergistic interaction, this workshop on corrosion-fatigue interactions was formed. The workshop had the general objective of promoting discussion on the viability of the current approaches to addressing the corrosion-fatigue interaction. Other major objectives included the focussing of the corrosion-fatigue research of member nations on priority issues and the identification of technology areas where NATO-RTO activity could accelerate the development of improved technology to address corrosion-fatigue.

D.L. Simpson
Chairman
Sub-Committee on Corrosion-Fatigue Interactions

Sub-Committee Membership

Chairman

Mr. D. Simpson
Chief, Structures
Structures & Materials Laboratory
Institute for Aerospace Research, NRC
Montreal Road
Ottawa, Ontario, K1A 0R6
CANADA

Members

H. Goncalo	-	PO	R. Servent	-	SP
G. Günther	-	GE	E. Starke	-	US
P. Heuler	-	GE	J. Vantomme	-	BE
J.P. Immarigeon	-	CA	J. Waldman	-	US
L. Kompotiatis	-	GR	S. Welburn	-	UK
H.H. Ottens	-	NE	G. Zennaro	-	IT

Panel Executive

Dr. J.M. CARBALLAL, SP

Mail from Europe:

RTA-OTAN/AVT
B.P. 25
7, rue Ancelle
F-92201 Neuilly-sur-Seine
France

Mail from US and Canada:

RTA-NATO/AVT
PSC 116
APO AE 09777

Tel. 33 (0)1 55 61 22 90 & 92

TECHNICAL EVALUATION REPORT

John W. Lincoln
United States Air Force, ASC/EN
2530 Loop Road West
Wright-Patterson AFB
OH 45433-7101, USA

David L. Simpson
Chief, Structures and Materials Laboratory
National Research Council Canada
Montreal Road
Ottawa, Ontario K1A 0R6, Canada

INTRODUCTION

The NATO Applied Vehicle Technology Panel organized a workshop with the title "Fatigue in the Presence of Corrosion" held 7 – 8 October in Corfu, Greece with Mr. D. Simpson as the Chairperson. There were 18 papers given on this subject followed by a round table discussion and conclusions. The papers selected represented eight countries. Canada contributed two, France one, Germany one, Greece two, Italy two, Netherlands one, United Kingdom two, and the United States seven papers. The chairperson divided the workshop into four sessions. The topic of the four sessions were the following:

I. In-Service Experience with Corrosion Fatigue

II. Simulation/Test Evaluation Programs

III. Fatigue Prediction Methodologies in Corrosive Environments

IV. Structural Integrity – Corrosion and Fatigue Interactions

The papers in these four sessions were primarily oriented towards the airplane corrosion problem although the content of many of the papers could well apply to land or sea vehicles. The attendance at the workshop, which exceeded 70, consisted of specialists in the fields of aircraft design, airline operation, and aircraft maintenance. This mix of interests contributed to considerable discussion of the individual papers.

The stated objectives of the workshop were to; promote general discussion on the viability of the current approaches to addressing corrosion-fatigue interactions, to exchange technical and life cycle management experiences related to cost effective and safe approaches to fleet management and repair of corrosion, and, to identify potential areas for coordinated and prioritized collaborative activities amongst the NATO nations.

The opinion of the Technical Evaluator Recorders is that the workshop met these objectives. In a two-day meeting, it is impossible to cover all aspects of this complex problem. However, the scope of the papers given provided the attendees with a remarkably good insight on the issues associated with the corrosion problem.

The workshop would have been an even greater success if Dr. W. Schütz of Germany had been able to attend. Health considerations prevented him from attending. He had planned to present the first paper entitled "Corrosion Fatigue of Structural Materials and Components." Unfortunately, the attendees missed hearing this paper and his contribution through intelligent critiques of the other papers. All wish him a speedy recovery. Although his paper was not presented at the meeting, it is included in these proceedings. His paper provides an excellent overview of the corrosion fatigue problem and the extensive background of research that has been accomplished and reported in earlier AGARD Structures and Materials Panel meetings. He discusses the problems with testing structures with the combined cyclic and corrosion environments and proposes some guidelines for the accomplishment of such testing. He emphasizes that these tests should be performed with components with the best possible simulation of the protection systems and the environment rather than on coupons which only test the material.

SESSION I - IN-SERVICE EXPERIENCE WITH CORROSION FATIGUE

This session consisted of three papers. The first was an overview paper "Corrosion and Fatigue: Safety Issue or Economic Issue" given by Dr. J. Lincoln from the United States Air Force (USAF). Dr. Lincoln emphasized several points. The first is that safe and economic operation of aging aircraft is a team effort involving the operators, maintenance personnel, and the original equipment manufacturer. Second, one should place primary emphasis on research in corrosion on detection and prevention methods rather than prediction. If researchers can develop useful prediction methods, then they should incorporate them in the management of corrosion. Finally, he gave a brief summary of the work done for the Boeing 707 aircraft that showed the influence of pitting corrosion on the onset of widespread fatigue damage in the wings of that aircraft.

Mr. M. Worsfold's paper "The Effect of Corrosion on the Structural Integrity of Commercial Aircraft Structure," from British Aerospace Airbus, provided an overview of corrosion concerns. His paper emphasized the importance of surface protection, drainage, and ventilation in controlling corrosion damage. He made the point that the Airbus aircraft have not suffered from corrosion fatigue in the wing structures. He indicated, however, that corrosion is a major economic problem. He is looking forward to insertion of new technology to reduce the cost burden.

Captain M. Colavita's presentation of the paper "Ageing Aircraft: In Service Experience on MB-326" cited the importance of teardown inspections in identifying corrosion prone areas. He accomplished this on the Macchi MB-326, a small trainer aircraft. In this case, they observed the effects of good conservation practices in a 30 year-old aircraft. He also reported on the results of a fatigue test of an aging wing spar and the development of multiple site damage in the attachment to the fuselage. He noted that the cracking found was considerably different than that found in similar aircraft in Australia where they found evidence of stress corrosion cracking.

Mr. J. Komorowski, from the National Research Council in Canada, provided the final paper in this session entitled "Local Stress Effects of Corrosion in Lap Splices." His paper summarized the economic and potential safety concern with pillowing in joints. The work accomplished in Canada has focused attention on this problem in aging aircraft that researchers often overlook. Their calculations and in-service experience observations confirm that cracking can result from this effect. He points out that these cracks may be hard to detect because of their aspect ratio that is unfavorable for nondestructive inspection. He indicated that there was a scarcity of data on cracking with sustained stress. Pillowing has the potential for reducing the time to the onset of widespread fatigue damage and, consequently, must be a serious consideration.

SESSION II - SIMULATION/TEST EVALUATION PROGRAMS

This session consisted of six papers. The first was by Prof. S. Pantelakis, from the University of Patras in Greece. He reported on the effects of corrosion on the properties of 2024, 6013, 8090, and 2091 aluminum alloys. Most of the test results were from strength testing of these materials (primarily 2024-T3). Although he found some loss in ultimate strength from corrosion, the loss in elongation and energy density was dramatic. He attributes this to a bulk embrittlement of the material from hydrogen penetration. When one removes the corrosive material, the ultimate strength increases to its uncorroded value, but the elongation does not. The reason that the ultimate strength is not degraded when they find the elongation significantly lowered is not clear. However, the implication on current metrics for corrosion damage could be significant. He found in his cyclic testing that corrosion had a major influence on S-N testing, but little effect on crack growth rate testing.

The paper given by Dr. B. Journet showed the results of a test program for pitting corrosion on 2091-T351 aluminum. His objectives are to develop an understanding of the transition to fatigue cracks in this material and to develop an approach for prediction of corrosion fatigue. He used the results of tests in a corrosive environment to develop equations for pit depth dependence on time in the environment. He also performed S-N testing, which showed a large effect from the saline environment. The crack growth rate testing showed that the effect of the environment was quite large at the low ΔK region. He concludes that the study provides the basis for a model from which he could make predictions of corrosive damage. The missing element is the definition of the in-service environment.

Prof. M. Marchetti's presentation on "Influence of Corrosion on Fatigue Crack Growth Propagation of Aluminum Lithium Alloys" described the effect of environment on three aluminum-lithium alloys. The aim of the paper was to look at the effect of the effect of both NaCl and moist air on the crack growth behavior in a range of loading frequencies from 1 to 10 Hz. They examined the fracture faces of the test specimens to ascertain the failure mode. This paper is a good example of the care required to obtain valid test data and reach meaningful interpretations from the results.

Mr. C. Brooks presented Dr. G. Bray's paper "Effect of Prior Corrosion on Fatigue Performance of Toughness Improved Fuselage Skin Sheet Alloy 2524-T3" since he was unable to be at this meeting. The primary purpose of this paper was to show the improvement in several important areas of design where 2534-T3 is superior to 2024-T3. These areas included smooth axial fatigue with prior corrosion and multi-hole fatigue with prior corrosion. The authors accomplished their purpose adequately. There was a question on whether the 23 percent increase in fracture toughness was a significant improvement in resistance to foreign object damage.

Ms. B. Schmidt-Brandecker presented the paper "The Effect of Environment on Durability and Crack Growth." This paper probed into those issues that face the designer of a new aircraft. One of the most important of these is the selection of materials considering cost, weight, and compliance with forthcoming regulations. She emphasizes the problem with material selection for a corrosive environment based on standardized crack growth procedures. She is of the opinion that the manufacturers should develop an international cooperative approach to testing that will provide a process for material evaluation and selection. As stated by other authors, the effect of protection systems is extremely important.

The paper "Combined Effect of Hydrogen and Corrosion of High Strength Aircraft Structures under Stress Conditions" presented by Dr. Z. Marioli-Riga, of the Hellenic Aerospace Industry, examines the embrittlement of high strength steels because of hydrogen absorption. This effort is to be part of a major project to develop standard qualification tests for these materials. The results presented lead to the conclusion that engineers should include cyclic sustained loads in the qualification test program.

SESSION III - FATIGUE PREDICTION METHODOLOGIES IN CORROSIVE ENVIRONMENTS

This session consisted of four papers with the first "Corrosion is a Structural and Economic Problem: Transforming Metrics to a Life Prediction Method" being presented by C. Brooks of APES, Inc. The paper defines the structure for making predictions based on an extension of the existing crack propagation formulation. He does derive; however, a time dependent term that is not typically used in fracture mechanics calculations. Since the current state of corrosion understanding does not permit the quantification of all the terms in his equations, he assumed what he believes to be reasonable values for them. His calculations show that for the example chosen, the effect of corrosion is to sharply decrease the life of the structural component. This would seem to place more emphasis on detection and protection since maintenance must find and fix the corrosion problem as soon as possible. For these highly corrosion sensitive cases, prediction methods have limited applicability for influencing in-service management practices for existing aircraft. For less corrosion sensitive cases, this information may allow life cycle managers to safely delay repairs to a more appropriate time. Application of prediction methodologies to assess corrosion sensitivity early in the design process could result in effective corrosion resistant designs.

The next paper presented was "Crack Growth on the Basis of the Strip-Yield Model" by Mr. A. de Koning, from the NLR in The Netherlands. This was a detailed description of the issues in the fracture mechanics analyses of corroded structures. He describes the ability of the strip-yield model to define the strain rate at the crack tip. A threshold level of this function is then useful to formulate a criterion for initiation of time-dependent accelerated fatigue crack growth. He concludes that one should consider the formulation provided

as a reference solution for a description of frequency and load wave effects on crack growth behavior.

The paper "Corrosion in USAF Aging Aircraft Fleet" presented by Messrs. R. Kinzie and G. Cooke is another study of the problem of prediction. This effort is; however, different in that the basis is empirically derived from measurements using the Superconducting Quantum Interference Device (SQUID). This effort appears to be progressing well and could be the basis for future efforts in corrosion prediction. The paper provides an in-depth examination of some of the problems in aging USAF aircraft and the cost of the remedial actions related to corrosion.

Dr. A. Vasudevan's paper "Environmental Effects on Fatigue Crack Growth" represents a quite different approach than that offered by A. de Koning. He proposes that to completely describe fatigue damage, one needs two independent loading parameters ΔK and Kmax. This concept, he believes, is independent of closure, testing methods, and is applicable to all crack growth regimes. He further contends that all deviations from steady state constant amplitude behavior are due to internal stresses introduced during service loading. He cites the need for a systematic test program to obtain the data required for the implementation of his approach.

The paper "Role of Surface Pitting Corrosion on Effectiveness of Hole Cold Expansion" presented by Mr. R. Cook, from DERA in the UK, shows that corrosion may adversely affect the benefits derived from the cold expansion process. He performed tests with both plain holes and holes that were cold expanded. Surprisingly, he found that the corrosive environment and the exposure times did not affect the plain holes. The cold expanded holes in a previously corroded specimen did suffer a significant loss of life because of cracking away from the hole. It was again surprising that the cold expanded holes when subsequently subjected to a corrosive environment did not show a loss of life.

The paper "An Experimental Study of Corrosion/Fatigue Interaction in the Development of Multiple Site Damage in Longitudinal Fuselage Skin Splices" presented by Mr. G. Eastaugh discussed their work on this important subject. The motivation for the effort is to find an economical experimental technique for the study of degradation of fuselage splices from fatigue and corrosion. He appears to have been accomplished this goal. They have made several observations from tests that relate to fretting, pillowing, and crack initiation.

Dr. A. Berens presented a paper entitled "Risk Assessment of Fatigue Cracks in Corroded Lap Joints." This is work he has been pursuing using the University of Dayton developed computer program called PRobability Of Fracture (PROF). He demonstrated, through an example of lap splice cracking with corrosion, how to combine the results of multiple PROF runs to reach the desired result. He also showed how the results could be used to determine the time to a fixed risk.

The final paper of the meeting "Tailoring the Structural Integrity Process to Meet the Challenges of Aging Aircraft" presented by Mr. C. Brooks of APES, Inc. discussed a process for building in corrosion considerations into structural integrity management. He used the USAF Aircraft Structural Integrity Program as a template and showed how this process could be improved through some specific additional corrosion tasks. These recommendations were generally in agreement with existing USAF plans to incorporate the effects of corrosion in their maintenance program.

CONCLUSIONS

Some of the workshop papers discussed the significance of corrosion-fatigue as a safety issue or an economic issue. There is ample data to support the contention that it is definitely an economic issue. There is also ample data to support the contention that it has not been a significant safety problem. However, the problem is certainly a potential safety concern if maintenance does not perform their task diligently. In addition, management must continuously update established maintenance and inspection practices to address additional real-time degradation threats for aircraft operated well beyond their initial design certification life. The economic issue alone is sufficient to motivate the support of research and development that can reduce the maintenance burden. This research will also reduce the threat of catastrophic failure from the corrosion damage.

Many questions about corrosion need to be resolved. The first of these concerns is the ability of nondestructive inspections to detect corrosion adequately. The word "adequately" refers to (1) the detection of what is today referred to as hidden corrosion and (2) the quantification of corrosion pitting and thinning such that corrosion management becomes viable. It would be supportive for maintenance to have the capabilities of nondestructive inspections quantified by means of probability of detection for corrosion in the same manner that one is able to quantify the ability of nondestructive inspection for crack detection.

The second question is on the need for institutionalizing the corrosion management process. Currently, there are no strong linkages between the structural engineer and the corrosion engineer. The structural engineer sizes the components of the aircraft based on strength, durability, damage tolerance, and stiffness requirements. There is no formal approach for combining the effects of corrosion with fatigue in a maintenance program. This type of program should start with the designer working for the original equipment manufacturer and be a part of the policy of the systems (or program) manager. It should be passed down to the depots performing the major maintenance and finally to the base and squadron level for the implementation in the field. One virtue of this approach is that all elements of the maintenance chain are completely aware of criticality of corrosion found in operational aircraft. Another virtue is that this effort should reduce the cost burden through prevention at the design level.

Another question is on the return on investment from the use of corrosion prediction methods. Researchers have expended considerable effort on tool development for the prediction of corrosion damage in the future from the observance of the current state of corrosion. The return on investment of this effort should be examined carefully. Many structural components are designed to zero static margins. This has been the accepted policy for both military and commercial aircraft for many years. Consequently, they are unable to withstand any thinning without causing the static margins to become negative. When the nondestructive inspection process indicates that corrosion is present, it may be that, at that time, the margins have become negative indicating that remedial actions are required. In such a case, the use of predictive capability would not be justified. Alternately, some components do have residual strength capability in the

presence of corrosion. If detected early, repair actions for these components may be delayed based on engineering assessment using the prediction methods. There may be availability and cost benefits to delaying repairs for these components. The question on return on investment is a difficult one because the actual cost of corrosion maintenance and repair is typically poorly tracked. A focussed effort is needed to remedy this situation so that the researcher can better determine if his work has the potential to reduce the cost burden from corrosion damage.

Another question is whether the testing that currently performed provides the proper data for the corrosion-fatigue problem. There is a need to establish the corrosion fatigue data for the commonly used materials in aircraft. The paper by Ms. B. Schmidt-Brandecker highlighted the need for a test approach involving corrosion fatigue for material selection.

A final question is on the current capability of corrosion prevention compounds and their potential uses in the future. Questions such as (1) should they be an integral part of airworthiness, (2) should there be increased process control on parts that are non-inspectable, and (3) is there a need for process qualification? Item number (3) refers to issues such as long-term breakdown of the compounds, technician training, and performance standards for durability, and assurance of sufficient coverage through nondestructive inspection.

Any of the questions above could be the subject of another workshop.

CORROSION FATIGUE OF STRUCTURAL COMPONENTS

Dr. Ing. Walter Schütz
Industrieanlagen-Betriebsgesellschaft (IABG)
Einsteinstrasse 20
D-85521 Ottobrunn
Germany

SUMMARY

Corrosion fatigue is a very complex phenomenon, because two very different loading systems are acting together. In addition, its correct simulation in the lab-relatively easy, if expensive, for fatigue alone - is nearly impossible for cost and duration reasons. Also, little is known about the corrosion environment of aircraft (and of ground vehicles).

Components, always notched, behave differently from unnotched material specimens in corrosion fatigue.Therefore, materials tests are useless, it is necessary to test components, with their protection system, under the relevant variable amplitude stress-time history and to simulate also the typical sequence: Corrosion-Corrosion Fatigue-Corrosion etc., in order to obtain a result which corresponds to the real behaviour in service. This has never been done up to know - and would be very expensive anyway. One way out of this problem would be to corrosion-fatigue test components which have suffered corrosion damage in service. This has been done a number of times, as some papers in this Workshop show.

Finally a number of rules for improving corrosion fatigue tests in the lab are presented, including the suggestion to fit "corrosion boxes" to some typical components of an aircraft during it's full scale fatigue test.

1. INTRODUCTION

Over the last 25 years the AGARD Structures and Materials Panel has been quite active in the field of corrosion and corrosion fatigue. We had at least two Specialist Meetings [1, 2], a collection of four Pilot Papers [3], the Corrosion Handbook [4] and two large cooperative programs [5, 6]. Since especially the latter one, the "FACT" program differed in all important aspects from any previous work on corrosion fatigue, it will be described in some detail here:

- Structural components of several typical aircraft materials in the form of rivetted joints with the relevant corrosion protection schemes (of different aircraft) were used.
- The mechanical and corrosive service loads were simulated as far as possible:
- First, two high tensile loads (near limit load) were applied at ≈ 210 K to simulate typical high-g loads during the flight test period of every tactical aircraft. This was to possibly crack the paint system around the fastener holes (and loosen the rivets?).
- Then, a precorrosion period of 72 hours in artificial seawater, acidified by H_2SO_4 followed, to simulate the highly corrosive environment aboard a carrier or near industrial plant, as far as possible in so short a time.
- The stress-time history "Falstaff" was then applied, either in air or in a seawater spray.
- Every detail of these tests was exacty specified.
- Some laboratories also performed crack propagation and other fatigue tests on the materials concerned or used other stress-time histories ("Twist"), specimens etc.
- A huge number of parameters was thus investigated.
- Every fracture surface was examined as to the fatigue origin and to the presence of NaCl.
- Highly sophisticated statistical methods were used to determine the effect of individual parameters on fatigue life.
- The result were, qualitatively: The effect of the most severe conditions - i.e. precorrosion plus corrosion during the fatigue test - on fatigue life was relatively small (less than a factor of four) compared to the usual constant amplitude corrosion fatigue tests on unnotched and unprotected material specimens, where it can easily surpass one hundred or more.

Paper presented at the RTO AVT Workshop on "Fatigue in the Presence of Corrosion", held in Corfu, Greece, 7-8 October 1998, and published in RTO MP-18.

2. A MATERIAL'S AND A COMPONENT'S RESISTANCE TO CORROSION FATIGUE IN LAB TESTS

Consider an unnotched material specimen and a typical aircraft or automobile component: The former's complete surface is attacked by corrosion and fatigue during the typical constant amplitude fatigue test, which usually does not contain hold times under corrosion and is run at high freguency.

The component, however, has, at most, a few fatigue critical locations, whereas all the other regions are not stressed highly enough by the repeated loads to show fatigue damage, not even in a corrosive atmosphere. Hold times under corrosion alone, if any, are short; to compensate for this the corrosion agent is usually made more severe (as in the FACT program). The stress-time history is either constant amplitude or something like "Falstaff", "Twist" or the individual aircraft's history. The component surface is either bare, typical for thick - section aluminium automotive applications - or protected - typical for all aircraft applications and all automotive steel and aluminium sheet applications..

As long as this protection is not breached, corrosion has no effect on fatigue life and the "corrosion fatigue" test is simply a fatigue test.

Even if it is breached sometime during the test, the time period before inflicted no additional corrosion damage, i.e. the component has a longer fatigue life than if it had been unprotected. Since **all** metallic structural materials are **corrosion fatigue** sensitive while some are **corrosion resistant** (see chapter 4), the location of such a breach is important: If it is not fatigue critical, i.e. away from a notch or (in bending) near the neutral axis, or if the design criterion was not fatigue, but stiffness or crash resistance, as in some automotive applications, there will be no reduction in test life. Instead, if the material was not corrosion resistant, a pure corrosion failure might result if the fatigue test would last long enough. These simple thoughts alone show that it is not possible to draw correct conclusions as to the corrosion fatigue behaviour of a component from tests on fatigue specimens of the component's material.

In addition to the above, the simulation of cathodic corrosion and crevice corrosion and their possibly deleterious effect on fatigue life are only possible with components. The influence of unintentional or intentional residual stresses produced for example by machining or shotpeening, cannot be simulated in unnotched specimens.

3. THE DIFFERENCE BETWEEN A CORROSION FATIGUE TEST IN THE LAB AND CORROSION FATIGUE LIFE IN SERVICE

As our 30 years' experience with modern full scale fatigue tests on aircraft prove, we will find

- most, if not all, the fatigue critical locations
- their correct order of occurrence and
- with somewhat reduced confidence - even the real service life

By the way, the German Automobile makers have a similar 20 years' experience with their complex full scale fatigue tests on automobile structures, at least with regard to fatigue critical locations and their order of occurrence.

Why is this so? Because the fatigue loads in service are well known and well simulated in these full scale tests. If there were deviations from the above experience in the past, the loads had changed in service (typical for tactical aircraft) or were not simulated correctly, as in many such tests of the 1960ies.

We therefore can state: Know your fatigue loads and simulate them well and you can rely on the results of the full scale fatigue test. That is true, at least, for locations in the structure which are not **corrosion** fatigue critical.

However, if in addition corrosion comes into play, we cannot state this with any confidence because

- there is practically no experience with corrosion fatigue tests on large components and their correlation with service behaviour and
- we have not simulated the **real** service conditions very well, not even in a dedicated program like the AGARD SMP "FACT" program described above.

Consider the corrosion and fatigue loads on a tactical aircraft: It performs 100 to 200 flights of about one hour each per year. For the rest of the time - 97 to 98 per cent of it's life - it is standing on the ground, corroding away, if the environment is corrosive enough or if corrosive products

from previous service are present on the inside and outside of the structure.

It is this prolonged, purely corrosive period - especially in military aircraft - which is impossible to simulate in a lab test for cost and test duration reasons and which makes the result of **any** corrosion fatigue test so questionable with regard to correlation with service.

The typical way to somehow shorten the pure corrosion time is to increase the corrosiveness of the enviroment involved, as was done in the "FACT" program, or to use altogether different media, as in some other corrosion programs. This is a difficult problem, as proved by many famous or infamous examples from the literature. Either the required effect did not occur or a misleading effect occurred which was not critical in real service (the great "hot salt stress corrosion" scare of the American SST program comes to mind).

Also in practically all corrosion fatigue tests, the precorrosion periods, if any, were followed by the fatigue period.

In aircraft service however, each short fatigue period (flight) is followed by a long pure corrosion period, followed by another short fatigue period and so on. The protection could have been breached by high fatigue strains around the notches or it could have been damaged by wear, abrasion etc. All these effects are usually not simulated in test and thus the dictum "Simulate what happens in service" is violated.

4. CORROSION RESISTANCE AND CORROSION FATIGUE BEHAVIOUR

As mentioned before, there are corrosion resistant materials in every Fe-, Al- and Ti-based materials group. However, this does not mean these materials are corrosion-fatigue resistant; on the contrary, all of them are highly sensitive to additional corrosion during fatigue, at least in some state, like welded (for stainless steels) or cracked (for titanium alloys).

One example is shown in Fig. 1: The "seawater resistant" Al-alloy 5456 shows a disastrous effect of seawater in the unnotched state, especially at high mean stresses. On the other hand some materials which are known to be corrosion sensitive, like 2024-T3 because of it's copper content, are quite good in crack propagation under corrosion conditions, at least in the usual lab tests in salt water spray. If a thin-gage component of this material were tested slowly and long enough in fatigue crack propagation, it might just corrode away before failing in fatigue crack propagation, as it probably would in aircraft service under the typical prolonged corrosion hold times described above.

Were the material "corrosion resistant" like the 5456 alloy above, this would not happen (neither in a prolonged test nor in service). A typical crack propagation test in a corrosive medium might show no difference between 2024-T3 and 5456 (and for both materials only a small influence of corrosion on the crack propagation rate); however, in service or in tests with long hold times, 5456 would not fail in corrosion, but 2024-T3 would.

Based on the typical short corrosion fatigue test, our conclusion would be: "Both materials are equal", and thus would be wrong with regard to service. This deceptively simple example shows, how difficult it is to draw correct conclusions from corrosion fatigue lab tests (and we **must** draw conclusions from tests because we cannot wait for results from service and these are difficult to interpret anyway).

Other unexplained (and unexplainable) questions with regard to corrosion fatigue exist:

- In **all** test programs known to the author, variable stress - time histories resulted in a less detrimental effect of corrosion on fatigue strength than constant stress amplitudes. Many examples are given in [7], one is shown in Fig. 2 [8]: A large effect of corrosion on constant amplitude strength of notched specimens of 7010 alloy at $6 \cdot 10^6$ cycles (none at 10^4 cycles) and none at all at 4000 and 55000 flights on "Falstaff" fatigue strength. The time in the environment was quite similar at $6 \cdot 10^6$ cycles and 55000 flights respectively. The author has discussed this general effect (also found in steels) with many corrosion and fatigue experts since about 1973, but no explanation came forward.
- Different materials behave differently in a corrosive environment in their crack initiation and crack propagation periods. The most pronounced difference occurs with some titanium alloys, as shown in Fig. 3 [8]: Both 2024-T3 and 7075-T6 showed relatively small effects of corrosion on the number of flights to crack initiation and Ti 6Al4V showed no effect at all

even at a larger number of flights. In crack propagation however, 2024-T3 showed a small effect, 7075-T6 a somewhat larger one, but Ti6Al4V a reduction of one about one order of magnitude due to corrosion!

- Corrosion alone takes time to take effect, but even in high-frequency corrosion fatigue tests a few minutes in the corrosive environment are enough to show it's detrimental effect. Prolonging the test time by lower test frequencies or reduced stress amplitudes (thus increasing the number of cycles to failure) will in many cases not increase this detrimental effect under veriable stress amplitudes, i.e. the Gassner curves are more or less parallel up to quite high numbers of cycles; in contrast to this, at constant amplitudes the SN-curves in air and under corrosion are sometimes parallel up to the point where the fatigue limit in air is reached and the corresponding SN-curve becomes horizontal, while the corrosion-fatigue SN-curve goes on at the slope of the finite life region.

Some other effects of corrosion on fatigue strength are understandable, at least in a qualitative way:

- The allowable omission level in variable amplitude corrosion fatigue tests is lower than in air. This is the experience of some German automobile makers and also of IABG.
- If the component is sharply notched, i.e. has a low fatigue strength in air, the effect of additional corrosion on fatigue strength is much less severe than if it is mildly notched, as shown in Fig. 4.

5. RULES FOR CORROSION FATIGUE TESTS

In order to improve the present unsatisfactory state of the art in corrosion fatigue, the following rules are suggested:

- Test the component, not the material.
- Test the component complete with it's corrosion protection system. If this can suffer damage in service (cracks, scratches) or deteriorates over time in some other way (wear, erosion, exhaustion of the cathodic protection potential etc.) this must be simulated in test. (The paint system of automobile springs, for example, is damaged in service by gravel thrown around in the wheelhouse and this is simulated by shooting gravel at the springs before the corrosion fatigue test).
- Test the component with any attached parts (bolted-on for example). Crevice corrosion and contact corrosion, if they occur, are included in this way.
- Simulate the mechanical stresses in service as best you can be applying the relevant stress-time histories like "Falstaff", "Twist,", "Helix-Felix" etc. or, better, by the individual component's stress-time history. Individual high loads (overloads) if they can occur in service, must be included.
- The omission level, if necessary, must be selected carefully. For tactical aircraft, which see less than 10^6 cycles in their lifetime - even with a safety factor of four - no omission is necessary. Anyway the omission level must be lower than in fatigue tests in air.
- Increase the severity of the corrosion by alternating corrosion periods with drying periods (The German "VDA-Wechseltest" is an example. Originally developed for testing paint systems, it's effect in corrosion fatigue is not yet clear).
- In the long term, use a more severe corrosion medium, if the location and type of failure are not changed. This is a difficult problem and requires further research and development.
- Increase the corrosion time (as apart from the corrosion fatigue time) as much as possible within the time and cost limitations available. Precorrosion alone is not sufficient, it often has no effect on the corrosion fatigue life. However, interspersed corrosion periods will often have a more degrading effect, because the corrosion protection system may have been damaged or breached by the fatigue loads or by the intentional damage applied to the component.
- Fatigue test (in air or in the corrosive medium) components corroded in previous service, with damaged protection system etc.
- Compare the result with the fatigue life of identical new components, which should be available anyway dating back to the development period. This results in a "life reduction factor" due to the corrosive environment in service.
- Try to achieve a similar reduction factor by corrosion fatigue tests in the lab on new components. (Difficult, further research and development are required). Fig. 5 shows the effect of a corrosive 10 year service life of the wing upper surface of a Lufthansa Boeing 707 made of 7178-T6, on fatigue behaviour: A severe decrease for the almost unnotched condition, a

less severe, but still considerable decrease for the notched condition [10]. We then tried to simulate this effect in lab tests with 2024-T3, because 7178 was not available. However, we did not succeed, 2024 showed a sudden drop of the SN-curve at intermedite fatigue lives, not the gradual decrease shown in Fig. 5.
Aluminium truck wheels, used for two winters in a highly corrosive environment (service over the Brenner pass) showed some effect on fatigue life, despite the (originally) good protection system.

- Finally, fit "corrosion boxes" of about one half to one square meter over typical design details of the structure for the full scale fatigue test (a window for example) inside and outside of the structure. The FSFT takes a long time, the individual aircraft's stress-time history is the best simulation of service available etc., so the results of such a "partial" corrosion fatigue test are the nearest approach to reality possible and a direct comparison with the fatigue life in air of nearby similar components is possible.

6. CONCLUSIONS

- The only question of **engineering** significance in corrosion fatigue is "How long is my structure going to last in its corrosion and fatigue environment in service and what can be done to improve that performance?"
- The conjoint action of corrosion and fatigue during the (usually short) fatigue periods and of corrosion alone during the (usually long) corrosion periods in typical aircraft service would be extremely difficult, costly and time consuming to simulate in laboratory component or structure tests. Such tests would also have to simulate the slow deterioration of the corrosion protection system over time.
- Such tests have never been carried out up to now.
- Therefore **all** available results of corrosion fatigue tests in the laboratory, even very complex ones, are questionable. (This is also true for some of the following conclusions, because they are based on such tests.)
- No correlations between service life and corrosion fatigue test life have been established.
- At the state of the art, fatigue tests on components corroded in service in comparison with identical, new, uncorroded components are a possible way out of this problem.The deleterious effects of service corrosion on fatigue life, if any, can be established in this way.
- The next step would be to try and simulate this effect by chosing suitable corrosion conditions for lab tests, resulting in equally reduced fatigue lives, identical failure locations etc.
- Any generalisations of such results, however, are questionable.
- Testing unprotected and unnotched fatigue specimens of the material in question is useless; the corrosion effect usually is catastrophic, in direct contradiction to service experience with components of the material.
- Notched fatigue specimens may give qualitative answers in the sense "Sharply notched components suffer less from additional corrosion than mildly notched ones", leading to conclusions like: "The better the design quality i.e. the smaller the K_t, the more important is a long-lasting corrosion protection system" etc.
- Qualitative answers may also be provided by crack propagation tests on the material in the sense. "Material A has better fatigue crack propagation properties under corrosion than material B". No generalisation of the type "Therefore A is better in corrosion fatigue than B" is allowable, because in the crack initiation stage this could be exacty wrong.
- All corrosion fatigue tests from notched or cracked specimens to complex components should be carried out under the relevant stress-time history. The greater cost of such tests is balanced by the always less severe effect of corrosion than in constant amplitude tests.
- If future full scale fatigue tests could be fitted with several "corrosion boxes" over typical details of the structure, the results would be the nearest approach to service possible. The additional cost would be negligible compared to the test cost (and that of the structure, which is destroyed by the test anyway).

7. REFERENCES

[1] N.N.: Aircraft Corrosion, AGARD Conference Proceedings No. 315, 1981

[2] N.N.: Corrosion Fatigue. AGARD Conference Proceedings No 316, 1981

[3] N.N.: Corrosion Fatigue of Aircraft Materials. AGARD Report No 659, 1977

[4] Wallace, W. and D.W. Hoeppner: AGARD Corrosion Handbook. Volume 1, Aircraft Corrosion. Causes and Case Histories. AGARDOGRAPH No 278, 1985

[5] Wanhill, R.J.H. and J.J. DeLuccia. An AGARD-coordinated Corrosion Fatigue Cooperative Testing Programme. AGARD Report No 695, 1982

[6] Wanhill, R.J.JH., J.J. DeLuccia and M.T. Russo: The Fatigue in Aircraft Corrosion Testing (FACT) Programme. AGARD Report No 713, 1989

[7] Schütz, W.: Corrosion Fatigue, the Forgotten Factor in Assessing Durability, in: Estimation, Enhancement and Control of Aircraft Fatigue Performance, ICAF 1995, Melbourne, EMAS 1995

[8] Kemp, R.M.J.: The RAE Contribution to the FACT Programme, in: [6]

[9] Wanhill, R.J.H., J. Schijve, F.A. Jacobs and L. Schra: Environmental Fatigue under Gust Spectrum Loading for Sheet and Forging materials, in: Fatigue Testing and Design. The Society of Environmental Engineers 1976

[10] Schäfer, R., H. Bügler and W. Schütz: Schwingungsrisskorrosion von Flugzeugstrukturen. IABG-Report TF 2323, May 1988

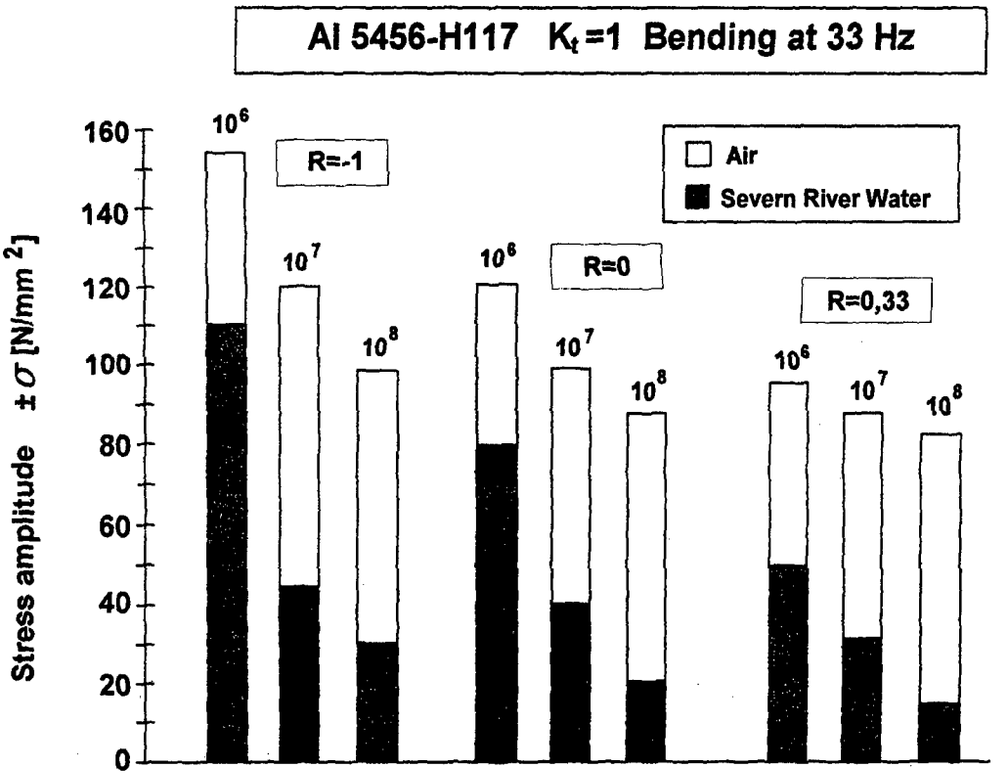

Fig 1. Effect of Corrosion on Fatigue Strength

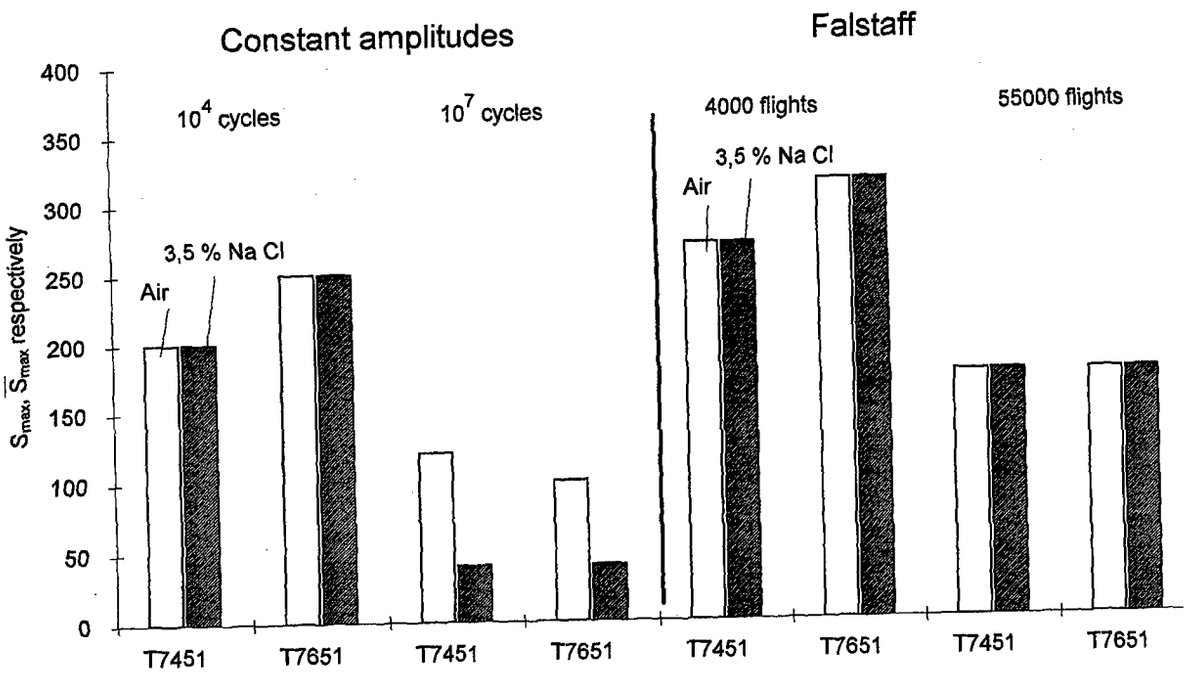

Fig 2. Fatigue Strength under Constant and Variable Amplitudes [8]

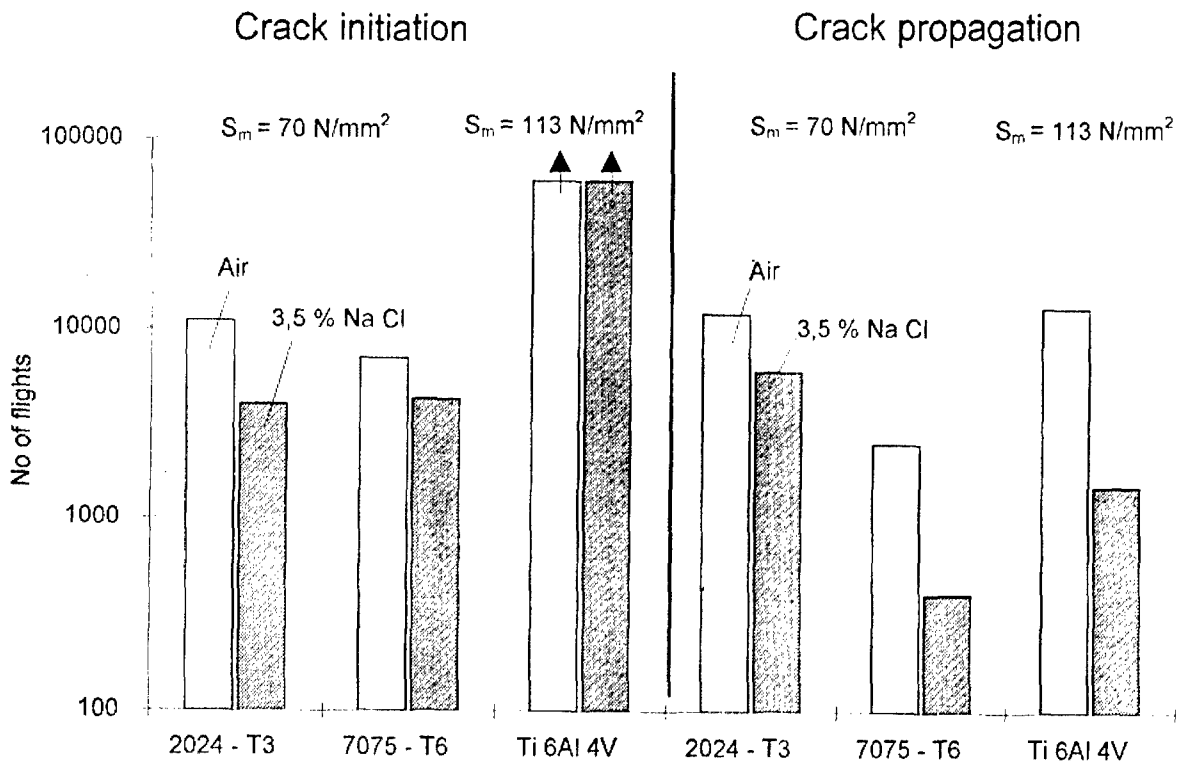

Fig 3. Crack Initiation and Crack Propagation Lives [9] Twist Sequence

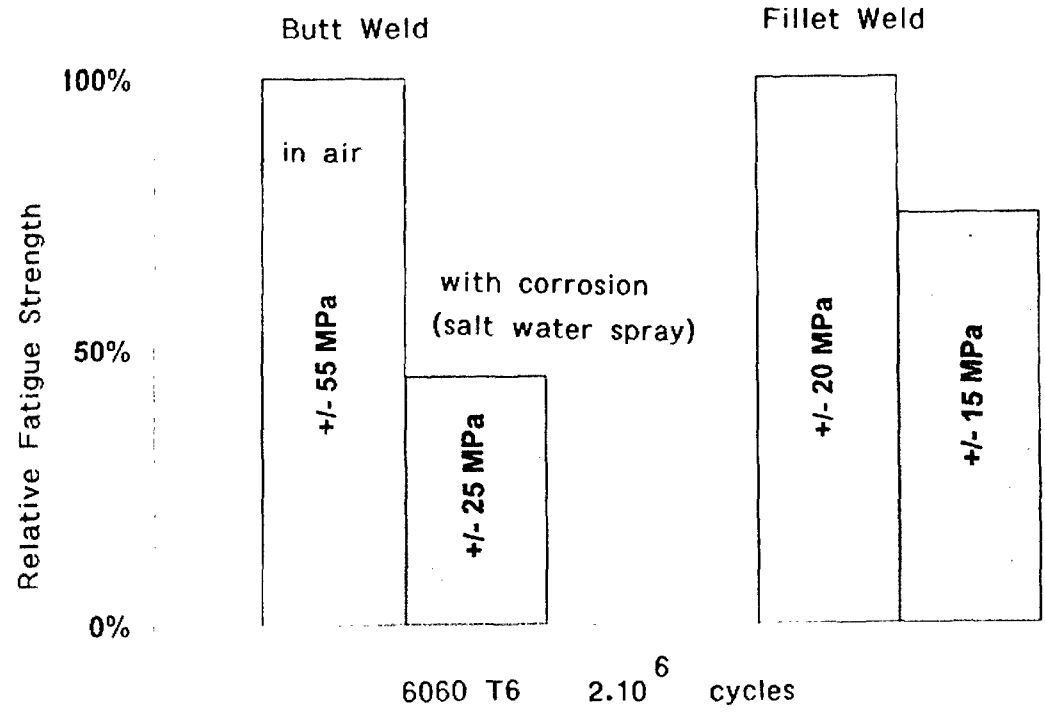

Fig 4. Effect of Corrosion on Fatigue Strength of Sharply and Mildly Notched Aluminium Weldments

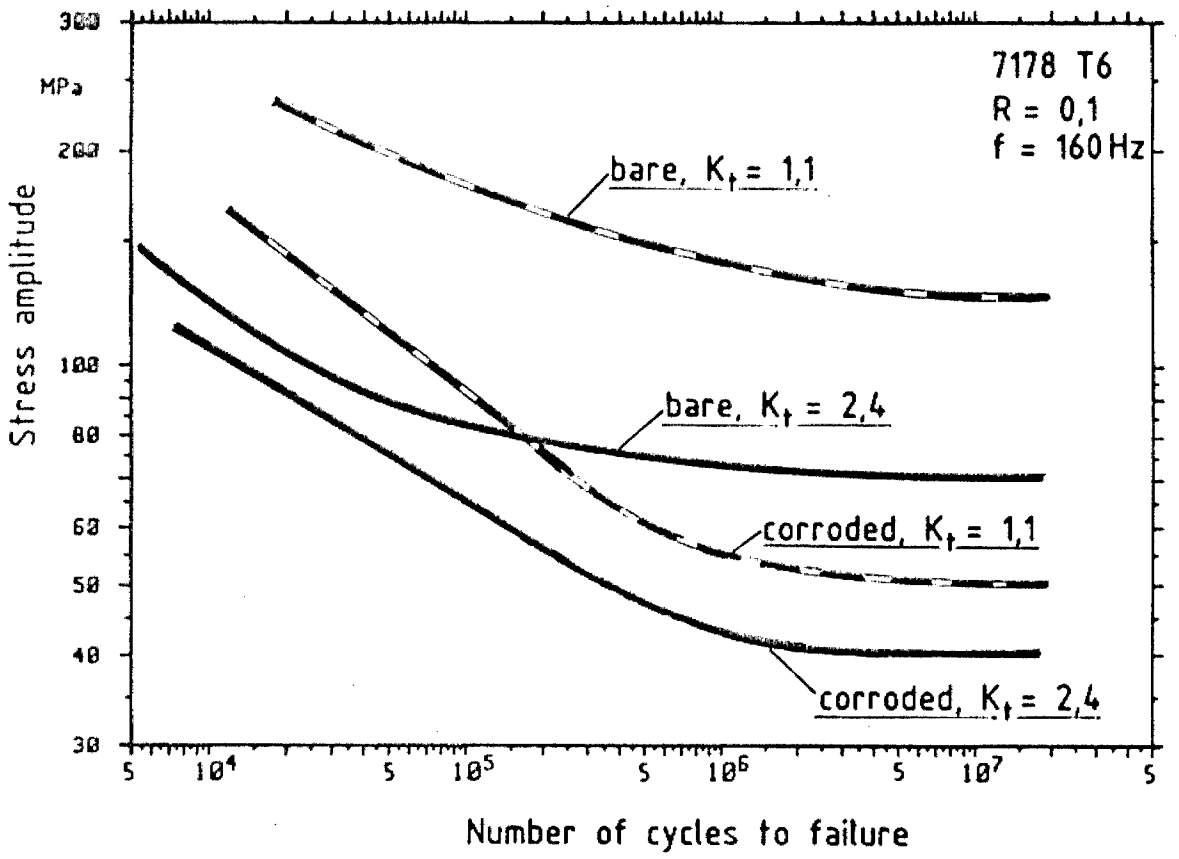

Fig 5. Effect of Precorrosion in Service (10 years) on Fatigue Life in Air

CORROSION AND FATIGUE: SAFETY ISSUE OR ECONOMIC ISSUE

John W. Lincoln
ASC/EN
2530 Loop Road West
Wright-Patterson Air Force Base, Ohio 45433-7101

SUMMARY

Corrosion and fatigue separately have both led to serious safety as well as economic problems. Corrosion alone, in forms such as uniform corrosion or exfoliation, may reduce the strength of aircraft and lead to failure. Both of these forms of corrosion may lead also to expensive component repair or replacement. There are many cases where corrosion alone is not significant from a safety consideration, but is a very significant economic problem. In the case of corrosion alone, one must judge the seriousness of this problem on an individual basis. Nondestructive inspections have found fatigue problems where there is essentially no influence from corrosion. Researchers have documented many cases over the years where the consequences were catastrophic. The results of fatigue cracking have caused many expensive repairs and modifications to the structure including component replacement. Fatigue often combines synergistically with corrosion. In these cases, the term corrosion fatigue is more appropriate. In most cases, corrosion, fatigue, or corrosion fatigue becomes a safety consideration only when either maintenance is not performed properly or the maintenance program is inappropriate. Experience derived from diligent maintenance has repeatedly shown that the operator need not compromise safety resulting from these problems. The purpose of this paper is to describe some experiences with corrosion, fatigue, and corrosion and fatigue and to review some of the relative literature on this subject.

1 INTRODUCTION

Based on historical evidence, there can be no question that corrosion is a major economic problem with both military and commercial aircraft. Many of the older military aircraft that are currently operating were victims of the zeal for increased performance that prompted the development of high strength alloys without any consideration of the threats that they could have on structural integrity. One such development was 7178-T6 that the United States Air Force (USAF) used for the lower wing skins of KC-135. This material was selected rather than the 2024-T3 material used in the Boeing 707 to provide additional tanker capacity for aerial refueling. Experience has shown that high strength was the material's only virtue. That material exhibited low fracture toughness, poor crack growth rates, susceptibility to corrosion, and low resistance to stress corrosion cracking. To make matters worse, the USAF elected to save money by omitting corrosion protection of the material by faying surface sealing or wet-installation of fasteners. The result was that the USAF had to replace the lower wing skins at 8,500 flight hours. By that time, the structure had lost its fail-safe capability because of widespread fatigue damage (WFD). Recent teardown inspections of a high time 707 wing with 2024-T3 indicates the onset of WFD occurs at about 50,000 flight hours of commercial usage [1]. The results of previous laboratory full-scale durability testing would not have indicated that the KC-135 wing structure would be in a state of WFD at 8,500 flight hours. Corrosion fatigue undoubtedly played an important role in the demise of this structure. The economic impact of this problem was enormous. However, the alertness of the engineers at the Oklahoma Air Logistics Center (OC-ALC) at Tinker Air Force Base prevented this problem from causing loss of an aircraft

This same material, 7178-T6, is used in the upper wing skins of the KC-135. It is now causing a significant problem in that there is considerable exfoliation corrosion around the fastener holes. The OC-ALC finds these problems through the process called search peening. In the performance of this process, maintenance personnel shotpeen the upper wing skins with glass beads that cause corroded areas to reveal themselves through local deformation around fastener holes. In some cases, the problem is severe enough to cause panel replacement. When the OC-ALC replaces upper wing panels, they select a replacement material that is much more resistant to corrosion than the original material. The troublesome part of this problem is that the USAF does not have a solution that would preclude further replacements in the future. The use of peening; however, does appear to extend their lives. There is evidence of beneficial effects of shotpeening from the B-52H upper wing. These wings, which had the upper surfaces shotpeened at the time of fabrication, are showing only minor corrosion damage although they have been in service for many years.

The USAF's C-141 is another aircraft that has experienced problems sooner than indicated by the results of full-scale durability testing. The USAF believes that a least part of this difference could be explainable by the environmental effect found in operational usage. However, this difference could be attributed to the variations in quality that could be expected from aircraft-to-aircraft. The manufacturer sealed the faying surfaces and wet-installed the steel fasteners. These actions appear to have diminished the corrosion problem significantly.

The AGARD Corrosion Handbook [2] discusses the problems found on these aircraft and many others through case studies. This document places the cost of corrosion in the United States alone in 1978 at $70 billion overall. The USAF can account for approximately one of those billions for their airplanes. The case studies in this handbook show the results of corrosion that remained undiscovered by maintenance personnel until it was a large economic or safety problem.

These problems include both military and commercial aircraft. As evidenced by the currently documented cost of the major maintenance visits by large category transport aircraft, the cost of corrosion is a major factor in commercial maintenance budgets. However, the use of corrosion prevention compounds in commercial aircraft has significantly reduced the burden. It is encouraging that the airframe manufacturers are doing a much better job of applying corrosion protection during fabrication. One would anticipate that these improvements would relieve some of the

Paper presented at the RTO AVT Workshop on "Fatigue in the Presence of Corrosion", held in Corfu, Greece, 7-8 October 1998, and published in RTO MP-18.

maintenance cost burden when the operators bring these aircraft into the inventories.

Also, based on historical evidence, there is no question that fatigue is a major economic and safety problem for aircraft. A history of fatigue [3] shows that aircraft have suffered fatigue problems since the late twenties. In the USAF, fatigue became particularly acute in the late fifties. Even the USAF Aircraft Structural Integrity Program initiated in 1958 did not completely alleviate this problem from affecting flight safety. The "safe life" approach adopted by the USAF in 1958 proved to be ineffective in eliminating fatigue problems as evidenced by the cracking problems in the KC-135, F-5, F-111, and others. The introduction of damage tolerance principles by the USAF in their structural inspection program in the early seventies virtually eliminated fatigue as a safety problem in their aircraft. However, fatigue cracking of operational aircraft in the USAF is still a significant economic problem. The USAF estimates that this problem cost approximately $250 million in 1997. The USAF attributes much of this burden to operational usage being more severe than the usage assumed for design.

The commercial approach of designing structures to be fail-safe and then augmenting this design principle with damage tolerance driven inspections has also virtually eliminated fatigue as a safety problem in large category transport aircraft. The remaining issue with some of these commercial aircraft is to determine the time of onset of WFD. That is, the time when their fail-safe capability is degraded. The work done by the FAA Technical Center and NASA Langley since 1988 has established the methodology for the determination of the time of onset of WFD. The commercial aircraft manufacturing community is now using this technology to assess their aircraft for the occurrence of this problem.

The synergistic effect of corrosion and fatigue together, called corrosion fatigue, is also a safety and economic problem. The author of the ICAF Plantema lecture of 1995 [4] discusses this problem in detail and provides a large bibliography for further study. The author suggests that a factor of two should be acceptable as a life reduction factor to account for the effect of corrosion on fatigue. This appears to be larger than would be expected from USAF experience. The specific reduction factor for the damage tolerance driven inspections would need to be determined on a case-by-case basis. Since pitting corrosion could affect the total life, it is likely that the factor would be significantly less than two. The reason is that the size of defects derived from pitting corrosion are considerably less than those assumed as initial flaws for damage tolerance. Consequently, the crack nucleation time from corrosion pits would not affect the inspection interval. This situation could change for an aircraft that has a long history of pitting corrosion that was not corrected through maintenance. In this case, multiple cracks from corrosion pits could require that the operator shorten the inspection intervals. Since this pitting may not have been recognized it could constitute a safety problem. In [4], the author indicates that the result may be different for constant amplitude loading and spectrum loading. The effect of pitting corrosion on life is another shortcoming of the "safe life" approach. In this approach, the analyst may not adequately account for the reduction in crack nucleation time from corrosion pits. Consequently, the "safe life" derived from laboratory fatigue testing could be unconservative.

The fail-safe design augmented by damage tolerance derived inspections is largely responsible for preventing the combined effect of corrosion and fatigue from becoming a major problem on large category transport aircraft. For the USAF, the inspection program derived from damage tolerance principles is certainly the primary means of maintaining safety from corrosion fatigue. The USAF also uses another inspection process called the Analytical Condition Inspection (ACI) to augment the damage tolerance inspections. The USAF initiated the ACI program many years ago to help the maintenance personnel discover distressed areas of the aircraft not identified by the design analyses or testing. For this process, the USAF selects a small sample of aircraft from the inventory and inspects the entire aircraft thoroughly. To gain better access to concealed areas they remove fasteners and panels to interrogate the structure. This is done as completely as possible nondestructively to ensure that the structure is not experiencing corrosion or fatigue cracking that could jeopardize continued flight safety or economic operation. When they find an area that does not correlate with design experience, they make appropriate changes to the Force Structural Maintenance Plan (FSMP) which is an integral part of the ASIP. The FSMP tells the maintenance personnel how, when and where to inspect the structure to maintain its safe operation.

2 DISCUSSION

A paper written in 1997 [5] describes the forms of corrosion that could compromise flight safety. The authors of this paper list pitting corrosion, intergranular corrosion, exfoliation corrosion, stress corrosion cracking, corrosion fatigue and uniform corrosion as safety issues. In this document, they suggest a number of research and development activities that should enhance the state of knowledge about the effects of corrosion. They suggest many activities including teardown inspections of ex-service aircraft and scheduling of maintenance on a time basis as well as a usage basis.

The USAF Aircraft Structural Integrity Program (ASIP) initiated in 1958 and modified in 1975 makes an assumption about the effects of some of the forms of corrosion listed above. It presupposes that corrosion damage will not raise the stress sufficiently to change the inspection program to ensure flight safety. This infers that the maintenance program is able to control corrosion damage through inspections and preventative measures. Experience has shown that this assumption has not led to serious consequences. The USAF maintenance program is outstanding. One reason for its success is the advice given to them by the resident ASIP Managers and other engineers at the Air Logistics Centers. These engineers provide them with a tailored inspection program for each individual aircraft from data collected from operational aircraft. The USAF experience, since they introduced damage tolerance, has shown that the failure rate from structural causes is less than one in fifteen million flight hours. The USAF cannot attribute any catastrophic failure since the early seventies to corrosion or corrosion related phenomena. There have been; however, numerous local failures from corrosion, particularly stress corrosion cracking. This has been a chronic problem in many landing gear systems and in large bulkhead forgings.

The applications of the 1975 version of ASIP addressed corrosion fatigue by modifying the crack growth rates in an attempt to account for the corrosion environment such as moisture, salt or sump tank water as appropriate. The validity

of these corrections is subject to question because of such factors as loading frequency, temperature and the use of crack growth rate data from constant amplitude testing. However, the USAF has found few errors in the damage tolerance assessments that they can directly attribute to the manner in which they accounted for the effects of the environment. Most often, the increase in crack growth rates in critical locations in the structure is associated with operational usage spectra that are more severe than the design spectrum of loading. The USAF accounts for these differences through individual aircraft tracking for loads.

Specific Corrosion Concerns

The USAF sponsored a contract in 1997 to determine the cost of corrosion in USAF aircraft and found in this study as in a previous study performed in 1990 that the cost of corrosion prevention and repair is significant. They found that the total cost from corrosion in 1997 was approximately $795 million dollars. This was an increase of 4% over the 1990 costs although the USAF reduced the force structure by 28%. The C-5, KC-135, and the C-141 account for 50% of all direct corrosion maintenance costs. Of the $795 million spent, painting the aircraft cost $136 million. The USAF spent approximately $425 million of the $795 million specifically on corrosion repairs. The survey highlighted the A-10 as a success story in defeating a serious corrosion problem.

There are serious concerns about the impact of corrosion on structural integrity. The first and most obvious is the effect of lapses in proper maintenance that have led to significant loss of structural strength. Thinning of the structure will increase the stress in the structure such that the inspection intervals required for flight safety will need to be decreased. There is limited nondestructive inspection capability to accurately quantify the amount of material loss due to corrosion. A much easier task is to interrogate the structure for the existence of corrosion. Consequently, at this time, the safest approach is to remove corrosion indications when found. As the capability for nondestructive inspection is improved, then the opportunity for corrosion management is improved. Further, it is essential that those areas that are damage tolerance critical be an integral part of the corrosion detection program.

As an example of the potential danger of damage from corrosion, a Far East Transport (FAT) 737 experienced a fuselage failure by explosive decompression in Sanyi, Taiwan on 22 August 1981. The operator had been using the aircraft for transporting fish in open barrels in the cargo compartment. The failure was due to severe undetected skin corrosion over a length of approximately 2.5 meters in the lower lobe of the fuselage. Corrosion caused significant thinning in the skin which resulted in an increase in hoop stresses due to cabin pressure. There was some evidence of fatigue in some areas on the final fracture surface. This likely occurred because of the increased stress. The thin skin must have eventually caused the stress to exceed the tension ultimate capability in at least one area. This aircraft had received a D check one-month before the accident. The inspection instruction required outboard cabin floor panels removal. A proper inspection would most likely have found the corrosion before it became catastrophic.

Corrosion was also present in the lap splices of ALOHA 737 aircraft that had an accident on 28 April 1988. This failure; however was not in the lower lobe of the fuselage as was the August 1981 failure discussed above. The aircraft suffered loss of adhesion causing the stresses to increase at the fastener holes. The knife-edge countersink caused the local stress at the fasteners to further increase. What remained of the skins themselves indicated that the corrosion had not thinned the skins below normal tolerances. Subsequent tests on simulated lap splices without corrosion indicated that the knife-edge was the major influence in the formation of cracks. Corrosion was only a minor factor, if any, in this accident since the environmental effects on the metallic material used for the fuselage skins is small. The accident report [6] issued on 14 June 1989 stated that the probable cause was the failure of the maintenance program to detect the presence of significant disbonding and fatigue damage that ultimately led to failure of the lap joint.

The USAF has had poor experience in the purchase of older aircraft from the commercial market. Some of these were so badly corroded that they could not be economically repaired. The USAF believes the decision by the owners to sell the aircraft exacerbated the extent of corrosion damage in these aircraft. After they made that decision, the aircraft evidently received very little maintenance until the owners could sell them. Under these conditions, it did not take long before the damage from corrosion was so extensive that the USAF had to condemn the aircraft immediately after they were purchased. If the USAF had used the current nondestructive inspection capability at the time of purchase, they would not have purchased these aircraft. Examples such as this highlight the diligence needed in a maintenance program. The owners of these aircraft, up to few years before they sold them, maintained them properly and they were flying in an airworthy condition.

Another major concern is that pitting corrosion may accelerate the onset of widespread fatigue damage (WFD). This is a safety concern since WFD is a condition where the cracks degrade the fail-safe capability of the structure from its original design requirement. This could be a serious concern unless the operators take proper care to use teardown inspections and nondestructive inspections to reveal the problem. The damage tolerance initial flaw requirements as adopted by the USAF in the early seventies are well in excess of the size of defects associated with pitting corrosion. The criterion used by the USAF for damage tolerance design of new aircraft is that the initial flaw will not grow to critical in two design lifetimes. Further, the damage tolerance requirements force the selection of ductile materials that are tolerant to defects. As a further safety measure, the USAF requires that the contractor design the structure such that it is inspectable. This is an advantage, not only for crack detection, but also for corrosion detection. The effects of pitting corrosion; however, could affect the safety of older aircraft that were not designed to the current damage tolerance requirements. Therefore, for these aircraft it is likely that cracks derived from pitting corrosion will need to found by the inspection program. The other concern with pitting corrosion is that it could result in a significant degradation of the durability of the structure and hence shorten its useful life in service. Experiments with specimens exhibiting pitting corrosion show that cracks appear much sooner than otherwise expected. These cracks could degrade the fail-safe capability of the aircraft and consequently precipitate the need for structural modifications. A teardown inspection of high time Boeing 707 wing revealed many significant cracks. These cracks appeared to be predominantly in holes where the manufacturer used steel fasteners. The steel was not protected from the aluminum wing skins and stringers. Consequently, it

These cracks appeared to be predominantly in holes where the manufacturer used steel fasteners. The steel was not protected from the aluminum wing skins and stringers. Consequently, it is likely that pitting corrosion did contribute to the cracking found in this structure. In contrast, the teardown inspection of the C-141 wing structure with wet-installed steel fasteners did not indicate evidence of pitting corrosion. For this aircraft, the steel fasteners were wet-installed. The Federal Aviation Administration (FAA) has sponsored extensive studies in pitting corrosion [7] [8] and corrosion fatigue. The studies show that for bare materials, the cracks nucleated from constituent particles, and for clad materials, the pitting promoted cracking a nearby favorably oriented grain. The work done to date on this subject has led to a good qualitative understanding of the problem and has quantified many aspects of the phenomenon. However, the researchers will not be able to provide a predictive method for the effects of pitting corrosion until sometime in the future.

Hidden corrosion is also a major concern for continuing structural integrity. Hidden corrosion is that corrosion that remains undetected after inspection with the specified method for the area. Based on this definition, the amount of hidden corrosion is dependent of the equipment used in the nondestructive evaluation. It is essential that the maintenance personnel have a clear understanding where they may find corrosion in the structure so that they may use appropriate inspection procedures to find it when it is present. It is also incumbent on the laboratory to develop the inspection equipment to improve the likelihood of detecting corrosion. Since corrosion damage appears to reoccur in the same locations in a population of airplanes, the use of teardown inspections is helpful for locating potential damage. The Oklahoma Air Logistics Center performed a teardown inspection on a KC-135 on an aircraft retired to Davis Monthan Air Force Base in 1991. This aircraft, delivered to the USAF in 1962, had spent twenty-nine years at Mildenhall Air Base in the UK. Therefore, the aircraft saw a severe corrosion environment during its life. The inspection interrogated the structure for cracking as well as corrosion. The USAF found little cracking since the aircraft had only 16,521 flight hours and 2,942 flights. They cleaned the parts and etched them approximately thirty micrometers to enhance corrosion and crack detection. The USAF, for this study, classified corrosion as light if it was less than 25 micrometers, moderate if it was between 25 and 250 micrometers, and severe if it was greater than 250 micrometers. For the fuselage, there was extensive light corrosion in the skin and doubler faying surfaces. They found limited moderate and severe corrosion below the cargo door, lower bilge, and at the spotwelds. None of the fuselage corrosion was severe enough to affect flight safety. For the wing, there was extensive moderate and severe pitting at the steel fasteners in the upper surface. Most of these had not progressed to exfoliation and none was severe enough to affect safety of flight. There were several areas of severe corrosion at the upper wing skin and spar interface. The center section of the horizontal tail suffered from severe exfoliation on the lower spar caps. They also found stress corrosion cracking in the horizontal tail. This inspection is significant in that it provided considerable insight on the extent of corrosion. It also served as an excellent representative aircraft for identifying areas of hidden corrosion that the USAF did not address in previous depot maintenance activities. In addition, it assessed the ability of available nondestructive inspection (NDI) procedures to locate corrosion. However, the NDI community has made significant progress in detecting corrosion since the completion of this work.

Another concern about the affect of corrosion on structural integrity is the affect of corrosion products on stresses in structural joints. Mostly, maintenance personnel will find evidence of this problem in the longitudinal lap splices in the fuselage. The corrosion products are much less dense than the original material and consequently the trapped powder causes the joint to expand. The stresses derived from this expansion are significant. At the lower limit of detectability of joint thinning, the stresses may reach yield. There have been many cases found where the stresses are sufficiently high to cause cracking in the skins. The National Research Council in Canada has studied this problem extensively. They have developed an optical device for detecting this problem on operational aircraft. There is no known case where this problem has caused a catastrophic failure or the onset of widespread fatigue damage. However, the potential is there for the cracks to turn into fatigue cracks and propagate. There is also the possibility that even without cracking the stresses may degrade the fail-safe capability of the structure. The USAF plans to investigate this problem as part of their aging aircraft program.

The potential for stress corrosion cracking to become a fatigue problem is another concern. This seldom happens, but the result can be serious if the maintenance does not find the crack. There is no known case where a stress corrosion crack in an airframe has resulted in a catastrophic failure. The use of 7079-T6, 7178-T6 and 7075-T6 in aircraft designed in the sixties and seventies has led to numerous cases of stress corrosion cracking. In the USAF the C-130, C-141, C-5A and the T-38 are aircraft where stress corrosion cracking is a significant economic burden. The Materials Information Analysis Center performed a study [9] in 1996 and found that 70 out of 115 or 60.9% of the corrosion failures (problems) in C-130 airplanes were attributed to stress corrosion.

The FAA took a firm stand on maintaining safety of corroded aircraft when they issued Airworthiness Directives (AD) against Part 25 and some Part 23 aircraft. These ADs provided guidance to the commercial operators on the amount of corrosion that would be allowed. It has been the policy of the USAF that if corrosion was found it would be removed. This policy has not always been followed because of the cost and the pressure to get aircraft back into service operations.

There is at least one other known case where diligent maintenance defeated a corrosion problem. FAA's Technical Oversight Group for Aging Aircraft (TOGAA) visited Petroleum Helicopter Inc. (PHI) in Layfayette, Louisiana on 27 March 1996. They found that PHI had defeated their corrosion problem resulting from the harsh environment of warm moist salt air associated with flying from the coast to the Gulf of Mexico oil platforms. PHI had earlier experienced the severe corrosion damage that one would expect in this environment. They decided to take matters in their own hands and through careful washing of the aircraft and the use of corrosion prevention compounds reduced the problem to insignificance. It is success stories such as this that should hearten even the most pessimistic about the impending doom associated with corrosion.

Future Corrosion Research and Development

The National Research Council in the United States recently published their findings [10] on USAF aging aircraft. This study sponsored by the Air Force Research Laboratory

(AFRL) identified many research and development activities. Their primary emphasis was in the area of corrosion. In response to this report, the USAF formed the Aging Aircraft Technologies Team (AATT) whose objective is to reduce the maintenance burden for aging aircraft while maintaining long-term safe operations. One of the primary research and development activities of the AATT will be on corrosion.

More recently, a paper [11] given by a member of the AFRL begged the question on when a predictive model would be available for corrosion. Unfortunately, no one appears to posses the strategy to develop such a tool. R. Wei from Lehigh University put this problem in perspective. He said "When we can make a metal specimen corrode in the laboratory in a week, how can we predict what it would look like on an operational aircraft in thirty years."

3 CONCLUSIONS

The dangers from corrosion, fatigue or corrosion fatigue are ever present in operational aircraft. Presently, the largest danger by a considerable margin is economic rather than flight safety. All of the collective experience from both military and commercial operations indicates this to be true. No one can foretell with any degree of accuracy what to expect as both military and commercial aircraft push further into the uncharted waters of aging. Thus far, experience has not indicated that there is "falling off point", as once imagined when there was widespread belief that the world was flat. It is incumbent; however, for the researcher, the engineer and the maintenance personnel to maintain a diligent approach to the problem. They must use all available techniques such as damage tolerance scheduled inspections, ACIs, and assessments for the onset of WFD to help ensure that they maintain the safety of future aircraft operations. Diligent use of CPC's and research into better means of corrosion detection and prevention appear to be the most promising ways to reduce the economic burden of these problems in the future.

4 REFERENCES

1. Lincoln, J.W. "Aging Aircraft - USAF Experience And Actions," Proceedings of the 19th Symposium of the International Committee on Aeronautical Fatigue, 16th Plantema Memorial Lecture, Edinburgh, Scotland, 1997.

2. Wallace, W., Hoeppner, D. W., Kandachar, "AGARD Corrosion Handbook, Volume 1, Aircraft Corrosion: Causes and Case Histories," July 1985

3. Schütz, W., "A History of Fatigue," Engineering Fracture Mechanics, Vol. 54, No. 2, pp. 263-300, 1996.

4. Schütz, W. "Corrosion Fatigue - The Forgotten Factor in Assessing Durability," Proceedings of the 18th Symposium of the International Committee on Aeronautical Fatigue, 15th Plantema Memorial Lecture, Melbourne, Australia, 1995.

5. Cole, G. K., Clark, G., Sharp, P. K., "The Implications of Corrosion with Respect to Aircraft Structural Integrity," DSTO-RR-0102, March 1997.

6. NTSB/AAR-89/03, National Transportation Safety Board Aircraft Accident Report, Aloha Airlines, Flight 243, Boeing 737-200, N73711, Near Maui, Hawaii, April 28, 1988.

7. Wei, Robert P. and Harlow, D. Gary, "Corrosion and Corrosion Fatigue of Airframe Materials," DOT/FAA/AR-95/76, February 1996.

8. Schmidt, C. G., et al, "Characterization of Early Stages of Corrosion Fatigue in Aircraft Skin," DOT/FAA/AR-95/108, February 1996.

9. Mindlin, H., Gilp, B. F., Elliott, L. S., "Corrosion in DoD Systems: Data Collection and Analysis (Phase 1), February 1996.

10. National Research Council, "Aging of U.S. Air Force Aircraft," Publication NMAB-488-2, National Academy Press, Washington, D.C., 1997

11. Paul, C. A. and Mills, T, "Structural Integrity of Aging Aircraft," presented at AeroMat '98, June 1998.

THE EFFECT OF CORROSION ON THE STRUCTURAL INTEGRITY OF COMMERCIAL AIRCRAFT STRUCTURE

Dr Martin Worsfold
British Aerospace Airbus
New Filton House
Filton, Bristol
BS99 7AR, United Kingdom

SUMMARY

The purpose of this paper is to discuss the effect of corrosion on the structural integrity of commercial aircraft wing structure. Data is presented for fatigue specimens tested with corrosion damage and following a spotface repair operation. The data demonstrates that failure initiates earlier from specimens with corrosion damage, when compared to corrosion free specimens, and that the reduction in fatigue life was due to a shortened crack initiation period.

INTRODUCTION

British Aerospace Airbus Ltd has responsibility within the Airbus Industrie consortium for the design, manufacture and in-service support of the wings for all Airbus products. In addition to these activities, British Aerospace Airbus Ltd continues to support the development and operation of BAC One Eleven and Concorde aircraft.

Airbus wings have gained an excellent reputation within the industry for an aerodynamic efficient, lightweight and durable design. To date there are nearly 1800 Airbus aircraft in operation, with 1200 aircraft on order and due to enter service in the near future.

Airbus wings are designed to achieve a Design Service Goal in the order of 20 years. During this period the primary structure is designed to be free from significant fatigue and corrosion damage. Nevertheless, structural problems in the form of accidental damage, corrosion and fatigue do occasionally occur prior to this goal and require repair action.

Although British Aerospace Airbus has not encountered fatigue-cracking problems in the presence of corrosion, the purpose of this study was to assess the effect of corrosion on the structural integrity of aircraft wing structure. Test data is, therefore, presented on the residual fatigue life of a riveted wing skin/stringer component with existing corrosion damage and following a repair action.

WING BOX STRUCTURE

Airbus wings are manufactured in the three main components that comprise the centre wing box, the port and starboard outer wing sections. Current practice is to fabricate the outer wing box structure from separately machined spars, ribs and skin/stringer panels. Figure 1 presents a schematic layout of the outer wing structure.

Paper presented at the RTO AVT Workshop on "Fatigue in the Presence of Corrosion", held in Corfu, Greece, 7-8 October 1998, and published in RTO MP-18.

Wing skin panels are machined from aluminium alloy plate to include detailed design features such as manhole apertures, stringer runout pads and local reinforcements. Skin and stringer details are currently riveted together in an automated process to produce the wing skin panel assembly. During final assembly these panels are mounted and attached to interfacing ribs and spars to form the wing box structure. The stringers are generally machined to shape from extruded section.

High strength aluminium alloys are used extensively in the wing structure and account for more than 75% of the total wing weight. Experience has shown that the alloys and tempers listed in Table 1 offer adequate resistance to corrosion damage and fatigue cracking.

Table 1. Aluminium alloys used in Construction of Current Airbus Outer Wing Box Structure.

Component	Aluminium Alloy
Upper Skin	7150-T651
Upper Stringers	7150-T6511
Lower Skin	2024-T351
Lower Stringers	2024-T3511
Front Spar	7010-T7651
Rear Spar	7010-T7651
Ribs	7010-T7651

CORROSION EXPERIENCE

British Aerospace Airbus wings are protected from the environment and the aggressive fluids used in the aircraft by a range of efficient protective treatments. Special attention is given to areas of potential contamination, high condensation and where different metals may contact.

Current experience indicates that British Aerospace Airbus protective treatments perform well. When corrosion does occur it is usually due to the local breakdown of the protective treatments (by chipping, fretting or abrasion), causing the underlying material to be exposed and damaged. Most corrosion findings are relatively minor and occur at the site of structural discontinuities, i.e. fastener holes and panel edges. The usual repair method is to mechanically remove the corroded material by grinding or spotfacing, which is then followed by the re-application of the surface protection.

Experience has also shown that the dry bay regions of the wing are subject to relatively mild corrosive conditions. More severe corrosive conditions are found in the wet bay regions (such as the main landing gear bay), on the exterior aerodynamic surfaces and in the integral wing fuel tanks. In these areas the structure can be exposed to heavy condensation, water spray and contamination, leading to a particularly aggressive cyclic "wetting and drying" environment.

British Aerospace Airbus has had recent experience of corrosion at fastener holes on the outer wing box structure. It is a problem that has occurred on only a few Airbus aircraft and has been reported to affect other aircraft types and manufacture.

The corrosion is generally restricted to a small area of the upper wing skin panel, where the damage occurs in the form of intergranular corrosion at the countersink of fastener holes, as shown in Figure 2.

The problem is caused by the breakdown of the protective treatments around the fastener head. Corrosion damage may then occur if the riveting process fails to develop an intimate fit between the rivet head and the countersink hole. Rivets with large head gaps can allow moisture to ingress and attack the unprotected countersink area. For manufacturing reasons surface protection can not be applied to the countersink areas during the riveting process.

The material used in the construction of the upper skin/stringer panels is the aluminium alloy 7150, in the peak aged T651 condition. This is basically a heat-treated high strength - high purity aluminium zinc magnesium copper alloy containing small additions of zirconium.

FATIGUE EXPERIENCE

In 1984 a study performed by the National Research Council of Canada reported on the fatigue initiation sites for fixed wing aircraft accidents, Ref 1. The percentage occurrence of fatigue at different types of initiation site is shown in Table 2. The main initiation sites were found to be threaded fasteners such as a bolt, stud or screw and holes such as those for fasteners.

Fatigue findings on British Aerospace Airbus wing structure has also included fatigue cracks at major fastener attachment holes, water drain valves, manhole apertures, stringer runouts and structural joints. As a result, considerable effort is made to minimise the occurrence of fatigue at fastener holes. This can be achieved with both careful attention to detailed design and the use of life improvement techniques, such as interference fit fasteners and hole cold expansion.

Table 2: Initiation Sites for Fixed Wing Accidents.

Initiation Site	%
Bolt, stud or screw	24
Fastener hole or other hole	16
Fillet, radius or sharp notch	13
Weld	12
Corrosion	10
Thread (other than bolt or stud)	7
Manufacturing defect	6
Scratch, nick or dent	6
Fretting	3
Others	4

CORROSION/FATIGUE EXPERIENCE

There are basically two ways in which a corrosion/fatigue interaction can occur:

Type 1: Corrosion-fatigue.

Corrosion-fatigue may occur under the conditions of simultaneous corrosion and cyclic loading. The potential loss in structural integrity being greater than the additive effects if each is considered either separately or alternatively.

British Aerospace Airbus has not encountered corrosion-fatigue problems on aircraft wing box structure. It is currently thought that corrosion-fatigue problems do not occur because the protective treatments perform well, while the normal operating environment does not favour the development of a corrosive-fatigue mechanism.

This is due to the fact that in flight the low atmospheric temperature and partial pressure limits the development of a corrosion mechanism on the external wing surfaces. Whereas parked on the ground, the absence of in-flight loads will limit the development of a fatigue mechanism, even though the local conditions may indeed be corrosive.

Type 2: Fatigue in the presence of existing corrosion.

British Aerospace Airbus has not encountered fatigue problems in the presence of corrosion. Nevertheless, recent experience with corrosion at fastener holes has shown the potential for such a mechanism. The purpose of this study was to quantify the effect of corrosion on the residual fatigue life of a wing skin/stringer component.

TEST PROGRAMME

An upper wing skin panel of the high strength aluminium alloy 7150-T651 was obtained with representative intergranular corrosion at the countersink of several fastener holes. The original fasteners and stringers were removed and the panel was subjected to a non-destructive examination by C-Scan, to determine the location and extent of the corrosion damage. The following types of fatigue test specimen were selected from the panel:

Type 1: Corrosion free - the first set of specimens which were nominally free of any corrosion, were required to define a baseline fatigue life for comparison purpose. Figure 3 shows the geometry (in inches) of the dog bone specimen selected for this study. In total six specimens of each type were tested.

Type 2: Corroded - these specimens were extracted from areas of the panel known to exhibit corrosion.

Type 3: Spotfaced - in these specimens the corrosion was removed by a spotfacing operation applied to the outside face of the specimen. The spotface depth used in this study was approximately 40 percent of the original skin thickness.

The two sides of the specimen were identified as the 'outside face', corresponding to the aerodynamic surface of the top skin, and the 'inside face', to which the stringers were originally attached. To achieve a standard thickness for each specimen, material was removed from the inside face. The existing stringer holes were drilled and reamed and filled with interference fit 5/16" countersunk bolts, or 5/16" pan head bolts in those holes that were spotfaced.

The specimens were then subjected to constant amplitude fatigue cycling at a nett mean stress of -66 MPa and a nett alternating stress of 132 MPa. This loading cycle was selected as it was considered to be representative of the in-service conditions.

Crack detection gauges were attached to the machined face of each specimen at a distance of 5mm from the edge of the fastener holes. The test was interrupted when a crack gauge was ruptured. The specimen was finally subjected to non-destructive examination by Rototest and surface scan eddy current techniques, along with ultrasonic inspection for detection of the corrosion.

TEST RESULTS

The results of this study are summarised in Table 3. The data indicates that both the corroded and repaired test specimen show a 60% reduction in fatigue lives when compared to the corrosion free specimens.

Table 3: Mean fatigue Lives of Test Specimens.

Specimen Type	Mean Fatigue Life (Cycles)
Corrosion free	793940
Corroded	310868
Spotfaced	335421

Examination with low magnification optical microscope showed that crack initiation in the corrosion free and spotfaced specimens was generally on the inside face of the specimen, which had been machined prior to testing. In contrast, the corroded specimens were seen to initiate cracks from areas of corrosion on the outside face of the specimens. The surface defects observed in the corrosion free specimens were not very deep, and appeared to originate from the concentric scoring caused by the fastener.

A scanning electron microscope (SEM) was used to examine the striations on both the corrosion free and corroded specimens, to estimate the average fatigue life of the 5mm fatigue failure. The rates confirmed that following initiation the cracks propagated at similar rates for both types of specimen, giving an average approximate figure of 6000-7000 cycles for a crack to reach 5mm. The growth rate for a striation averaged approximately 1 micron per cycle.

Chemical analysis using a SEM Electron Dispersion Spectrometer (EDS) detector was performed on a number of small corrosion fragments. A number of strong emission peaks were obtained for S, P, Cl and Zn. The presence of these elements in the corrosion product is normal and would suggest exposure to an aggressive environment.

DISCUSSION

The results of the visual inspection indicated that the fatigue cracks generally initiated from the tip of the corrosion flaws. It was clear that the initiation sites were greatly influenced by the shape and orientation of the in-plane corrosion flaws. Also, given the localised nature of the attack, it is reasonable to assume that the material losses from the corrosion process were relatively small.

Further analysis has shown that the reduction in the fatigue life of the spotfaced specimens was due to an increase in stress concentration at the fastener hole. This increase in stress concentration results from the spotface geometry and the loss of local skin thickness at the fastener hole. These effects combine to shorten the fatigue initiation period and the subsequent crack growth to failure. The conclusion to be drawn from these results is that the corroded and spotfaced specimens failed coincidentally at similar fatigue lives.

The short fall in the fatigue life of the corroded specimens can be attributed to a 60% reduction in the fatigue crack initiation period. The short fall in the fatigue life of the spotfaced specimens was due to the increase in stress

concentration associated with the repair operation.

The results of this study are also in broad agreement with the work of Cook who examined fatigue crack initiation and crack growth in 7010-T7651 material, Ref 2. In this work the mean fatigue lives of the corroded material were approximately 30% of the mean fatigue lives of the corrosion free specimens, i.e. 70% reduction in fatigue life. Furthermore, the mean initiation period for the corroded specimens was approximately 25% of that for the corrosion free specimens.

Static compression tests on corrosion free, corroded and spotfaced skin/stringer specimens has also shown that the corrosion has little impact upon the strength of upper skin panels with regard to local instability and wrinkling modes of failure. The corroded achieved 98% and the spotfaced specimens achieved 90% of the strength of the corrosion free specimens. The spotface result being consistent with the loss in area resulting from the spotfacing operation and the consequent rise in stress level.

CONCLUSION

The repair of corrosion and fatigue damage is an expensive and unwanted maintenance burden on the operator. In order to reduce this burden, British Aerospace Airbus is continuing to learn the in-service lessons and, are using this experience to develop the Airbus product.

British Aerospace Airbus is also engaged in a wide-ranging programme of research to develop alternative protection treatments, and to assess new aluminium alloys/tempers. The objective of this research is to develop environmentally friendly processes and generate the engineering data and understanding required for the selection of new materials for future aircraft projects.

Initial data for exfoliation corrosion tests of new high strength aluminium alloys indicates that greater resistance to corrosion can be achieved without penalty to fatigue or static strength, Table 3.

Table 3: Summary of Accelerated Exfoliation Tests in ANCIT Solution at 25°C for 96 Hours.

Aluminium Alloy	Rating	Max. Loss (mm)
7150-T6511	EC	0.51
7150-T77511	EA	0.03
7055-T77511	EA	0.05

Activity is also progressing in the development of new manufacturing methods that can offer enhanced structural performance in wing box design. Areas of interest include advanced carbon fibre composites and novel welding technologies. These manufacturing routes offer the possibility of using more corrosion resistant materials and may eliminate the need for potentially damaging stress-raising fasteners.

In conclusion, the work described in this paper has demonstrated that even if corrosion should initiate, long fatigue lives are achievable in corrosion damaged and repaired structure. Continued structural integrity can therefore be achieved with careful attention to detailed design, material selection, manufacture and corrosion control.

REFERENCES

1: Campbell, G. S. & Lahery R. *"A Survey of Serious Aircraft Accidents Involving Fatigue"*. Int. J. Fatigue, Vol. 6, No 1 – January 1984.

2: Cook, R. "*Deteriorating effects – Experiment conducted at DERA"*. Task 4 – Sub Task 4.2, SMAAC-TR-4.2-07-1.3/DERA, (1998)

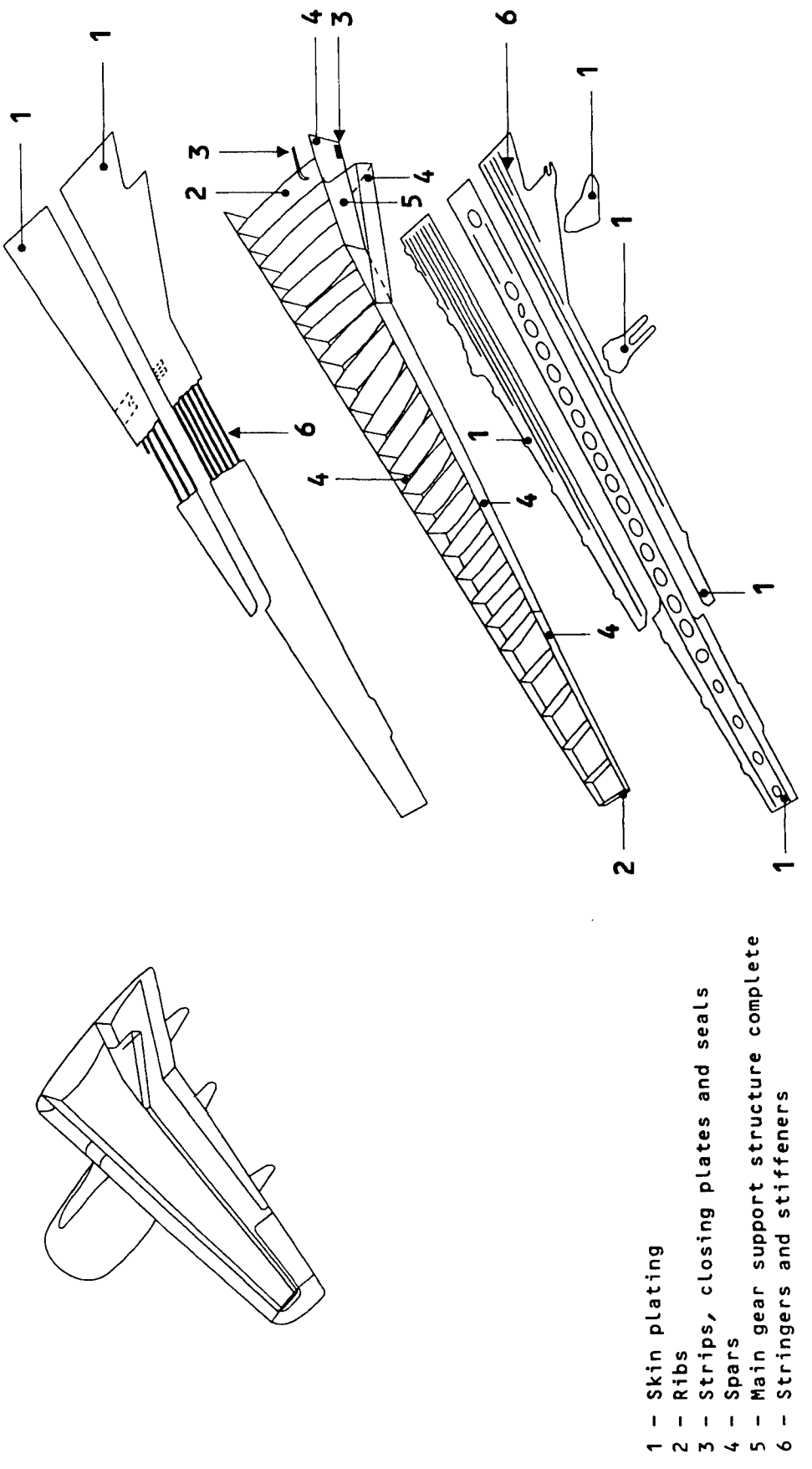

Figure 1: A Schematic Layout of a British Aerospace Airbus Outer Wing Structure.

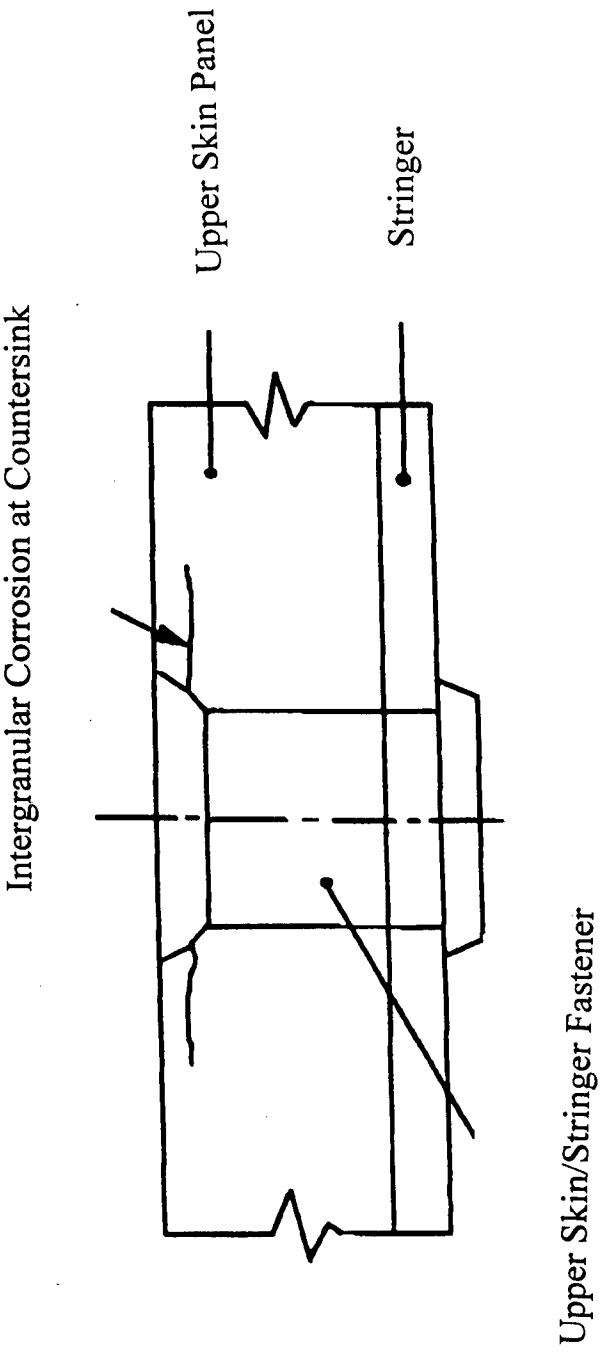

Figure 2: Intergranular Corrosion at the Countersink of Fastener Holes.

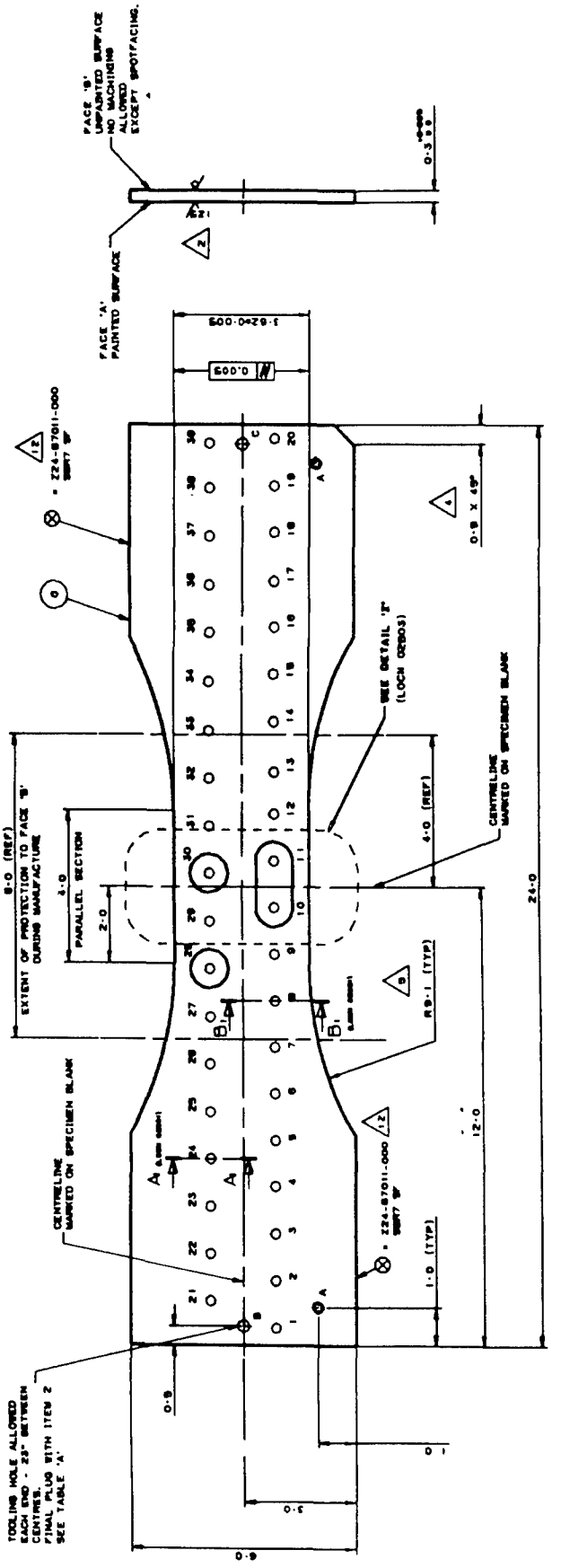

Figure 3: Geometry of the Dog Bone Fatigue Specimen selected for the study.

AGING AIRCRAFT: IN SERVICE EXPERIENCE ON MB-326

Capt. Mario Colavita
Capt. Enrico Dati
Lt.Col. Giovanni Trivisonno
Chemical-Technological Department of D.A.S.R.S. - Italian Air Force -
Aeroporto Pratica di Mare, Italy I-00040

1. INTRODUCTION

In 1996 started an European research project on Structure Maintenance of Aging Aircraft (SMAAC) where a consistent number of partners decided to cooperate in order to offer an answer to this problem.
The first purpose of the research project was joining the In-Service Experiences that allow to relate all structural and chemical degradation induced by corrosion to the potential interactions with fatigue.
Italian Air Force (IAF) and AerMacchi decided to carry out a tear-down inspection on a 30 years old Macchi MB-326, a small trainer aircraft, having 4685 flight hours with respect to 5979 safe life hours.
For this purpose the chosen test articles were fuselage center section, tailplane, wings, and front fuselage. The first two of them were investigated at the Air Force laboratories and the other ones at the AerMacchi research department. Particular attention was focused on the components subjected to the high stress and potential corrosion in areas not accessible during routine servicing.

2. EXAMINATION

The test articles, except the wings already available by Aermacchi, were chosen in the Air Force hangar in Capodichino, in accordance to the following requirements:
- high safe life spent;
- the test articles had not been modified or replaced during the aircraft service life;
- good conservation state.

The used procedure for the examination can be summarized in nine phases:
1. Photographic and video documentation of the items as received and in every steps of inspection.
2. Tear-Down of structural components.
3. Visual inspection and Non Destructive Testing (NDT) on the test articles before panels removal.
4. Remove rivets, Deutsch fasteners, bolts and screws as necessary.
5. Cleaning and paint removal as necessary.
6. Visual inspection inside the items and NDT of the critical areas.
7. Check of bolts and holes of the attach fittings.
8. Break open critical areas and holes as necessary.
9. Examine critical areas with the aid of a low-powered microscope.

2.1. FUSELAGE CENTER SECTION

The fuselage center section is a two beams metallic structure, separated by three magnesium alloy spacers and connected to the wings by two attachment lugs each side. Two aluminum alloy panels cover the center section rear and front sides.

2.1.1. Magnesium Spacers, Port and Starboard

The spacers of the fuselage center section were inspected before the removal of the aluminum sheet covering the center section.
Below, the results of the radiographic inspection are presented:

Item	*Material*	*Method of examination*	*Results*	*Comments*
Spacer Port	magnesium alloy (AZ91 C)	radiographic and visual inspection	Nil cracks found	severely corroded
Spacer Starboard	magnesium alloy (AZ91 C)	radiographic and visual inspection	Nil cracks found	severely corroded

After de-skinning, the external spacers, in magnesium alloy AZ91 C, were found severely corroded, as visible in Figg. 1-2.

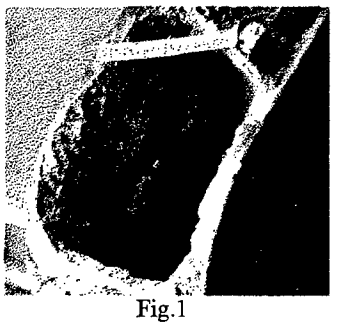

Fig.1

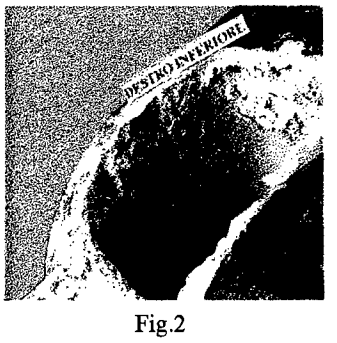

Fig.2

The corrosion distribution was not symmetrical and appeared concentrated on the lower part more than on the upper one, both cases especially on the rear surface.
Metallographic inspection revealed the galvanic nature of the corrosive attack (Fig. 3) produced by the moisture penetrated between the spacers and the steel beams. Geometrical shape explains the corrosion pattern.
In the past this corrosion problem was already found, and AerMacchi carried out a study to evaluate its effect on the static and fatigue life of the entire center section[1].

Paper presented at the RTO AVT Workshop on "Fatigue in the Presence of Corrosion", held in Corfu, Greece, 7-8 October 1998, and published in RTO MP-18.

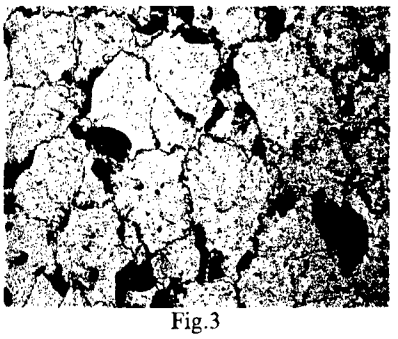

Fig.3

Using three different corrosion development phase models (Fig. 4) and a detailed Finite Element Modeling, it was stated that:

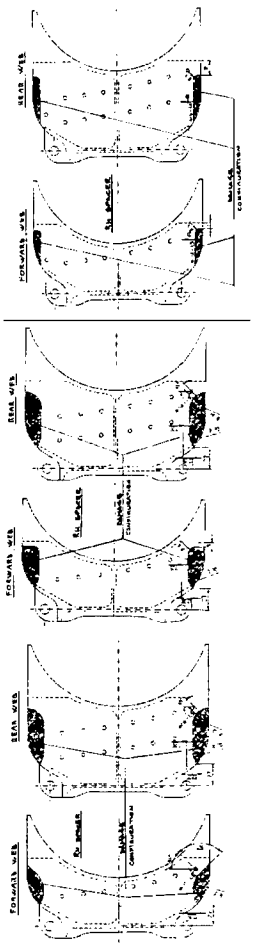

Fig.4

- there is no reciprocal influence between lower and upper damage;
- maximum permissible damage is as for 1st corrosion model (lower and upper part).

2.1.2. Center Section lower beam holes

The critical holes of the lower beam were investigated by means of Magnetic Rubber inspection (MRI). No hole was found cracked.

2.2 TAILPLANE

Major focus in analyzing the MB-326 tailplane was given to the stabilizer.

The tailplane was at first visually inspected after cleaning and washing, to discover defects or corrosion on the skin and near the screws and rivets.

Then the stabilizer was separated from other components.

2.2.1. Stabilizer

The MB 326 stabilizer is a typical aluminum alloy two spars structure, having printed ribs, skins and lugs.

The entire stabilizer was exposed to radiographic inspection to detect any preliminary defect on the main spar, consisting of an upper and lower L-shaped extruded caps joined by a web with self-aligning Hi-Locks.

No defect was found and then it was de-skinned and all the fasteners drilled out.

a. Spar

The central section of the upper spar cap considered to be the most stressed region, was cut and the dark green coat stripped by means of plastic media blasting method.

All the holes were subject to visual inspection and the whole central region submitted to ultrasonic inspection in order to determine if it was affected by Stress Corrosion Cracking (SCC). The C-scan obtained didn't reveal any presence of SCC.

Further, several holes were broken and inspected under a low-powered microscope: no crack propagation was found.

The microstructure of the extruded 7075-T6 alloy appeared regular, with grains typically elongated in the extrusion direction.

In the past, the Australian Aeronautical Research Laboratory investigated some MB-326 tailplanes[2]. In that occasion a small number of shallow fatigue cracks and a significant number of fastener holes containing SCC was found. The SCC seems to initiate in the bores of the fastener holes (mainly in their lower half) at corrosion pit sites. The growth pattern is unusual and due to the cracks' preference to follow the circular-shaped metal flow induced by the extrusion process of the cap.

In order to detect these defects, just a de-skinning approach to permit ultrasonic inspection along the aft side face of the cap was in some degree successful.

b. Elevator Hinge Brackets

The tailplane of aircraft MB 326 consists of four elevator hinge brackets, two on the starboard side and two on the port side, which were investigated for fatigue failure.

Item	*Material*	*Method of examination*	*Results*	*Comments*
Inboard Starboard	aluminum alloy extrusion	eddy currents and penetrant test	Nil cracks found	
Outboard Starboard	aluminum alloy extrusion	eddy currents and penetrant test	Nil cracks found	
Inboard Port	aluminum alloy extrusion	eddy currents and penetrant test	Nil cracks found	Corrosion initiated
Outboard Port	aluminum alloy extrusion	eddy currents and penetrant test	Nil cracks found	
Bolts and nuts	steel	magnetic particle testing	crack on a bolt head	mild corrosion

Bolts and nuts were also investigated and a crack on the head of a bolt was discovered, Fig. 5.

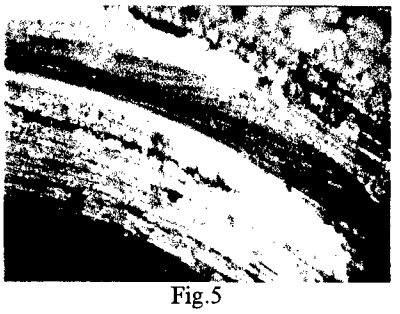

Fig.5

In the past[3] occurrence of fatigue failure on the elevator hinge bracket was related to intergranular corrosion acting as the initiating mode for major cracks. Other fatigue cracks were found at the inner radii of the two elevator lugs[4].

c. Stabilizer - torque tube bolts and nuts

All the bolts and nuts that keep the torque tube joined to the stabilizer were inspected.

Item	*Material*	*Method of examination*	*Results*	*Comments*
Bolts	steel	magnetic particle testing	bolt thread cracks	——
Bolts and Nuts	aluminum	penetrant test	cracks on the thread of four bolt	all nuts corroded

Some aluminum bolts shows cracks propagated on the thread, Figg. 6-7.

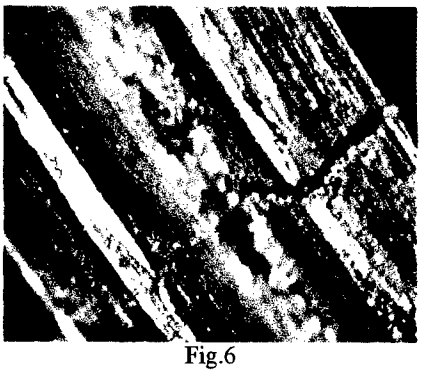

Fig.6

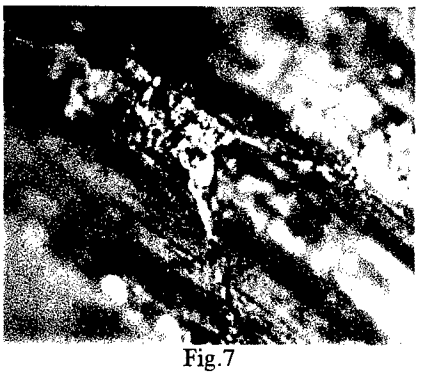

Fig.7

d. Front Stabilizer-to-Fuselage Attach Fittings

After the removal of the lugs, holes and bolts were investigated.

Item	*Material*	*Method of examination*	*Results*
Attach fitting starboard	aluminum alloy	eddy currents	Nil cracks found
Attach fitting port	aluminum alloy	eddy currents	Nil cracks found
Bolts	steel	magnetic particle testing	Nil cracks found

e. Rear Stabilizer-to-Fuselage Attach Fittings

Item	*Material*	*Method of examination*	*Results*
Attach fitting starboard	aluminium alloy	eddy currents	Nil cracks found
Attach fitting port	aluminium alloy	eddy currents	Nil cracks found
Bolts	steel	magnetic particle testing	crack on a bolt head

2.1.2. Elevators

a. Upper and lower skin

After cleaning and washing elevators were at first visually inspected to discover defects or corrosion on the skin and near the screws and rivets.

Item	*Material*	*Method of examination*	*Results*	*Comments*
Upper skin	aluminum alloy	visual inspection	Nil cracks found	mild corrosion around the screws
Lower skin	aluminum alloy	visual inspection	Nil cracks found	mild corrosion around the screws

b. Balance Tabs

The magnesium alloy Balance Tabs were investigated using radiography and severely corroded areas were found near the edge.

After panel removal visual inspection confirmed the presence and the extension of the corroded areas; metallographic inspection revealed the exfoliation nature of the selective attack and gave a measure of the corrosion depth.

On both tabs deep corrosions below the hinge were also found by means of visual inspection (Fig. 8).

Fig.8

In these cases corrosion was generated by galvanic coupling with tinplated copper wires used for grounding.

Item	*Material*	*Method of examination*	*Results*	*Comments*
Balance Tabs	AZ 91C Magnesium alloy	radiographic and visual inspection	Nil cracks found	Severely Corroded areas

2.3 FRONT FUSELAGE

The pressurized cockpit section between the front and the rear bulkhead is a multi-stringer metallic structure where two spars on both left and right sides transfer the canopy pressure loads to the fuselage structure.

Item	*Material*	*Method of examination*	*Results*	*Comments*
Skin	Alclad 2024-T6	visual inspection	Nil cracks found	no defect
Frame	Alclad 2024-T6	visual inspection	Nil cracks found	no defect
Lh spar	Alclad 2024-T6	visual inspection	Nil cracks found	no defect
Housing canopy lug	AZ91 C magnesium alloy	visual inspection	Nil cracks found	Corrosion

Here following the most critical expected areas are reported:

- Front and rear bulkheads;
- Cockpit floor;
- Cockpit spars;
- Lateral frames and frames to spar joint;
- Skin to frames lap joint and splices;
- Longitudinal stringers to skin and frames connection.

The preliminary inspection results indicated corrosion on the Magnesium alloy casting (AZ91 C) housing canopy lug.

2.4 WINGS

The MB 326 wing is a typical two spars metallic structure, with tip tank configuration and main landing gear bay. No fuel tanks are placed inside.

The wing root joint is a triple point lug: the upper and lower lugs at the front spars sustain wing bending loads, vertical shear loads and wing torque; the single lug at the auxiliary rear spar withstands only wing vertical shear loads and torque.

The most critical expected areas are:

- upper and lower spar caps and webs;
- ribs;
- longitudinal stringers;
- main landing gear supports;
- skin-stringers lap joints;
- angular brackets.

On the next table just inspection results [5] relative to defect items are reported.

Item	*Material*	*Method of examination*	*Results*	*Comments*
♦ Main wing root lugs (Rh-Lh)	4340 steel	visual inspection	Nil cracks found	Corrosion Superficial
♦ Bolted joints between ♦ Lower main lugs (Rh-Lh) and spar caps	4340 steel 7075-T6	visual inspection visual inspection	Nil cracks found	Pitting Corrosion Fretting Corrosion
♦ Bolted joints between front web and spar cap in the wing root area Lh	7075-T6	visual inspection	Crack starting at rivet hole	————
♦ Rear wing root lugs (Rh-Lh)	2014-T6	visual inspection	Nil cracks found	Corrosion Superficial
♦ Fitting between rear spar and T.E. structure in the wing root area (Rh-Lh)	AZ91 C Magnesium alloy casting	visual inspection	Nil cracks found	Corrosion
♦ Rib angle fittings on front & rear spars (MLGB area) (Rh-Lh)	AZ91 C Magnesium alloy casting	visual inspection	Nil cracks found	Corrosion
♦ Tip tank front fuel duct (Rh-Lh)	AZ91 C Magnesium alloy casting	visual inspection	Nil cracks found	Corrosion
♦ Main landing gear pivots fittings (Rh-Lh)	AZ91 C Magnesium alloy casting	visual inspection	Nil cracks found	Corrosion
♦ MLG bay wing rib	2024-T42	visual inspection	Nil cracks found	Exfoliation

After the completion of the NDT activity, a fatigue test was carried out on the front spars in order to study the development of the Multiple Site Damage (M.S.D.); the test articles are is summarized as follows:

Test Article	Material
RH WING MAIN SPAR	
Wing Upper Attachment Fitting	AISI 4340
Wing Lower Attachment Fitting	AISI 4340
Upper Spar Cap	AA7075-T6
Lower Spar Cap	AA7075-T6
LH WING MAIN SPAR	
Wing Upper Attachment Fitting	AISI 4340
Wing Lower Attachment Fitting	AISI 4340
Upper Spar Cap	AA7075-T6
Lower Spar Cap	AA7075-T6

Steel Front Center Section for Spars Connection (MB-339A Rejected Item)
Outboard Aluminum Lug for Hydraulic Jack (Tip Lug)
Rear Beam for Strut to Spar Joint
Wing Root Dummy Rib for Correct Torque Realization
Strut Linking the Spar Mid Point with Rear Beam
Adapter for Center Section - Wing Spar Attachment Fitting Connection

Both spars, having 4900 flight hours, i.e. 90% of safe life, were symmetrically loaded in accordance with a quite severe training use.

The test spectrum of the load factor (Nz) was a flight by flight spectrum type constituted by 35967 load steps, representing 200 flight hours and the occurrences are shown in Fig.9. Five strain gages (E_1-E_5) were located on both spars (Fig 10); E_1 and E_2 were used in order to calibrate the stress spectrum.

Peak g-Level																						
-2.76	0																					
-2.24	0	0																				
-1.71	0	0	0																			
-1.19	0	0	0	0																		
-0.66	0	0	80	695	0																	
-0.14	0	0	0	0	2225	0																
0.39	0	0	0	0	0	0	0															
0.92	0	0	0	0	0	215	0	0														
1.44	0	0	0	0	0	45	2420	0	0													
1.97	0	0	0	0	0	45	20245	0	0	0												
2.49	0	0	0	0	5	130	6855	13735	0	0	0											
3.02	0	0	0	0	5	140	2895	3030	3205	0	0	0										
3.54	0	0	0	30	40	440	3535	2535	2390	2500	1415	0	0									
4.07	0	0	0	50	80	425	2945	1480	1095	710	870	1270	780	0								
4.59	0	0	10	95	110	350	2175	775	345	305	200	235	1020	245	0							
5.12	0	0	5	125	85	460	1465	270	160	60	60	60	85	250	100	0						
5.65	0	0	15	200	105	315	580	90	20	10	10	10	15	35	70	15	0					
6.17	0	0	40	180	50	135	135	20	10	0	0	0	5	0	5	20	5	0				
6.70	0	0	35	80	15	15	10	0	0	0	0	0	0	0	0	0	10	0	0			
7.22	0	5	15	15	0	0	0	0	0	0	0	0	0	0	0	0	0	0	0	0		
7.75	0	10	0	0	0	0	0	0	0	0	0	0	0	0	0	0	0	0	0	0	0	
8.27	0	0	0	0	0	0	0	0	0	0	0	0	0	0	0	0	0	0	0	0	0	0
Trough g-Level	-2.76	-2.24	-1.71	-1.19	-0.66	-0.14	0.39	0.92	1.44	1.97	2.49	3.02	3.54	4.07	4.59	5.12	5.65	6.17	6.70	7.22	7.75	8.27

Fig.9

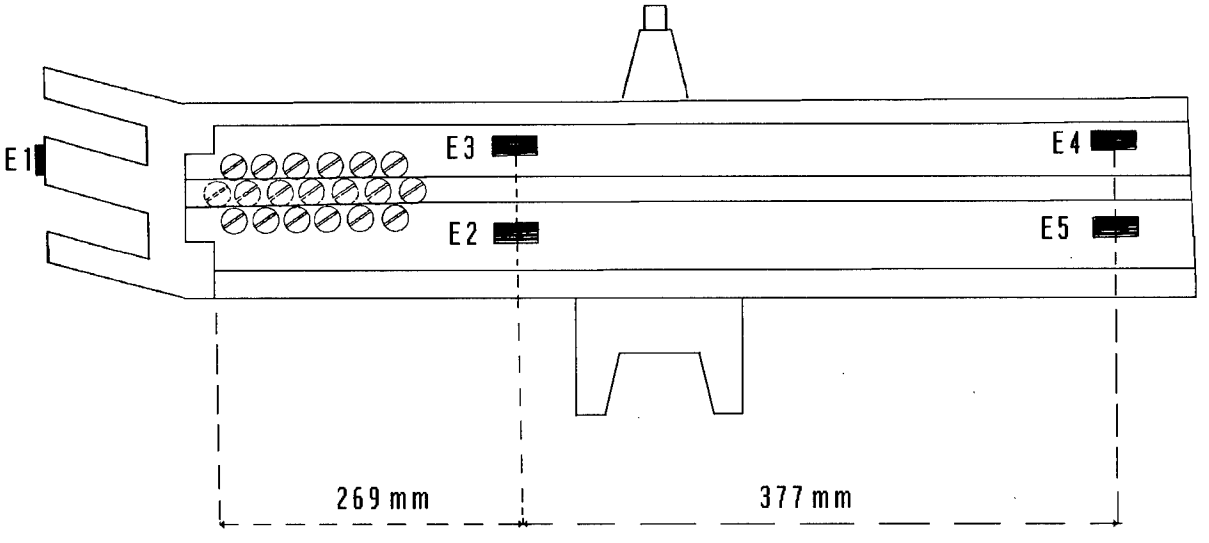

Fig.10

From 0 to 3000 SFH (Simulated Flight Hours) a stress/Nz value of 1.9 Kg/mm^2 were adopted, while over 3000 SFH this value was fixed in 2.5 Kg/mm^2.
The Non Destructive Inspections planned during the test are reported in the following schedule:

SFH	TYPE	AREAS TO BE INSPECTED
At Start	NDI and Visual	• Dye Penetrants on Wing Attachment Fittings • Eddy Currents on Spar Caps Flanges • Visual on Spar Webs • Eddy Current on Main Landing Gear to Spar Bolts Holes
Each 500	Detailed Visual	• Boroscope inside Rear and Front Flanges Box • Wing Attachment Fittings Lugs
Each 1000	NDI and Visual	• Spar Caps Flanges • Main Landing Gear to Spar Bolts Holes • Wing Attachment Fittings Lugs Bores and Corners

The failure occurred at 5032 SFH concerns the sections corresponding to the first two bolts rows of the RH lower Wing Attachment Fitting (Fig. 11). This area was not inspectable during the test but some defects were detected after 2000 SFH on both spars at the lower cap front ligaments corresponding with the rivet hole n° 7.

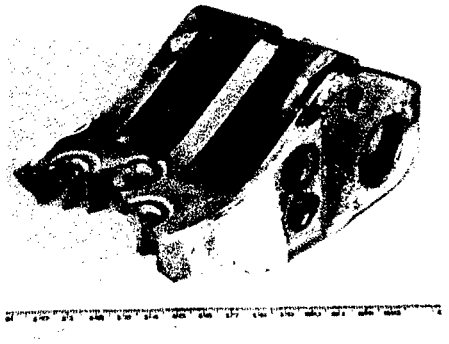

Fig.11

The stress direction shows a slant (plant view) equal 3 degrees which introduce a stress transversal component. It makes the rear side the most stressed one; considering the side view the same situation can be found and in this case the stress level is higher at the lower surface of the Wing Attachment Fitting.
These stresses caused the appearance of a crack on the lower surface of the first row, initiated on the rear side. This crack generated more stresses on the near bolts row which propagated more quickly. The failure occurred when this Multi Side Damage reached the critical extension.

After the RH spar failure the fatigue test has been continued on the left one introducing the following artificial defects on the lower spar cap:

LOCATION	ACTION
Front Lower Spar Cap and Web	• Four rivets have been removed • 2 mm long artificial cracks (saw cut) have been introduced on each side of the hole - downward and upward
Rear Lower Spar Cap	• One rivet has been removed • A defect simulating a bad drilling has been introduced
Main Landing Gear Pivot to Spar Bolt Hole	• A saw cut -25 mm long - has been introduced at the lower bolt hole along the direction of the leading edge

The test, still on going, restarted with a dummy RH spar installed on the rig.

3. CONCLUSIONS

The tear-down activity gave useful information about the good conservation of the thirty years old aircraft observed structures.
The most interesting corrosion event has concerned the spacers of the center section fuselage and its effect on the fatigue and static load on the entire region.
No cracks were found on the main spar of the stabilizer and this phenomenon appeared very different from what has been experienced in the Australian previous investigation activity where SCC often occurred: differences in environmental effects and applied loads could explain this discrepancy.
The fatigue test carried out on the aged main wing spar gave information about the development of Multi Side Damage on the Wing Attachment Fitting in accordance with the expected stress profile.

ACKNOWLEDGMENTS

Authors wish to thank S. Peyronel, R. Martelli and G. Cattaneo from AerMacchi for their helpful discussions.

REFERENCES

1. Report AerMacchi N°560/MB-326H/021, 1995.
2. N. Athiniotis, "Defect Assessment & Failure Analysis Report N° 73/93", 17 September 1993.
3. N. Athiniotis & S. A. Barter, ARL letter report N° M48/90, "Failure of a Macchi Elevator Hinge Bracket", 20 August 1990.
4. S.A. Barter, N.Athiniotis, B.C. Bishop, G.C.S. Booth, "Defect Assessment & Failure Analysis Report N° 35/93", 3 May 1993.
5. V. Bossini, "Brite-Euram Document N° SMAAC-WP-1.3-01-1.3/AEM", May 1997.

LOCAL STRESS EFFECTS OF CORROSION IN LAP SPLICES

J. P. Komorowski
N.C. Bellinger
R. W. Gould
Institute for Aerospace Research
National Research Council
Building M14, Montreal Road, Ottawa ON Canada K1A 0R6
Email: jerzy.komorowski@nrc.ca

1. SUMMARY

Corrosion pillowing in fuselage joints has been modelled using finite element techniques and close-form solutions and shown to result in very high stress, which may lead to non-surface breaking high aspect ratio cracks. These cracks have been identified in a number of transport aircraft. Fractographic studies identified intergranular corrosion and in some cases fatigue striations at the crack front. Corrosion may have a greater impact on the structural integrity of joints than previously recognised and may require durability and damage tolerance reassessments including corrosion damage scenarios.

2. INTRODUCTION

The late 80's and early 90's saw the introduction and updating of Corrosion Prevention and Control Programs (CPCP) for all transport aircraft. These programs were deemed to be so effective that corrosion in aircraft was regarded by some as being brought under control, an economic problem but not a safety issue (Ref 1). The Federal Aviation Administration discontinued the funding of aircraft corrosion related research in 1996. Aircraft manufacturers who were showing significant corrosion related maintenance cost reductions in newer models due to better corrosion prevention measures (Ref 2) apparently supported these views.

The CPCPs are based on visual inspections for corrosion and as was shown by Akindez et al. (Ref 3) are not adequate for the case of hidden corrosion. They showed that severe corrosion was accidentally discovered within a year of a major maintenance activity (D Check). Their conclusions represent a significant departure from the views described above. Essentially, they indicted that NDI systems will have to be deployed to detect hidden corrosion and expressed concern that corrosion may have more significant impact on structural integrity than previously recognised. It should be noted that all Durability and Damage Tolerance (DADT) assessments have been conducted assuming that structures are free of corrosion damage.

This new position corroborates recent studies supported by United States Air Force Corrosion Programs Office, which will be presented by Kinzie at this workshop (Ref 4). Modelling efforts relating corrosion damage such as pitting and surface morphology to stress or stress intensity factors (Brooks et al. (Ref 5) Perez et al. (Ref 6) also supports it. Work at the National Research Council of Canada (NRCC), which has demonstrated the significant impact of corrosion pillowing on the structural integrity of lap joints, will be summarised in this paper.

3. MODELING CORROSION PILLOWING STRESS

Fuselage joints have two basic forms, lap or butt splice. There are many differences among these two basic types, some are bonded or wet sealed while a few are assembled dry. The common feature of all joints is the overlapping of two or more sheets joined by rivets. Corrosion of the faying surfaces of these sheets, typically made of aluminium alloy 2024 T3, is known as crevice corrosion and manifests itself as corrosion pillowing or bulging of the sheets between rivets. To support the development of an enhanced visual technique (D Sight™) for the detection of this pillowing, the molecular volume of the corrosion product retrieved from fuselage joints was found to be nearly 6.5 times that of the alloy from which it was formed (Ref 7). This volume ratio was used to develop an analytical relationship between corrosion material loss and volume of corrosion products contained between two riveted sheets. This mathematical formula was later used in conjunction with a finite element (FE) model to relate pillowing deformation to the amount of material lost. Both a simple lap splice (Fig 1.) and a complex multilayer joint with finger doublers (Fig. 2) were modelled. The pillowing deformations predicted by the model and those measured in joints retrieved from retired aircraft were very similar, giving some confidence in the modelling technique. It was also shown that quantification of corrosion is possible using an enhanced visual technique (Ref 8). Significant understanding of the limitations of visual inspections of fuselage joints for corrosion was gained from these models. Based on these models and the inspections of corroded joints, it was concluded that the generally accepted threshold for visual detection of 10% thickness loss may be significantly higher, and that a 30% thickness loss or more could remain undetected. On this basis, it was recommended that enhanced visual inspections were necessary for fuselage joints, which led to the development of the D Sight Aircraft Inspection System (Ref 9).

The FE models of corroded lap joints indicated that pillowing deformation might result in high stress, which led to the development of new FE models for the joints shown in Figures 1 and 2. These models were linear elastic, with one exception – gap elements were used. The final analysis was a superposition of three loads: corrosion pillowing deformation, rivet interference and hoop stress from pressurisation of the fuselage. The resulting maximum stress indicated that a typical simple two layer lap splice would yield locally at 5.5% loss of material in one layer (38% increase in stress over the non-corroded condition). At 10% loss, this stress increased by 91% over the non-corroded condition. In the multilayer joint the increase was even more significant. Local yielding started at a 5% thickness loss, which represented a 113% increase over the non-corroded condition. (Ref 10, 11).

Paper presented at the RTO AVT Workshop on "Fatigue in the Presence of Corrosion", held in Corfu, Greece, 7-8 October 1998, and published in RTO MP-18.

Results for both the simple and multilayer joints indicated that even the low levels of corrosion considered in the models can shift the location of the critical stress to other layers and rivet rows as compared to the non-corroded condition. The models also demonstrated that corrosion in one area could make a previously non-critical area become critical even though this new critical area is free of corrosion. Often these new critical areas are difficult to inspect, as the cracks are located in second or third layers. The models suggest that corrosion free DADT assessments and the supporting full scale tests do not identify these critical areas and therefore should not be the sole basis for defining in-service inspections, particularly where corrosion detection is only based on visual inspection.

4. STRESS MODEL VERIFICATION

The predicted magnitude of the pillowing effect and its potential consequences required verification. Disassembly of lightly corroded joints (5 to 10%) showed that permanent pillowing deformation is evident after the removal of rivets (Ref 11). Further verification of the stress results came from a study that measured the strain and deformations in a riveted sheet, which was deformed using hydraulic pressure. Strain gauge data, photoelastic coating readings and Shadow Moiré deformations were all compared to the FE model of the experimental rig containing the sheet (Ref 12). As can be seen in Fig 3 the photoelastic and FE results compare very well.

Recently, the NRCC stress predictions were confirmed by the corrosion pillowing modelling work of Welch (Ref 13) and Koch et al. (Ref 14), and by the experimental work by Groner who used bolts to induce pillowing in a strain gauged sheet pinned down with rivets (Ref 15).

5. MODELING CORROSION PILLOWING CRACKS

In an attempt to begin to quantify the impact of corrosion pillowing on the damage tolerance of fuselage joints, a through crack was introduced into the top rivet row of the simple lap joint shown in Fig. 1. Since the model was three-dimensional, the stress intensity factor was calculated for the crack tip at the faying and outside skin surfaces for the first layer. For a 3.8 mm crack, the corrosion pillowing induced by a 5% thickness loss in the outer skin, doubled the stress intensity factor at the faying surface. At the same time, on the outside surface, the stress intensity factor was reduced to zero since the pillowing induced a compressive stress in this area. It was therefore concluded that elliptical high aspect ratio cracks would tend to grow in these joints and that they would not break through to the outside surface before significant crack growth had occurred. The crack shape proposed is shown in Fig. 4 (Ref 11, 12). Later, such cracks were identified in lap joints retrieved from aircraft and some of these were studied under optical and scanning electron microscopy (Ref 16). This work is described below.

Welch (Ref 13) using boundary element methods has confirmed NRCC's predictions of high aspect ratio cracks.

6. IN SERVICE EVIDENCE FOR PILLOWING CRACKS

NRCC has found pillowing cracks in a number of different aircraft. These cracks usually form a star shaped pattern around adjacent rivet holes (Figure 5). Bueno et al. (Ref 17) reported finding similar cracks in a corroded area of a 707 joint. Although Bueno et al. have not indicated that these cracks were non-surface breaking, the limited angle 3D computed tomography used to detect them suggests that could have been the case. SEM analysis performed on some of the cracks that were found in corroded pillowed joints confirmed that they had high aspect ratios (eg. 24.5 for a crack 10.5 mm long) and were usually non-surface breaking (Figure 6) (Ref 16).

The non-surface breaking shape of these cracks has an important in-service impact. Typical inspections for cracks are performed using high frequency eddy current techniques which are not suitable for finding these cracks even if they are in the first layer, which often is not the case (Table 1). Therefore, it would appear that regular inspections for fatigue cracks do not provide sufficient protection against potential premature failure modes involving these pillowing cracks.

Using scanning electron microscopy striations typical of cyclic fatigue were identified in some of the pillowing cracks along the crack front, providing evidence of interaction between corrosion and fatigue in aircraft joints. The authors have uncovered an Airbus Service Bulletin (SB) (Ref 18) that was prompted by a significant corrosion finding. The SB mentioned that cracks were found around the rivets in the corroded area. These cracks were attributed to corrosion pillowing. While this is not surprising in light of present corrosion pillowing work, the aircraft involved, an A300, was only 5 years old at the time. With the exception of the A300, all other cracks listed in Table 1 have not been identified by the operators. Thus it is reasonable to assume that cracks of this nature exist in some operational aircraft.

The investigations of corroded joints and the SEM and optical microscopy work have provided some clues as to the possible initiation mechanisms for pillowing cracks. From FE modelling it is known that these cracks form in areas of very high stress (yielding) around the rivets. However, Figure 7, which shows the distribution of pillowing cracks found to date, does not indicate a strong correlation between fuselage loads and pillowing crack formation. Thus the sustained stress from corrosion pillowing and rivet pre-stress would seem to be the major contributing factors. The other contributing factor is the presence of a corrosive medium, which points to environmentally assisted cracking.

A simple laboratory experiment involving a 1mm thick sheet of 2024 T3 and a 4 mm thick plate of Plexiglas joined with screws and exposed to a corrosive environment was recently completed. After 65 days in EXCO solution, the accumulated corrosion products from the 2024 T3 sheet caused significant pillowing in both materials. As a result the Plexiglas sheet was severely cracked (Fig. 8) at the screw holes, as expected from modelling, and midway between the screws (mid-bay). Both of these locations experienced high bending from pillowing. The mid-bay cracks have not been observed in aircraft because of the significant contribution of the rivet interference (included in the FE models but absent from this simulated joint) to the stress state near the rivets. In aircraft joints, the concentration of the corrodent would not be expected to be as high on the outside surface of the joint as on the faying surface thus making environmentally assisted cracking in the mid-bay area less likely. Further experimental studies are required to establish conditions required for pillowing crack formation.

Koch et al. (Ref 14) identified and modelled a potentially significant new element, which further undermines the structural integrity of corroded joints. In a KC-135 lap joint, local zones with intergranular corrosion were found, which when combined with the high stress from corrosion pillowing could further weaken the joint providing potential nucleation sites for crack formation. This scenario is more likely in KC-135 joints because of the use of one-sided clad sheets in the construction of this aircraft. Typically fuselage skins are made

of sheets that are cladded on both sides. Until corrosion passes through the clad layer, the alloy is well protected from intergranular attack. Since the clad layer represents 5 to 7% of the sheet thickness, corrosion pillowing will usually be present before the intergranular zones observed by Koch et al. appear.

7. MAINTENANCE AND REPAIR IMPLICATIONS

The significance of corrosion pillowing has only recently been recognised. Early attempts at quantifying the effect of pillowing stress on life and residual strength have been carried out by Brooks et al. and the results will be presented at this workshop (Ref 5). The results indicate that the effect is significant at very low levels of corrosion (below 10% thickness in one skin). This level of corrosion is very difficult to detect using the currently deployed system of visual inspection followed by hand held low frequency eddy current probe inspection. Sophisticated scanner based multi-frequency eddy current inspections will improve detection of thinning, however, they will not identify pillowing which will be needed to assess the impact of corrosion in a lap joint.

Lap joints are inspected regularly for fatigue cracks in critical rivet rows. The high frequency EC systems used are incapable of detecting non-surface breaking cracks such as pillowing cracks. The shifting of the critical stress location to other rivets and layers predicted by the models further supports the position that current NDI inspections are not adequate for detecting corrosion pillowing cracks.

Teardowns of joints, which were subject to in-service corrosion removal, indicated that pillowing is often ignored during maintenance. As shown in the Figure 9 the sanding or grinding used to remove corrosion, after wedging open the joint, often removes an excessive amount of metal around the rivets. Post repair measurements indicate that more than 30% thickness reduction had occurred in the skin shown in Fig. 10 due to the grinding process.

A possible scenario, which has to be considered in the future evaluations of the impact of pillowing cracks on structural integrity, is the performance of a repaired lap joint with pillowing cracks. Following abrasive removal of corrosion, a joint with significant metal loss around the rivet holes and pillowing cracks might be re-riveted and the aircraft returned to service. While the sealant and corrosion preventing compounds applied before re-assembly may prevent further corrosion, some corrosion pillowing cracks could provide the initiation sites for significant MSD after a relatively low number of cycles.

8. CONCLUSIONS

- Analytical and numerical models relating corrosion in lap joints to high stress and cracking in fuselage skins around rivets have been demonstrated.
- Pillowing corrosion stress in simple and multilayer joints becomes significant before corrosion can be detected visually.
- Corrosion pillowing cracks have high aspect ratios and may grow along the faying surfaces without becoming through cracks. Non-surface breaking cracks are very difficult to detect.
- Fatigue striations observed at the front of some of the pillowing cracks provide evidence for corrosion and fatigue interaction.
- The shifting of the critical stress location, predicted by FE models, to previously non-critical areas indicates a further potential mode of corrosion and fatigue interaction.
- Repair processes must account for the effects of corrosion pillowing.
- Future DADT assessments should include corrosion damage and corrosion repair effects.

9. ACKNOWLEDGMENTS

We are greatly indebted to our NRC colleagues and students who have contributed to this work over the years. In particular to K. Shankar, C.E. (Ted) Chapman, A. Marincak, S. Sparling, M. Lockman and A. Othman. The support of US Air Force Corrosion Program Office, NCI Information Systems and Department of National Defence AVRD organisation is gratefully acknowledged.

10. REFERENCES

1. Goranson, U. G., Miller, M., "Aging Jet Transport Structural Evaluation Programs", Springer Series in Computational Mechanics Atluri, Sampath, Tong (Eds.), Structural Integrity of Aging Airplanes, Springer Verlag Berlin Heidelberg 1991.
2. Varanasi, S. R., McGuire, J. F., "Boeing Structural Design Technology Improvements", Airliner, April-June 1996, p 12-19, Boeing Commercial Airplane Group.
3. Akdeniz, A., Das, G., "Influence of Undetected Hidden Corrosion on Structural Airworthiness of Aging Jet Transports", The Second Joint NASA/FAA/DoD Conference on Aging Aircraft, Williamsburg, Virginia, August 31 – September 3, 1998.
4. Kenzie, R., Cooke, G., "Corrosion in USAF Aging Aircraft Fleets", NATO RTO Workshop "Fatigue in the Presence of Corrosion", 7-8 October 1998, Corfu, Greece.
5. Brooks, C. L., Prost-Domasky, Scott, Honeycutt, K., "Corrosion is a Structural and Economic Problem: Transforming Metrics to a Life Prediction Method", NATO RTO Workshop "Fatigue in the Presence of Corrosion", 7-8 October 1998, Corfu, Greece.
6. Perez, R., "Corrosion/Fatigue Metrics", Proceedings of ICAF '97 Symposium on Fatigue in New and Ageing Aircraft, June 16-20, 1997, Edinburgh, Scotland.pp.215-229.
7. Bellinger, N.C.; Krishnakumar, S.; and Komorowski, J.P.: Modelling of Pillowing Due to Corrosion in Fuselage Lap Joints. Canadian Aeronautics and Space Journal, Vol. 40, No. 3, September 1994, pp.125-130.
8. Komorowski, J.P, Bellinger, N.C., Gould, R.W., Marincak, A., Reynolds, R., "Quantification of Corrosion in Aircraft Structures with Double Pass Retroreflection", Canadian Aeronautics and Space Journal, Vol. 42, No.2, June 1996, p76-82.
9. Karpala, F., Hageniers, O.L., Komorowski, J.P., et al., "Development of a D Sight Aircraft Inspection System", phase 3, Final Report". Transportation Development Centre, TP 13098E, September 1997.
10. Bellinger, N.C., Komorowski, J.P, "Corrosion Pillowing Stresses in Fuselage Lap Joints", AIAA Journal, Vol. 35, No. 3, pp317-320, March 1997.
11. Komorowski, J.P., Bellinger N.C. and Gould, R.W., "The Role of Corrosion Pillowing in NDI and in the Structural Integrity of Fuselage Joints", Fatigue in New and Aeging Aircraft – Proc. of the 19th Symposium of the International Committee on Aeronautical Fatigue Edinburgh, 16-20, June 1997, pp251-266, EMAS Publishing 1997.
12. Bellinger, N.C., Komorowski, J.P, Gould, R.W., "Damage Tolerance Implications of Corrosion Pillowing on Fuselage Lap Joints", Journal of Aircraft, Vol. 35, No. 3, pp487-491, May-June 1998.
13. Welch, D. W., "Fracture Mechanics Analysis of a Corroded Aircraft Fuselage Lap Joint", Master of Science

thesis, the University of Oklahoma Graduate College, Norman, Oklahoma 1997
14. Koch G.H., Yu, L., Katsube, N. and Paul, C. A., "Mathematical Model to Predict Fatigue Crack Initiation in Corroded Lap Joint", The Second Joint NASA/FAA/DoD Conference on Aging Aircraft, Williamsburg, Virginia, August 31 – September 3, 1998
15. Groner, D. J., ASC/SMA, WPAFB, OH., private communication.
16. Bellinger N.C., Komorowski, J.P., Gould, R.W., "Corrosion Pillowing Cracks in Fuselage Joints", The Second Joint NASA/FAA/DoD Conference on Aging Aircraft, Williamsburg, Virginia, August 31 – September 3, 1998
17. Bueno, C., Barker, M.D., Betz, R.A.,Barry, R.C., Buchanan, R.A., "Real Time Digital Radioscopy for Structural Assessment", Air Force 3rd Aging Aircraft Conference 26-28 September 1995.
18. Service Bulletin No: A30053178, Jan 08/82, revised 7 SEP 19/88, Airbus Industrie.

TABLE 1. RECORDED INCIDENCES OF PILLOWING CRACKS

Type of Aircraft	Hours / Cycles	Location of crack	Layer	WFU / CUT
L1011	38,040 / 31,370	33R / BS589-609	First	Dec. 92 / Sept. 93
B727-235	55,640 / 48,660	4R / BS1100	Second	Sept. 92 / May 93
B727-200	D Check	S30 / BS1090	First	In service / Aug 95
B727-100	61,890 / 54,150	S19R / BS600-640	Second	July 94 / July 96
B727-90C	72,400 / 56,700	S19-26L / BS440	First	In service / Oct 95
B727-235	56,870 / 49,530	S19R / BS700-720	First	Mar 92 / Feb 93
A300(Ref 18)	10,400 / 6,940	S31L / FR26-31	First	In service / Oct 81
B727-295	61,854 / 55,465	S19R / BS660-680	First	Jan 90 / Feb 98
B727-295	63,349 / 55,676	S19R / BS720A-720B	First	Aug 89 / Feb 98
B707(Ref 17)		Floor to skin joint	First	

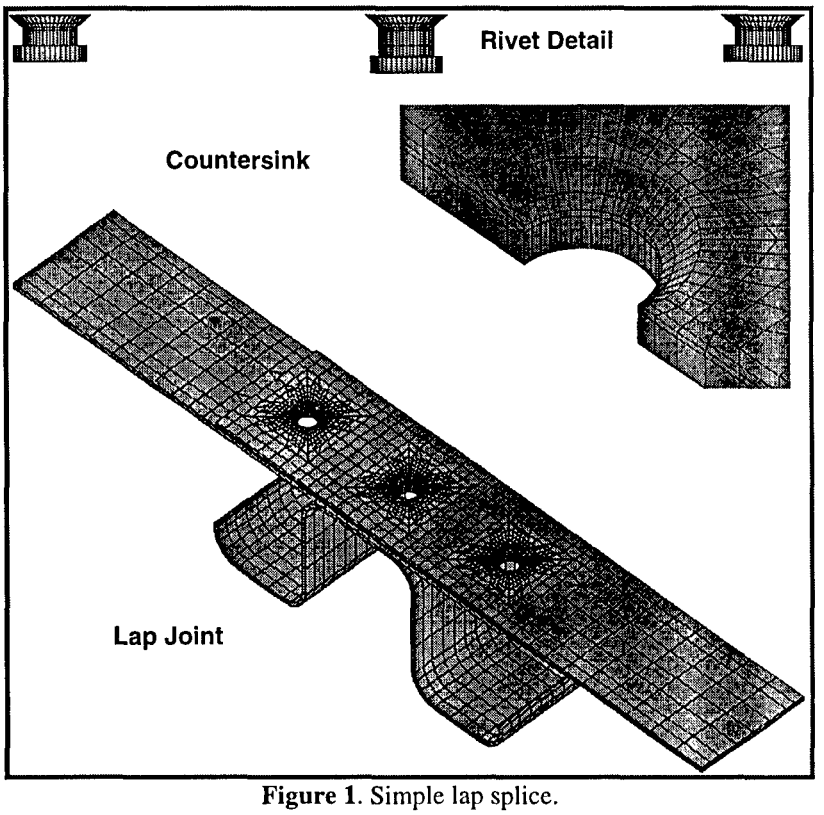

Figure 1. Simple lap splice.

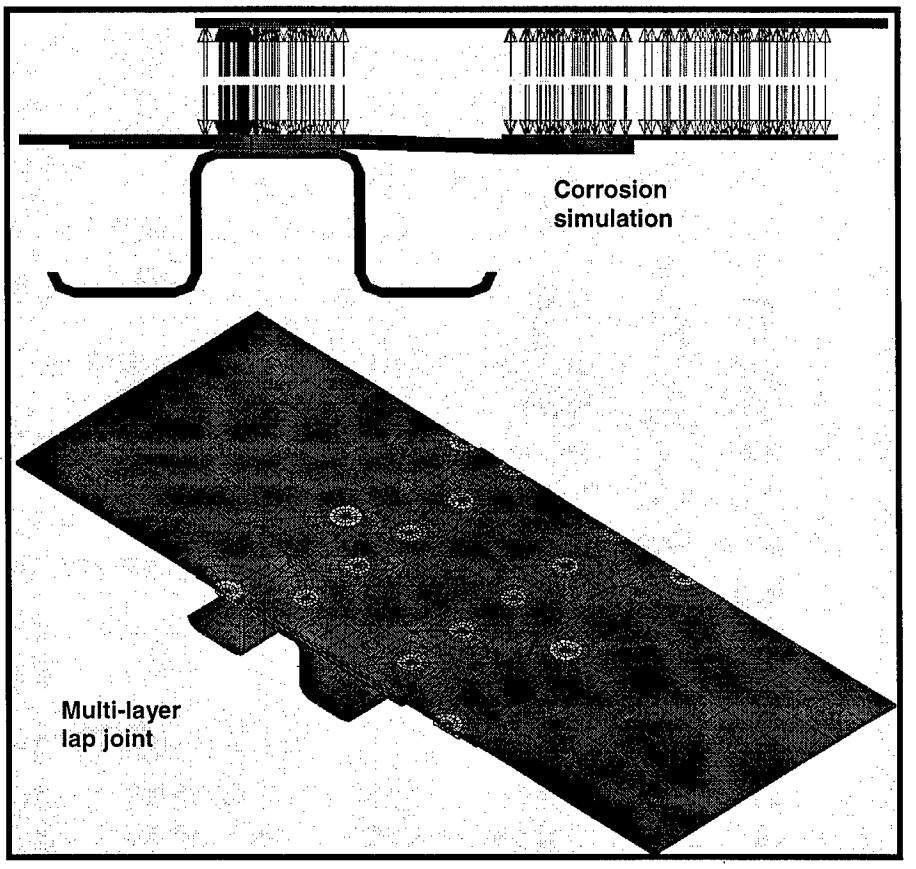

Figure 2 Complex multi-layer joint with finger doublers.

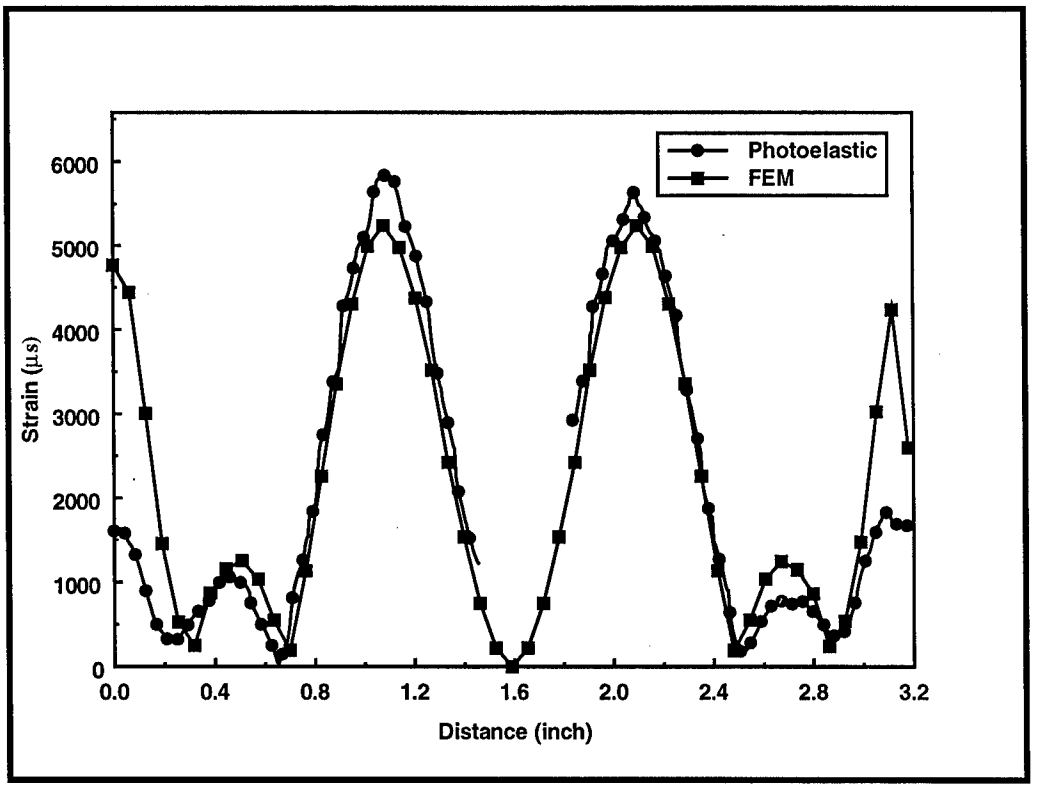

Figure 3. Comparing photoelastic coating and FE modeling results.

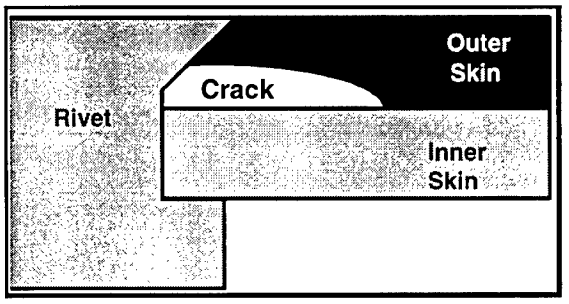

Figure 4. The proposed corrosion pillowing crack shape.

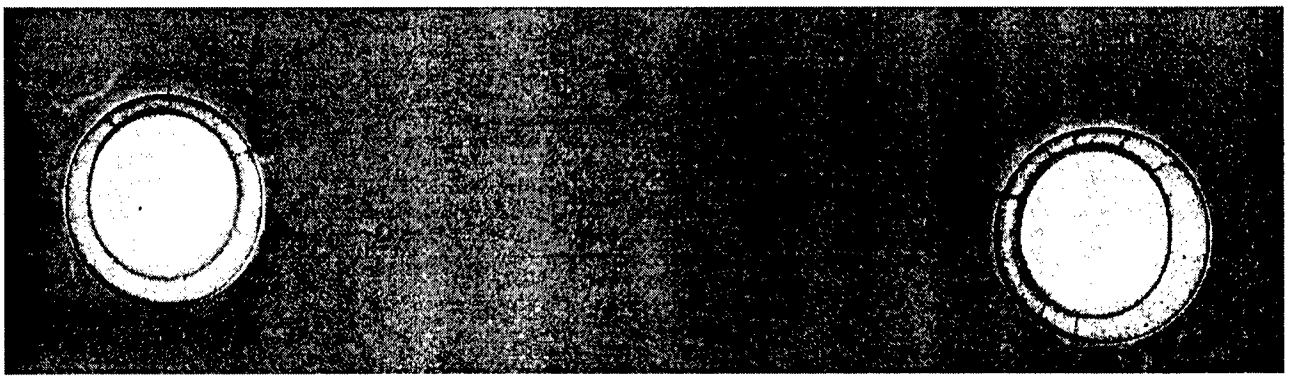

Figure 5. Star shaped patterns around adjacent rivet holes.

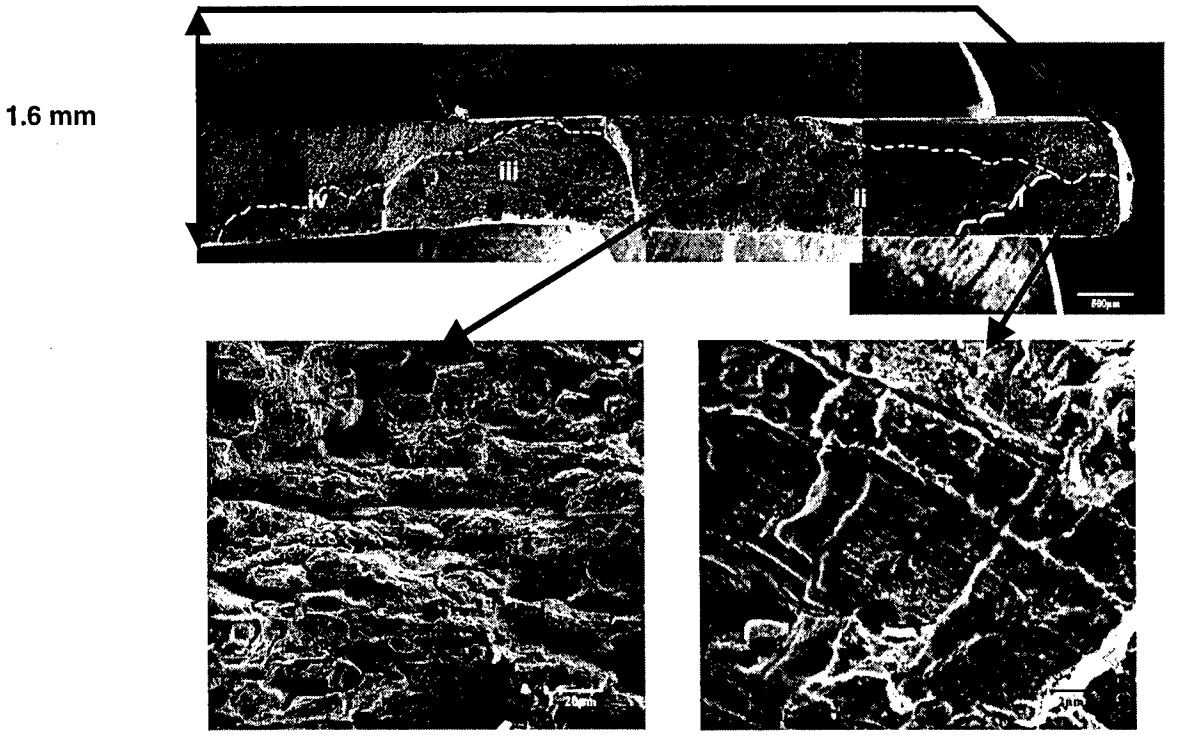

Figure 6. Microscopy of non-surface breaking crack from L1011 aircraft skin. Close-ups show intergranular corrosion and fatigue striations.

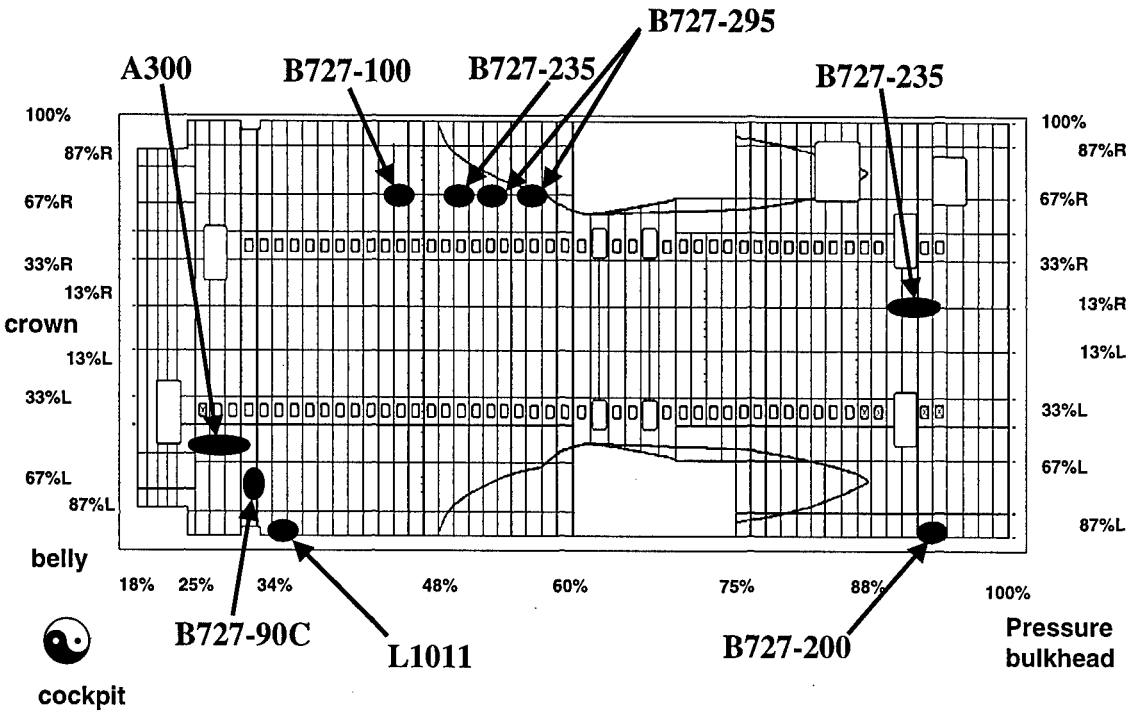

Figure 7. Turtle diagram of a generic fuselage showing locations of pillowing cracks.

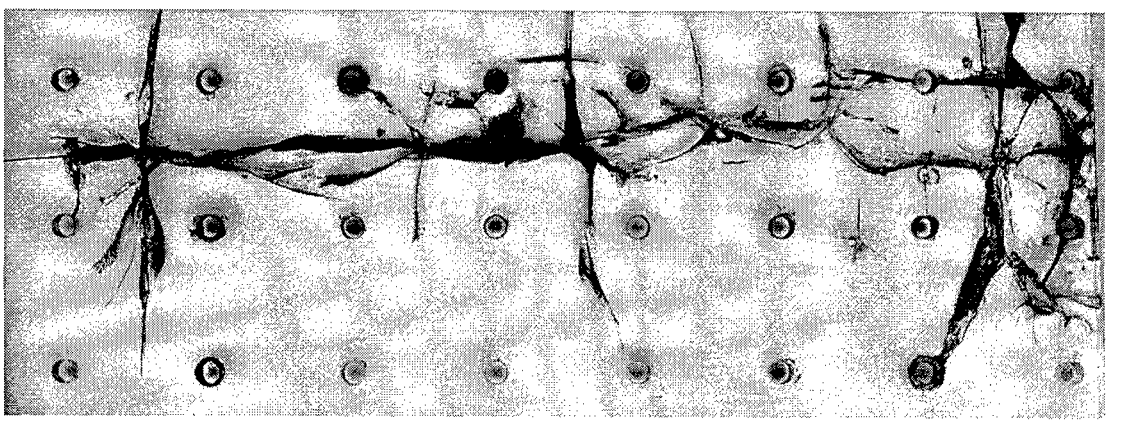

Figure 8. Plexiglas sheet severely cracked by corrosion pillowing.

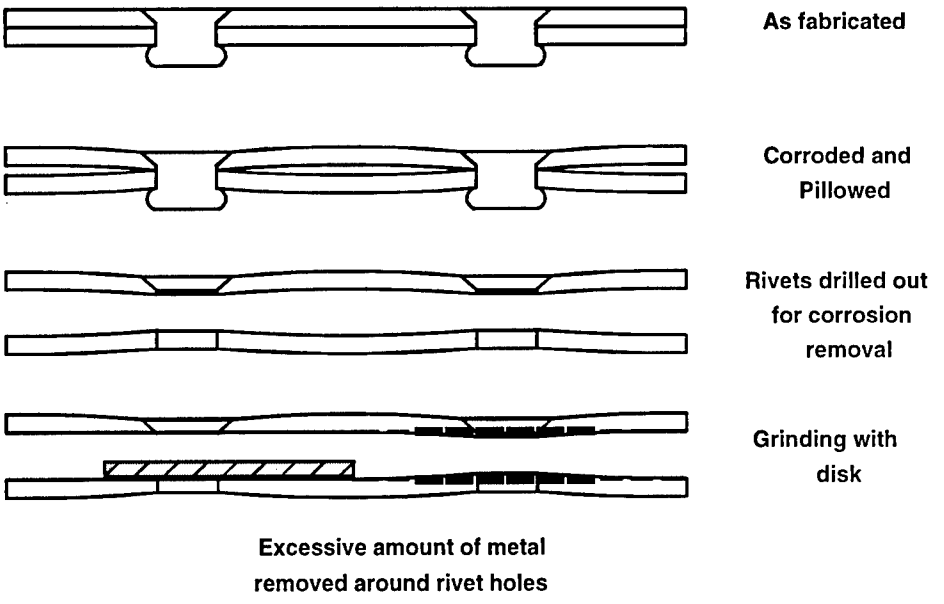

Figure 9. Improper corrosion removal procedure.

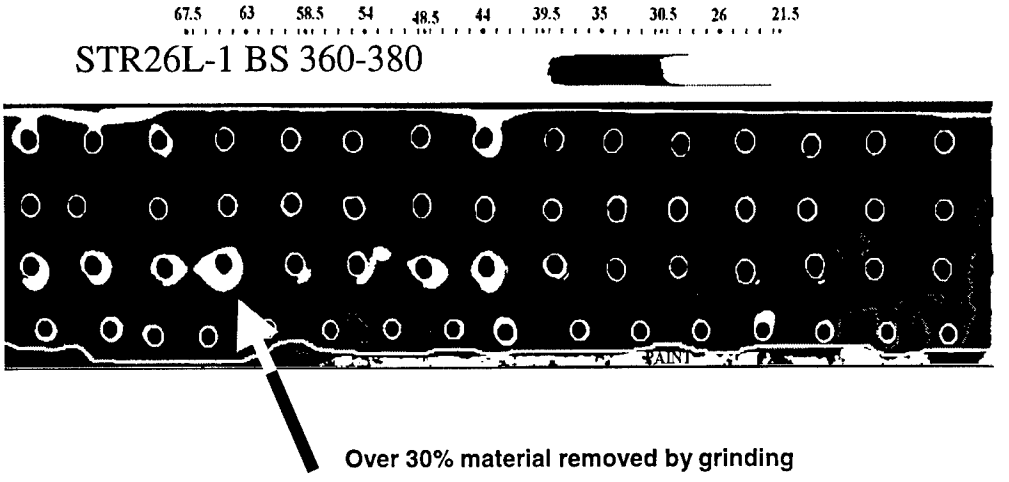

Figure 10. Thickness map from X-ray image showing the effect of improper corrosion removal.

THE EFFECT OF EXISTING CORROSION ON THE STRUCTURAL INTEGRITY OF AGING AIRCRAFT

Sp. G. Pantelakis
Th. B. Kermanidis
P.G. Daglaras
Ch. Alk. Apostolopoulos
Laboratory of Technology & Strength of Materials
Department of Mechanical Engineering & Aeronautics
University of Patras, Panepistimioupolis Rio, 26500 Patras, Greece

ABSTRACT

Investigation on effects of existing corrosion on the structural integrity of aging aircraft structures was made. The study included characterization of the tensile behaviour as well as determination of the fatigue and fatigue crack growth behaviour of structural aircraft aluminium alloys following to corrosion exposure.
The investigation of the tensile behaviour following corrosion exposure was performed on the aluminium alloys 2024, 8090, 2091 and 6013. The materials were exposed to five different accelerated laboratory corrosion tests ; alloy 2024 T351 was also subjected to out-door exposure. Evaluation has shown an appreciable decrease of yield and ultimate tensile stress caused by corrosion attack on the materials surface layers. In addition, a dramatic volumetric embrittlement of the corroded materials was observed ; it has been associated to hydrogen penetration and absorption.
The influence of existing corrosion on fatigue life and fatigue crack growth of 2024 alloy was evaluated as well. Obtained S-N curves are confirming the expected decrease of fatigue life following corrosion. Fatigue crack growth tests performed for several R-ratios have shown that crack growth rates are practically not practically influenced by existing corrosion ; yet, this result should not be misinterpreted as insignificance of existing corrosion for the damage tolerance behaviour of the structure.

1. INTRODUCTION

In service mechanical loads and the occurrence of corrosion present significant causes of structural degradation in aging aircrafts. To account for the influence of the several forms of damage caused by mechanical loads on the structural integrity essential efforts have been made ; they include models for calculating the growth of a single crack under in service spectra [e.g. 1 to 4], concepts to estimate damage accumulation during the several phases of the complex wide spread fatigue damage phenomena [e.g. 5, 6], numerical tools for reducing the enormous calculation time required for assessing the integrity of an aging aircraft structure which presents multiple side damage [e.g. 7 to 9], etc. Yet, the effect of existing corrosion on the structural integrity of aging aircrafts remains still underestimated although it has been recognized that the potential interaction of corrosion with other forms of damage such as single fatigue cracks or wide spread cracking at regions of high stress gradients can result to loss of structural integrity and may lead to fatal consequences, [e.g. 7,10]. The available data to face the corrosion induced structural degradation issue refer mainly to results from accelerated laboratory corrosion tests and, more rarely, to results from out-door atmospheric corrosion tests. With the exception of the atmospheric corrosion tests where according to the relevant specification [11] the tensile properties of corroded specimens are periodically measured as well, said tests are evaluated by measuring weight loss and characterizing depth and type of corrosion attack ; the tests are exploited for evaluating the corrosion susceptibility of the materials. Yet, above viewpoint to understand corrosion susceptibility of a material does not relate the occurrence of corrosion to their impact on the materials mechanical behaviour and residual properties. The corrosion induced mechanical degradation is considered on the basis of results from stress corrosion cracking tests or from fatigue tests carried out in a corrosive environment [e.g. 12-14]. Despite of the fact that presently no quantitative correlation exists between the accelerated

Paper presented at the RTO AVT Workshop on "Fatigue in the Presence of Corrosion", held in Corfu, Greece, 7-8 October 1998, and published in RTO MP-18.

laboratory corrosion tests and the expected in-service or even the out-door corrosion attack the data obtained by means of mentioned SCC or corrosion/fatigue tests may be exploited for the cases where a structural member is stressed or fatigued within a corrosive medium but not in situations where the already corroded member is subjected to mechanical loads. Present day considerations of the corrosion induced structural degradation relate the presence of corrosion with a decrease of the load bearing capacity of the corroded structural member, [e.g. 7, 9, 10, 12]. Said decrease is associated to the occurrence of corrosion notches which lead to local increase of stresses and support fatigue crack initiation, as well ; in addition corrosion induced reduction of the members load bearing thickness which, in the case of the thin aluminium alloy skin sheets, may be essential, can lead to appreciable increase of stress gradients [10].

Classical understanding of the corrosion attack of aluminium alloys as the result of complex oxidation processes [e.g 12, 15], is supporting above considerations of the corrosion induced structural degradation issue. Yet, it has been recognized that additionally to oxidation processes, hydrogen produced during the corrosion process may diffuse to the material interior and lead to hydrogen-metal interaction, [e.g. 13, 16-18] ; macroscopically, it is reflected to as material embrittlement. For the alloy system Al-Zn-Mg the role of hydrogen for observed material behaviour has been early recognized [17]. In [18] determined embrittlement of the Al-Mg and Al-Zn-Mg aluminium alloy systems was explained as the result of the formation of magnesium hydrides on the grain boundaries. Yet, a dramatic embrittlement of the alloys 2024 following exposure in several corrosive environments has been reported in [19 to 22] ; 2024 belongs to the Al-Cu system. Same behavior was observed for the 6013, 8090 and 2091 alloys as well [19 to 22]. The works in [21,22,23] give evidence for the responsibility of hydrogen penetration and absorption for observed embrittlement . Latterly referred results demonstrate the need to include information on the remaining mechanical properties of the corroded member when assessing the integrity of an agining aircraft structure.

In present work the tensile behaviour of the 2024, 6013,8090 and 2091 alumunium alloys following exposure to several accelerated laboratory corrosion tests as well as to out-door atmospheric corrosion was investigated. The effect of existing corrosion on the fatigue life and the fatigue crack growth behavior of the 2024 alloy was studied as well. Determined results are discussed along with a critical appraisal of the sufficiency of current practice to evaluate material corrosion susceptibility with regard to structural integrity.

2. EXPERIMENTAL

The experiments included firstly the exposure of the specimens to corrosive environments as they are specified in the respective standards for accelerated laboratory corrosion tests and out-door exposure. Then the corroded specimens were subjected to mechanical testing. Metallografic and stereoscopic analyses were made as well to derive type and depth of corrosion attack.

2.1. Materials and specimen preparation

The investigation was performed on the aluminium alloys 2024,6013,8090,and 2091 ; their chemical compositions are given in **Table 1**. The selected alloys refer to the aluminium alloy systems Al-Cu, Al-Si-Mg-Cu and Al-Li. All alloys were received in sheet form of 1.6mm nominal thickness in the temper conditions T351 for 2024, T6 for 6013, T81 for 8090 and T3 for 2091; the latter was aged to T84 to make it comparable with 2024 T351 and 8090 T81. To investigate the protective role of anodizing and sealing a number of specimens from material 2024 were subjected to anodizing and sealing prior to corrosion exposure. In the following this material is referred to as 2024, "ref. 2" alloy. Prepared have been tensile, fatigue and fatigue crack propagation specimens. Tensile specimens were machined according to ASTM E8m- 94 a ; specimens were cut in both, longitudinal (L) and long transverse (LT) direction. For the fatigue tests specimens were cut according to ASTM E466-82 specification; the specimens were cut in (L) direction. For the fatigue crack growth tests the specimens were machined following to the ASTM E647-93 specification ; they were cut in (L) direction. Prior to mechanical testing all specimens were subjected to corrosion tests with the exception of a certain number of specimens used to derive the reference mechanical behaviour of the uncorroded

material. The corrosion tests considered and the respective specifications used to perform the tests are given in **Table 2.**

2.3. Mechanical testing

All tensile tests performed are summarized in the **Table 3**. The tensile tests aim to provide information on : i) the influence of accelerated laboratory corrosion tests according to the specifications or of out -door exposure on the tensile properties of the material, ii) the gradual decrease of the tensile properties during exfoliation corrosion exposure (tests were performed for all materials) or during out-door exposure (tests were performed only for 2024) , iii) the question whether observed property degradation during corrosion exposure is volumetric, iv) the protective role of hard anodizing and sealing against corrosion (tests were performed only for alloy 2024). All tensile tests were performed according to ASTM E8m-94a specification using a 200 KN Zwick universal testing machine and a servohydraulic MTS 250 KN machine by a deformation rate of 10 mm/min
As it is obvious from Table 3 focal point of the investigation was alloy 2024. Investigation on fatigue and fatigue crack growth behaviour has been limited to this alloy 2024, "ref. 2". The specimens were precorroded in exfoliation corrosion solution with the exception of the specimens used to obtain reference material behaviour. All fatigue tests performed to obtain S-N curves as well as performed fatigue crack growth tests are summarized in **Tables 4 and 5** respectively.

Fatigue crack growth tests were performed for the R-values 0.01, 0.1, 0.5 and 0.7. For each R- value two tests were performed on as recieved specimens and 2 tests on specimens subjected to 36 hours exfoliation corrosion exposure prior to fatigue crack growth test. The frequency for all tests was constant, 20 Hz.

2.4 Tests for metallographic and stereoscopic corrosion characterization

Corrosion characterization included determination of weigth loss, type and depth of corrosion attack as well as measurement of pitting density. Evaluation was made by stereomicroscopie at 30 x and metallographic analysis of specimens.

3. RESULTS AND DISCUSSION

Performed metallographic and stereoscopic corrosion analysis has shown that in all accelerated laboratory corrosion tests corrosion developed gradually from pitting into integrannular attack. Out door exposure for durations up to 24 months does not lead to appreciable occurrence of corrosion. **(Figure 1)**. For long exposure time in exfoliation corrosion solution major intergrannular cracks were also found. Protection by anodizing and sealing decreases significantly the rate of corrosion attack. Yet, for all cases investigated in present study exposure in a corrosive environment results to mechanical degradation of the material. Tensile properties of the investigated materials 2024, 2024 "ref. 2" and 6013 determined after their exposure in accelerated corrosion tests are summarized in **Figures 2 to 4** respectively. Same behaviour was determined for the materials 8090 and 2091. For the accurate data refer to the works in [19-21]. As it can be seen, decrease of yield and ultimate tensile stress was appreciable where corrosion exposure occurred for long duration and/or in aggressive environments. Yet, in all cases investigated a dramatic material embrittlement was determined ; it is demonstrated in the low values for elongation to failure and energy density measured for the corroded materials. Remarkable is the appreciable tensile ductility loss of all materials investigated already after a short exposure in atmospheric corrosion conditions. Determined tensile ductility decrease caused by anodizing of the 2024 alloy is noticeable as well. Tensile property degradation occurs gradually. **Figures 5 to 6** refer to tensile property degradation of the materials 2024 and 6013 respectively following exfoliation corrosion. Yield and ultimate tensile stress degrade following power functions with the exposure time. Tensile ductility properties are decreasing following exponential functions with the exposure time. In both cases the power exponents are <1. Materials 8090 and 2091 showed same behaviour ; the data have been presented in [20, 21]. Illustrated in **Figure 7** has been the dependency of the tensile properties of alloy 2024 on the exposure duration in atmospheric corrosion. For the investigated duration of two years, yield and ultimate tensile stress have been practically not affected. On the contrary, a clear trend of an appreciable tensile ductility decrease has been observed. Yet, for formulating derived dependency further data

are still needed. Obtained yield and ultimate tensile stress decrease is caused by corrosion induced material surface degradation. It was found that after machining of the corrosion attacked material surface layer yield and ultimate tensile stress increase again almost to their initial values. Yet, tensile ductility drop is volumetric. Machining of the corrosion attacked surface layer had practically no influence on the determined tensile ductility values although the tensile tests were performed on the "uncorroded" material core after the removal of the corrosion attacked layer [21, 22]. In the works [19, 23] observed bulk embrittleemnt has been associated to hydrogen penetration and absorption. As expected, exposure in a corrosive environment prior to fatigue tests is reducing the fatigue life of the material . Displayed in **Figure 8** have been S-N curves derived for the material 2024 "ref 2" following exposure to exfoliation corrosion solution for 36 hours for specimens without hole (K_t=1) or including a hole (K_t=2,5). For comparison the S-N curve of the uncorroded and uncoated (reference) material and the S-N curve of the uncoroded but coated material ("ref 2") have been plotted as well. Remarkable is the fact that anodizing and sealing is reducing fatigue resistance appreciably. Specimens including hole (K_t=2,5) show, as expected, reduced fatigue life as compared to specimens without hole stressed at same stress amplitude. The exponents of the Weibull distribution describing the plots in Figure 8 are summarized in **Table 5** ; the respective curves are plotted in figure 8 as well. Yet, above discussed corrosion induced fatigue degradation was not reflected to the fatigue crack propagation tests performed on both, uncorroded and corroded 2024 "ref 2" alloy specimens for four different $R=\sigma_{min}/\sigma_{max}$ values. The results are displayed in **Figure 9**. In the figure the influence of the R-value on fatigue crack propagation rate may be well recognized. The occurrence of corrosion caused by the exposure in exfoliation corrosion solution for 36 hours has practically no influence on determined fatigue crack growth behaviour. Summarized in **Table 6** have been determined constants C and n for the Paris equation.

$$\frac{da}{dN} = C(\Delta K)^n$$

where ΔK stands for the stress intensity factor range. Derived results are consistent with experimental results from [24]. Determined independancy of the FCP behaviour on existing corrosion is a result which is not intuitively understandable. Further investigation is needed to quantify whether observed fatigue resistance drop due to corrosion may be explained solely by the occurrence of corrosion notches which, no doubt, are reducing the fatigue crack initiation phase significantly, or may be related to determined ductility drop as well.

REFERENCES

[1] J.B. Chang, M. Szamossi and K.W. Lin, in Methods and Models for Predicting Fatigue Crack Growth under Random Loading, ASTM STP 748, ASTM, Philadelphia, PA 19103, 1981, p. 115.

[2] G.C. Sih and D.Y. Jeong, Fatigue Load Sequence Effect Ranked by Critical Available Energy Density, J. Theor. Appl. Fract. Mech. 14, 1990, p. 1.

[3] X. Zhang, A.S.L. Chan and G.A.O. Davies, Numerical Simulation of Fatigue Crack Growth under Complex Loading Sequences, Engineering Fracture Mechanics 42, No.2,, 1992, p. 305.

[4] Sp. Pantelakis, Al. Kermanidis, P. Daglaras, "Crack-growth analysis code for assessing fatigue life of 2219-T851 aluminum specimens under aircraft structure service spectra" , Theor. and Appl. Fract. Mech. 28, 1997, p. 1.

[5] "FAA / NASA Int. Symp. On Advanced Structural Integrity Methods for Airframe Durability and Damage Tolerance", ed. C.E Harris, Hampton, Virginia, USA, 1994.

[6] P, Horst, H.-J. Schmidt, "On the Significance of Probabilistic Parameters for the Assessment of MSD in the Case of Aging Aircraft" Proc.of the 19th International Council on Aerospace, p. 1773.

[7] BRITE-EURAM No BE 95-1053 Structural Maintainance of Ageing Aircraft, Mid Term Assessment Report, CEC, Brussels, 1996.

[8] Th. Kermanidis, G. Labeas, J. Lentzos and J. Diamantakos, Efficient computation of stress intensity factors under MSD conditions using FE substructuring technique, presented at Structural Maintenance of Aging Aircraft, Task 2 Internal Conference at NLR Amsterdam, 16-17 Oct. 1997.

[9] Th. Kermanidis, G. Labeas and J. Diamantakos, Corner crack growth simulation using through crack equivalence and sub-modelling techniques, presented at Structural Maintenance of Aging Aircraft, Task 2 Internal Conference at NLR Amsterdam, 16-17 Oct. 1997.

[10] M.E. Inman, R.G. Kelly, S.A. Willard and R.S. Piascik, Proc. of the FAA-NASA Symposium on the Continued Airworthiness of Aircraft Structures, Atlanda, Georgia, August 28-30, 1996, National Technical Information Service, Springfield, Virginia 22161, USA, 1997, p. 129.

[11] ASTM G50-76, Annual Book of ASTM Standards, Section 3, Metal Test Methods and Analytical Procedures, West Conshohocken, ASTM, Philadelphia, U.S.A., 1995, p. 185.

[12] FAA-NASA Symposium on the continued airworthiness of aircraft structures, FAA Center of Excellence in computational modeling of aircraft structures, Atlanda, Georgia, USA, August 28-30, 1996.

[13] M. O. Speidel, in R. Gibala and R.F. Heheman (eds.), Hydrogen Embrittlement and Stress Corrosion Cracking, Materials Park, OH: ASM, 1992, p. 271.

[14] H. F. de Jong, Influence of environment and temperature on the stress corrosion crack growth rate of aluminum 7075, Aluminium, 58, 1982, p. 526.

[15] W. Wallace, D.W. Hoeppner and P.V. Kandachar, Aircraft corrosion : Causes and case histories, AGARD Corrosion Handbook Vol. 1, AGARD AG 278, 1985.

[16] Sp. Pantelakis, Th. Kermanidis, P. Daglaras, "Mechanical behaviour of pre-corroded advanced Al-Li alloys 2091 and 8090 and the conventional aerospace Al alloy 2024" In : Proc. of the "Fourth International Conference on Production Engineering and Design for Development", Dec. 27-29, 1993, Cairo, Egypt, Vol. 1, p. 128.

[17] G.M. Scaman, R. Alani and P. R.. Swann,Pre-exposure embrittlement and stress corrosion failure in Al-Zn-Mg alloys, Corrosion Science, 16, 1976, p. 443.

[18] C.D.S. Tuck, Proc. of the 3rd Int. Conference of Hydrogen on the Behaviour of Materials, Jackson, Wyoming 1980, p. 503.

[19] BRITE/EURAM No BE92-3250, Investigation on Aluminium-Lithium alloys for Damage Tolerance Application, Final Report, CEC Brussels 1993.

[20] Sp. G. Pantelakis, N. I. Vassilas, P.G. Daglaras, Effects of corrosive environment on the mechanical behaviour of the advanced Al-Li alloys 2091 and 8090 and the conventional aerospace alloy 2024, *Metall* 47 Jahrgang, Heft 2,1993, p. 135.

[21] Sp. G. Pantelakis, P. G. Daglaras and Ch. Alk. Apostolopoulos, Tensile Behaviour of 2024, 6013, 8090 and 2091 Aircraft Aluminium Alloy Specimen Following Corrosion Exposure, sumbitted for publication.

[22] EPETII/30, Damage tolerance behaviour of corroded aluminium structures, Mid Term Assessment Report General Secretariat for Research and Technology, Greece, 1996.

[23] G.N. Haidemenopoulos, N. Hassiotis, G. Papapolymerou and V.Bontozoglou, Corrosion, 54, 1998, p. 73.

[24] J.P. Chubb, T.A. Morad, B.S. Hockenhull and J.W. Bristow, The effect of exfoliation corrosion on the fatigue behaviour of structural aluminium alloys. Springer Series in Computational Mechanics Atluri, Sampath, Tong (Eds.) Structural Integrity of Aging Airplanes, Springer Verlag Berlin Heidelberg 1991, p. 87.

Chemical composition (in wt %)											
aluminium alloy	**Si**	**Fe**	**Cu**	**Mn**	**Mg**	**Cr**	**Zn**	**Ti**	**Ni**	**Zr**	**Li**
2024	.10	.18	4.35	.67	1.36	.02	.07	.03	-	.01	-
6013	.25	-	.90	.35	.95	-	-	-	-	-	-
8090	.02	.05	1.26	.04	.83	.003	.02	.024	.004	.06	2.34
2091	.044	.034	2.02	-	1.25	-	-	.025	-	.085	1.97

Table 1: Chemical composition (in wt %) of the aluminium alloys 2024, 6013, 8090 and 2091.

Corrosion test	**Exfoliation corrosion**	**Intergran-nular corrosion**	**Alternate immersion**	**Salt spray**	**Cyclic acidified Salt fog**	**Out-door exposure**
Specification	ASTM G 34-90	ASTM G 110-92	ASTM G 44-94	ASTM B117-94	ASTM G85-94 Annex A2	ASTM G50-76

Table2: Corrosion tests performed on the specimens prior to mechanical loading.

Test series description	Corrosion exposure prior to tensile test	Specimen direction	Material
Tensile tests on reference materials	none	L/LT	2024, 6013, 2091, 8090
Tensile tests on specimens following to their exposure to corrosion processes according to ASTM specifications	Exfoliation corrosion 48h	L/LT	2024, 6013, 2091, 8090
	Exfoliation corrosion 96h	L/LT	2024, 6013, 2091, 8090
	Intergrannular corrosion 6h	L/LT	2024, 2091, 8090
	Alternate immersion 30 days	L/LT	2024, 6013, 2091, 8090
	Salt spray 30 days	L/LT	2024, 2091, 8090
	Cyclic acidified salt fog (mastmaasis)30 days	L/LT	2024, 2091, 8090
	Atmospheric corrosion 12 months	L/LT	2024, 2091, 8090
Tensile tests following to the exposure of specimens to exfoliation corrosion solution or to atmospheric corrosion for different exposure times	Exfoliation corrosion (exposure times : 0.3, 2.0, h 8.0 16.0 h 24, 48, 72, 96 h	L/LT	2024 8090 2024, 6013, 2091, 8090
	Atmospheric corrosion (exposure times : 3, 6, 9, 12, 15, 18, 21 months)	L/LT	2024
Tensile tests on reference specimens subjected to anodizing and sealing	none	L	2024
Tensile tests on protected specimens following to their exposure to corrosion processes according to ASTM specifications	Exfoliation corrosion 24h	L	2024
	Exfoliation corrosion 48h	L	2024
	Alternate immersion 30 days	L	2024
Tensile tests on specimens following to their exposure to exfoliation corrosion solution and mechanical removal of the corroded material surface layer	Exfoliation corrosion (exposure times : 48h and 72h)	L/LT	2024, 6013, 2091, 8090

Table 3: Performed tensile tests

Specimens preparation prior to fatigue	K_t	$R=\sigma_{min}/\sigma_{max}$	Number of tests to derive the S-N curne
as recieved	1	0,1	17
anodization coating and sealing	1	0,1	11
anodization coating and sealing	2,5	0,1	11
anodization coading and sealing and then exposure to exfoliation corrosion	1	0,1	11
anodization coating and sealing and then exposure to exfoliation corrosion	2,5	0,1	12

Table 4: Fatigue tests performed on the 2024 alloy to derive S-N curves ; f=25Hz

Specimen preparation prior to fatigue	C_1	C_2	C_3	C_4
as recieved. K_t=1	499	171.3	4.3	-8.8
anodization coating and sealing, K_t=1	450	129	4.16	-7.09
anodization coating and sealing, K_t=2,5	350	83.8	4.15	-8.41
anodization coading and sealing and then exposure to exfoliation corrosion, K_t=1	450	93.03	3.77	-5.11
anodization coating and sealing and then exposure to exfoliation corrosion, K_t=2,5	350	40.97	3.94	-5.14

Table 5: Derived exponents of the Weibull distribution $\sigma_{max} = C_1 + \frac{C_2 - C_1}{\exp\left(\frac{\log N_f}{C_3}\right)^{C_4}}$ for the alloy 2024.

Stress Ratio R	"ref 2" 2024		"ref 2" 2024 corroded	
	C	n	C	n
R = 0.01	$2,87.10^{-10}$	2,20	2.10^{-10}	2,24
	$9,31.10^{-10}$	2,01	$3,29.10^{-10}$	2,20
R = 0.1	$2,8747.10^{-9}$	1,876	$8,73.10^{-11}$	2,42
	3.10^{-9}	1,87	$6,32.10^{-10}$	2,12
R = 0.5	$2,66.10^{-13}$	3,45	$3,13.10^{-12}$	3,04
	$4,899.10^{-13}$	3,36	$5,90.10^{-13}$	3,356
R = 0.7	$4,46.10^{-13}$	3,47	$6,03.10^{-11}$	2,53
	$2,71.10^{-12}$	3,108		

Table 6: Dependency of the constants of the Paris equation on R-values and existing corrosion for the alloy 2024.

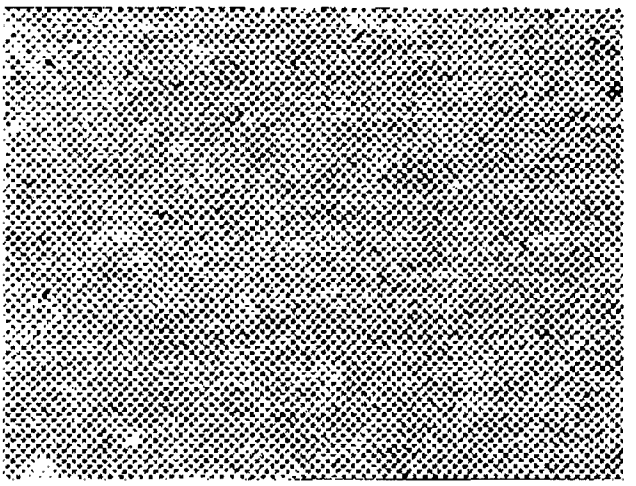

Figure 1: Characteristic micrographs of corroded material 2024 after 24 months outdoor exposure (stereoscopic at 30 x)

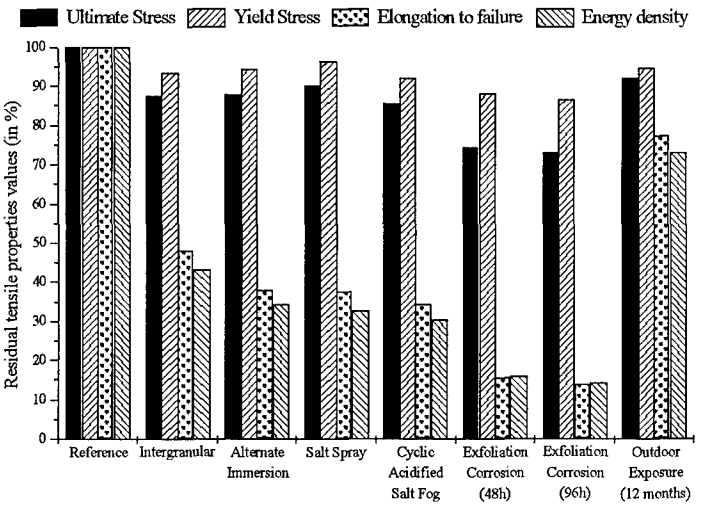

(a)

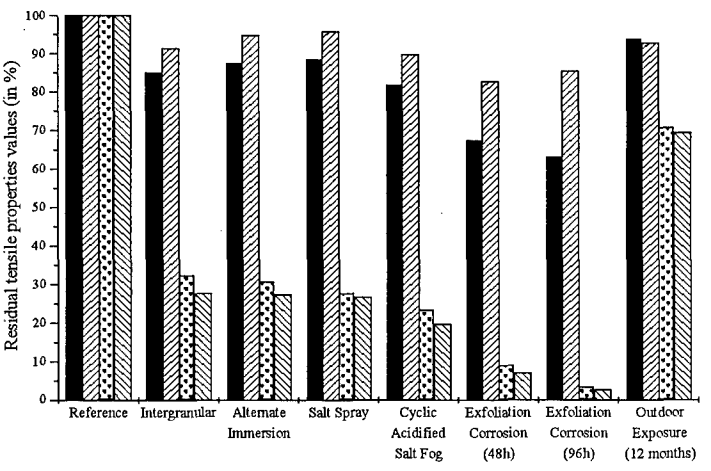

(b)

Figure 2: Tensile behaviour of the alloy 2024 following corrosion exposure according to the relevant specifications for accelerated corrosion tests: (a) L direction, (b) LT direction.

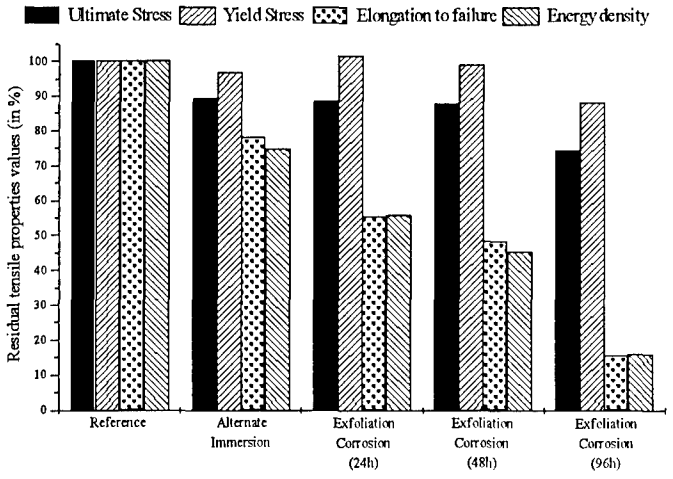

Figure 3: Tensile behaviour of the alloy 2024 "ref. 2", for the L direction, following corrosion exposure according to the relevant specifications for accelerated corrosion tests.

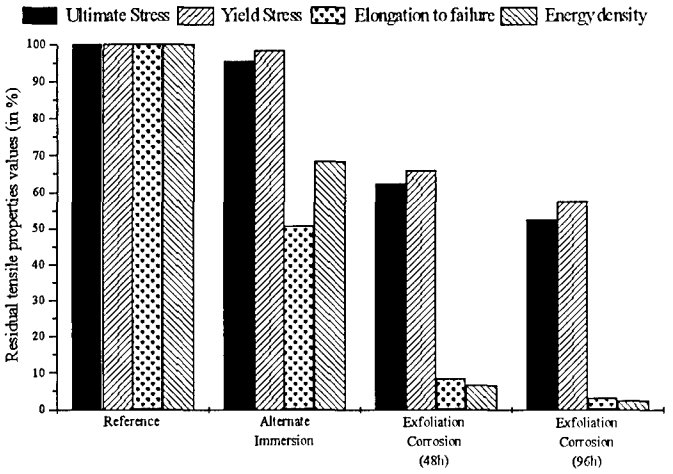

(a)

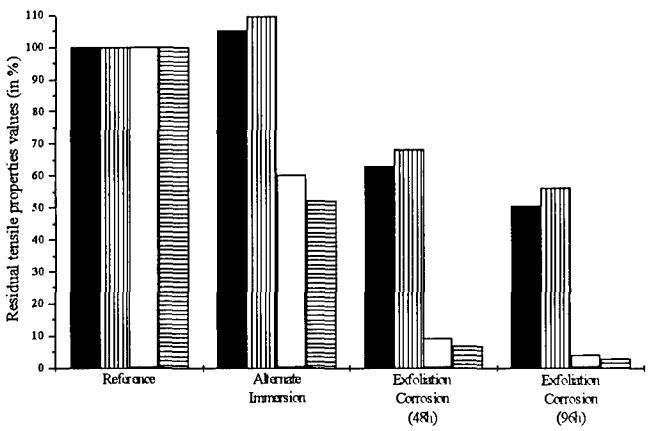

(b)

Figure 4: Tensile behaviour of the alloy 6013 following corrosion exposure according to the relevant specifications for accelerated corrosion tests: (a) L direction, (b) LT direction.

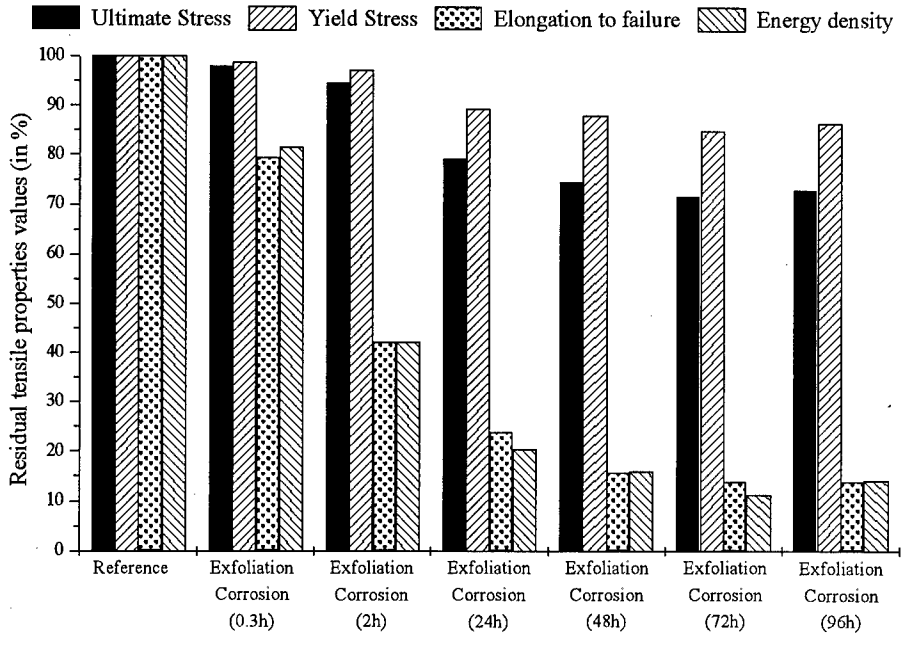

(a)

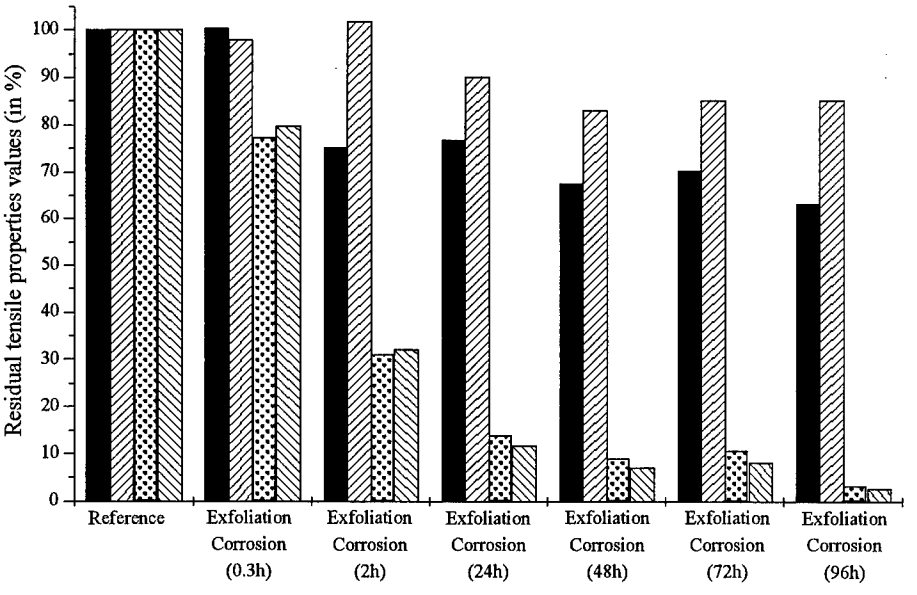

(b)

Figure 5: Gradual tensile property degradation for the alloy 2024 during exposure in exfoliation corrosion solution: (a) L direction, (b) LT direction.

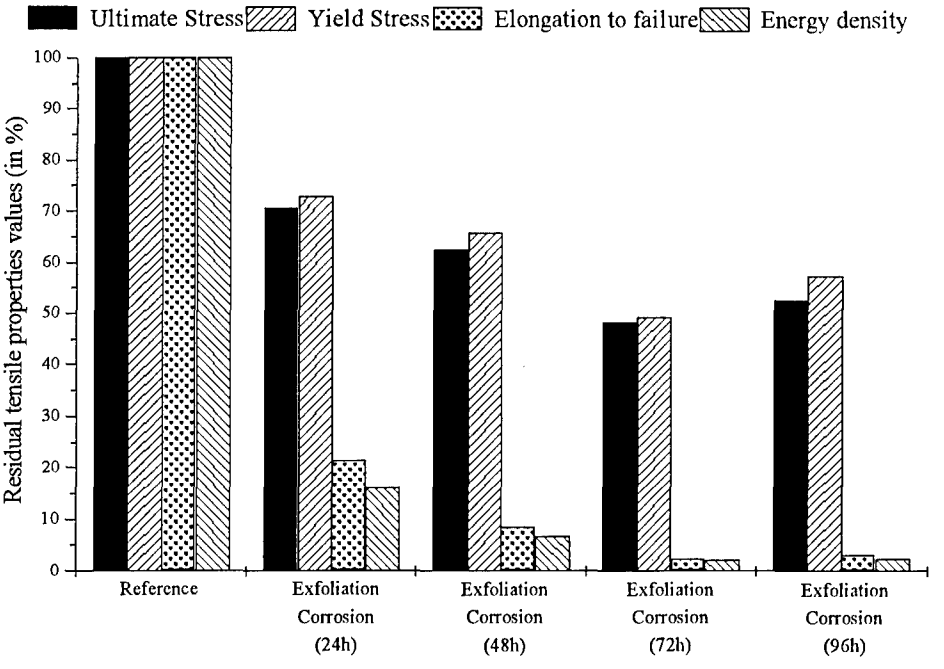

(a)

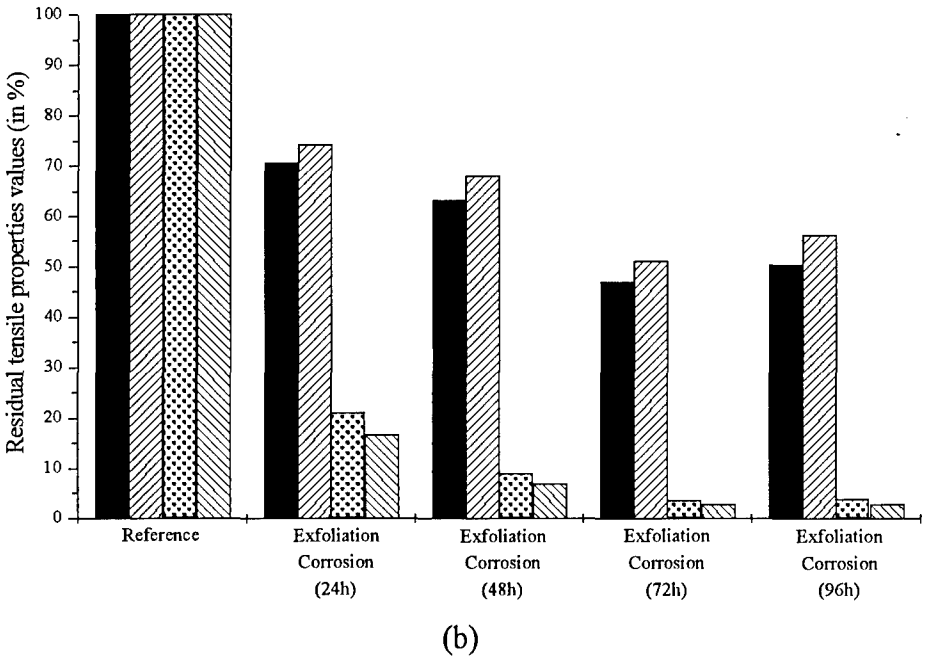

(b)

Figure 6: Gradual tensile property degradation for the alloy 6013 during exposure in exfoliation corrosion solution: (a) L direction, (b) LT direction.

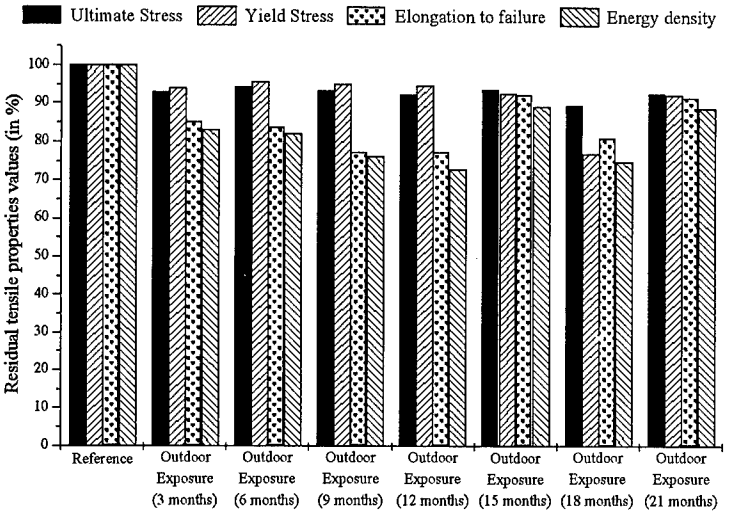

(a)

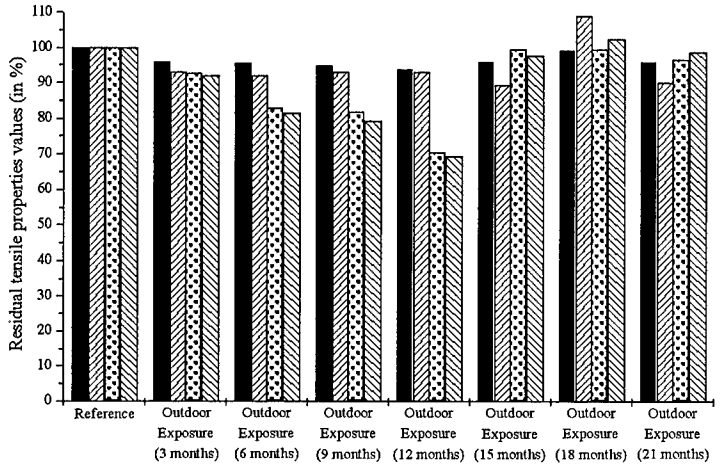

(b)

Figure 7: Gradual tensile property degradation for the alloy 2024 during exposure in atmospheric corrosion: (a) L direction, (b) LT direction.

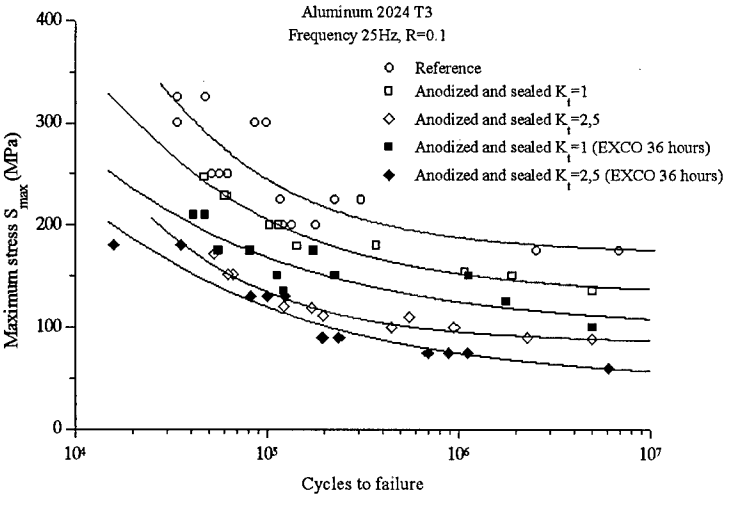

Fig. 8: S-N curves for the anodized and corroded for the 2024 alloy.

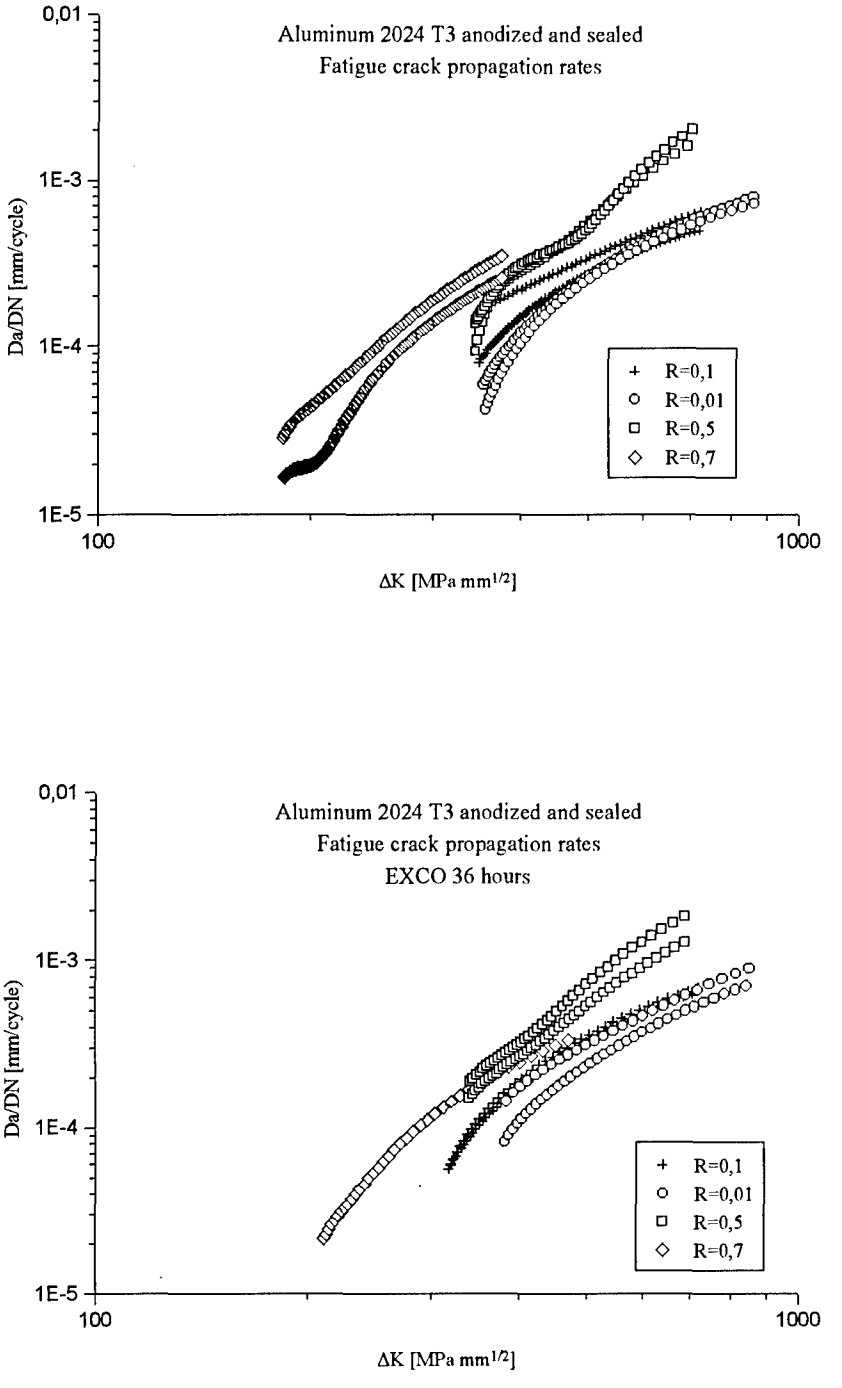

Fig. 9: Fatigue crack growth curves for the anodized and corroded 2024 alloy.

CORROSION FATIGUE OF ALUMINUM ALLOYS TESTING AND PREDICTION

J-M. Genkin*, B.G. Journet

AEROSPATIALE, CCR Louis-Blériot
12, rue Pasteur, BP 76
92152 Suresnes, France

* formerly with AEROSPATIALE

ABSTRACT

Since the Aloha in-flight failure, the ageing aircraft issue has prompted some renewed effort from the research community in the area of corrosion fatigue. This paper presents a methodology which deals with corrosion fatigue crack initiation in a pitting environment. The investigation is carried out on an aluminum lithium alloy. The obtained results shed a new light on the understanding of corrosion fatigue. Before corrosion fatigue cracks take over, the propagating flaw is a hybrid half pit / half corrosion fatigue crack. Both pitting and corrosion fatigue contribute to the flaw growth. A predictive model has been derived. The validation was made by comparing the predictions to experimentally measured pit depths and fatigue lives. A set of guidelines is given for the prediction of in-service corrosion fatigue. It highlights the materials parameters to be evaluated and the testing conditions to use.

1-INTRODUCTION

Ageing aircrafts are prone to corrosive degradations that may result in Multi Site Damage (MSD). On the Aloha airplane which lost a considerable part of its fuselage upper skin in 1988 during its flight, the rupture was caused by the coalescence of a series of corrosion initiated cracks at adjacent rivet holes. Furthermore this MSD was not detected during the last inspection. It means that the cracks do not need to be too long for the MSD to become an impending threat.

MSD reduces the residual strength of a structural part in a much worse manner than a single crack does. Nowadays the fatigue propagation and link-up of MSD is understood and can be calculated (1, 2).

In-house studies have shown that the effect of saline environment (A3 type 3.5% NaCL and ASTM G69) on the crack growth rates of alclad 2024 and 6013 is less than a factor of 2 (3, 4). Tests run at very low frequency such as 0.33 mHz show that the growth rates are the same as in air in Paris' regime. On 2024 the investigation concluded that crack tip blunting and branching balanced the accelerating effect of reduced crack closure. Furthermore low frequency does not increase the effect of hydrogen embrittlement because the diffusion of Hydrogen would be at saturation. On the other hand low frequency does not promote anodic dissolution because the protective oxide film has time to build up. Figure 1 shows the fatigue crack growth rates on alclad 2024 in air and saline environments (3, 4). Tests with lap joints made out of alclad 2024 have shown that as long as the cladding is there to sacrifice itself in the corrosive environment, there is no pitting in the rivet holes. The fatigue properties in air of precorroded joints are therefore preserved (3).

The next step should involve corrosion fatigue when the cladding is no more protecting (dissolved or broken due to low cycle fatigue aound rivet hole). If the propagation stage can be assessed, effort must be placed to clarify and quantify the initiation stage which involves pitting in rivet holes and initiation of corrosion fatigue cracks from pits. This knowledge will help improve the predictions in the application of the damage tolerance philosophy, namely in the assessment of residual life of pitted components. This will further help in defining the initiation scenarii taking into account the influence of corrosion, since initiation is the major source of scatter.

The literature reports few works on the transition from pits to fatigue cracks. Kondo (5) has successfully demonstrated that in steel the transition occurs at a critical stress intensity factor. The underlying principle of Kondo's

Paper presented at the RTO AVT Workshop on "Fatigue in the Presence of Corrosion", held in Corfu, Greece, 7-8 October 1998, and published in RTO MP-18.

model states that fatigue craking is observed when the fatigue crack growth rate exceeds the pit growth rate (Figure 2). In order to make this assessment, the pit is considered as a sharp semi-elliptical crack. Therefore corrosion fatigue crack initiation is a competition between pitting and cracking. This type of approach has not been applied to aluminum alloys.

2-OBJECTIVES

The objectives of the present research work are twofold : understand the transition from pits to fatigue cracks in 2091 alclad alloy, develop a new approach based on a formalism laid down by Kondo to predict the corrosion fatigue behavior of 2091 alclad alloy. The monitored key parameters are the electrochemical potential of the corrosive environment, the frequency and level of the mechanical applied loads.

3-WORK PROGRAMME

The following tasks are carried out (6) :

- pitting behavior evaluation
- fatigue testing in air and saline environment, fractographic examination of crack initiation
- fatigue crack growth rate testing in air and saline environment
- development of model and validation

4-MATERIAL AND TEST SET-UP

4.1-Material

The material is an aluminum lithium alloy supplied by Pechiney-Cégedur : 2091T351 alclad sheet, 1.6 mm thin. The chemical composition and mechanical properties are given in Tables I and II.

4.2-Experimental set-up

Figure 3 shows the experimental set-up for the study of the corrosion fatigue behavior in an NaCl environment under potential control. There are three electrodes : the working sample being the specimen, two platinum foils on each side of the specimen being the counter electrode, and a fine glass tube (Luggin probe) connected to a reference saturated calomel electrode (SCE) through a potassium chloride salt bridge. The potential of the solution is controlled using a Schlumberger 1286 potentiostat.

Polarisation curves for 2091 base and clad were determined (6). Table III gives the respective breakdown, rest and repassivation potentials.

5-PITTING BEHAVIOR

5.1-Specimens

The pitting curves are determined immersing rectangular pieces of alloy mounted in a resin so that only one plane is in contact with the corrosive environment, namely the L-S plane, representative of the orientation of the rivet hole (Long-Short). The specimens were polished down to a 3 micron diamond paste finish.

5.2-Testing conditions

The potential is maintained constant to -660 mV(SCE), just above bare 2091T351 breakdown potential. With this value, both the cladding and 2091 pit. Measurement of the potential response of ASTM G69 solution with clad 2091 yields a stabilized value of -695 mV(SCE), and pitting is observed (6).

5.3-Results

Figure 4 shows the measured pit depths as a function of the immersion time on bare 2091T351. There is a breaking point at 24,000 s. The pits develop around precipitates and are spread evenly across the specimen thickness during the first 20,000 seconds. Then coalescence of pits starts close to the edges. Pitting proceeds with two steps : dissolution takes place along lines in the rolling direction, then bulk dissolution takes on (Figure 5). Power laws can be fitted to the maximum pit depth with exponents of 2/3 for short times, which denotes microstructure effect, and 1/3 for long times where the phenomenon is isotropic (Figure 4) :

$t<24{,}000$ s $\quad d_{max} = 0.74\, t^{2/3}$ microns

$t>24{,}000$ s $\quad d_{max} = 25\, t^{1/3}$ microns.

Bare alloy and clad alloy pit the same way. The curves are shifted and the difference is only the time it took the cladding to dissolve. The pits aspect ratio is 0.2.

6-FATIGUE TESTING

6.1-Test specimens

The specimen geometry used for fatigue testing is shown in Figure 3. The orientation is transverse to the rolling direction. It simulates a section of a fuselage skin with a rivet hole.

The hole surface is ground down to a 3 micron finish with a diamond paste. The surface around the rivet hole was also polished finishing with the diamond paste over an area of 1 cm^2 on both sides. Lacquer was then applied all over the specimen except for the polished areas.

6.2-Testing conditions

The R ratio is 0.05. The environment is lab air and 1M NaCl solution at 25°C. The potential of the saline environment is maintained at -660 mV(SCE). The mesurement of crack initiation to 400 microns is made using a travelling microscope. The frequency goes from 0.1 to 10 Hz in the saline water. Both clad and unclad alloys are tested according to the testing matrix given in Table IV. Interrupted tests are also run for fractographic purpose. Additional tests are also run to investigate crack initiation in the passive range of the alloy.

6.3-S-N data

The results are shown in Figure 6. There is a dramatic effect of the saline environment. A life factor reduction of 3 to 5 is noted. There is a negligible effect of the frequency from tests run under 100 MPa. Tests at different potential values on the clad alloy show that crack inititation time decreases when the potential becomes more anodic.

6.4-Fractography

SEM fractography has allowed to identify four modes of crack initiation, depending on the combination of applied potential, stress and frequency :

- slip band cracking : the combination leaves time for mechanical damage due to cycling to initiate cracks in slip bands at the interface clad/metal on the free surface of the hole. If the potential is passive, this mechanism operates at any stress or frequency levels. In the non passive range, this mechanism will be effective if the clad does not have time to dissolve away (high stress and high frequency).
- initiation from seperated pits and stage I fatigue : few pits forms but cracks readily initiate around them. The pit does not have time to fully develop and remains small (no bulk dissolution). This mechanisms is effective at high/medium stress and medium/high frequency.
- initiation from pits with existence of a transition zone : there is a flat, smooth, pitted zone perpendicular to the applied load axis, between fully developed pits and the corrosion fatigue cracks that has taken over (Figure 7). This clearly shows the competition between pitting and corrosion fatigue crack growth. At this stage the effect of cyclic stress is to homogenize the environment composition and pitting is no more 3 dimensional. This type of mechanisms is observed at low/medium stress and medium/low frequency. Furthermore, pitting is predominant at the apex of the flaw, corrosion fatigue cracking is prevailing at the bottom of the flaw on the edge of the hole. A schematics, Figure 7, skectches the way the corrosion flaw grows.
- initiation due to general pitting : multi pits form and the pit spacing is small so that fatigue initiates in the ligaments between the pits. A through thickness crack readily forms and its propagation takes place in parallel with pitting. This mechanism operates at low/medium stress and low frequency.

Table V gives a summary of the tests with the corresponding initiation modes.

7-FATIGUE CRACK PROPAGATION

7.1-Test specimens

The specimen geometry used for da/dN data is a typical CCT panel, 76.2 mm (3.0 in) wide. The orientation is T-L.

7.2-Testing conditions

The R ratio is 0.05. The applied potential is -750 mV(SCE), which is just above the breakdown potential of alclad 2091. The test frequency is 1 and 5 Hz. The crack length is monitored using a travelling microscope.

7.3-da/dN data

The results are plotted in Figure 8. There is a dramatic effect of the environment at low ΔK.

The effect of frequency as seen on the low ΔK regime is negligible. A change of slope is observed around 9 $MPam^{1/2}$. The crack growth rate (mm/cycle) can be fitted with two straight lines :

$\Delta K<9$ $MPam^{1/2}$; $da/dN=2.67\ 10^{-7}\ \Delta K^{2.76}$

$\Delta K>9$ $MPam^{1/2}$; $da/dN=2.57\ 10^{-6}\ \Delta K^{1.74}$.

For the subsequent modelling purpose, short crack and above-threshold behavior will be

accounted for by extrapolation of the above low ΔK line.

8-MODELLING

8.1-Basics

The modelling deals with crack initiation from pits. Linear Elastic Fracture Mechanics is assumed to be valid shortly after crack initiation from pits. Equivalent stress intensity factors are calculated on corrosion pits. Pits and corrosion fatigue cracks are modelled as sharp semi-elliptical cracks. Stress intensity factors are calculated at the tip or at the hole surface edge only, since those two give the maximum and the minimum values on the crack contour. Pit growth rate and corrosion crack growth rates are computed. The comparison of the two with the threshold for corrosion fatigue crack growth tells whether pitting prevails or not on each point.

The notch effect is accounted for. Flaw interaction and coalescence is also taken into account. Flaw interaction between neighboring pits is calculated, assuming similar flaws as is often seen on the fractographies, with an interaction parameter $\lambda=2a/d$, where 2a is the flaw width on the surface edge and d=2a+flaw spacing : $K=K(1+\lambda^7)$ (ref 6). Coalescence is assumed to take place when the cyclic plastic zones on the surface edges are in touch with each other. Finally the threshold for fatigue crack propagation has been determined from a flaw that has initiated a crack on the edge only : between 0.6 and 1.2 $MPam^{1/2}$.

8.2-Simulation when there are transition zones

This is the case when pits are isolated or in a cluster. The schematics in Figure 9 illustrates the different three phases to account for. Phase I which is initiation where the flaw is hybrid half pit / half corrosion fatigue. The flaw propagates by dissolution at the tip and fatigue at the surface edges. Phase II which is unconstrained / constrained transition to crack formation depending on whether the pits are isolated or mechanically interacting with each other. Phase III is the coalescence of the cracks to form a through thickness crack. The analysis computes the number of cycles to transition, to coalescence, to form a through thickness crack, to initiate a 400 microns surface crack and to failure.

Simulations were run at 1 Hz and 10 Hz with differents sets of active pits at the beginning. Figure 10 gives an example of the output of the simulation at 100MPa and 1 Hz. The window gives the number of active pits that should be there : 3 to 7. The corresponding experimental values are 4 to 7. Figures 11 and 12 show the comparison between the predictions and the experiments in terms of pit depths and fatigue lives.

At 1 Hz, there is fair agreement. At 10 Hz, the agreement is not as good. The model overestimates both fatigue life and pit depth. It seems that the transition to corrosion fatigue is earlier. At 65 MPa and 1 Hz, the simulation seems to work but general pitting was observed as well. At 140 MPa and 10 Hz, pitting is actually very limited.

At 100 MPa and 0.1 Hz, the simulation works out but general pitting also took place. At 100 MPa and 0.5 Hz, the simulation is also reasonably good but general pitting is also observed.

In the cases where pitting with transition zone is not the only mechanism (Table V), an extension to the model is proposed thereafter (§8.3 and 8.4).

8.3-Simulation in the case of limited pitting

The pits do not have time to develop as is the case at 140 MPa, 10 Hz on the unclad alloy. Fatigue develops everywhere. In this case the life is calculated with a through crack the length of which is that of the pit depth. The results are plotted in Figure 12, curve labeled « minimum fatigue life ». This curve is actually a lower bound for fatigue lives. The prediction is good at 140 MPa. However the real behavior at lower stresses stands between the two dimensional flaw model and this short pit model.

8.4-Simulation in the case of general pitting

Pitting and corrosion fatigue cracking are decoupled. A through thickness corrosion fatigue crack forms from pit coalescence. The model therefore calculates on one hand the corrosion fatigue crack growth, on the other hand the pit growth (Figure 13). From fractographic analysis, the cases of general pitting involved 15 pits. The fatigue life is given by the addition of three times : time to dissolve the cladding + time to grow the pit to

coalescence and initiate the through crack + time to grow the initiated corrosion fatigue crack (initial length equal to the plastic zone size in the interpit ligament when the pits coalesce) until failure.

Under the condition of 65 MPa and 1 Hz, the simulation yields a life of 10,000 + 4900 + 154,000 =170,000 cycles which fairly agrees with the experimental values of 160,000 and 185,000 cycles. Furthermore the calculated maximum pit depth is 1020 μm which is close to the experimental 1100 μm.

Under the condition of 100 MPa and 0.1 Hz, where the test was stopped at 16,000 cycles, the simulation calculates a crack length of 814 μm and a maximum pit depth of 1300 μm . The measured crack depth is between 800 μm and 1000 μm, the measured maximum pit depth is 1200 μm at most.

8.5-Mechanisms mapping

Figure 14 gives an overview of the prevailing mechanisms with respect to stress range $\Delta\sigma$ and frequency f relative to the carried out tests. The boundaries of the different domains (limited pitting, transition zone, general pitting) can be fitted with a power law :

$$\Delta\sigma \times f^{2.76} = \text{constant.}$$

9-CONCLUSION

The corrosion fatigue behavior of 2091 alloy was investigated with respect to the following parameters : electrochemical potential of 1M NaCl environment, applied stress range and frequency. In a pitting environment, corrosion fatigue is a competition between pitting and fatigue. Fatigue cracks initiate around the pit on the surface edge while pitting prevails at the pit tip.

The model which has been developed gives satisfactory results. The model could be refined taking into account the short crack behavior (acceleration) especially when the pits leading to crack initiation are small (less than 100 μm). The present study gives grounds to define a methodology in order to make predictions once the operating conditions are known : electrochemical potential of the corrosive environment, applied stress range and frequency. The innovation stands in handling the half pit / half corrosion fatigue flaw. The needed data, with respect to an identified environment (nature and potential) are pit growth, da/dN (long and short cracks) down to threshold, pit shape and population.

This methodology could be applied to ageing airplane. The predictions will deal with the worst case (no protection from the cladding). Corrosion can be assumed to be effective when the plane is on ground. The fuselage pressurization cycle (R=0) with corrosion is the stress range of concerned. The da/dN data could be those in air since the frequency of the fuselage cycle is low and past experience have shown that in this case the growth rates in saline environment fall onto those in air. The only hard point is to define an equivalent in-service corrosive environment.

ACKNOWLEDGEMENTS

This work was carried out by J-M. Genkin at M.I.T., under the supervision of Professor R.M. Pelloux and Professor R. Ballinger. During this time J-M. Genkin was with AEROSPATIALE. This collaboration between M.I.T. and AEROSPATIALE was technically monitored by Louis-Blériot Corporate Research Center and supported by the Aircraft Division.

REFERENCES

1. BRITE EURAM « SMAAC »
2. ICAF 1993
3. J. Foulquier, D. Schuster : « Influence d'un milieu corrosif sur l'amorçage et la propagation de fissures de fatigue dans les alliages légers ». AEROSPATIALE report n° DCR/M-62198/F-96.
4. J-M. Genkin, R.M. Pelloux and B. Journet: « La fatigue corrosion dans le domaine de l'aéronautique commerciale - rapport final CSN ». AEROSPATIALE report n° DCR/M-62704/F-96.
5. Y. Kondo : « Prediction of Fatigue Crack Initiation Life Based on Pit Growth ». Corrosion, vol. 45, n° 1, pp. 7-11, 1989.
6. J-M. P. Genkin : « Corrosion Fatigue Crack Initiation in 2091-T 351 Alclad Aluminum-Lithium Alloy ». Ph. D. Dissertation, MIT, june 1996.

- Table I -

Chemical composition in w% of 2091

elements	Li	Cu	Mg	Fe	Si	Mn	Cr	Zn	Zr
2091	1.7-2.3	1.8-2.5	1.1-1.9	0.3	0.2	0.1	0.1	0.25	0.04-0.16

- Table II -

Mechanical properties of alclad 2091T351

L			LT			45°		
Y (MPa)	UTS (MPa)	elongation (%)	Y (MPa)	UTS (MPa)	elongation (%)	Y (MPa)	UTS (MPa)	elongation (%)
265	364	10	265	384	10	236	350	15

- Table III -

Potential values of alclad 2091T351 in 1M NaCl at 25°C

material	breakdown potential mV(SCE)	rest potential mV(SCE)	repassivation potential mV(SCE)
2091	-685	-940	-1,000
cladding	-760	-910	-960

- Table IV -

Fatigue testing matrix

alloy	frequency	65 MPa	80 MPa	100 MPa	120 MPa	140 MPa
clad	0.1 Hz	-	-	Y	-	-
clad	0.3 Hz	-	-	Y	-	-
clad	0.5 Hz	-	-	Y	-	-
clad	1 Hz	Y	Y	Y	Y	Y
clad	5 Hz	-	-	Y	-	-
clad	10 Hz	-	-	Y	-	-
unclad	10 Hz	Y	Y	Y	-	Y

- Table V -

Fatigue crack initiation modes

alloy	frequency	65 MPa	80 MPa	100 MPa	120 MPa	140 MPa
clad	0.1 Hz	-	-	GC/P	-	-
clad	0.3 Hz	-	-	P/GC	-	-
clad	0.5 Hz	-	-	P/GC	-	-
clad	1 Hz	GC/P	P	P	P	P
clad	5 Hz	-	-	SBC	-	-
clad	10 Hz	-	-	SBC	-	-
unclad	10 Hz	P	P	P	-	P/SBC

GC : General Corrosion - P : Pitting - SBC : Slip Band Cracking

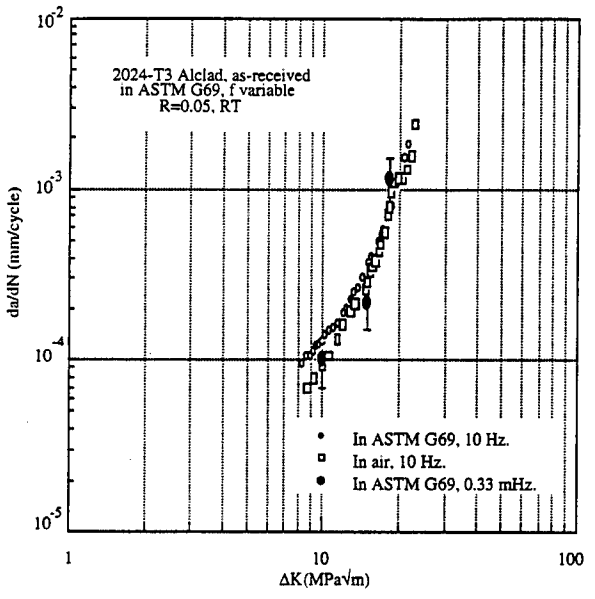

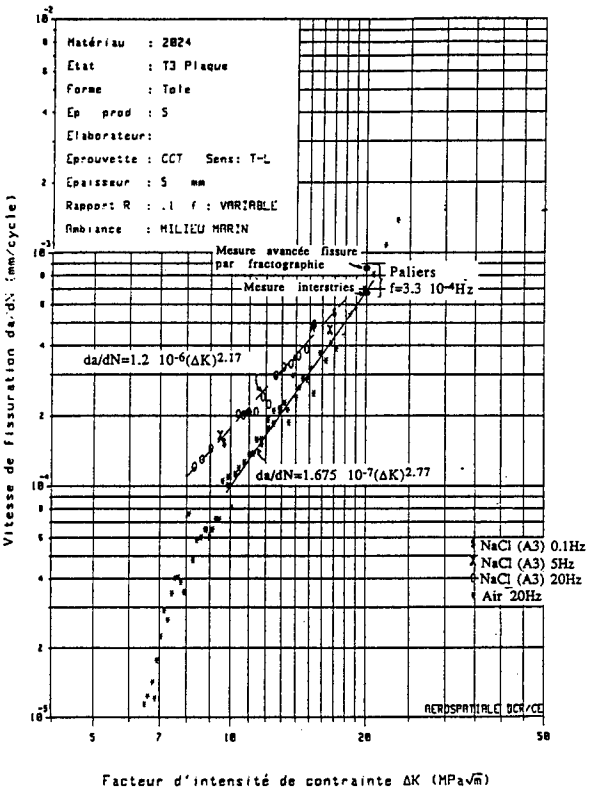

Figure 1
Crack growrh rate data on alclad 2024 in air and in saline environment (A3, ASTM G69) at different frequencies (3, 4).

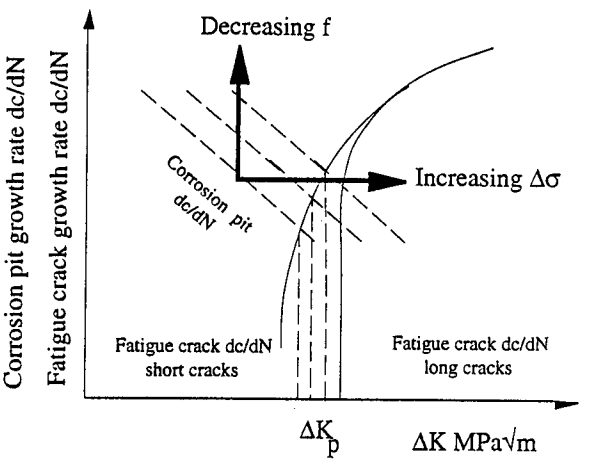

Figure 2
Basics of Kondo's model (5).

Figure 3
Test set-up and fatigue specimen geometry (dimensions in inches)

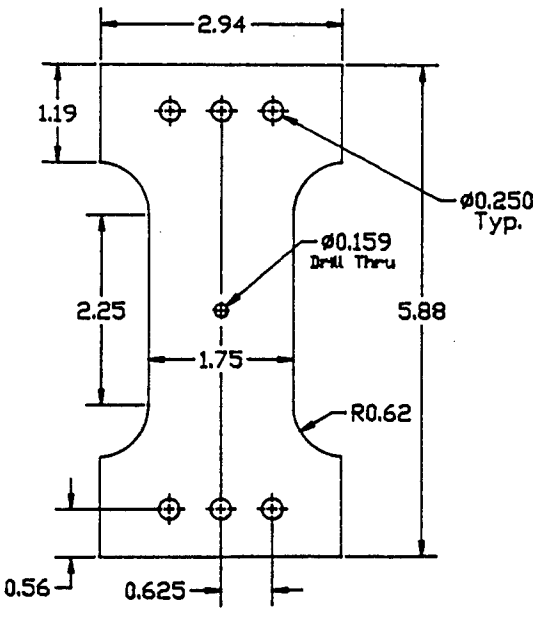

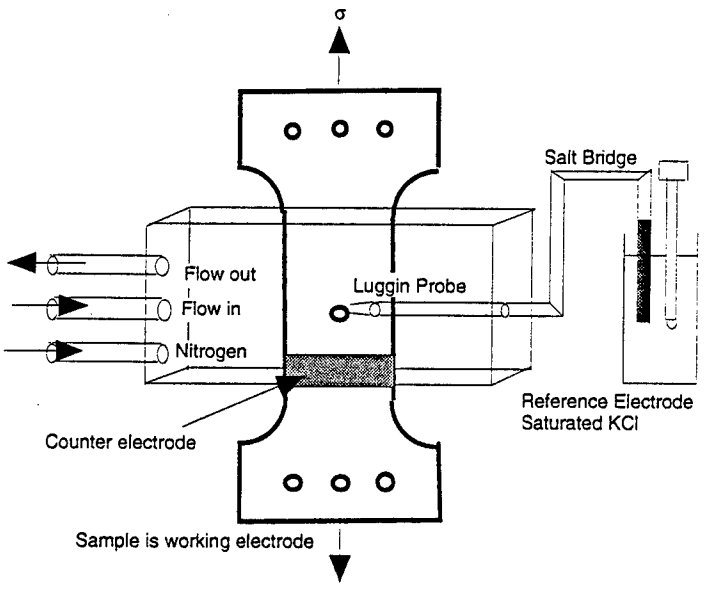

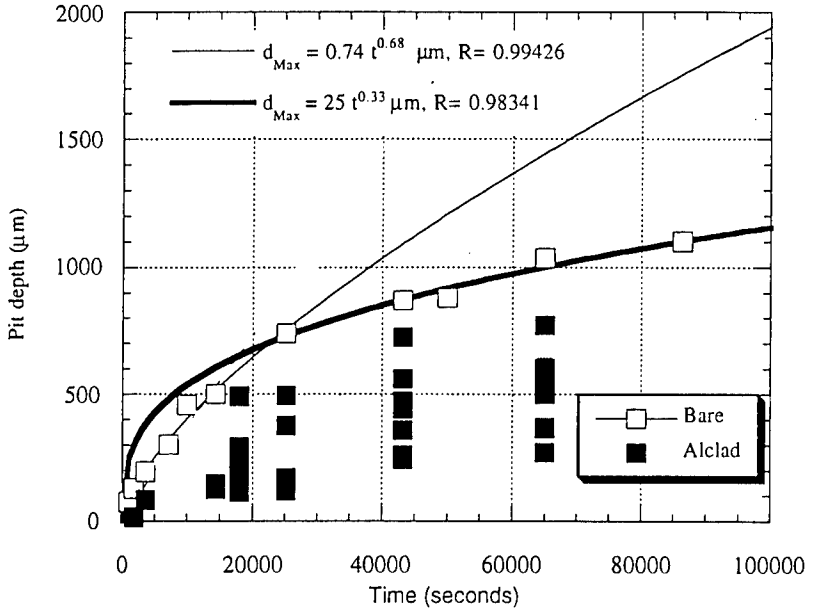

Figure 4
2091T351, maximum pit depth on bare alloy and pit depth on clad with time. 1M NaCl, -660 mV(SCE), RT, deaerated. There is a time shift between clad and unclad alloys.

Figure 5
Two-stage corrosion pitting on 2091T351,1M NaCl, -660 mV(SCE) for 0.5 hour, LT cross-section : dissolution of thin lines along the rolling direction in stage 1, bulk dissolution in stage 2.

Figure 6
2091T351, effect of environment on fatigue life and initiation (400 µm crack).

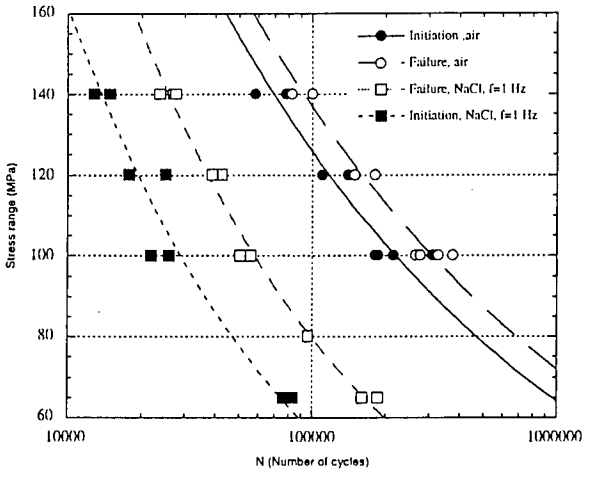

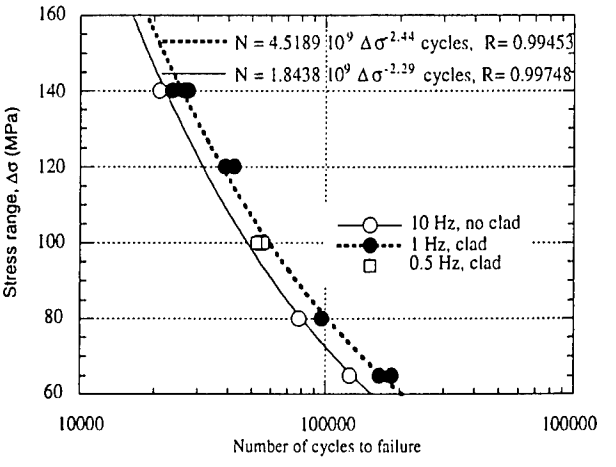

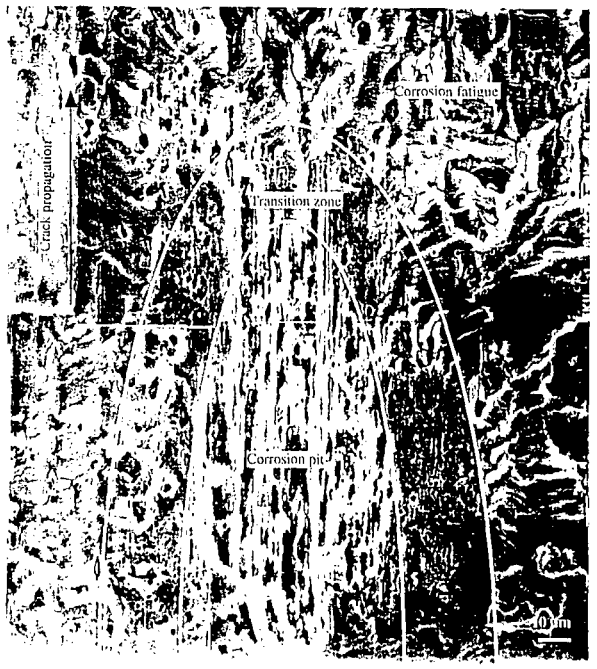

Figure 7
Initiation from pits with the existence of a transition zone.

Top, LH side, 2091T351, 1M NaCl, -660 mV(SCE), $\Delta\sigma$ =120 MPa, R=0.05, 1 Hz : fully developed pit, flat pitted transition zone around leading to corrosion fatigue crack initiation.

Top, RH side, 2091T351, 1M NaCl, -660 mV(SCE), $\Delta\sigma$=100 MPa, R=0.05, 1 Hz : fully developed corrosion pit, the flaw is elongated with a transition zone, the tip of the pit is in contact with the flaw front.

Bottom : schematics giving a proposed interpretation of the corrosion flaw growth : pitting and corrosion fatigue crack growth contribute to the flaw growth.

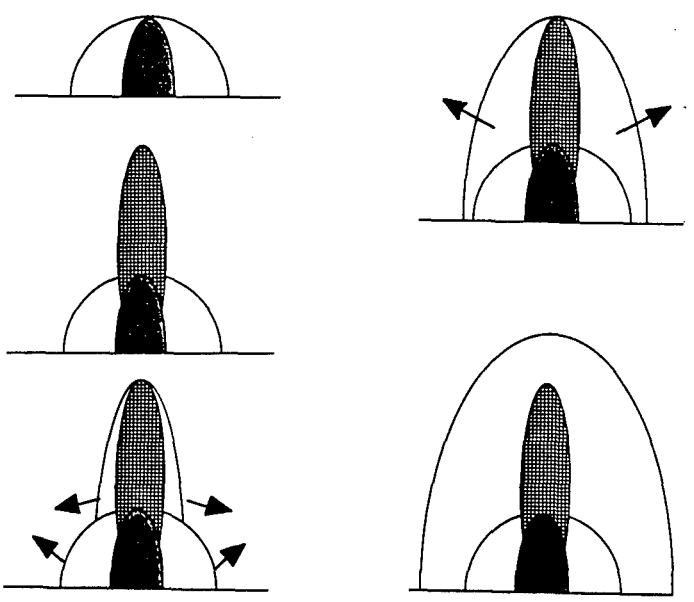

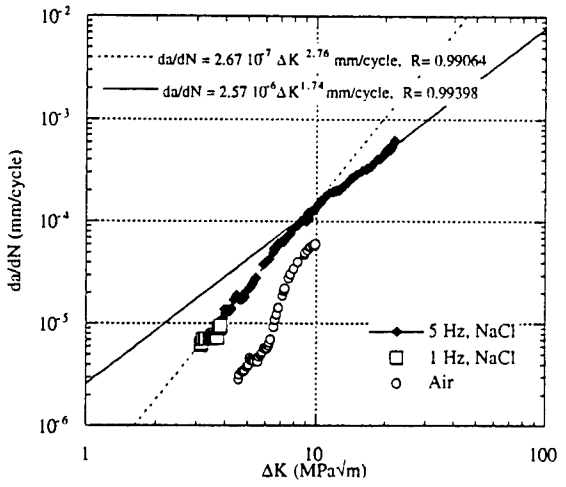

Figure 8
da/dN data on clad 2091T351, R=0.05, in air and in 1M NaCl at -750 mV(SCE), 1 and 5 Hz.

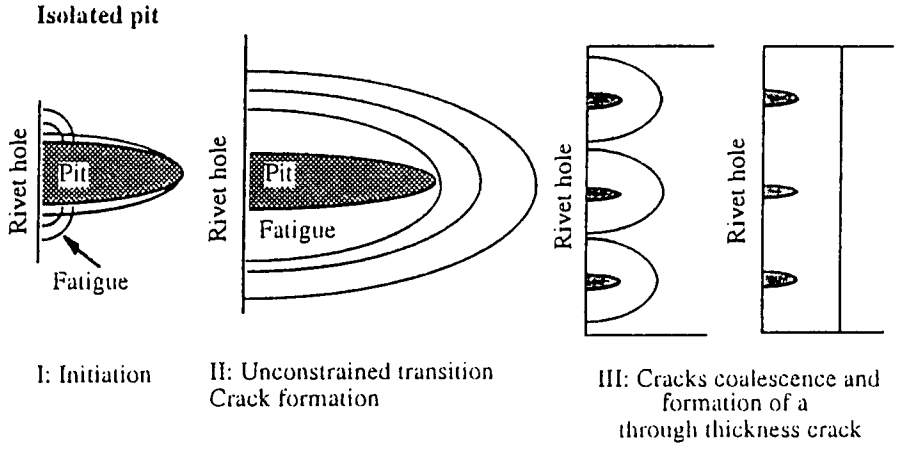

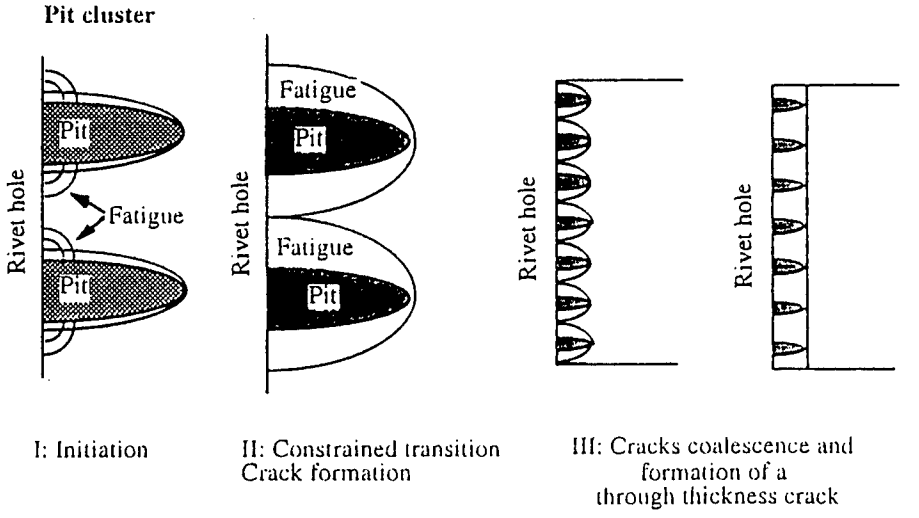

Figure 9
The three phases of flaw growth when there is a transition zone. Two cases are told apart whether pits are isolated or in clusters.

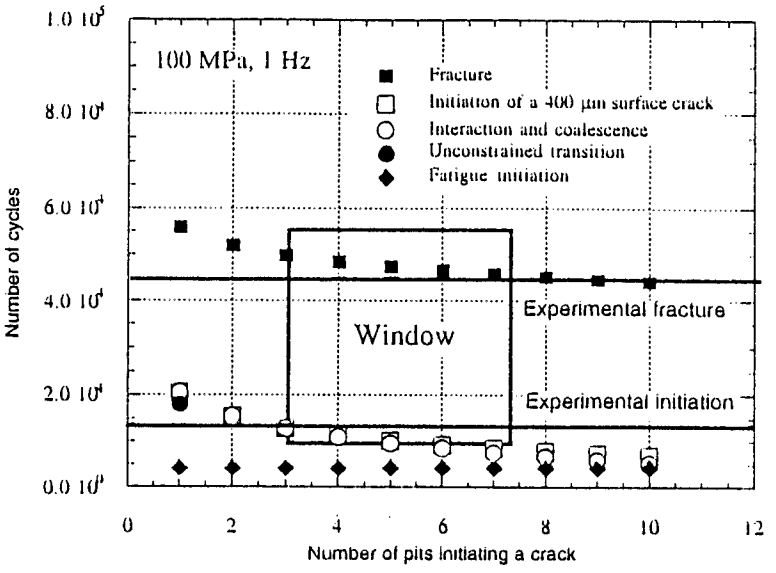

Figure 10

Simulation results on 2091T351, 100 Mpa, 1 Hz : number of cycles to obtain the different phases of corrosion fatigue life with the number of active pits. The window gives the conditions for best agreement with the experimental data.

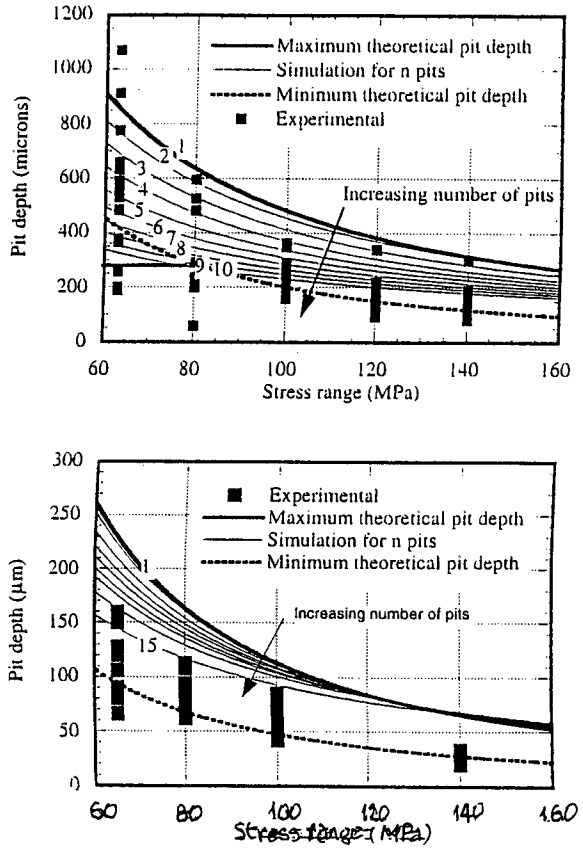

Figure 11

2091T351 alclad : pit depth versus stress range, R=0.05, frequency of I Hz (top) and 10 Hz (bottom) in 1M NaCl at -660 mV(SCE), RT. Comparison simulation with experiments.

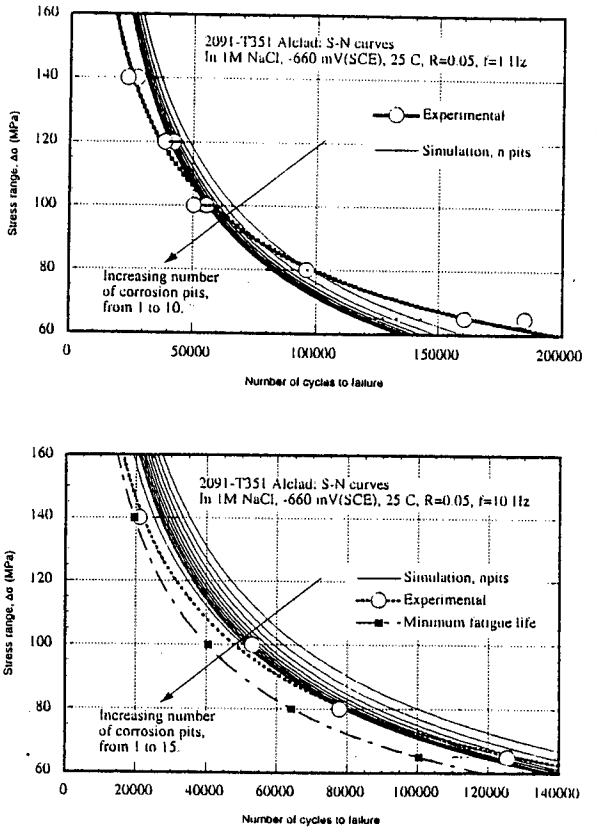

Figure 12

2091T351 alclad : S-N curves, R=0.05, frequency of I Hz (top) and 10 Hz (bottom) in 1M NaCl at -660 mV(SCE), RT. Comparison simulation with experiments.

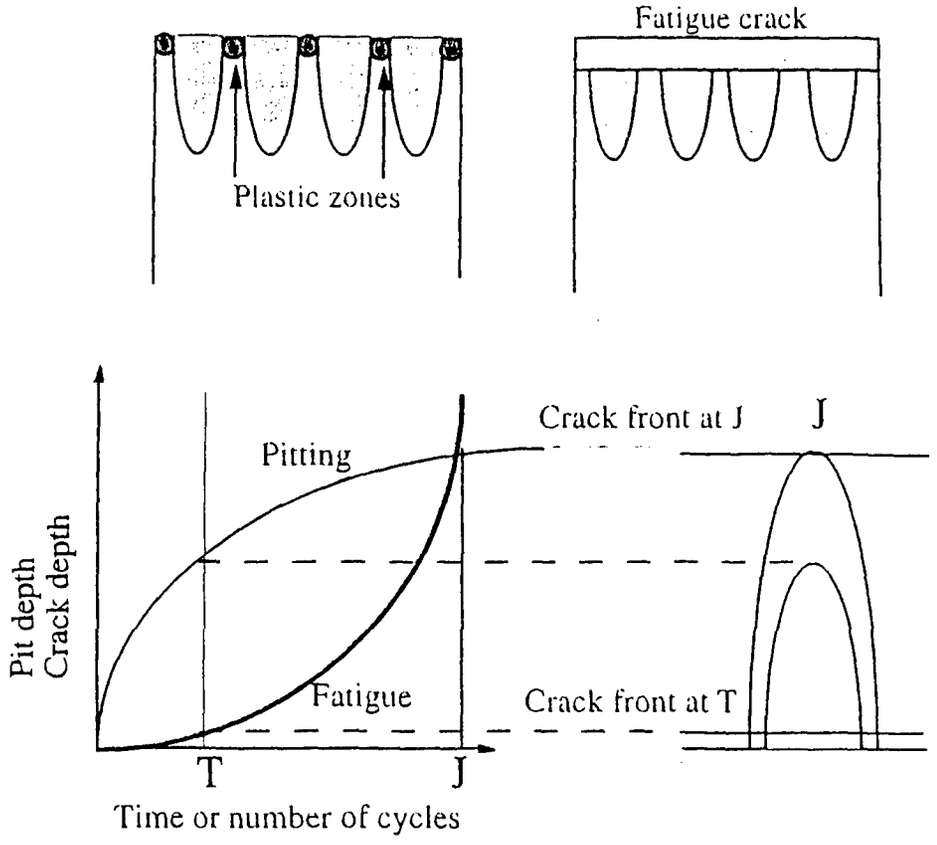

Figure 13

Simulation in the case of general pitting. A through crack forms as soon as all the pits coalesce. The length of the crack is equal to the plastic zone size in the pit ligament upon coalescence. The growths of the pit and of the through crack are decoupled. Maximum pit depth can be predicted as well as time for the through crack to inititiate and run to failure.

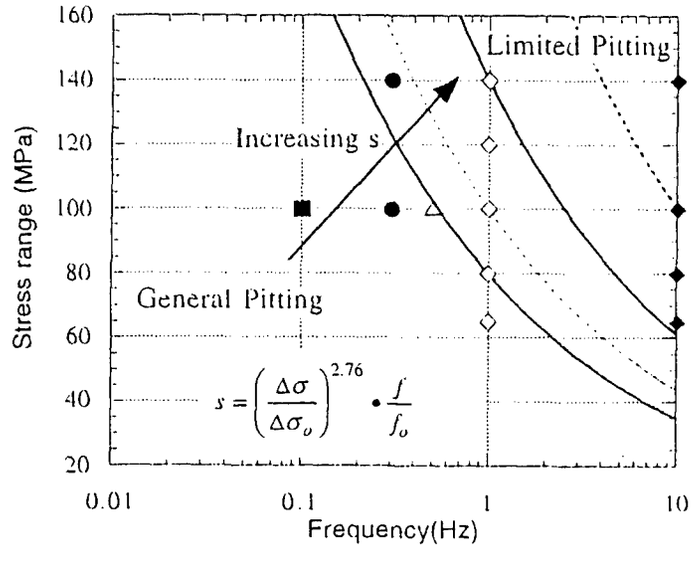

Figure 14

Mapping of the corrosion mechanisms with respect to fatigue stress range and frequency on 2091T351 in 1M NaCl solution at -660 mV(SCE).

INFLUENCE OF CORROSION ON FATIGUE CRACK GROWTH PROPAGATION OF ALUMINIUM LITHIUM ALLOYS

A. Brotzu
M. Cavallini
F. Felli
M. Marchetti
University "La Sapienza" of Rome
Via Eudossiana 18 - 00184 - Rome - Italy

Summary:
The fatigue crack propagation behaviour of three commercial Al-Li alloys (2091, 8090 and Weldalite® 049), supplied by the manufacturer in form of plate, have been studied. A great number of the test have been carried out in order to obtain a reliable set of data. The tests were conducted in air and 3.5 $\%_w$ NaCl aqueous solution at different frequencies (1, 2, 5 and 10 Hz). Fractographic examinations with a scanning electron microscope and a particular etching technique have been done in order to individuate the possible fatigue damage mechanisms.

1. Introduction

Today, designers of military and commercial aerospace vehicles are continuously in search of new materials with lower density and higher strength. The aluminium industry has recently introduced a new generation of aluminium-lithium alloys (Ref. 1-4). Aluminium-lithium alloys are a class of high strength, low density, high stiffness monolithic metallic materials, candidates for replacing in the future the conventional 2000 and 7000 series aluminium alloys currently employed in military and commercial aircraft.
Compared with the other new class of high strength, high stiffness, low density materials, the aluminium matrix composites, Al-Li alloys offer several advantages. Al-Li alloys are only three times more expensive as conventional aluminium alloys, while composites are 10÷30 times more expensive. Al-Li alloys fabrication technologies are compatible with the existing manufacturing methods developed for the conventional aluminium alloys, while composites need more complex production techniques. Al-Li alloys have ductility and fracture properties higher than those of the composites (Ref. 5).
For these reasons, Al-Li alloys became one of the principal alternative to the conventional materials for the applications in safety critical aerospace structures. For this motive their durability and damage tolerance performance are of considerable importance (Ref. 6).
In the past a great number of investigations have been carried out to study various aspects of Al-Li alloys fatigue behaviour (Ref. 6-15). Particularly crack initiation and crack growth behaviour in function of mechanical, microstructural and environmental factors have been examined. These studies have reported superior fatigue crack growth resistance of these alloys in air related to a great influence of closure phenomena induced by an high crack path tortuosity (roughness induced closure) and often to the presence of delamination phenomena. However, much less is known concerning the corrosion fatigue sensitivity of these alloys in more aggressive environment as the marine water (Ref. 16-22). Lithium is one of the most reactive elements; so one would expect that Al-Li alloys are fairly corrosion fatigue susceptible. It was found that these alloys, in marine environment, are more susceptible to corrosion fatigue than Al-Cu alloys (2000 series alloys), while are less sensitive than Al-Zn alloys (7000 series alloys). (Ref. 18)
An other not much investigated aspect of the fatigue behaviour of these alloys is the effect of frequency on the fatigue crack propagation both in air and in aggressive environments (particularly chloride aqueous solution). The few data reported in literature are sometimes contradictory (Ref. 23-25).
The aim of the present work is to investigate the fatigue behaviour of three commercial Al-Li alloys in two different environment (moist air and NaCl aqueous solution) at different frequencies in the range 1÷10 Hz and to correlate the results to some damage mechanism proposed which better interpret them. A statistically significant number of test in each condition, using also different testing machines, have been carried out in order to obtain a reliable set of data.

2. Experimental

Three different commercial Al-Li alloys were studied: 2091, 8090 and Weldalite® 049 (2195). The 2091 alloy was supplied by Pechiney in the form of 12 mm thick plate . The material was in the T8X51 condition (solubilized, quenched, 2% stretched and artificially aged 12 h at 135 °C). The 8090 alloy was supplied by Alcan in the form of 46 mm thick plate. The material was in the T8771 condition (solubilized, quenched, stretched and artificially aged 32 h at 170 °C). The Weldalite® 049 alloy was supplied by Reynolds in the form of 9.5 mm thick plate. The material was in the T8 condition (solubilized, quenched, stretched and artificially aged).
The composition of the alloys, in weight percent, is reported in table 1.

Tab.1 Chemical composition of the alloys

	8090	2091	Weldalite
Li	2.34	2.00	0.96
Cu	1.14	1.90	4.03
Mg	0.55	1.50	0.38
Zr	0.14	0.09	0.12
Fe	0.05	0.05	0.05
Si	0.03	0.03	0.03
Ti	0.03	0.03	0.02
Zn	---	---	0.01
Ag	---	---	0.40
Ni	---	---	0.01
Mn	---	---	<0.005

Mechanical properties of these materials in the longitudinal direction are reported in table 2.

Paper presented at the RTO AVT Workshop on "Fatigue in the Presence of Corrosion", held in Corfu, Greece, 7-8 October 1998, and published in RTO MP-18.

Tab. 2 Mechanical properties of the alloys

	8090	2091	Weldalite
TS MPa	519	497	589
0.2PS MPa	444	379	571
El_5 %	11.5	11.0	10.5

Fatigue tests were performed on compact tension (CT) test specimens machined from the plates in the L-T orientation with B ≈ 9.5÷12 mm and W ≈ 40 mm. These tests were performed using three different fatigue test machines (mechanical, electromechanical and hydraulic). All test were conducted at $R=P_{min}/P_{max}=0.3$ with a maximum load P_{max} of 4 KN and a constant load sinusoidal amplitude waveform. An optical microscope was used to measure the crack length on both side of the specimens.
All da/dn vs. ΔK data were fitted using the different semiempirical models (Paris, Collipriest and Forman), but in this work we show only the curves fitted using the Collipriest model. (Ref. 26-28)
The fatigue tests were conducted in two different environments (air and 3.5%$_w$ NaCl aqueous solution) and at different frequencies (1, 2, 5 and 10 Hz). For each test combination at least 3 specimens were tested. Fracture surface were examined using a scanning electron microscope (SEM). Some fracture surfaces were etched with a particular reagent in order to identify the crystallographic orientation of fatigue crack surface facets. The fracture surface was etched at 25 °C for 5 seconds in a solution of 50 ml H_2O, 50 ml HNO_3, 32 ml HCl and 2 ml HF, immediately flushed with distilled water and dried. Pit geometry (figures 1 a-c) is produced by preferential etching of specific intersecting crystallographic planes. Cracks along {111} planes is characterised by equilateral triangular pits, along {100} planes by square pits and along {110} planes by rectangular pits. (Ref. 17, 22, 29)

3. Results and discussion

Figures 2.a-c show the microstructures of the three studied alloys. The grains are flatted and elongated along the rolling direction. These alloys show a different ricristallization grade, higher in 8090 and lower in Weldalite® 049. The mean grain size is about 20×80×70 μm (respectively in the direction S×L×T) for 8090, 15×50×60 μm for 2091 and 10× 150×150 μm for Weldalite® 049. Intermetallic particles and dispersed phases are observed both along boundaries and inside grains. The maximum quantity of these particles is found in 2091, the lower in 8090.
Figures 3 a-f show the plot of the fatigue crack propagation rate da/dn vs. ΔK of two representative tests (one in air and one in NaCl aqueous solution) for each alloy. The reference test frequency is indicated in the caption. The experimental point scatter is the result of many tests carried out with different fatigue test machines. In this figure the experimental point scatter has been interpolated by the Collipriest model represented by the continuous curve. In general for all the test condition the experimental points are scattered inside a band well fitted by the employed models.
Figures 4 a-f show the comparison between the results obtained at different frequencies for each alloy and environment. In the figure are indicated only the Collipriest curves.
Figures 5 a-c show the comparison of the fatigue crack growth rate vs. ΔK in air and in NaCl aqueous solution for the indicated alloy. Figures 6 show the comparison between the fatigue crack propagation behaviour of the three studied alloy in air (a) and in NaCl aqueous solution (b). The scatter bands in the figures 5 and 6 are the result of all the tests conducted on each alloy in the indicated environment.
From all the results proposed, it's clear that there isn't a direct correlation, in the frequency range 1-10 Hz, between the applied frequency and the fatigue crack growth rate both in air and in chloride solution. It can be only observed that fatigue crack growth rates are higher at 10 Hz for 2091 and Weldalite® 049 alloys. Aqueous chloride solution clearly enhances the rate of fatigue crack propagation in 2091 and 8090 alloy at any used frequency. While Weldalite® 049 alloy seems less sensible to the environment.
The comparison between the three alloys in air doesn't show any appreciable difference in the fatigue behaviour. Only the 2091 alloy, near the threshold region, show higher propagation rates. In aqueous chloride solution Weldalite® 049 shows lower propagation rate at any ΔK.
Figures 7-10 show the fracture surfaces micrographs of the tested alloys carried out after the above-mentioned etching. In the Weldalite® 049 we have found equilateral triangular pits (figure 7, cracks along {111} crystallographic plane) only in the near threshold region, while at higher ΔK levels rectangular pit (crack along {110} crystallographic plane) have been observed (figure8). In 2091 alloy we have found only rectangular pits (cracks along {110} plane) at any ΔK level (figure 9). In 8090 alloy we have found only square pits (cracks along {100} plane) at any ΔK level (figure 10).No difference in the crystallographic propagation planes have been observed between tests carried out in air or in NaCl aqueous solution. However, in this last environment we never observe equilateral triangular pits.
As regard the effect of the frequency, previous studies of other researchers on 8090 alloy are in quite accord with our results. It was found (Ref. 23), for an 8090 alloy, that the fatigue crack growth rate decreases with the increasing of the frequency, in the range 1 -10 Hz, especially at lower ΔK level. For this alloy we have found a tendentialy similar behaviour; in any case, the curves at different frequency are very closer. However the tests of the other researchers were carried out with modalities different from those of our tests.
For the other alloys we have found a tendetialy opposite behaviour.
The good fatigue properties of this class of materials results from a series of phenomena that reduce the crack growth driving force (Ref. 6). Usually Al-Li alloys show an intergranular fracture with evident signs of delamination. Delamination phenomena increase fracture toughness and fatigue resistance in the TL and LT orientations because they divide the specimen in thin sheets, and thus change the expected plane strain state (triaxial load) in a global plane stress state (biaxial load, lower stress level). The higher elastic modulus of Al-Li alloys reduces the crack tip opening displacements, which result at a fixed ΔK in lower crack growth rates per cycle. However, the main phenomena that reduces the crack growth driving force are those related to the roughness induced closure mechanisms (Ref. 6, 16, 17, 23) In fact, Al-Li alloys fatigue fracture surfaces usually show highly non linear and tortuous crack path morphologies. The microscopic crack path deflection results in a reduction of the ΔK which effectively acts at the crack tip, first because the macroscopically applied mode I

load became at the crack tip a mixed mode load, and then because the deflections cause a not complete closure of the crack. This last phenomenon reduces the crack growth driving force because the effective applied K minimum (K_{cl}) is higher than the nominal one (K_{min}) and then the effectively applied ΔK (K_{max}-K_{cl}) is lower than the nominal ΔK (K_{max}-K_{min}). This tortuosity results from the particular fracture mechanism of these alloys.

Two different fatigue fracture mode have been identified which are in competition: a shear facet mode and a flat tensile mode (Ref. 6, 16, 23).

Particularly shear facets fracture mode is prevalent in pure gas (He, H_2, N_2) or in vacuum, while the tensile mode is the result of the interaction of the metal with aggressive environments (i.e. moist air or NaCl aqueous solution).

Usually the first fracture mode is characterised by shear facets protruded by the fracture surface to form "pinnacles". These "pinnacles" produce a zig-zag geometry of the crack path and a mixed mode stress at the tip of the crack. In this kind of fracture the facets were formed by a localisation of the slip on particular crystallographic planes that bring to a slip plane decohesion. This localisation is due to the high coherency and low mismatch between the δ' (Al_3Li) strengthening phase and the Al matrix on the {111} crystallographic plane. In fact, along this crystallographic plane the mobility of dislocation is higher then in other planes in virtue of the coherency between the strengthening phase and the matrix that allows an easy shear of this phase. This shear creates an antiphase boundary. Further shearing by groups of dislocations pairs occurs on the same slip plane in order to minimise the area of antiphase boundary formed. Repeated particle shearing leads to a slip plane softening and may results in particle dissolution, and thus it could lead to a local softening of the materials and a concentration of the deformation with a rapid formation of shear bands and of cracks which deviate from the fracture plane.

The second fracture mode is characterised by a macroscopically flat fracture. Microscopically the fracture surfaces show the presence of transgranular cleavage with river line and sometimes a transgranular features with "herringbone" appearance with some evidence of cracking along subgrain boundaries.

Different mechanisms for the tensile fracture mode have been proposed: local alternate slip, local ductile slip, increased flow stress due to dislocation entanglement that favours cleavage on plane {100}, shear mode growth on intersecting {111} plane that produce a final macroscopic {100} fracture plane. All these mechanisms result from a slip homogenisation (multiple slip).

Macroscopically the difference between these two kind of fracture is in the crack path morphology, and thus in the closure level. The first fracture mode results in higher roughness, and thus in higher closure level and lower crack growth.

Kemp observed on his tests both these fracture mechanisms (Ref. 23). He found that the transition from tensile to shear mode is influenced by the test and R values.

We have observed in our specimens mainly tensile fracture. We have noticed that there is no significative correlation between the kind of fracture mode and the frequency. Figures 11 and 12 show the typical aspect of the fracture surface of 8090 alloy of specimens tested in air at different frequency. It can be noted the typical "herringbone" aspect of the tensile mode fracture. However, the fracture surface aspect is different between specimens broken in air or in aqueous chloride solution. Particularly, the fracture is still in tensile mode, but in aqueous chloride solution the aspect of the surface is more oxidised and corroded. Figures 13 and 14 show the fracture surfaces of the Weldalite® 049 at 5 Hz in air and in chloride aqueous solution at the same ΔK level. As it can be seen the fatigue striations are more corroded and irregular in aqueous solution. Figures 15-17 show the fracture surface of the three alloys tested in chloride aqueous solution. It can be observed the flat tensile mode aspect of the fracture and the corroded and oxidised aspect of these surfaces, particularly manifest in the high magnification micrograph of figure 17. As in the specimens broken in air, also in these there are signs of delamination. Delamination is present also in Weldalite® 049 alloy, which, however, is less susceptible to this phenomenon.

Rarely in air we have found a little shear component in the fracture surface. This component was found always in specimens with the lower fatigue crack growth rate. Figure 18 shows the fracture surface of the 8090 alloy tested at 5 Hz in air. This fracture surface has a more corrugated aspect with more marked "pinnacles" which protruded from the mean propagation plane. As it can be seen from figure 4 c, for this alloy, in these conditions, the fatigue crack growth rate is the lowest.

As it can be observed from figure 5.a-c, aqueous chloride solution enhances the fatigue crack propagation rate of the 2091 and 8090 alloys. Particularly the maximum rise was shown by 8090. On the contrary Weldalite® 049 shows no or very little differences between the crack propagation rate in salt solution or in air.

This behaviour is similar to those reported in literature for this kind of materials (Ref. 6, 16-22). Many authors have noticed that aluminium lithium alloys are particularly susceptible to enhanced fatigue propagation rate in NaCl aqueous solution. In examples a 2090 T81 alloy tested in salt water shows crack propagation rates threefold higher than those measured in moist air (Ref. 6). The mechanisms involved in this rate enhancement are still not well known. Usually this behaviour is attributed to the diminished contribution from roughness induced crack closure, arising from the combined action of the corrosive attack and mechanical fretting in flattening the fracture surface asperities. In fact the fracture surfaces of specimens broken in salt solution are usually more flat and less rough than those of specimens broken in moist air or in other non aggressive environment. However this is not the only mechanism proposed. For instance it has been proposed that the reduced faceting and closure observed in specimens broken in salt solution may be the result of an intrinsic change in the cracking mechanism. The influence of the chloride environment on the cracking mechanisms could be related to the presence of atomic hydrogen at the crack tip or of the oxide surface film. The atomic hydrogen at the crack tip, produced by the reaction between water and not oxidised aluminium on the fracture surface, could enter inside the metal in the processing zone bringing to the embrittlement of the metal. However, the effect of the frequency on the propagation rate suggests that this is not the principal mechanism. In fact usually in most conventional aluminium alloy the crack growth rate increases as the frequency decreases. This is the

typical behaviour of the 7000 alloys. This fact is correlated to the enhanced surface reactions or to the higher mass transport during the longer time period of the cycle that results in an higher hydrogen quantity adsorbed by the metal. On the contrary in aluminium-lithium alloys crack growth rate decreases as the frequency is reduced. This reduction is usually little and it was observed tendentially also in the tested alloys. These considerations suggest that hydrogen embrittlment is not the principal damage mechanism and that the mass transport is not the rate limiting step in the corrosion fatigue process of aluminium-lithium alloys. Rather this effect could be correlated to the higher crack tip strain rates at the higher frequency that results in enhanced anodic dissolution or crack advance by film rupture. This effect may be coupled with the effect of the hydrogen on the fatigue behaviour previously illustrated.
The fracture surface morphology of corrosion-fatigue broken Al-Li alloys is similar to those broken in moist air tough they show a flatter aspect and a greater degree of intersubgrain boundary fracture ({110} and {100} crystallographic fracture plane)and a reduced quantity of slip band cracking ({111} crystallographic fracture plane) especially at higher ΔK levels. At low ΔK levels a transgranular cleavage fracture is often observed. The evident path tortuosity reduction is caused by an environmentally induced change from faceted slip band cracking along {111} crystallographic plane to relatively intersubgranular and {110} and {100} type cracking. This lower roughness is the principal cause of the reduced closure level measured in salt water than in air.

Conclusion

From the fatigue crack growth rate tests carried out in air and in NaCl aqueous solution, in the frequency range of 1÷10 Hz, for three different alluminium-lithium alloys (Weldalite® 049, 8090 and 2091), it can be noted that:

- there isn't any clear correlation between frequency and fatigue crack growth rate in air; there is only a little trend towards higher propagation rates at the highest frequency testes (10 Hz) in 2091 and Weldalite® 049.
- 2091 alloy shows the higher propagation rates at low ΔK level (near threshold).
- fatigue crack growth rate raises when the specimens are tested in NaCl aqueous solution, especially for the 8090 and the 2091.
- Weldalite® 049 is less sensible then the other tested<alloys to the propagation in this environment.
- in NaCl aqueous solution, all alloys show the lower propagation rate at the lower frequencies.
- all fracture surfaces of specimens broken in air show a mainly tensile aspect.
- all fracture surfaces of specimens broken in NaCl aqueous solution show a flat tensile aspect with clear sign of oxidation and with rounded and blunted asperities.
- little components of shear mode fracture have been found in the specimens tested in moist air with the lowest propagation rate.

Bibliography

1. R. Grimes et al, Sixth International Aluminum-Lithium Conference, Garmish-Partenkirchen (1991), M. Peters and P.I. Winkler eds.), Vol. 1, pp. 3-14.
2. R. H. Graham et al., ibidem, Vol. 1, pp. 15-24.
3. T. Wakiyama et al., ibidem, Vol. 1, pp. 25-34.
4. I. N. Fridlyander et al., ibidem, Vol. 1, pp. 35-44.
5. F. Felli et al., *Mater. Sci. And Techn.*, Vol. 13, pp. 420-429, (1997).
6. K.T. Venkateswara Rao and R.O. Ritchie, *Int. Mater Rev.*, Vol.37, No. 4, pp.153-185, 1992.
7. M. Cavallini, F. Felli and M. Marchetti, *L'Aerotecnica - Missili e Spazio*, Vol. 66, No. 3, pp. 149-158
8. M. Cavallini, F. Felli and P. Delogu, *Met. Sci and Tech.*, Vol. 9, No. 1, pp. 3-9, 1991.
9. M. Cavallini and F. Felli, in "Aluminum-Lithium" Sixth International Aluminum-Lithium Conference, Garmish-Partenkirchen (1991), M. Peters and P.I. Winkler eds.), Vol. 1, pp. 627-631.
10. D. Buttinelli et. al., in "EUROMAT 95", 4th European Conference on Advanced Materials ans Processes, Padua-Venice (1995), Symposium F, pp. 495-498.
11. K. J. Park et. al., *Mater.Sci. and Eng.*, Vol. A190, pp. 99-108, (1995).
12. K. T. Venkateswara et al., in Aluminum-Lithium Alloys, Fifth International Aluminum-Lithium Conference, Williamsburg, Virginia (1989, T. H. Sanders Jnr. And E. A. Starke Jnr. Eds.), Vol.3, pp. 955-971.
13. J. Petit et al., Sixth International Aluminum-Lithium Conference, Garmish-Partenkirchen (1991), M. Peters and P.I. Winkler eds.), Vol. 1, pp. 521-532.
14. M. Darvish and S. Johansson, ibidem, Vol. 1, pp. 557-562.
15. B. O'Brien and A Pradier, ibidem , Vol. 1, pp. 657-662.
16. R.S. Piascik and R.P. Gangloff, *Met. Trans. A*, Vol. 22A, pp. 2415-2428, 1991
17. R.S. Piascik and R.P. Gangloff, *Met. Trans. A*, Vol. 22A, pp. 2751-2762, 1993.
18. P.S. Pao et al., *Corrosio n*, Vol. 45, No. 7, pp.530-535, 1989., (1987).
19. T.S. Srivatsan and E.J. Coyne, *Eng. Fract. Mech.*, Vol. 36, No. 1, pp. 123-135, (1990).
20. S-I. Pyun and Y.G. Chun, *Corrosion Science*, Vol. 35, Nos. 1-4, pp. 611-619, (1993).
21. R. M. J: Kemp and R. N. Wilson, Sixth International Aluminum-Lithium Conference, Garmish-Partenkirchen (1991), M. Peters and P.I. Winkler eds.), Vol. 1, pp. 575-580. (1995)
22. M. Darvish and S. Johansson, *Fatigue Fract. Engng. Mater. Struct.*, Vol.18, No. 3, pp. 319-327,
23. Kemp et al., *Fatigue Engng Mater. Struct.*, Vol. 15, No. 3, pp. 291-308, 1992.
24. H. Mayer and C. Laird, *Mater. Sci and Eng.*, Vol. A187, pp. 23-35, (1990).
25. R. P. Wei et al., *Met. Trans. A*, Vol. 11A, pp 151-158, (1980).
26. P.C. Paris and F. Erdogan, *J. Basic. Eng*, Vol 85n, p 528, (1963)
27. J. E. Collipriest et al., "Fracture mechanics equation for cyclic crack growth", Technology Utilisation Report MFS 24447, NASA, USA, (1973).
28. "Fracture Control Guidelines" ES PSS-03-1203, ESTEC, ESA, Noordwijk, the Netherlands, (1986).
29. M. Gao et al., *Met. Trans A*, Vol 19A, pp. 1739-1750, (1988).

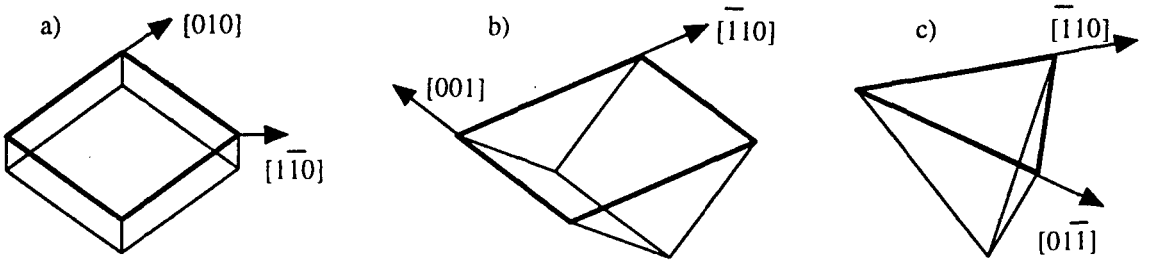

Fracture plane (100) Fracture plane (110) Fracture plane (111)

Fig. 1 Etch pits shapes more commonly observed

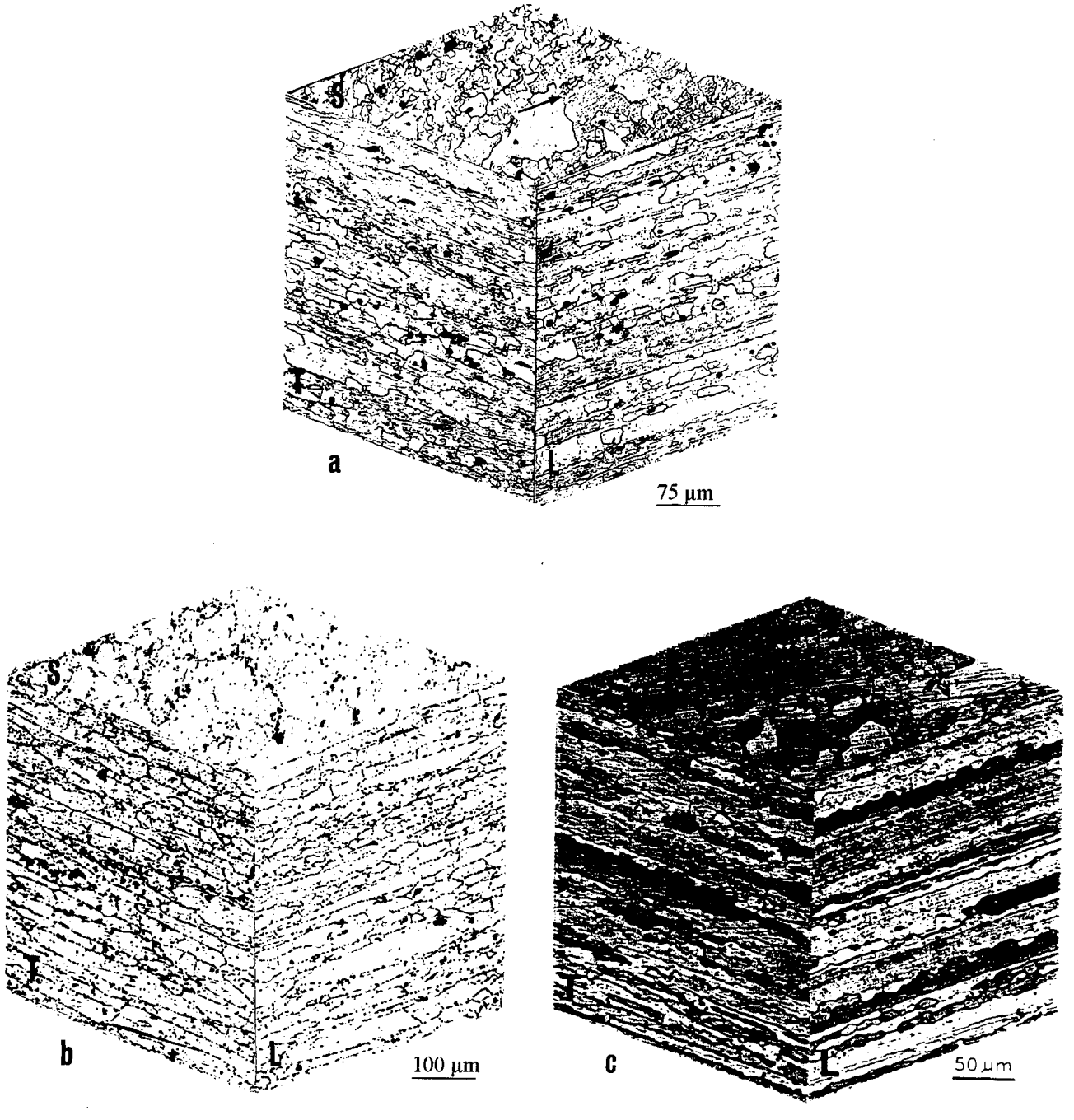

Fig. 2 Three dimensional optical micrographs of: a) 2091, b) 8090, c) Weldalite® 049

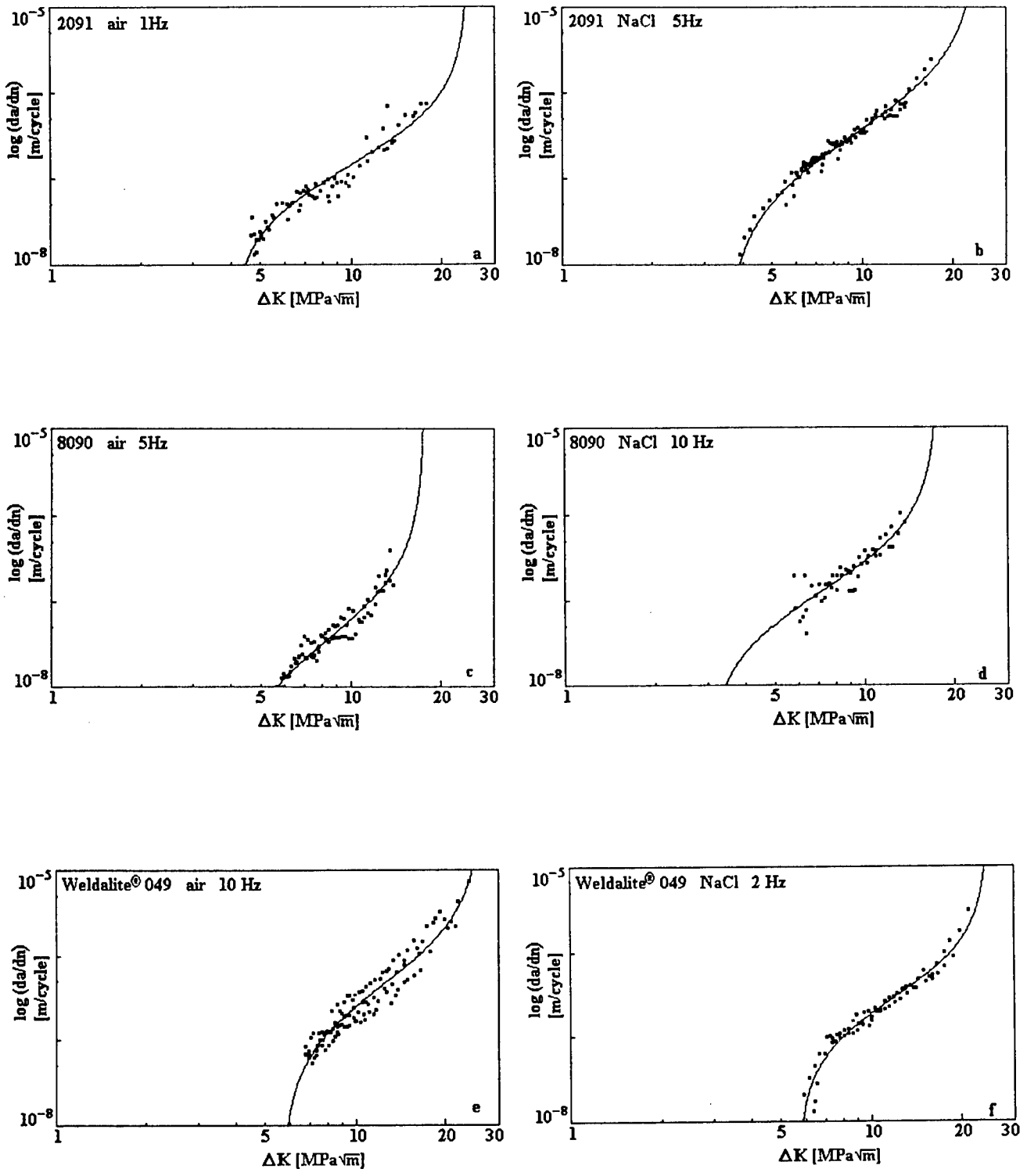

Figg. 3 a-f Fatigue crack propagation rate vs.ΔK of two representative tests (one in air and one in NaCl aqueous solution) for each alloy.

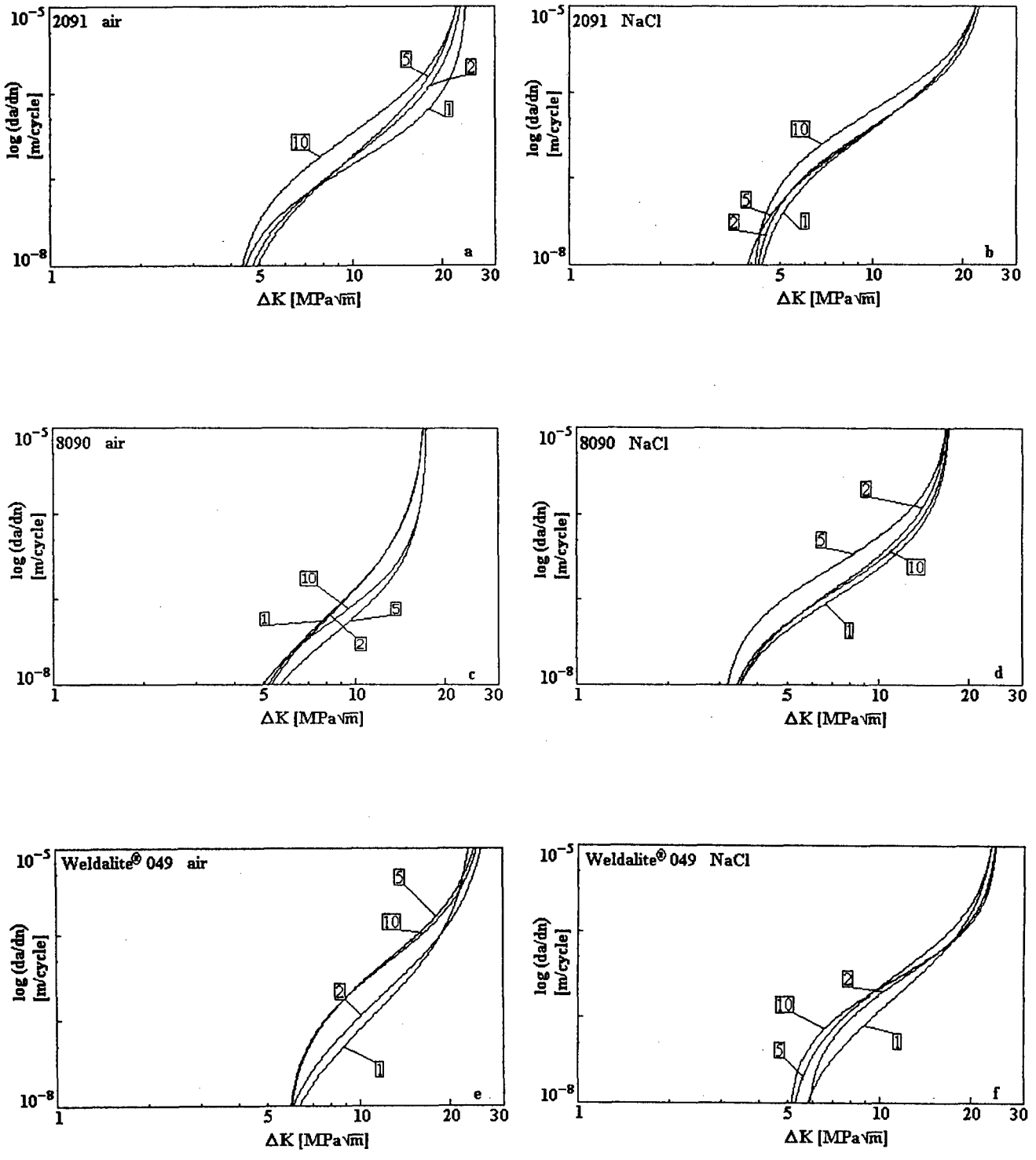

Figg. 4 a-f Comparison between the results obtained at different frequencies for each alloy and environment.

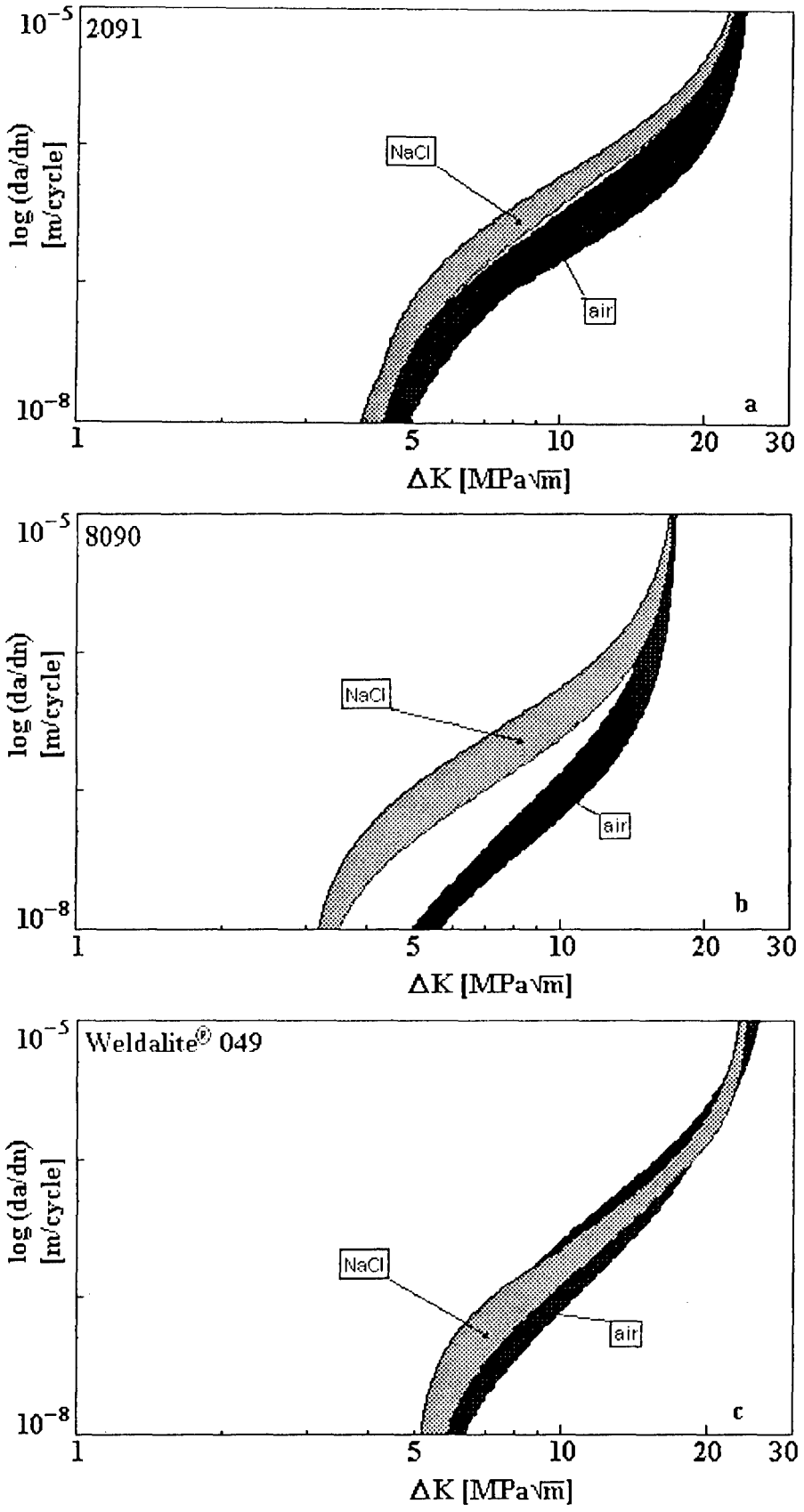

Figg. 5 a-c Comparison between the fatigue crack propagation rate in different environment for the indicated alloy.

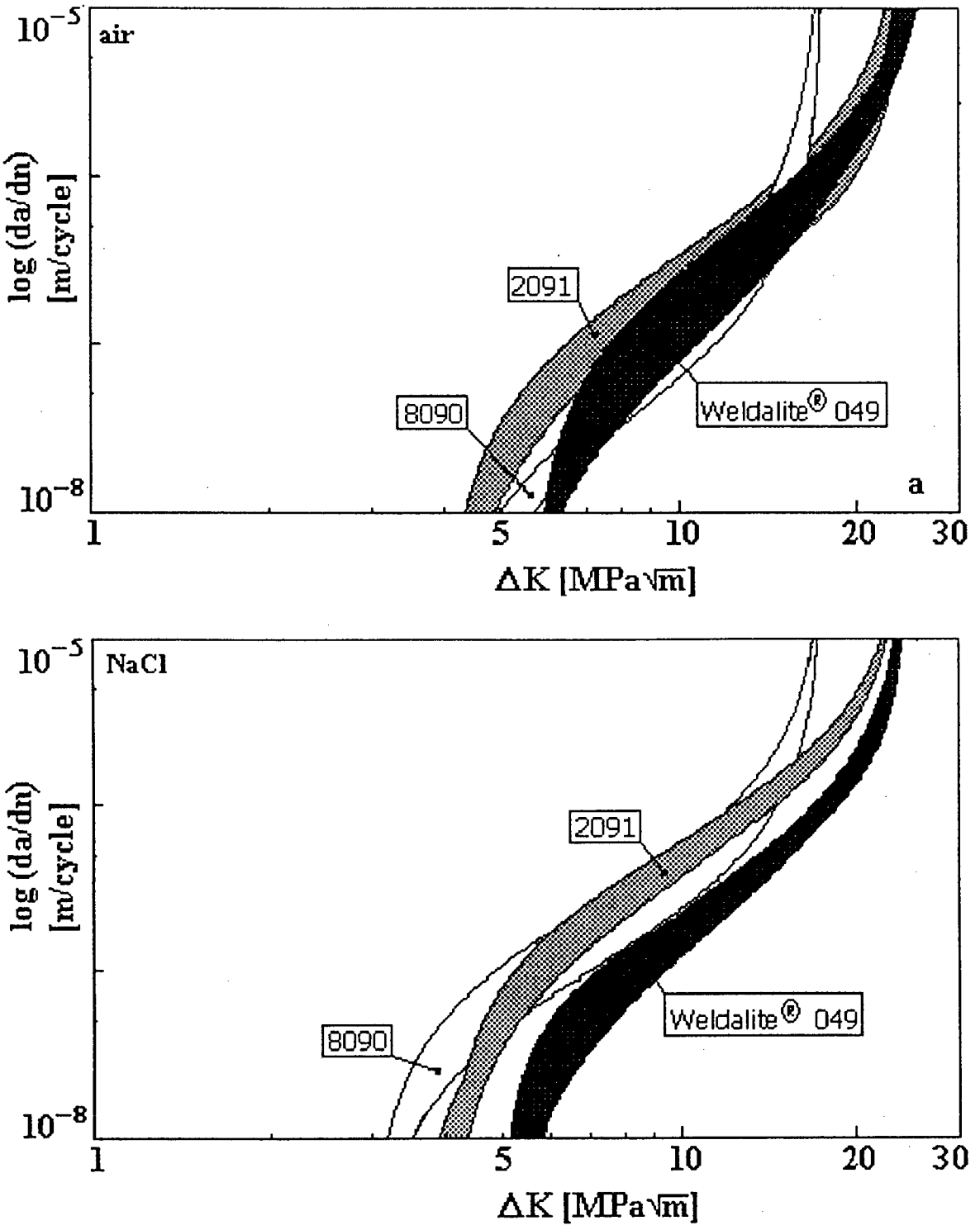

Figg. 6 a-b Comparison between the fatigue crack propagation rate of the three studied alloys in: a) air and b) NaCl aqueous solution.

Fig. 7 Etch pits in the fracture surface of Weldalite® 049 in the near threshold region (crack along the {111} crystallographic plane).

Fig. 8 Etch pits in the fracture surface of Weldalite® 049 at a higher ΔK level (crack along the {110} crystallographic plane).

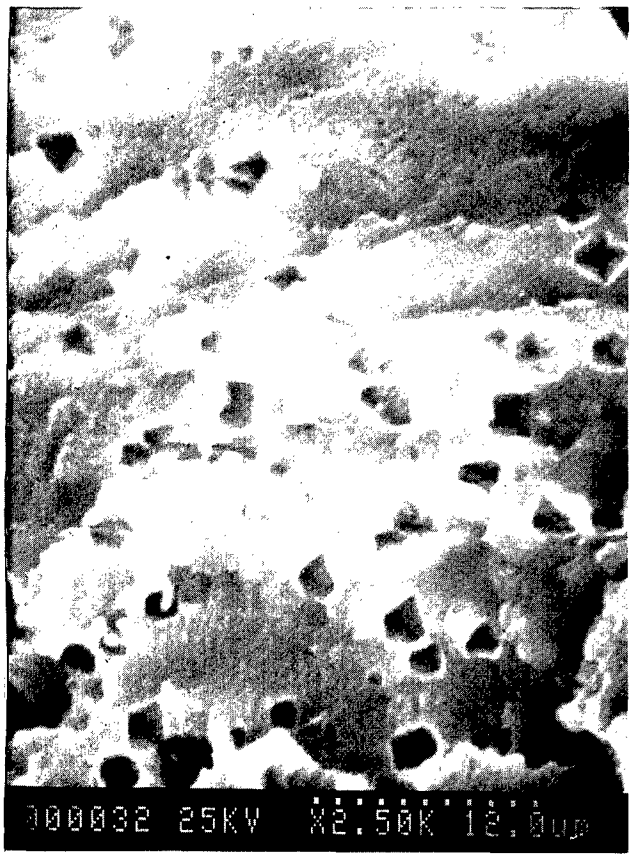

Fig. 9 Etch pits in the fracture surface 2091 (crack along the {110} crystallographic plane).

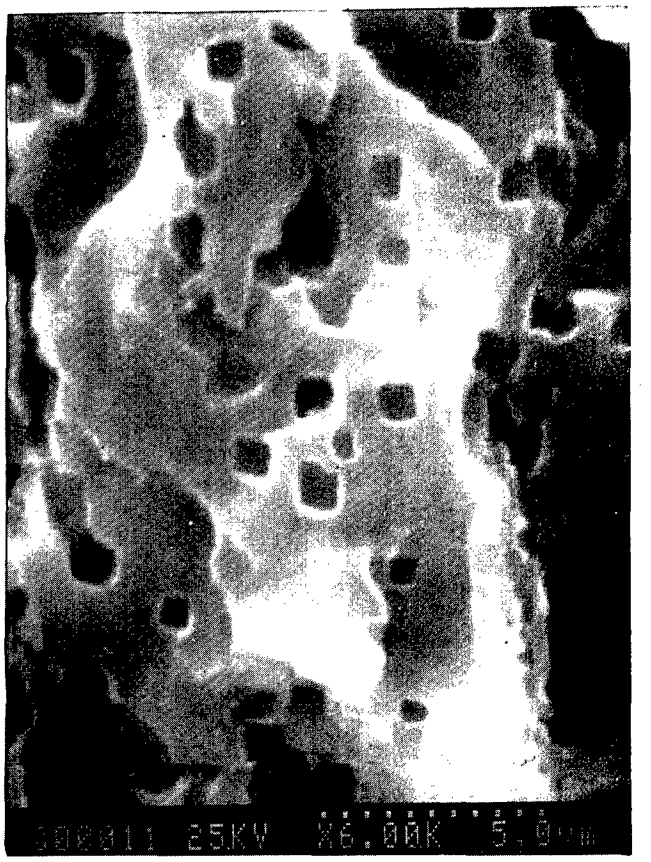

Fig. 10 Etch pits in the fracture surface of 8090 (crack along the {100} crystallographic plane).

Fig. 11 Fracture surface of 8090 alloy tested in air at 10 Hz (2÷3 mm from the notch).

Fig. 12 Fracture surface of 8090 alloy tested in air at 1 Hz (2÷3 mm from the notch).

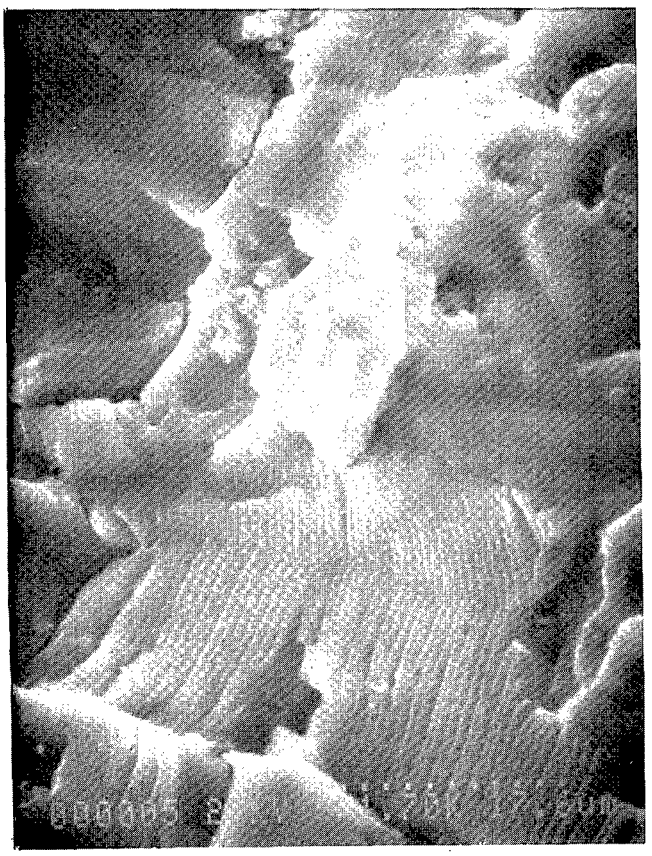

Fig. 13 Fracture surface of Weldalite® 049 alloy tested in air at 5 Hz (7≈ mm from the notch).

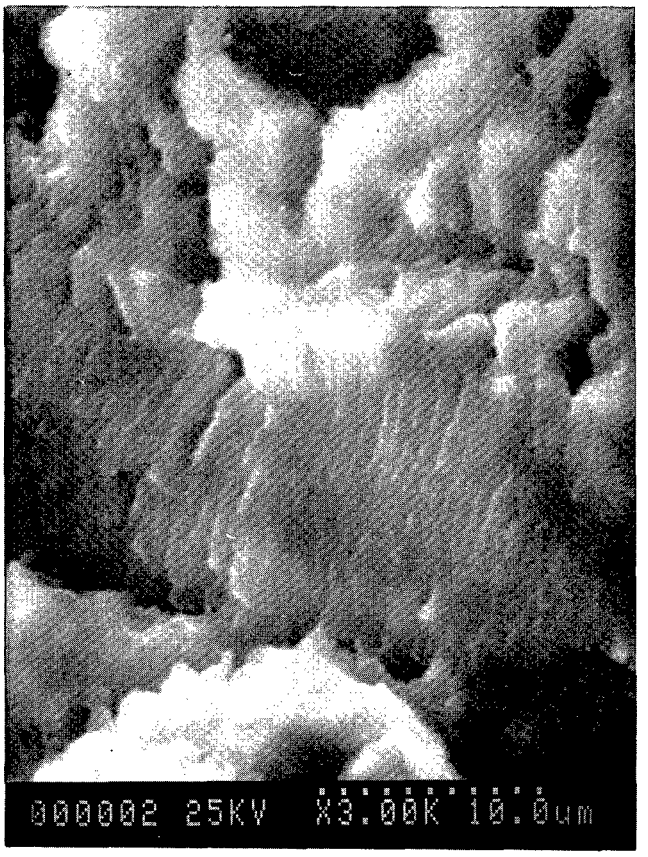

Fig. 14 Fracture surface of Weldalite® 049 alloy tested in NaCl aqueous solution at 5 Hz (≈7 mm from the notch).

Fig. 15 Fracture surface of 8090 alloy tested in NaCl aqueous solution at 10 Hz (3 mm from the notch).

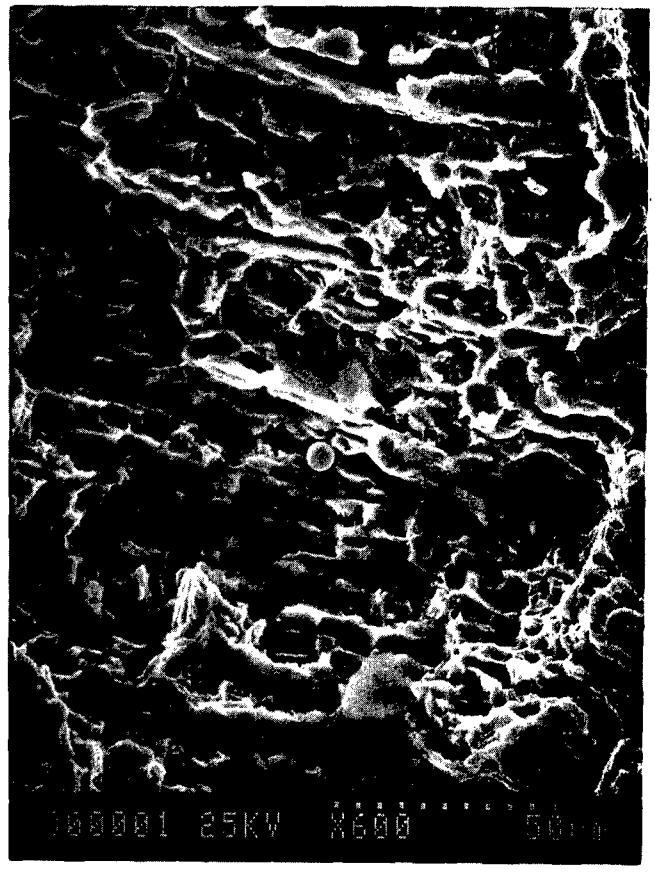

Fig. 16 Fracture surface of Weldalite® 049 alloy tested in NaCl aqueous solution at 5 Hz (10 mm from the notch).

Fig. 17 Fracture surface of 2091 alloy tested in NaCl aqueous solution at 2 Hz (2 mm from the notch).

Fig. 18 Fracture surface of 8090 alloy tested in air at 5 Hz (1÷2 mm from the notch).

EFFECT OF PRIOR CORROSION ON FATIGUE PERFORMANCE OF TOUGHNESS IMPROVED FUSELAGE SKIN SHEET ALLOY 2524-T3

G.H. Bray
R.J. Bucci
Aluminum Company of America
Alcoa Center, PA 15069 USA

P.J. Golden
A. F. Grandt
School of Aeronautics and Astronautics
Purdue University
West Lafayette, IN 47907 USA

SUMMARY

Aviation industry demand for continuous safety improvement in the face of trends toward increasing service life of aircraft and cost control necessitates stronger prevention and control measures to avoid the likelihood of structural failures linked to multi-site damage (MSD) involving corrosion and fatigue. New materials with improved damage tolerance attributes can improve the margin of safety in the presence of MSD. An excellent example of one such material is new aluminum alloy 2524 (formerly C188). In this study, the effect of prior pitting corrosion on the S/N fatigue performance of thin ($\leq$ 3.17 mm) 2524-T3 and 2024-T3 bare sheet was evaluated in a two part study. First, smooth axial fatigue specimens were corroded by accelerated methods to approximate 1yr seacoast exposure and then fatigue tested in lab air. The fatigue strength of 2524 was approximately 10% greater and the lifetime to failure 30 to 45% longer than that of 2024. Second, panels containing 24 open holes were similarly corroded and then fatigued in lab air for 100,000 cycles. The mean flaw areas following corrosion and fatigue were 18% smaller in 2524 and the corroded area alone 32% smaller. The results of this study indicate that thin, bare 2524 sheet is more resistant to MSD from pitting corrosion than thin, bare 2024 sheet. Alloy 2524 also offers improved structural damage tolerance in the presence of MSD due to its superior fatigue crack growth resistance and fracture toughness.

1. INTRODUCTION

The economic necessity to extend the operating lifetimes of both new and existing aircraft has given rise to new requirements that non-pristine or aging structure be accounted for in design and maintenance strategies. Explicit in these requirements is the upgrading of prevention/control measures to counter the potential emergence of a multi-site damage state, that in the presence of a larger rogue crack could imperil the structure's damage tolerance capability. As a result, corrosion is no longer viewed primarily as a maintenance issue, but as a potential threat to aircraft safety when combined with fatigue. This shift creates demand for affordable, replacement materials that not only can resist the occurrence of multi-site damage (MSD) from corrosion or other sources, but which also offer improved structural damage tolerance with MSD present.

An excellent example of one such material is new aluminum alloy 2524 developed to have improved fracture toughness and fatigue crack growth resistance relative to incumbent alloy 2024. Typical mechanical properties of 2524 and 2024 are compared in Table 1. The results of a separate study (Ref. 1) to quantify the improved resistance of 2524 to the consequences of MSD are shown in Fig. 1. The residual strength of 2524 panels containing a lead crack with MSD at adjacent holes was 9 to 10.5% higher than 2024 panels (Fig. 1a) and the fatigue life 27 to 45% longer (Fig. 1b) depending on MSD flaw size.

The objective of the present study was to determine if 2524 is more resistant than 2024 to MSD resulting from corrosion. The two alloys possess equivalent tensile (Table 1) and S/N fatigue properties (Fig. 2) when tested in an uncorroded condition. The classical rating systems of evaluating corrosion performance also rate both alloys as being nominally equivalent (Table 2). However, recent work by Wei et al. (Ref. 2) and Chen et al. (Refs. 3 and 4) indicates fatigue initiation resistance is degraded by pitting at large, second phase particles commonly referred to as constituent particles. Since 2524 has a significantly lower density of constituent particles as a result of compositional and processing improvements, it was hypothesized that the S/N fatigue performance of bare 2524 would be superior to that of 2024 in a precorroded condition.

2. EXPERIMENTAL PROCEDURES

2.1 Part I- Smooth Axial Fatigue with Prior Corrosion

Two thicknesses of clad 2024-T3 and 2524-T3 sheet, 1.60 mm and 3.17 mm, fabricated by Alcoa Davenport Works were procured for Part I of this study. Since these materials were clad and the desired test condition was bare, the cladding was removed by machining prior to testing. The final thicknesses after removal of the cladding were 1.37 mm and 2.54 mm, respectively. The materials will be referred to by their nominal thickness, 1.60 mm and 3.17 mm, for designation purposes. The morphology of constituent particles on the L-ST plane was examined using optical metallography. This plane was normal to the direction of loading in the fatigue tests. In addition, the number of particles and their areal size were measured with automated optical image analysis for the 3.17-mm sheet only. The sample area was 2.525 sq. mm. The minimum particle size that could be resolved was 2 sq. μm.

Smooth, sheet-type S/N fatigue specimens were machined in the long-transverse (LT) direction, seven per alloy from the 1.60 mm-sheet and thirteen per alloy from the 3.17-mm sheet. A smooth geometry was selected instead of a notched one because it samples a larger volume of material. The specimen had a gage length of 31.7 mm and a gage width of 12.7 mm. The tool marks from removal of the cladding were eliminated by wet sanding the specimen faces in the length direction with 600 grit paper. The specimens were corroded by 24 h exposure to sodium chloride/hydrogen peroxide solution prepared in accordance with ASTM G110. A comparison with seacoast data indicated the fatigue performance of 2024 sheet after 24 h exposure in sodium chloride/hydrogen peroxide is similar to that obtained after one year exposure to a seacoast environment. Both the faces and edges were exposed in the gage section of the specimens. The faces correspond to the L-LT plane and the edges to the LT-ST plane.

Paper presented at the RTO AVT Workshop on "Fatigue in the Presence of Corrosion", held in Corfu, Greece, 7-8 October 1998, and published in RTO MP-18.

One corroded specimen from each of the materials was cross-sectioned on a random L-ST plane and examined using optical metallography to determine the mode of corrosion attack. To characterize the severity of attack in the 3.17 mm-sheet, the number and depth of the corrosion features on the perimeter of the random plane were quantified by automated optical image analysis. The minimum depth of corrosion attack that could be resolved was approximately 12 μm. This information was also used to estimate the area loss due to corrosion.

The remaining corroded specimens were tested in laboratory air using a stress ratio of R=0.1. Duplicate specimens for each material were tested to failure at three stress levels, 172, 207 and 241 MPa, in order to define the S/N fatigue curve in the neighborhood of 100,000 cycles. The load applied to achieve a given stress level was based on the nominal specimen dimensions prior to corrosion. For the 3.17-mm sheet, four additional specimens were tested for each alloy at the intermediate stress level to better determine the variability in lifetime. Six failed specimens per thickness and alloy were examined in a scanning electron microscope (SEM) to determine primary initiating feature(s) and their sizes. The number of secondary cracks were also counted for the 3.17-mm sheet.

2.2 Part II- Multi-Hole Fatigue with Prior Corrosion

Bare 2024-T3 and 2524-T3 sheet, 2.54 mm thick, was procured for Phase II of this study. Panels 160 mm wide by 610 mm long containing four rows of six holes (24 total) at mid-length were machined from each alloy. The length dimension was in the long transverse (LT) direction of the parent sheet. The diameter of the holes was 4.0 mm and the hole spacing or pitch was 25.4 mm. The panels were corroded by 24 h exposure to sodium chloride/hydrogen peroxide solution prepared in accordance with ASTM G110. Three panels of each alloy were then fatigued at a gross stress of 69 MPa for 100,000 cycles in laboratory air at a stress ratio of 0.05. One panel of 2524 and two panels of 2024 were tested to failure.

Following fatigue cycling, each hole (72 total per alloy) was broken open and examined to determine the area of fatigue and corrosion. To break open each hole, a 25 mm square coupon of material containing the hole was excised from the panel. Notches were cut in the square piece perpendicular to the direction of loading in the plane of likely crack growth. Then each specimen was pulled to failure in a tensile test machine to expose the crack surfaces. The exposed cracks were examined and area measurements made using an optical microscope at magnifications up to 70x to determine the area of fatigue and corrosion. A portion of the fracture surfaces were examined in a scanning electron microscope to verify the accuracy of the optical measurement technique.

3. EXPERIMENTAL RESULTS

3.1 Part I- Smooth Axial Fatigue with Prior Corrosion

Optical metallography revealed that 2524 had significantly fewer constituent particles than 2024 in both sheet thicknesses as expected. The distribution of particle sizes obtained from the 3.17-mm sheet (Fig. 3) revealed that 2524 had fewer particles over the entire size range, but that the greatest difference between the two alloys was in the size range of 25 sq. μm and less. The overall density of particles was 800/sq. mm in 2524 compared to 2290/sq. mm in 2024.

The type of corrosion attack in all materials was predominantly pitting corrosion (Fig. 4). The pits on the specimen faces (L-LT plane) were hemispherical in shape, while those on the specimen edges (LT-ST) plane were elongated. It was not determined whether the pitting was associated with the constituent particles, but the work of Wei et al. (Ref. 2) and Chen et al. (Refs. 3 and 4) suggest this is probably the case. The distribution of pit depths obtained in the 3.17-mm sheet is shown in Fig. 5. The average density of resolvable pits (12 μm) on the specimen perimeter was 2.5/mm in 2524 compared to 3.2/mm in 2024. The density of smaller pits (<12 μm deep) may have been significantly greater in 2024, but these would be less likely to act as fatigue initiation sites. The area loss due to corrosion in the 1.60-mm sheet was estimated to be 4.6% for 2024 and 4.0% for 2524, while that in the 3.17-mm sheet was estimated to be 1.1 and 0.9%, respectively.

A Box-Cox equation (Ref. 5) was fit to the individual fatigue test results to obtain stress-life (S/N) curves for precorroded 2524 and 2024 (Fig. 6). The lifetime at each stress level and the fatigue strength at 100,000 cycles obtained from the Box-Cox fit are given in Table 3. The fatigue performance of precorroded 2524 was superior to that of 2024. For both thicknesses, the lifetime to failure of precorroded 2524 was 30 to 45% longer than that of precorroded 2024 depending on stress level, and the fatigue strength at 100,000 cycles approximately 21 MPa or 10% higher. Prior corrosion reduced the fatigue strength of both alloys approximately 140 MPa relative to the typical smooth (K_t=1) fatigue strength of 345 MPa for bare, uncorroded material (Ref. 6).

SEM fractography revealed that the largest or primary fatigue cracks originated on the specimen edges in all specimens examined. The edges correspond to the through-thickness orientation (LT-ST plane) which is representative of the surfaces of a fastener hole or splice edge. Fatigue cracking typically initiated at 4 to 8 pits and then coalesced to form a common crack front. Generally, the pits in 2524 were elongated and separated by uncorroded material, while those in 2024 were partially or fully coalesced (Fig. 7). The maximum depth of corrosion attack in the primary origin area varied significantly from specimen to specimen but on average was similar in the two alloys for the 1.60-mm sheet, while in the 3.17-mm sheet, 2524 exhibited shallower attack than 2024 (Table 4). The fracture surfaces exhibited many secondary cracks on both the faces and edges, each typically containing multiple pit initiation sites. The number of secondary cracks in the 3.17-mm sheet also varied significantly from specimen to specimen, but on average was slightly less in 2524.

3.1 Part II- Multi-Hole Fatigue with Prior Corrosion

The descriptive statistics from the examination of the broken open holes from the multi-hole specimens are given in Table 5. The areal measurements for each alloy have also been represented graphically by use of histograms in Fig. 8. Of the potential 144 sites (72 holes times two sides), corrosion was observed at 99% of the sites and fatigue at 97% of the sites in the 2024 specimens compared to 92% and 83% of the sites, respectively, in the 2524 specimens. The broken open holes revealed pitting corrosion and fatigue emanating from the bore of the holes very similar in appearance to that observed at the edges of the smooth specimen (see Fig. 7). Generally, the pits in 2524 were less deep and separated by uncorroded material while those in 2024 were deeper and partially or fully coalesced. As a result of these differences, the area of corrosion at each hole was on average 32% less in 2524 than in 2024. The distribution of corrosion area for all holes is compared in the histogram in Fig. 8a. It was anticipated that the fatigue area might also be smaller in 2524 since the starting flaw (i.e., the area of corrosion) was smaller in 2524 and its fatigue crack growth resistance is higher. This was not the case as seen in Table 5 and Fig. 8b possibly for several reasons. First, most of the fatigue area in 2524 is between the non-coalesced pits while in 2024 this material has already been corroded away. Second, because the pits are not

coalesced and the corrosion area is smaller in 2524, the fatigue cracks are experiencing greater stress intensification from the hole than in 2024. Third, the improvement in fatigue crack growth resistance of 2524 over 2024 is much greater at high ΔK than at the low ΔK present at the early stage of fatigue crack growth. On average, the total area of corrosion plus fatigue at each hole was 18% less and the maximum depth of attack 16% less in 2524 than in 2024 as seen in Table 5 and 8c.

Confidence intervals were calculated at the 95% level to determine the statistical significance of the differences in mean values of the area from corrosion, fatigue and total damage for 2524 and 2024 were statistically significant. The mean and confidence intervals are shown in Fig. 9. The differences between the two materials was calculated to be statistically significant for the corroded area and total area only. The difference in the fatigue area was calculated to be insignificant. The confidence intervals indicate that it can be stated with 95% confidence that the mean corrosion area of 2024 is 24 to 40% greater than that of 2524 and the total area of corrosion plus fatigue in 2024 is 8 to 28% greater than that of 2524.

The two 2024 specimens fatigued to failure had lifetimes of 204,300 and 151,200 compared to a lifetime of 263,000 in the 2524 specimen, an improvement of 22% and 42%, respectively. The improvement in 2524 is consistent with that observed in the smooth specimen results.

4. DISCUSSION

The results of this study indicate that thin, bare 2524 sheet is more resistant to the formation of MSD from pitting corrosion than thin, bare 2024 sheet. In Part I of this study, the smooth fatigue strength of corroded 2524 was approximately 10% greater and the lifetime to failure 30 to 45% longer than that of corroded 2024 depending on stress level. In Part II, the mean flaw area at open holes was 20% less in 2524 than in 2024 following corrosion and fatigue to 100,000 cycles. Alloy 2524 also offers improved structural damage tolerance in the presence of MSD due to its superior fatigue crack growth resistance and fracture toughness.

In a previous paper (Ref. 7) the factors contributing to the improved smooth fatigue performance of corroded 2524 relative to corroded 2024 were analyzed. Possible contributing factors were: (1) less cross-sectional area loss; (2) a less damaging configuration of initiating features (i.e., pits); and (3) and better fatigue crack growth resistance. The results of this analysis indicated that less than 5% of the life improvement was due to less cross-sectional area loss in 2524, its better fatigue crack growth resistance was responsible for 50 to 75% of the life improvement, and a less damaging configuration of initiating pits in 2524 was responsible for the remaining 20 to 45% of the lifetime.

The configuration of initiating pits was less damaging not because of far fewer pits in 2524 as first anticipated but because the shape of the pits was less damaging with respect to their depth and/or their aspect ratio. Based on the work of Wei et al. (Ref. 2) and Chen et al. (Refs. 3 and 4) which indicates that pits primarily form at large, second phase particles, it was anticipated that 2524 would have far fewer pits, since its particle density is only about a third of that in 2024. However, while the density of resolvable pits (>12 μm) measured in Part I (see Fig. 5) was less in 2524, the difference was not as large as expected. One possible explanation is that pits of resolvable depth were mainly associated with the larger particles in the upper tail of the size distribution where the difference between the two alloys was not as great (see Fig. 3). The number of smaller pits (<12 μm deep) may have been significantly greater in 2024, but these would be less likely to serve as fatigue initiation sites. As a result, the average number of secondary cracks and the total number of initiation sites (see Table 4) was not significantly different in the two alloys.

However, in both Parts I and II, the pits in 2024 were observed to be typically deeper and/or wider at their base (i.e., lower aspect ratio) than those in 2524 due to pit coalescence in the former. A possible explanation for this behavior consistent with the observations of Chen et al. (Refs. 3 and 4) is that pitting at the smaller particles abundant in 2024 (see Fig. 3) are acting to link up or coalesce the larger pits. The analysis performed in the previous paper (Ref. 7) showed that pit depth and aspect ratio of the initiating pits can affect fatigue lifetime just as signficantly as the number of initiating features as seen in Fig. 10. Thus, it appears that while the lower density of constituent particles of 2524 relative to 2024 did not result in fewer fatigue initiating pits as anticipated, it did result in the shape of these initiating pits being less damaging to fatigue performance.

While the observed improvement in 2524 with respect to 2024 is believed to be correct and plausible mechanisms for this improvement have been identified, it should be recognized that the test data is limited in scope with respect to the number of lots tested (3 each alloy) and are therefore insufficient to reliably quantify the magnitude of the performance improvement. It should also be noted that the improvement was observed for the case of pitting corrosion in thin, bare sheet only. Pitting corrosion is typically observed in 2X24-T3X products less than approximately 2 mm in thickness which can be quenched rapidly enough to be resistant to intergranular (IG) corrosion. As product thickness increases, the attack typically changes from pitting to a mixture of pitting and IG corrosion to primarily IG corrosion (Ref. 8). The corrosion behavior of both alloys can also vary considerably from lot-to-lot particularly in the intermediate thickness range where the mode of corrosion is mixed. Therefore, the relative performance of the two alloys may vary from lot to lot and in the presence of other forms of corrosion. However, the fatigue crack growth resistance and fracture toughness of 2524 sheet is expected to exceed that of 2024 sheet in nearly all cases. Thus, when multi-site damage (MSD) is present in the form of corrosion or any other form, alloy 2524 has an inherent advantage over 2024 (see Fig. 1).

The results of this study also point out the need to develop and standardize new metrics for assessing the combined effects of fatigue and corrosion. With respect to classical rating systems of fatigue and corrosion, 2524 and 2024 are nominally equivalent (see Table 2 and Fig. 2). However, the results of this study indicates that the fatigue performance of thin, bare 2524 sheet after corrosion is superior to that of 2024. One approach for discriminating such differences would be to determine the equivalent initial flaw size (EIFS) for corrosion damage. The EIFS approach has been applied to pores and microfeatures in aluminum alloy 7050 by Magnusen et al. (Ref. 9) and to corrosion damage in 2124 and 7050 by Perez (Ref. 10). Basically, in this approach, the equivalent corner or through-crack dimensions which gives the same lifetime as a corroded specimen is obtained through fatigue crack growth analysis. The better performance of an improved alloy like 2524 would be recognized by a smaller equivalent initial flaw size (EIFS) than that from a poorer performing alloy such as 2024. Before widespread use of such a rating system would be possible, protocols for corrosion exposure, crack growth analysis, test specimens, number of lots and thicknesses required to achieve representative and statistically meaningful comparisons, etc. would need to be agreed upon and standardized.

Because of the potential threat to aircraft safety from MSD resulting from the combination of corrosion and fatigue, it is recommended that similar information be generated for older incumbent alloys such as 7075 and newer alloys such as 7055 which are intended to replace them. Such information would be useful not only to designers of new aircraft but also to those selecting alloys for retrofit applications on existing aging aircraft. More fundamental studies on the role of constituent particles and their influence on the severity or corrosion features with respect to their number size and shape should also be performed since insight from such studies would be useful to alloy developers.

5. CONCLUSIONS

The results of this study indicate that thin, bare 2524-T3 sheet is more resistant to multi-site damage (MSD) from pitting corrosion than thin, bare 2024-T3 sheet. In smooth fatigue specimens with prior corrosion, the fatigue strength of 2524 was approximately 10% greater and the lifetime to failure 30 to 45% longer than that of 2024. In open hole specimens, the mean flaw areas following corrosion and fatigue were 18% smaller in 2524 than in 2024 and the corroded area alone 32% smaller. The improvements in 2524 are due to a less damaging configuration of fatigue initiating pits believed to result from a much lower density of constituent particles. The better resistance of 2524 to MSD could be particularly beneficial in small aircraft where the use of thin, bare sheet is common. 2524 also offers improved structural damage tolerance in the presence of MSD due to its superior fatigue crack growth resistance and fracture toughness.

This study points out the need to develop new, standardized metrics and a rating system for assessing the ability of an alloy with respect to the combined effects of corrosion and fatigue. A reasonable approach for ranking alloys in this regard would be to determine the equivalent initial flaw size (EIFS) for corrosion damage. It is also recommended that similar studies be performed on pairs of older incumbent alloys and the newer alloys intended to replace them. Such information would be useful to both designers of new aircraft and for those selecting alloys for retrofit applications on existing aging aircraft.

REFERENCES

1. Grandt, A.F et al., "A Comparison of 2024-T3 and 2524-T3 Aluminium Alloys Under Multi-Site Damage Scenarios," *ICAF '97 Fatigue in New and Ageing Aircraft, Vol. II*, R. Cook and P. Poole, Eds., Engineering Materials Advisory Services, Ltd, UK, 1997, pp. 659-669.
2. Wei, R.P, Gao, M. and Harlow, D.G., "Pitting Corrosion in Aluminum Alloys: Experimentation and Modeling," Presentation at Air Force 3rd Aging Aircraft Conference, Wright-Patterson Air Force Base, September 1995.
3. Chen, G.S et al., "Corrosion and Corrosion Fatigue of Airframe Aluminum Alloys," *FAA/NASA International Symposium on Advanced Structural Integrity Methods for Airframe Durability and Damage Tolerance, NASA Conference Publication 3274, Part 2*, September 1994, pp. 157-173
4. Chen, G.S., Gao, M. and Wei, R.P., "Micro-Constituents Induced Pitting Corrosion in a 2024-T3 Aluminum Alloy," *Corrosion*, Vol. 52, No. 1, January 1996, pp. 8-15.
5. Hinkle, A.J. and Emptage, M.R., "Analysis of Fatigue Life Data Using the Box-Cox Transformation," *Fatigue and Fracture of Engineering Materials and Structures*, Vol. 14, No. 5, 1991, pp. 591-600.
6. *Metallic Materials and Elements for Aerospace Vehicle Structures*, Mil-Hdbk-5G, 1994.
7. Bray, G.H. et al., "Effect of Prior Corrosion on the S/N Fatigue Performance of Aluminum Sheet Alloys 2024-T3 and 2524-T3, *Effects of the Environment on the Initiation of Crack Growth, ASTM STP 1298*, W.A. Van Der Sluys, R.S. Piascik, and R. Zawierucha, Eds., American Society for Testing and Materials, 1997, pp. 89-103.
8. *Aluminum: Properties and Physical Metallurgy*, J. Hatch, ed., American Society for Metals, 1984, p. 167-169.
9. Magnusen, P.E. et al., "Final Report: The Role of Microstructure on the Fatigue Durability of Aluminum Aircraft Alloys," ONR Contract N00014-91-C-0128, November 1995.
10. Perez, R., "Corrosion/Fatigue Metrics," *ICAF '97 Fatigue in New and Ageing Aircraft, Vol. I*, R. Cook and P. Poole, Eds., Engineering Materials Advisory Services, Ltd, UK, 1997, pp. 215-225.

Table 1. Typical mechanical properties for 2524-T3 and 2024-T3 sheet in the long-transverse direction.

Alloy	Condition	UTS MPa	TYS MPa	Elong. %	Kc[a] MPa√m	da/dN@ΔK=33[b] m/cycle
2524-T3	Clad	455	310	18	174	2.3E-06
	Bare	462	317	18	---	---
2024-T3	Clad	455	310	18	141	7.0E-06
	Bare	462	317	18	---	---

[a] M(T) specimen, T-L orientation, W=406 mm, $2a_0$= 102 mm tested per ASTM B646.

[b] T-L orientation, tested per ASTM E647 under constant ΔK conditions, R=0.1, relative humidity> 90%.

Table 2. Corrosion performance of several lots of bare 2524-T3 and 2024-T3 sheet.

Alloy	Thickness mm	EXCO[a] 48 h	EXCO[a] 96 h	MASTMAASIS[b] 2 week	MASTMAASIS[b] 4 week	Type of Attack[c]
2524-T3	0.81	P	P	P	P	P
	3.17	EA	EB	P	EB	IG
	6.32	EA	EB	P	EC	IG
2024-T3	1.02	P	EA	P	EA	P+IG[d]
	2.54	EA	EA	P	EA	P+IG[d]
	6.32	EA	EA	EA	EA	IG

[a] Tested at mid-thickness (t/2) per ASTM G34.
[b] Tested at mid-thickness (t/2) per ASTM G85, Annex A.2 (dry bottom).
[c] Tested per ASTM G110.
[d] Pitting with slight IG attack.

Table 3. Comparison of S/N fatigue performance of bare 2524-T3 and 2024-T3 sheet with prior corrosion [a].

Thickness mm	Alloy	Lifetime at Smax= 172 MPa	207 MPa	241 MPa	Smax at 10^5 cycles
1.60	2024	171800	82000	47900	196
	2524	221900	115000	70200	216
	% Improved	+29%	+40%	+46%	+10%
3.17	2024	197500	96400	57000	205
	2524	252600	135000	83500	228
	%Improved	+28%	+40%	+47%	+11%

[a] Smooth specimen tested in lab air after 24 h in NaCl/H_2O_2 solution (ASTM G110), R=0.1.

Table 4. Maximum depth of corrosion attack in primary origin area and number of secondary cracks on plane of failure.

Thickness mm	Alloy	Max. Depth of Attack, mm Range[a]	Max. Depth of Attack, mm Average[a]	No. Secondary Cracks Range[a]	No. Secondary Cracks Average[a]
1.60	2524	0.267-0.521	0.367	---	---
	2024	0.259-0.648	0.374	---	---
3.17	2524	0.292-0.632	0.416	5-26	15
	2024	0.439-0.681	0.550	6-28	16

[a] Range and average of six specimens from each thickness and alloy.

Table 5. Descriptive statistics for flaws in multi-hole specimens after corrosion and fatigue.

Metric	2024-T3	2524-T3	% Difference
Number of Sites (144 possible)			
With Corrosion	142	133	-6%
With Fatigue	140	127	-9%
With Corrosion and Fatigue	121	120	-1%
Mean Value			
Maximum Depth (mm)	0.81	0.68	-16%
Corrosion Area (sq. mm)	0.94	0.64	-32%
Fatigue Area (sq. mm)	0.56	0.59	+5%
Total Area (sq mm)	1.50	1.23	-18%

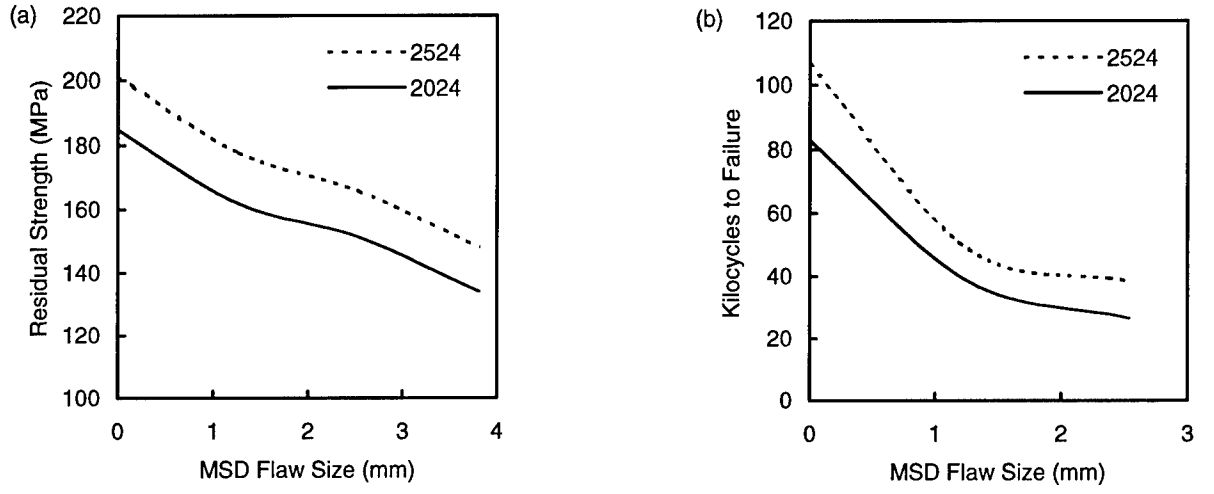

Figure 1. A comparison of (a) residual strength and (b) fatigue life in alloy 2524-T3 and 2024-T3 sheet with multi-site damage (MSD) present *after Grandt et al. (Ref. 1).*

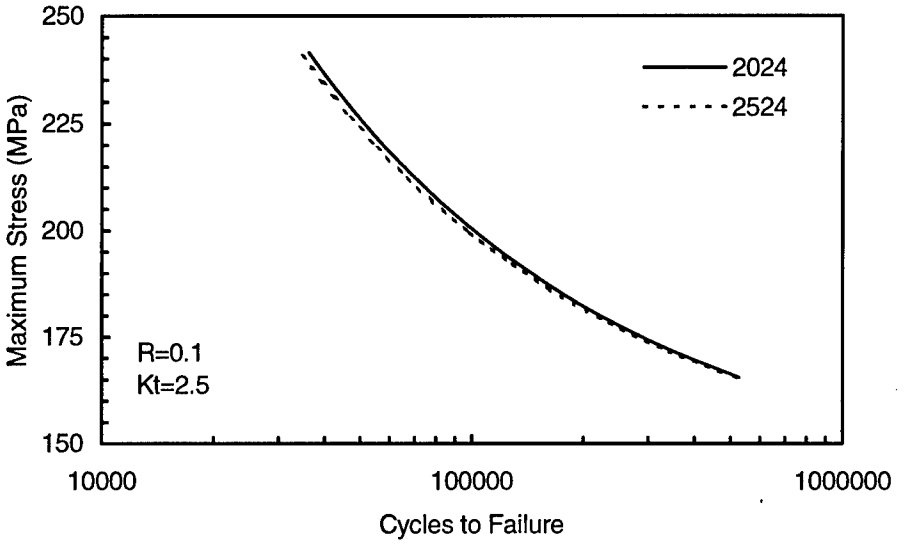

Figure 2. Comparison of S/N fatigue performance of bare 2524-T3 and 2024-T3 sheet in an uncorroded condition.

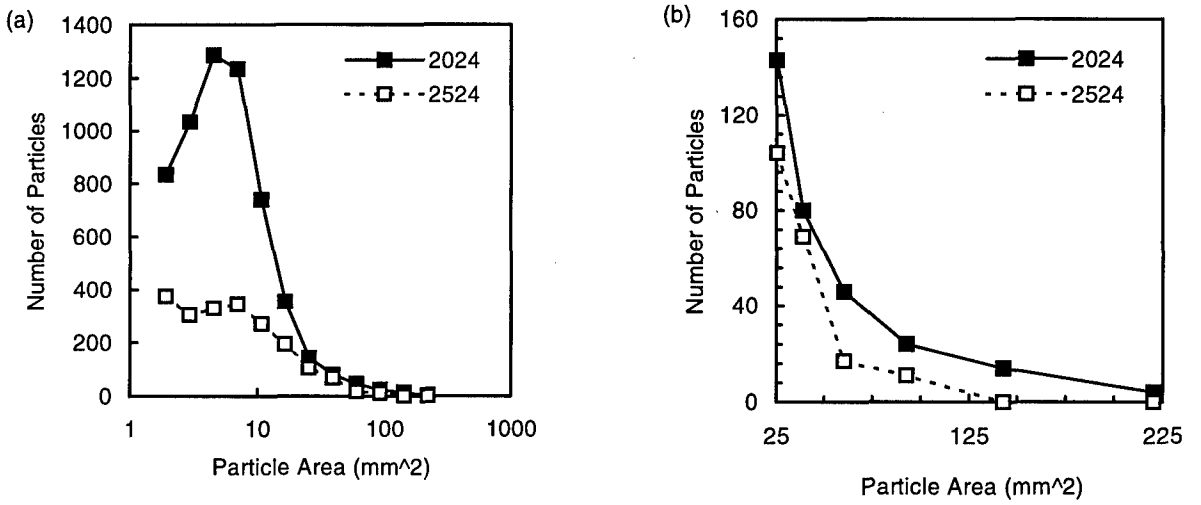

Figure 3. Histograms comparing (a) entire distribution and (b) upper tail of the distribution of particle sizes in 3.17-mm thick 2524-T3 and 2024-T3 sheet.

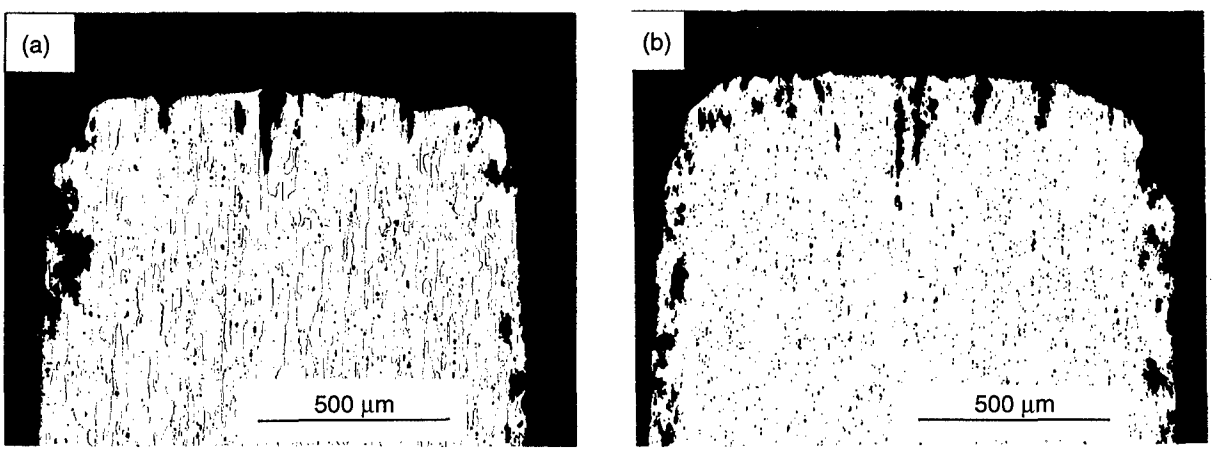

Figure 4. Optical micrographs of random plane showing pitting corrosion in bare 1.60-mm thick (a) 2524-T3 and (b) 2024-T3 sheet after 24h exposure to NaCl/H_2O_2 solution.

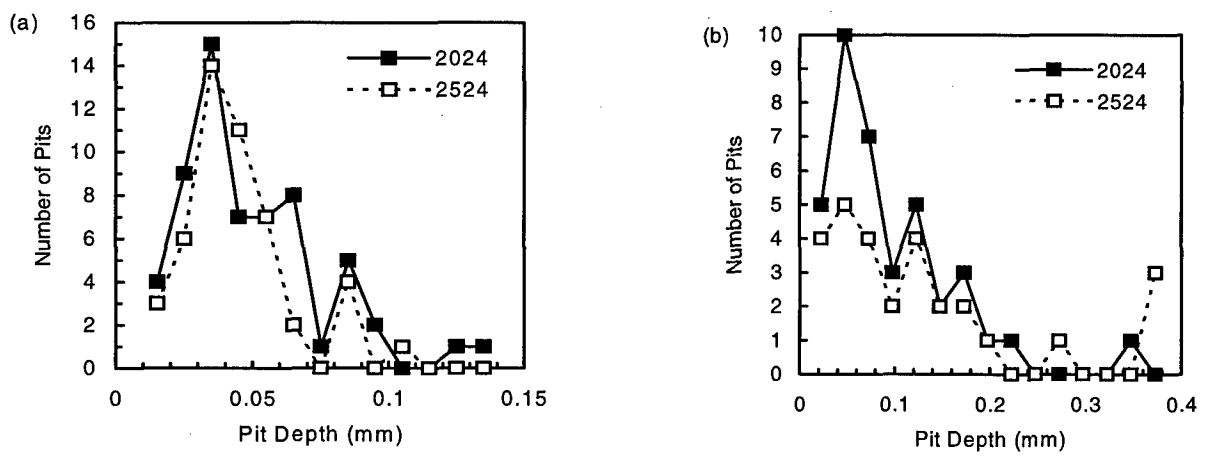

Figure 5. Histograms comparing distribution of pit depths (after 24 h in NaCl/H_2O_2) on random plane (L-ST) of 3.17-mm thick 2524-T3 and 2024-T3 sheet for (a) specimen faces and (b) specimen edges.

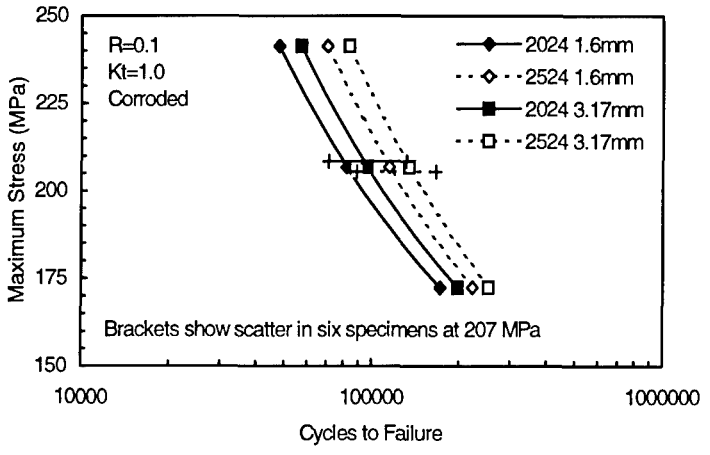

Figure 6. Stress-life fatigue curves for bare 2524-T3 and 2024-T3 sheet with prior corrosion (24h in $NaCl/H_2O_2$).

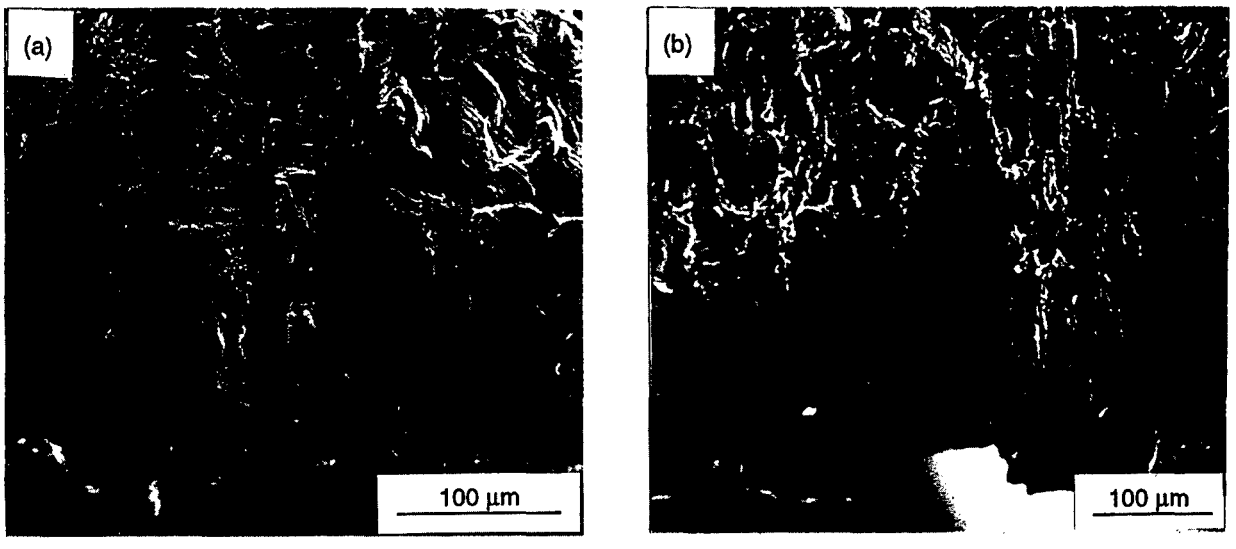

Figure 7. SEM fractographs from 3.17-mm thick sheet showing typical primary origin area on specimen edge in (a) 2524-T3 and (b) 2024-T3 sheet.

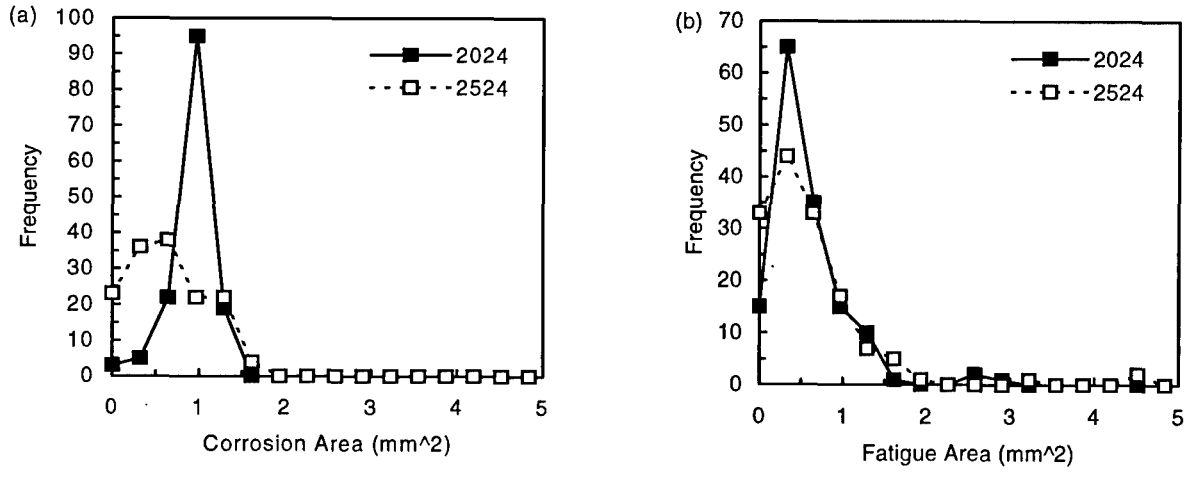

Figure 8. Histograms from 2.54-mm thick corroded and fatigued multi-hole specimens comparing: (a) area of corrosion, (b) area of fatigue (continued next page)

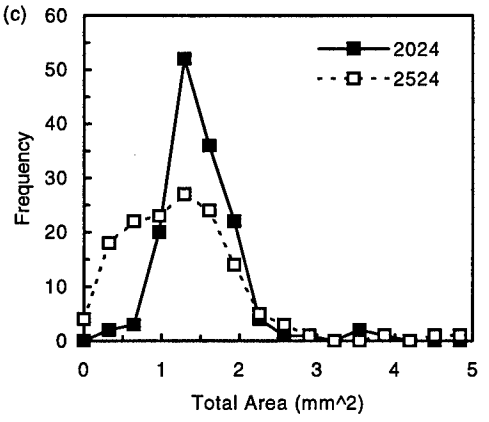

Figure 8 (continued). (c) total area of fatigue and corrosion.

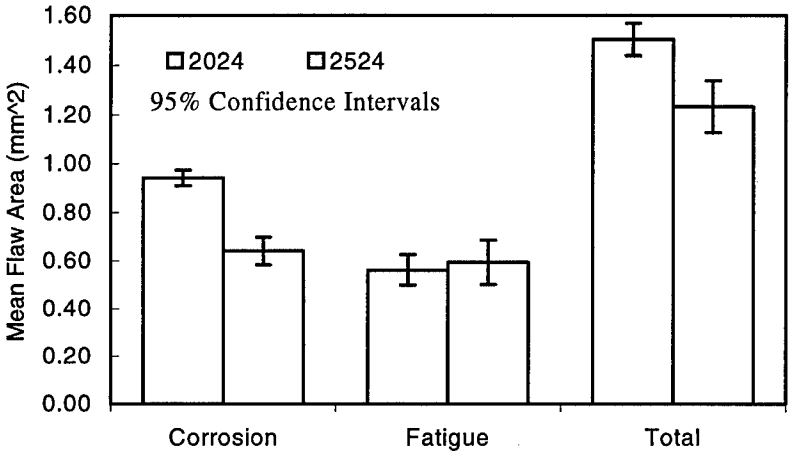

Figure 9. Comparison of mean values of area from corrosion, fatigue, and total damage from 2.54-mm thick multi-hole specimens (144 holes total) of 2524-T3 and 2024-T3 sheet.

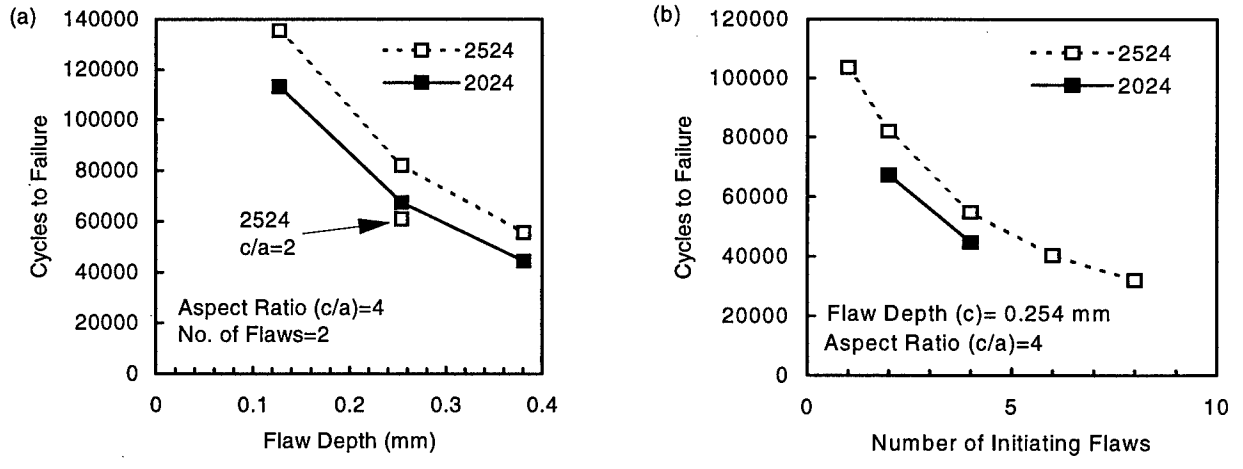

Figure 10. Results of crack growth analysis showing effect of (a) flaw depth and aspect ratio, and (b) number of initiating flaws on propagation lifetime *after Bray et al. (Ref. 7).*

THE EFFECT OF ENVIRONMENT DURABILITY AND CRACK GROWTH

B. Schmidt–Brandecker
H.–J. Schmidt
Fatigue and Fracture Mechanics Department
Daimler–Benz Aerospace Airbus
Kreetslag 10
D21129 Hamburg, Germany

SUMMARY

Structures of transport aircraft are to be designed for an optimum of weight, costs and performance. Amongst others this requires the investigation of the durability and the damage tolerance behavior of the structure. Both characteristics are significantly influenced by the environmental conditions. Additionally the load frequency has an effect on the crack growth behavior of aluminium structure. These aspects play a major role during the material selection for the next Airbus aircraft generation. For the fuselage of the planned Airbus Megaliner new materials are under consideration to comply with the forthcoming regulations and to reduce the production costs. This paper describes the results of crack growth and crack initiation tests of several aluminium alloys under varying environment and loading frequency.

1. INTRODUCTION

The design of aircraft structures requires the consideration of a large variety of aspects to reach an optimum design regarding weights, costs and performance. The design regarding static strength and damage tolerance has to be based on the airworthiness regulations and further recommendations. The major design aspects are the static and dynamic loading, the material data (for static strength, durability, damage tolerance), the environment, the detailed component design, the damage detectability and the production aspects..
This paper deals with the effect of the environment of the material behavior regarding durability and crack growth. This effect is presented using materials for fuselage shells as an example.

2. DESIGN OF FUSELAGE SHELLS

The design of fuselage shells is described here for the planned Airbus megaliner A3XX which has a design service goal of 24000 flights. In principle fuselage shells are loaded by longitudinal and circumferential loads caused by external and pressure loads. The design critieria to be met are static strength, residual strength, durability, crack growth, sonic fatigue strength and the so–called two–bay–crack criterion. Furthermore corrosion resistance, repairability and inspectability have to be considered.
Fig. 1 shows the design criteria in different fuselage areas for the A3XX if made of the conventional skin material 2024.

During the initial design phase of the Airbus A3XX the application of new materials and production methods is considered to reduce the production costs and the weight and to comply with the forthcoming regulations. To substitute the fuselage material of the current Airbus types, i.e. the aluminium alloy 2024, three different materials are under consideration; these are 2524, 6013 and GLARE, see table 1.
The materials 2524 and GLARE4 show significantly higher fracture toughness compared with 2024 which results in significant weight reductions in those areas which are designed by the two–bay–crack criterion. The disadvantage of both materials is the higher price. For the GLARE4 material this may be (partly) compensated by a simplified design and production, GLARE4 has additionally advantages with respect to the static strength, the yield strength and the corrosion resistance. Furthermore GLARE4 shows a very good burn through behavior which should be taken into account besides the structural aspects. The material 6013 leads to similar structural weights as 2524 considering the slightly lower yield strength which is approximately compensated by the lower density. 6013 can be welded which allows to substitute the bonding or riveting of the stringers to the skin by welding. This new production method is very promising with respect to the reduction of the production costs.

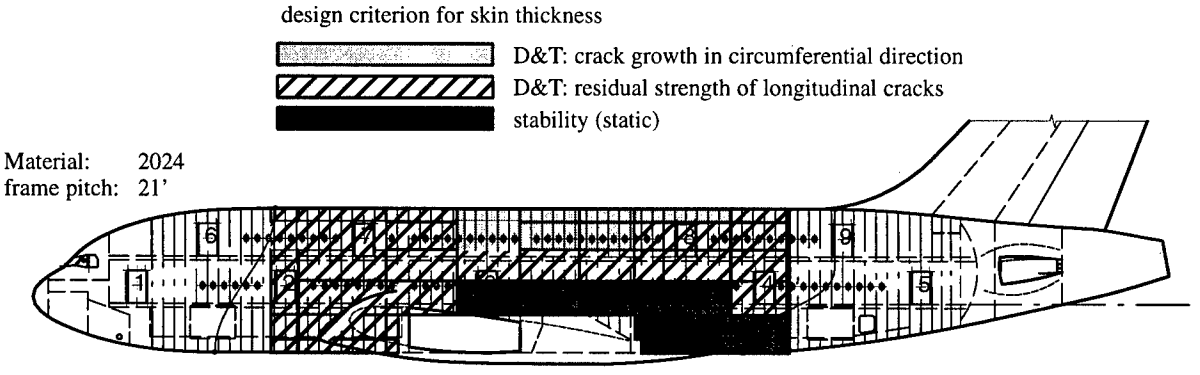

Fig. 1: Design criteria for A3XX fuselage sections

Paper presented at the RTO AVT Workshop on "Fatigue in the Presence of Corrosion", held in Corfu, Greece, 7-8 October 1998, and published in RTO MP-18.

Table 1: Materials for fuselage skin

material data		2024T3 clad	2524T3 clad	6013T4/T6 unclad	GLARE4 (LT/TL) unclad
R_m	(in %)	100	100	~75	190 / 120
$R_{p0.2}$	(in %)	100	100	~94	110 / 80
$\sigma_{\text{blunt notch}}$	(in %)	100	100	not tested	143 / 100
young's modulus (tension)	(in %)	100	100	~95	79 / 70
K_C	(in %)	100	~120	~115	~120 / ~110
ς	(in %)	100	100	97	87
corrosion resistance		basis	equal	equal / less	higher

3. CRACK GROWTH TESTS

One of the key issues during the material selection is the crack growth behavior under real environment. Any new material for the fuselage in areas where damage tolerance is the dimensioning case, can only be accepted, if the crack growth behavior under real environment and real frequency is not worse than the present 2024T3/T42 material. If the new material would not fulfill this requirement, either the skin thickness would have to be increased which is unacceptable due to weight reasons or more severe inspection programs have to be applied.

Comprehensive coupon tests have been carried out by Daimler–Benz Aerospace Airbus (DA) which are presented in the following as well as some investigations from other authors. For all DA tests the following conditions were applied: the 2024 specimens were cladded (except one test series to investigate the influence of cladding) as well as the 7475 specimens; all 6013 specimens were bare; the specimen geometry was: width 100 or 160 mm, thickness 1.6 mm; all specimens were manufactured without surface treatment and painting; the specimen direction was L–T; the tests were performed either in laboratory air or in 3.5 percent sodium chloride (NaCl) with inhibitors; all tests were performed at room temperature except those to investigate a lower temperature.

3.1 Crack Growth Tests under Constant Amplitude Loading

The effect of corrosive environments on the crack growth behavior has been investigated by comparative coupon tests performed at a frequency of approximately 20 Hz and using either laboratory air or 3.5 percent sodium chloride (NaCl). Table 2 presents the crack growth behavior of different materials obtained by tests with CCT specimens performed at 20 Hz. The comparison for the two lower ΔK values reveals that e.g. for 6013 and laboratory air the da/dn values are similar to the 2024T3 values. The same comparison for an environment of 3.5 percent sodium chloride shows significant differences.

Table 2: Crack Growth Data for a Frequency of 20 Hz

Material	Environment	da/dn (mm · 10^{-3}/cycle)		
		$\Delta K = 13\ \text{MPa}\sqrt{\text{m}}$	$\Delta K = 20\ \text{MPa}\sqrt{\text{m}}$	$\Delta K = 27\ \text{MPa}\sqrt{\text{m}}$
2024T3	laboratory air	0.20	0.65	2.40
6013T6	laboratory air	0.28	0.55	1.00
7475T76	laboratory air	0.45	1.00	1.90
2024T3	3.5 percent NaCl	0.27	0.65	2.30
6013T6	3.5 percent NaCl	0.65	0.80	1.50
7475T76	3.5 percent NaCl	0.85	1.50	2.20

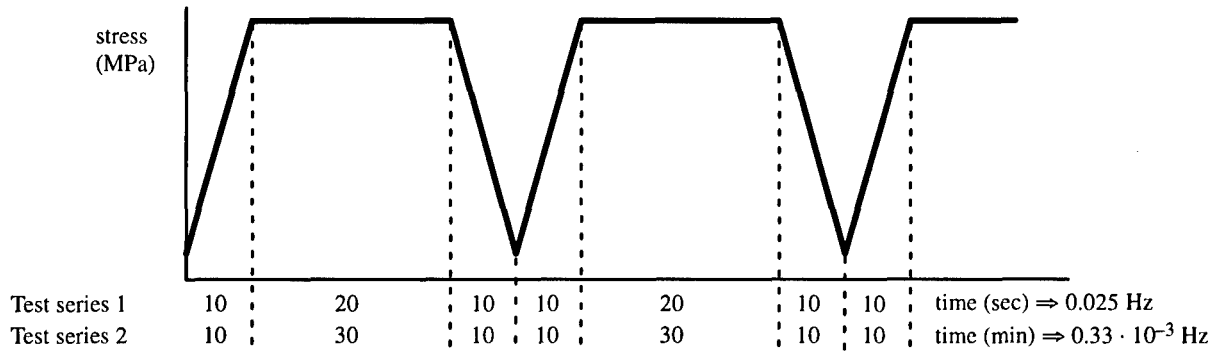

Fig. 2: Stress–time histories for crack growth tests

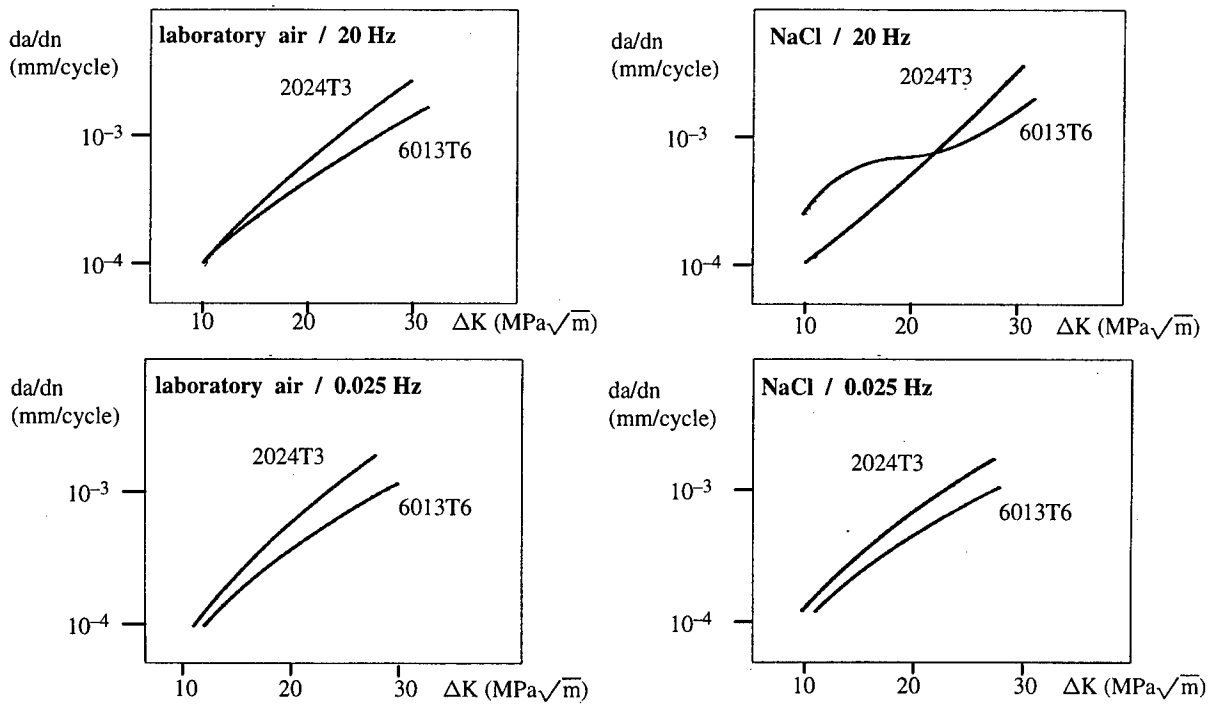

Fig. 3: Crack growth test results for 2024T3 and 6013T6 and frequencies of 20 Hz and 0.025 Hz

Considering the above mentioned comparison it would not be recommended to use these new materials. However, the test conditions are quite different from the reality, therefore new test procedures are to be developed and applied before a final decision is made. DA has accomplished crack growth tests using new test procedures. In general the effect of the frequency and the environment on the crack growth behavior has to be evaluated for longitudinal and circumferential cracks in a pressurized fuselage. The load spectra for these crack types are quite different, i.e. a constant amplitude spectrum due to internal pressure is driving the longitudinal cracks and a complex flight–by–flight spectrum due to internal pressure and external loading has to be considered for the circumferential cracks.

In test series 1 and 2 DA has analyzed the frequency and environmental effect for longitudinal cracks. Constant amplitude tests (R=0.1) have been carried out with CCT specimens and the stress–time–histories shown in Fig. 2. Figure 3 contains the results of the test series 1 compared with the data for the frequency of 20 Hz. The left hand figures show the da/dn data obtained under laboratory air. Independent from the test frequency the material 6013 shows a better crack growth behavior than 2024. The right hand figures, valid for the environment of sodium chloride, show different results: In case of a frequency of 0.025 Hz the crack growth behavior of 6013 is better. For a frequency of 20 Hz and lower ΔK values ($\Delta K \leq 22$ MPa$\sqrt{m}$) the crack growth behavior of 2024 is significantly better. For higher ΔK values ($\Delta K > 22$ MPa$\sqrt{m}$), which are less important, 6013 is superior to 2024.

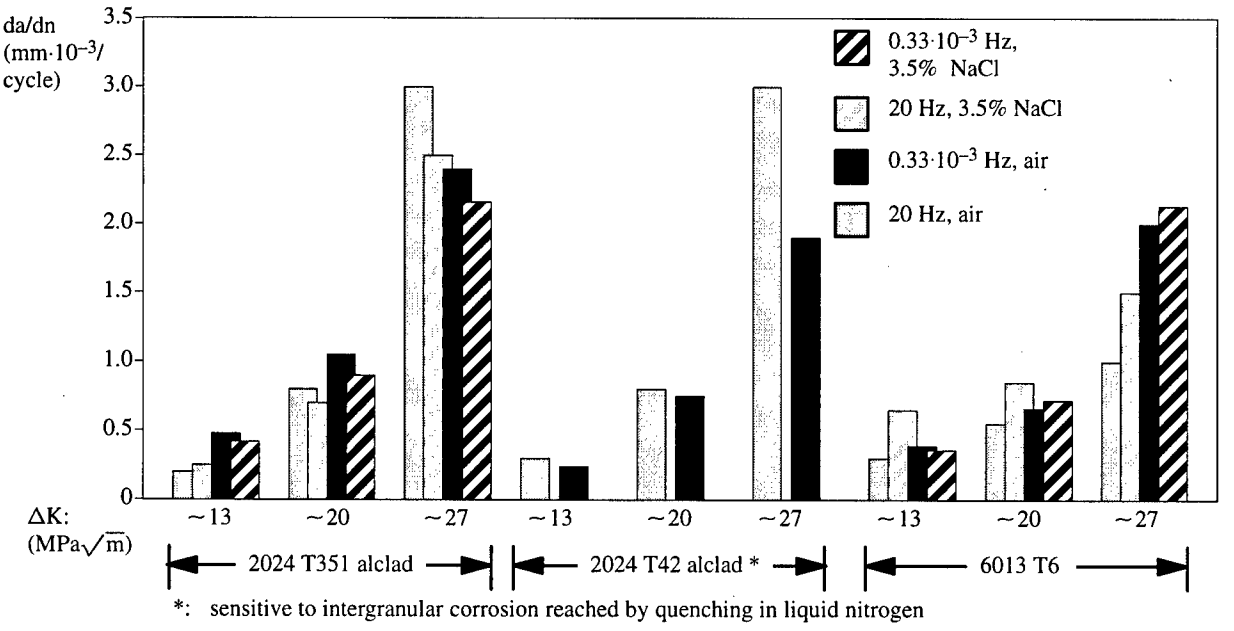

Fig. 4: Crack growth test results for 2024T351/T42 and 6013T6 and frequencies of 20 Hz and $0.33 \cdot 10^{-3}$ Hz

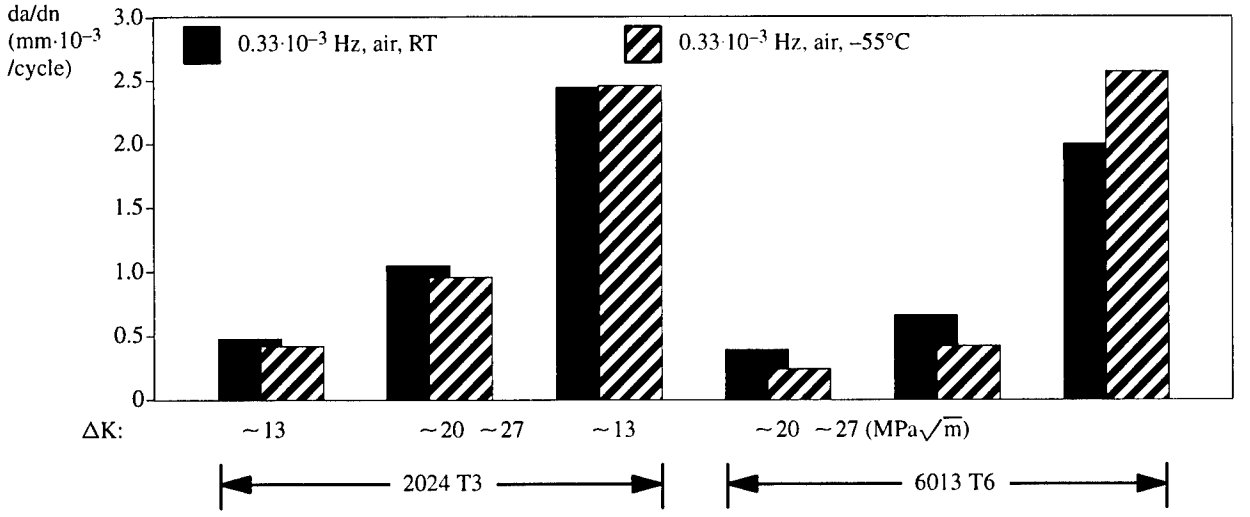

Fig. 5: Crack growth test results for 2024T3 and 6013T6 for low frequency and RT/–55 °C

Test series 2 contains similar tests with a frequency of $0.33 \cdot 10^{-3}$ Hz, see Fig. 4. As for test series 1 the material 6013 has a better crack growth behavior than 2024 for the frequency of $0.33 \cdot 10^{-3}$ Hz and 3.5 percent sodium chloride. The same behavior, i.e. 6013 better than 2024, is observed for laboratory air and the low frequency.

Furthermore some special effects such as temperature, application/deletion of cladding and other frequencies have been investigated with the following results.

Figure 5 presents a comparison of crack growth test results for specimens tested at low frequency of $0.33 \cdot 10^{-3}$ Hz in laboratory air and two temperatures (room temperature (RT) and –55°C). For the lower temperature of –55°C the crack growth is less than for RT for the two lower ΔK values of ~ 13 and ~ 20 MPa$\sqrt{m}$. For the highest ΔK value no decrease is observed for 2024 or even an increase for 6013.

Comparative crack growth tests with 2024 clad and bare specimens were performed at a frequency of 0.025 Hz and 3.5 percent sodium chloride, see Figure 6. The bare specimens show a slightly better crack growth behavior which can be explained by the thicker core material for the bare specimens.

The Technical University of Hamburg–Harburg, Germany, has carried out similar tests (ref. 1) and investigated the crack growth versus the frequency for the materials 2024T351, 6013T6 and 7475 (underaged) at two ΔK values. In principle the test results correlate with the DA investigations, but a maximum crack growth has been found at 1 Hz for all three materials and 3.5 percent sodium chloride environment with inhibitors, see Fig. 7. The possible reasons of these effects are discussed in ref. 1.

3.2 Crack Growth Tests under Flight–by–Flight Loading

For assessing the behavior of circumferential cracks in the upper shell of the pressurized fuselage complex flight–by–flight loading is necessary to comply with the in–service loading. Crack growth tests have been carried out using the stress–time history applied at the Airbus A330 full scale fatigue test of the rear fuselage. This flight–by–flight test program consists of 3920 normal (revenue) and 80 crew training flight types applied in a block of 4000 flights by 12 different flight types which are split into more than 100 sub–flight types in test. The flight types presented as examples in Figure 8 occur 5 times (A) and 980 times (G) in a block (the stress time histories are given in different scales).

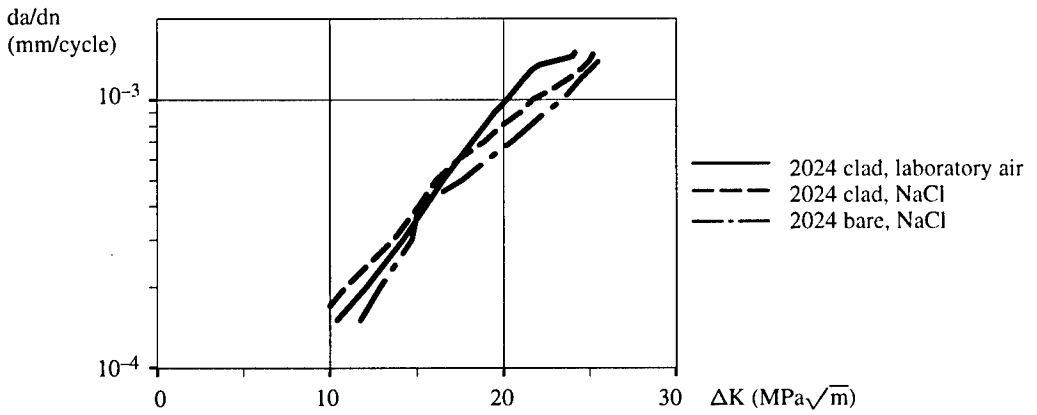

Fig. 6: Crack growth test results for 2024T3 clad and bare specimens at 0.025 Hz and 3.5 percent NaCl

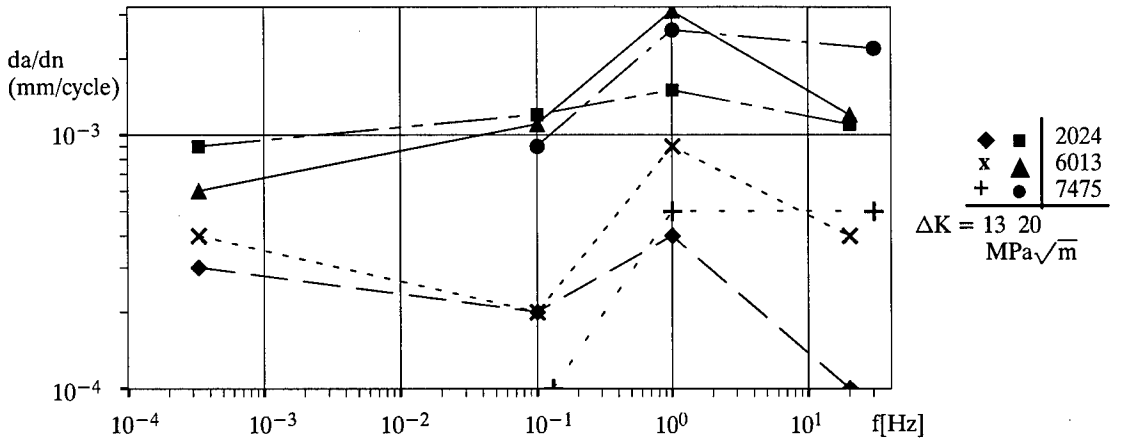

Fig. 7: Influence of frequency for 2024, 6013 and 7475

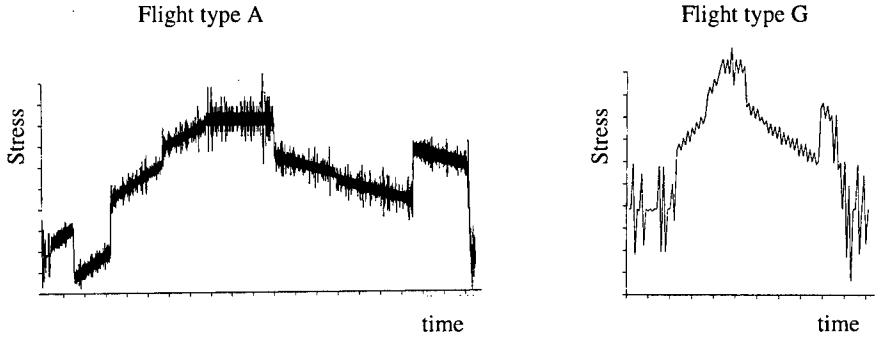

Fig. 8: A330–300 short range stress time histories for upper shell of rear fuselage

The tests with 2024T351 and 6013T6 specimens were performed at a frequency of approximately 15 to 20 Hz either in laboratory air or in 3.5 percent sodium chloride, see Figure 9. The crack growth behavior of 2024 for the two different environments shows small differences only, as expected from the experience with constant amplitude testing, see Table 2. In contrast 6013 shows an increased crack growth of factor 2 to 2.75 for the corrosive environment and the high test frequency. This result is also in line with the data presented in Table 2. However, the crack growth rates for 6013 and 3.5 percent NaCl are up to factor 2 higher than for 2024.

3.3 Crack Growth Test under Simplified Flight–by–Flight Loading

To investigate the effect of the flight–by–flight loading systematically simplified flight–by–flight stress–time histories were defined with major cycles of R=0.1 and incremental cycles of R=0.8, see Figure 10. The goal of this investigation is to understand the effect of incremental cycles during taxi and cruise (spectrum 1) and the effect of incremental cycles during climb, cruise and descent (spectrum 2). For both spectra the test frequency is 0.025 Hz for one flight allowing the comparison with the results of the constant amplitude testing (test series 1).

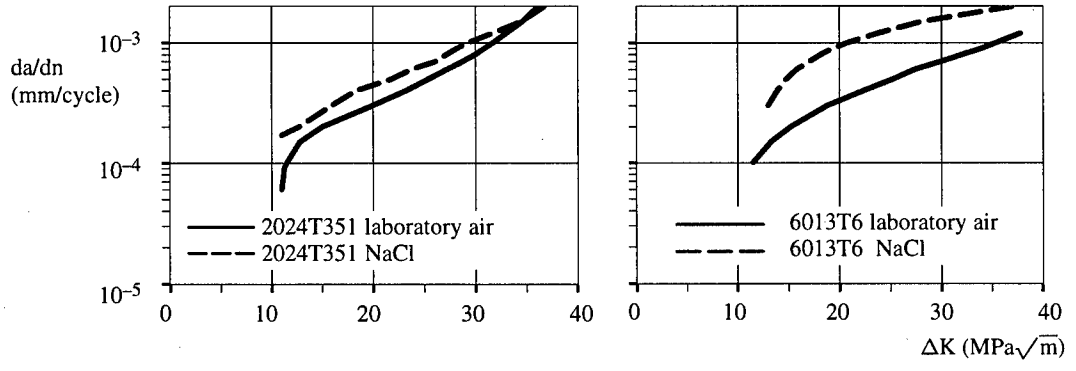

Fig. 9: Crack growth of 2024T351 and 6013T6 under Airbus fuselage spectrum loading (15 to 20 Hz)

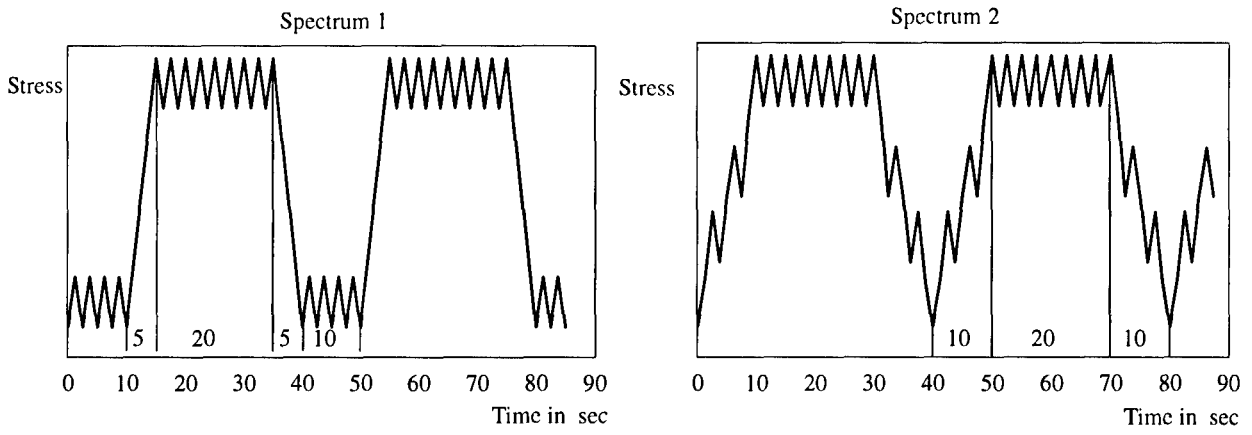

Fig. 10: Simplified flight-by-flight stress time histories

Figure 11 shows the results of the crack growth tests with spectrum 1. For 2024 no difference has been observed between the test conditions laboratory air and 3.5 percent NaCl which is in line with results presented in Figure 3. A similar behavior was observed for 6013 for ΔK values less than 17 MPa$\sqrt{m}$. Above this value the corrosive environment leads to an increased crack growth up to factor 2. The comparison of 2024 and 6013 under spectrum 1 loading and 3.5 percent NaCl reveals no difference in the crack growth rates.

The tests results with spectrum 2 loading show almost no differences in the crack growth rates under laboratory air and sodium chloride for both materials, see Fig. 12.

3.4 Crack Growth Tests under Variable Amplitude Waveforms

The Technical University of Hamburg-Harburg, Germany, investigated the effect of frequency on crack growth behavior of 6013T6. Besides the sinusoidal waveform, a sawtooth and two different types of variable amplitude waveforms were applied (ref. 2). The major cycles of all of the waveforms were applied with an R value of 0.1 (in addition 0.8 for waveform A) and a frequency of either 1 Hz (waveform A) or 0.1 Hz (waveform A and B) or 0.303 Hz (waveform C and D). Waveforms B and D were superpositions of the basic cycle and incremental cycles with R = 0.8 applied either at the maximum stress or during the climb flank, see Figure 13.

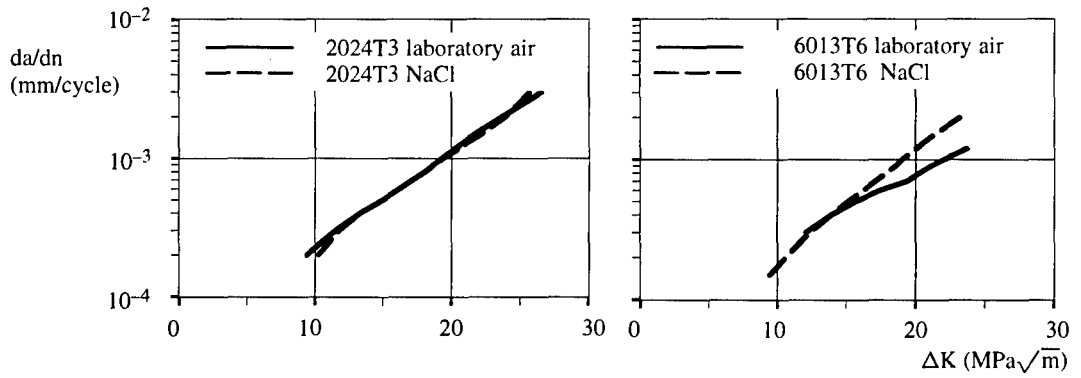

Fig. 11: Crack growth of 2024T3 and 6013T6 under simplified spectrum loading (spectrum 1, 0.025 Hz)

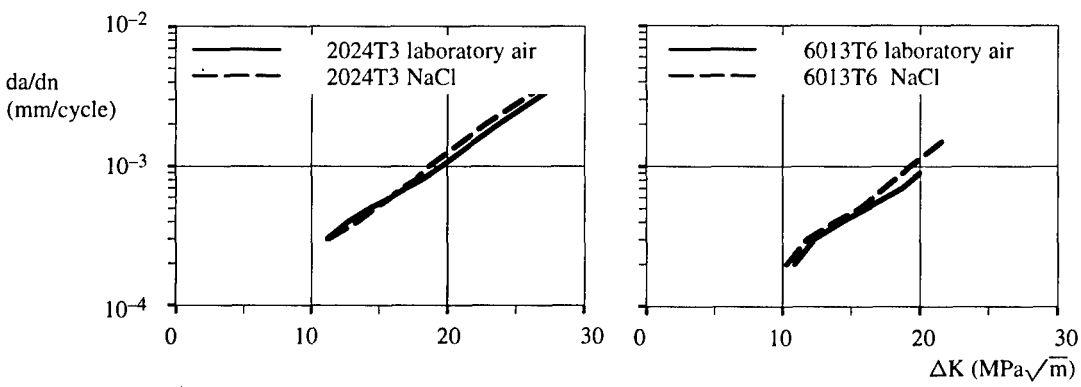

Fig. 12: Crack growth of 2024T3 and 6013T6 under simplified spectrum loading (spectrum 2, 0.025 Hz)

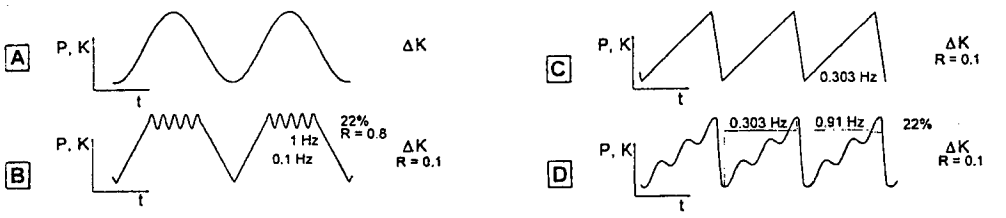

Fig. 13: Applied waveforms and corresponding frequencies

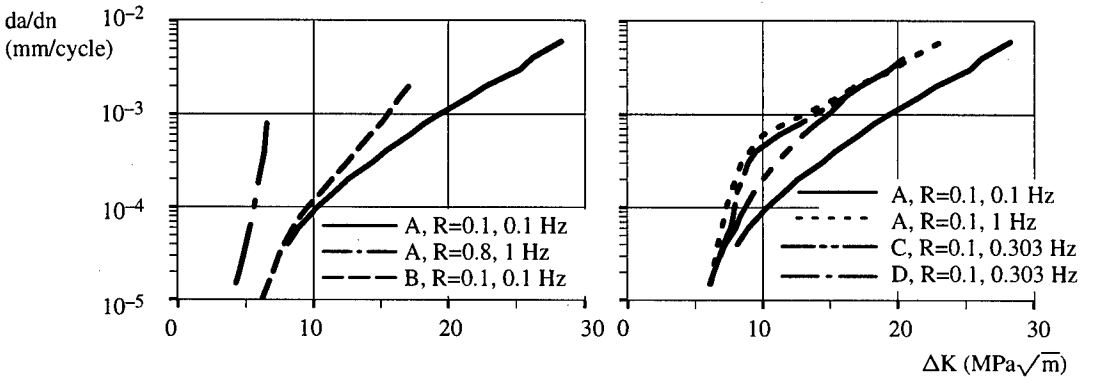

Fig. 14: Crack growth rates for 6013T6 in NaCl

The corrosive environment consists of 3.5 percent sodium chloride solution with an inhibitor. The specimens were 30 mm wide and 1.6 mm thick and tested in T–L direction.

The left hand diagram of Figure 14 presents results for the constant amplitude sinusoidal tests (waveform A) with either R = 0.1 and 0.1 Hz or R = 0.8 and 1 Hz and the variable amplitude trapezoidal tests (waveform B). The crack growth rates obtained for both waveforms are identical up to about $\Delta K = 10$ MPa$\sqrt{m}$, above this stress intensity waveform B leads to increased crack growth rates. The right hand diagram of Figure 14 contains first of all a comparison of test results for waveform A with the frequencies of 0.1 Hz and 1 Hz. The results are in line with data presented in Figure 7, i.e. increased crack growth rates for 1 Hz are observed. A further comparison between the sawtooth (waveform C) and the modified sawtooth by superposition of small cycles (waveform D) reveals slightly increased crack growth rates for waveform D. However, the increased crack growth rates do not exceed the data for waveform A with a frequency of 1 Hz.

3.5 Proposal of Spectrum Standardization

The investigations presented above revealed the complexity of the problem of material selection using the standard crack growth test procedure, i.e. frequency approx. 20 Hz, RT, air and 3.5 percent sodium chloride, resp., which may be misleading.

Therefore it seems necessary to develop new standardized test procedures which allow a sufficient prediction of the crack growth behavior for real conditions. A key issue is the standardization of the spectra to be applied for these tests, which should contain information about the stress–time–history, the corresponding frequencies, and the temperature distribution. The standardized spectra should be developed by an international co–operative approach. As an example Fig. 15 contains the DA proposal for the spectra to assess the skin of the pressurized fuselage of a widebody transport aircraft.

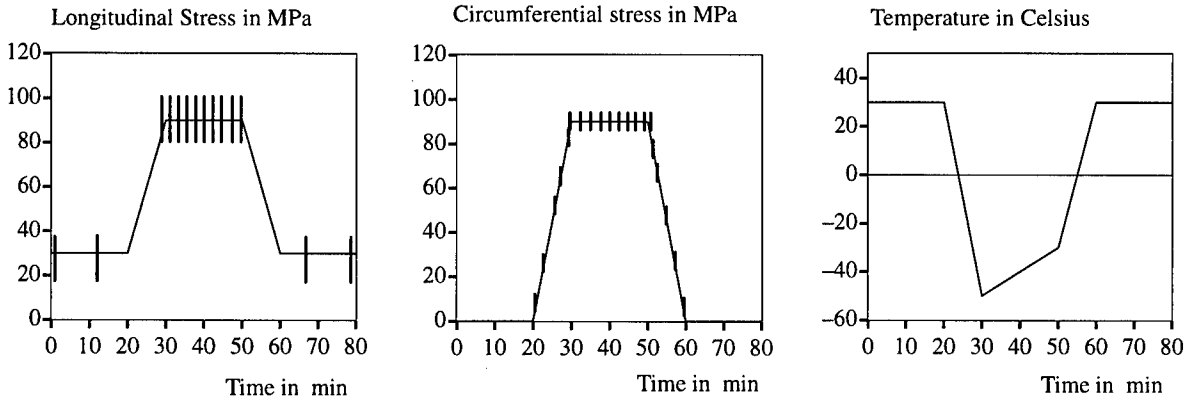

Fig. 15: Proposal of standardized spectra for fuselage skins

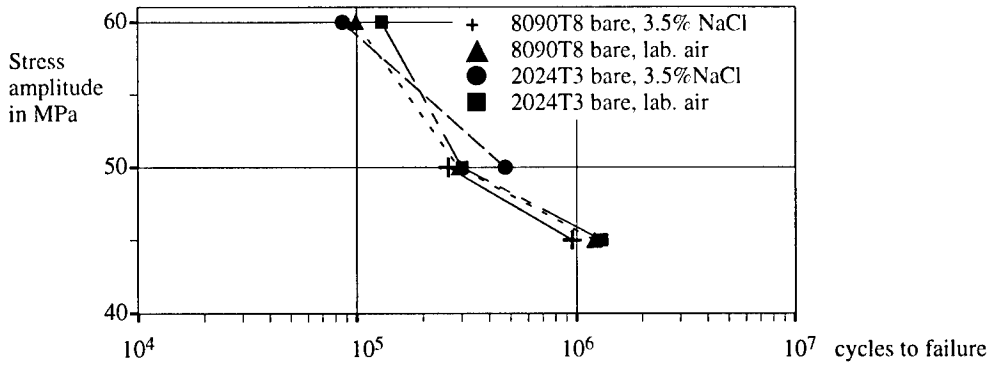

Fig. 16: Influence of the environment on the fatigue life of longitudinal lap joints

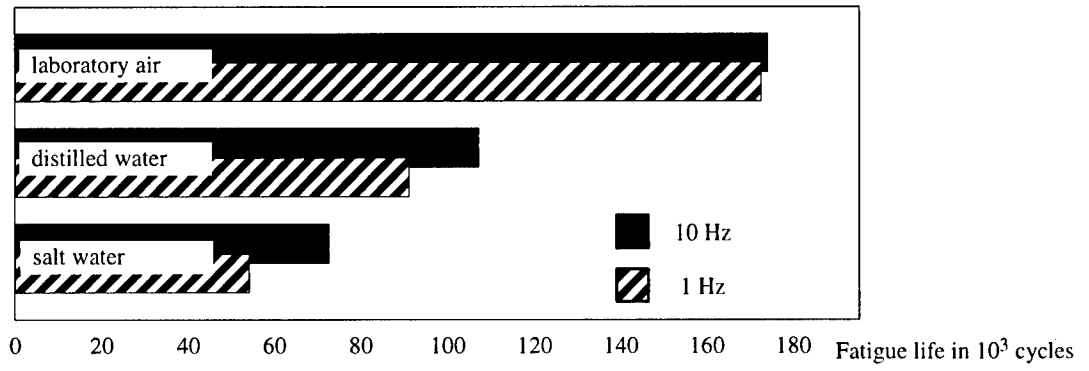

Fig. 17: Influence of the environment on the fatigue life of 2024T3 lap joints without surface treatment

4. CRACK INITIATION TESTS

Many investigations have been carried out to determine the effect of corrosive environment on fatigue life (crack initiation). For example DA tested several coupons representing the longitudinal lap joint. The test specimens were manufactured according to the production standard, i.e. with surface treatment (CAA, primer, top coat), wet assembly and wet riveting. The tests performed for two materials, the current skin material 2024T3 and the Al–Li alloy 8090T8, revealed no influence of the different environments, i.e. laboratory air and sodium chloride, see Fig. 16.

In contrast to the above mentioned results corrosion has a significant effect on the fatigue life of lap joints investigated in ref. 3. It has to be recognized that these 2024T3 specimens were manufactured without surface treatment and dry assembled. The results are nearly independent from the test frequency as shown in Fig. 17.

These test series lead to the conclusion that no reduction of the fatigue life has to be expected for in–service aircraft as long as the surface protection system is intact.

Figure 18 presents a typical example of the corrosion protection system used for the longitudinal lap joint areas in the pressurized A320 fuselage showing the internal and external protection, the application of sealant and an additional protection of the internal sealant beads in hydraulic fluid areas, e.g. in the bilge area. All rivets are wet installed and the driven rivet heads are protected by a paint touch–up.

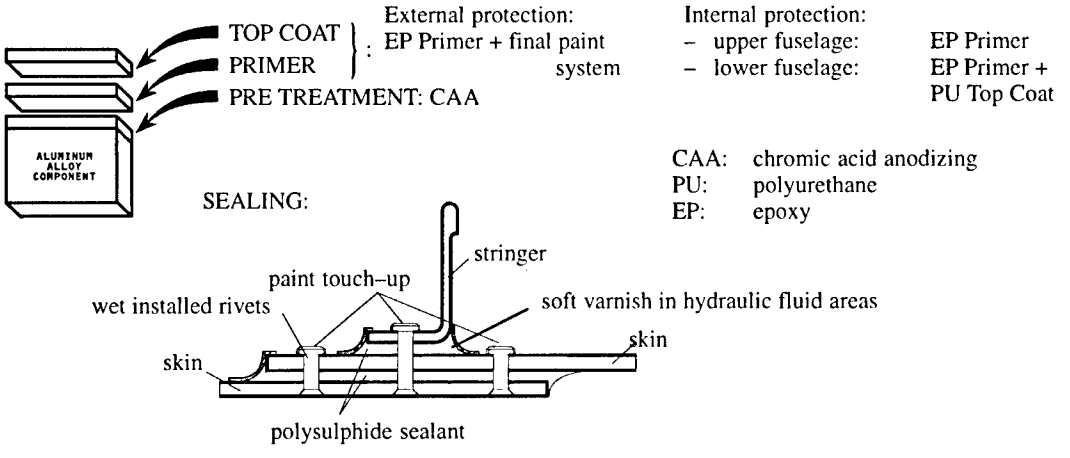

Fig. 18: Corrosion protection system for longitudinal lap joint area in A320 pressurized fuselage

5. CONCLUSION

The application of new materials to the next aircraft generation requires among others crack initiation and crack growth tests to verify that the new materials are not worse than the conventional 2024. Since this could not be concluded from the standard crack growth tests with 20 Hz in laboratory air or sodium chloride, DA has performed comparative crack growth tests with 2024 and 6013 specimens loaded by either constant amplitude or variable amplitude spectra and more realistic frequencies. The crack growth tests with the low frequencies in laboratory air or in corrosive environment revealed that the crack growth rates for 6013T6 are as good as or better than those for 2024T3/T42/T351, except for low temperature and high ΔK values. This result leads to the conclusion, that 6013 may be considered during the material choice for future aircraft as far as the crack growth aspect is concerned.

The results presented in this paper show that the current standard crack growth tests with high frequency and at room temperature may lead to decisions which are not on line with the conclusions from more realistic test. Therefore standardized test procedures considering the real conditions should be developed.

The crack initiation tests revealed that the surface protection plays the major role to prevent a fatigue life reduction in corrosive environment.

REFERENCES

1. Trockels, I.; Gysler, A.; and Lütjering, G.: Influence of Frequency on Fatigue Crack Propagation Behavior of Aluminium Alloys in Aggressive Environment. FATIGUE '96, The Sixth International Fatigue Congress; May 6–10, 1996; Berlin, Germany.

2. Trockels, I.; Lütjering, G.; and Gysler, A.: Effect of Frequency on Fatigue Crack Propagation Behavior of the Aluminium Alloy 6013 in Corrosive Environment. 5th International Conference of Aluminium Alloys; July 1–5, 1996; Grenoble, The Swiss.

3. Müller, R.P.G.: An Experimental and Analytical Investigation on the Fatigue Behaviour of Fuselage Riveted Lap Joints. Ph. D. thesis of Delft University of Technology, Faculty of Aerospace Engineering, Structures and Materials Laboratory, The Netherlands, 1995.

COMBINED EFFECT OF HYDROGEN AND CORROSION ON HIGH STRENGTH AIRCRAFT STUCTURES UNDER STRESSED CONDITIONS

Z.P. Marioli-Riga, A.N. Karanika
HELLENIC AEROSPACE INDUSTRY
R&D, ADVANCED MATERIALS AND PROCESSES Dept.

1. SUMMARY

The embrittlement of high strength landing gear steels is occurred due to hydrogen absorption during electro-chemical corrosion protection treatments. Accidents have been reported after service of high strength landing gear components at low applied cycles of stresses and have been attributed to Hydrogen Embrittlement.

For evaluation of the mechanical properties reduction of high strength structures, after re-treatment during maintenance, specific sustained load creep tests are carried out. When an electrochemical plated notched specimen is strained, hydrogen is carried by mobile dislocations to the root of the notch. Transient cracks formed by dislocation interaction, are stabilized by the hydrogen and stresses which would be relieved by deformation in absence of hydrogen are relieved by cracking when the hydrogen content exceeds a critical value.

However, these tests provide information of mechanical behaviour based only to Hydrogen absorption. In real cases the A/C components phases a combined effect of highly corrosive environment like seawater, hydrogen and loading.

The present investigation is aimed to create realistic qualification tests for high strength serviced aircraft components operated in a periodical fatigue and corrosive environment. A creep test program was developed and a series of notched specimen -attacked variously by Hydrogen and corrosion salt spray- have been subjected to different cycles of sustained load. The mechanism of failure was recorded and conclusions were extracted for establishing simulated qualification tests.

2. INTRODUCTION

The failure of metal resulting from the conjoint of stress and chemical attack usually called stress corrosion cracking. There are two different types of mechanisms by which stress corrosion cracking is believed to occur. Active path corrosion and hydrogen embrittlement. In the active path corrosion type, cracking is caused by localized corrosion at the crack tip and proceeds along the path that is electrochemically active with respect to the surrounding metal. The hydrogen damage results from the initial presence or absorption of excessive amounts of hydrogen in metals, usually in combination with residual or applied tensile stresses. It occurs most frequently in high strength steels and certain other high strength alloys.[3][4]

Embrittlement by hydrogen damage manifests itself as a decrease in tensile ductility (reduction in area in laboratory testing) or a decrease in notched tensile strength and delayed failure by fracture under static loading. Yield strength is not significantly affected.[1][2]

In hydrogen charging, atomic hydrogen is introduced in metals by processes like pickling, electroplating, galvanic coupling to a more anodic metal.[1][2][6]

Paper presented at the RTO AVT Workshop on "Fatigue in the Presence of Corrosion", held in Corfu, Greece, 7-8 October 1998, and published in RTO MP-18.

Corrosion reactions that generate hydrogen at metal surfaces also result in hydrogen charging.

Metal specimens for use in studying hydrogen embrittlement are internationally charged by electroplating at controlled current densities . If enough hydrogen is absorbed and diffuses into the metal lattice the metal can become embrittled. Embrittlement may occur when a critical amount of hydrogen precipitates out of solution within the metal as hydrogen gas at voids or points of weakness in the metal. However, internal voids and other imperfections lead to local formation of molecular hydrogen that can not be diffused gradually out of the metal. Heating at 150 ° to 200 ° C speeds up the removal of hydrogen. Ultra high strength steels are the materials of choice for highly loaded aircraft structural components. Examples of such components are landing gears, arresting structures, wing attach fittings etc.[5][6][7]

The materials used in a series of aircraft at the above mentioned structures are martensitic and maraging low alloy steels with tensile strength of 260ksi (1800 Mpa). These steels are susceptible to stress corrosion cracking and hydrogen damage. Martensitic structures absorb atomic hydrogen at an increasing rate with increasing tensile stress. During operation and maintenance these components are subjected to hydrogen and corrosive environment. All the repairs on the above mentioned items are followed by application of electroplated coatings which produce and induce hydrogen in the high strength metal of structure. Many aircraft accidents have been reported due to abrupt fracture of high strength steels in landing gears.[7][8]
Actually, trapped hydrogen operates inside the metal by producing a stress field and if this phenomenon be combined with a corrosive environment and externally applied cyclic loads the life of the component dramatically changes and it seems to be decreased, unpredictable.

For quality control purposes all processes used on aircraft high strength steels (plating, pickling) during maintenance, must be evaluated for hydrogen embrittlement by different tests in order to assess the influence of hydrogen absorption and corrosion to their mechanical properties.

3. PURPOSE OF INVESTIGATION

The main purpose of this investigation is to study the behavior of high strength steels used in critical aircraft structures subjected to hydrogen charging and corrosive environment under cyclic sustained loading. This will be a part of a major project to develop standard qualification tests more accurate and less time consumable.

The proposed qualification tests suggested in the pertinent specifications are depicted in Table 1. The investigation deals with destructive special tests on specimens with different attack of hydrogen, as well as, both hydrogen and corrosion (salt spray), under various type of loading as tension static, static sustained and cyclic sustained.

In addition, the reason for conducting this investigation is the establishment of engineering data to be used for the design of periodical repairs on aircraft structures, based on the environmental effects as:

- The influence of environments on the stress corrosion behavior of aircraft quality, high strength steels
- The effect of specific service environment for the possibility of stress corrosion cracking
- The effectiveness of electroplated coatings for reducing the susceptibility of high strength in stress corrosion.
- The effect of stress corrosion in the service life of structure.

Table 1: Suggested Methods for Hydrogen Embrittlement Tests [9][10][11][12][13][14][15][16][17]

SPECIFICATION	PROCEDURE	NOTES
MIL-STD-870 "Cd PLATING, LOW EMBRITTLEMENT, ELECTRODEPOSITION"	SUSTAINED LOAD ON NOTCHED SPECIMENS	200 HRS/MONTH PER TEST
AIR 3376 "INSTRUCTION FOR ELECTROLYTIC PROTECTIVE TREATMENT ON FERROUS METALS BY Cd AND Zn PLATING" AND MESSIER-HISPANO-BUGATTI 32-09-01 "ELECTROLYTIC Cd PLATING (LOW EMBRITTLEMENT PROCESS) OF HIGH TENSILE STRENGTH STEEL PARTS HEAT TREATED TO NOT LESS THAN 1450 MPa"	✓ SLOW BENDING TEST ✓ LAWRENCE GAUGE ✓ STATIC LOADING TEST (SUSTAINED LOAD)	TOO MANY SPECIMENS OF COMPLICATED SHAPE REQUIRED PER TEST (10 SPECIMENS) COMPLICATED CALIBRATION PROCEDURE EVERY 7 DAYS 200 HRS/MONTH PER TEST
I.G.C. 04.73.106 "ELECTROLYTIC Cd PLATING" A/DET 0073 "ELECTROLYTIC Cd PLATING OF NON-STAINLESS STEELS"	✓ SLOW BENDING TEST ✓ STATIC LOADING TEST	TOO MANY COMPLICATED SPECIMENS REQUIRED PER TEST (10 SPECIMENS) 200 HRS/MONTH PER TEST
FPS-1007 "Cd PLATING FOR FERROUS ALLOYS, 180 TO 240 KSI ULTIMATE TENSILE STRENGTH"	SUSTAINED LOAD	200 HRS/MONTH PER TEST
BAC5718 "LOW HYDROGEN EMBRITTLEMENT Cd PLATING" AND BSS 7321 "HYDROGEN DETECTION INSTRUMENT TEST METHOD"	✓ PLATING POROSITY METER ✓ STATIC TENSILE LOADING (SUSTAINED LOAD) AND MICROGRAPHIC EXAMINATION	COMPLICATED CALIBRATION PROCEDURE, TWICE EVERY 7 CALENDAR DAYS 150 HRS 150 HRS/EVERY 7 DAYS
AMS 2401 "Cd PLATING. LOW EMBRITTLEMENT CONTENT DEEPOSIT"	✓ ROOM-TEMPERATURE NOTCHED STRESS-RUPTURE PROPERTIES	200 HRS PER TEST AND TOO MANY SPECIMENS OF COMPLICATED SHAPE

4. MATERIALS AND SPECIMENS

The material selected for this study is SAE 4340 in accordance with MIL-S-8844. The chemical composition of this material is shown in Table 2. The specimens were round and notched, heat-treated to a tensile strength of 260-280 Ksi. Their configuration was in accordance with ASTM Standard E8 for round specimens, as shown in Fig.1. Specimens had a 60-degree V-notch located at the center of the gauge length. The cross section area at the root of the V-notch was approximately equal to half the area of the full cross section. The V-notch had a 0,254±0,0127mm radius of curvature at the base of the root.

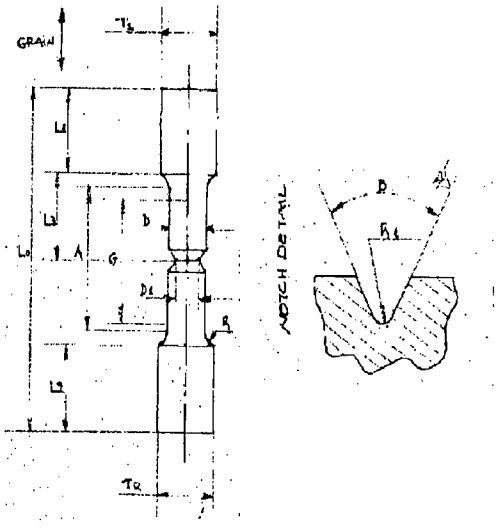

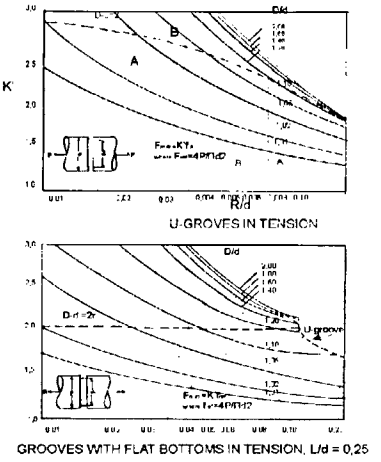

DASH No	L_0 ±0,100	L_1 ±0,05	L_2 ±0,05	L_3 REF	G ±0,005	D ±0,005	D_1 ±0,002	T_1	T_2	R ±0,0005	R_1 ±0,0005	A MIN	B ±30"
-001	3,125	0,75	0,75	13/16	1,000	0,250	0,177	M10x1,5	T_1	0,1875	0,0100	1 ¼	60"

Fig1 Configuration of tensile notched specimen and related toughness curves

Table 2: Chemical composition of SAE 4340

Element	Percentage
Carbon	0,38 to 0,43
Manganese	0,65 to 0,90
Phosphorous	0,010 maximum
Sulphur	0,010 maximum
Silicon	0,20 to 0,35
Nickel	1,65 to 2,00
Chromium	0,70 to 0,90
Molybdenum	0,20 to 0,30
Vanadium	-
Boron	-

5. EXPERIMENTAL PROCEDURE

After the heat treatment and machining, the specimens plated in accordance to MIL-STD-870. The cadmium plating process was followed by baking for hydrogen emrittlement relief at 375 ± 25 °F (191 ± 14 °C). Seven different groups of specimens baked for different times as shown in Table 3 (3hrs, 10hrs and 23hrs). By this way the remaining amount of the absorbed hydrogen was different in the specimens, depending on the time of baking for relieve.

After the completion of baking, 3 groups of the specimens exposed for 360 hrs in salt spray solution per ASTM B-117 (see Table 3).

Two specimens of the same configuration, heat-treated simultaneously with the above mentioned, but were not plated and used for the determination of ultimate notched tensile strength (u.t.s.). Thereinafter all groups submitted to cyclic sustained load. In the first cycle the load was the 50% of u.t.s. And applied for 100 hrs. Upon the completion of the first cycle a second cycle followed with a load equal to the 75% of u.t.s.

The specimens baked for 3 hrs failed during this second cycle. The average time of failure is shown in the Table 3. After this rupture the surfaces were fractographic examined by Scanning Electron Microscopy (SEM). (Photo 1and 2)

The specimens baked for 10 and 23 hrs passed successfully the test. After 265 hrs of loading in 75% of u.t.s. The test stopped and the specimens submitted to tensile test in order to examine the effect of corrosion and cyclic stress in the resistance of metal to tension (speed of tensile test = 3mm/min).

The fracture was accomplished at different load levels as shown in the following Table 3.

The fractured surfaces were examined by stereo-zoom. (Photo 3,4,5, 6 and 7)

Table 3: Experimental procedure & Results

SPECIMEN ID. MARKING	CADMIUM PLATING	TIME OF BAKING AFTER Cd PLATING (Hrs)	TIME OF EXPOSURE IN SALT SPRAY (Hrs)	TIME OF SUSTAINED LOADING AT 50% OF U.T.S. (Hrs)	TIME OF SUSTAINED LOADING AT 75% OF U.T.S. (Hrs)	U.T.F. AFTER Cd PLATING, BAKING, SALT SPRAY & LOADING (KN)
1	AS PER MIL-STD 870	3	0	100	10 FAILURE	-
2	AS PER MIL-STD 870	3	0	0	160 FAILURE	-
C1	AS PER MIL-STD 870	10	0	100	264	42,02
C2	AS PER MIL-STD 870	23	0	100	264	42,54
C1C	AS PER MIL-STD 870	10	360	100	264	40,74
C2C	AS PER MIL-STD 870	23	360	100	264	41,46
C*	See note	See note	360	100	264	41,54

NOTE: Specimen marked C* has already passed successfully the hydrogen embrittlement test during a periodic qualification of the cadmium plating process.

6. RESULTS AND DISCUSSION

The test results gathered from the following groups of specimen:

1. Notched specimens with remained hydrogen (only 3 hrs baking after electroplating) in the metal lattice ,subjected to :
   1) Static sustained load
   2) Cyclic sustained load
   The failure was occurred after 160hrs
   The same types of specimens were failed after 10hrs when subjected to cyclic sustained load.
   The variation in times to cracking seems to be affected seriously by a static fatigue loading sequence (see fig.2). For the same amount of absorbed hydrogen in the metal the endurance limit is shorten when subjected to static fatigue than to static stress fields

2. Notched specimens with less and no remaining hydrogen in the metal lattice (10hrs and 23hrs of baking after plating) , subjected to cyclic load. These group of specimens passed successfully cyclic sustained load for 100hrs at 50% of utf and 264hrs at 100% of utf (see fig.3). In addition there was no reduction of the ultimate tensile strength. All failed in tension at 42 KN. That means that the type of loading is less serious for the endurance of metal when the remained amount of hydrogen in the lattice is none or insignificant

3. The same notched specimens as in case 2 were subjected to corrosive environment (salt spray). A noticeable reduction of their static strength was measured (see fig.4). But they passed successfully the cyclic sustained load (100hrs at 50% of uts and 264 hrs at 75% of uts.

   According to the experimental results, for the same amount of entrapped hydrogen in the metal the cyclic sustained load (static) seems to be more critical

7. CONCLUSIONS

In high strength aircraft quality steels used for landing gears and fittings the presence of hydrogen after electroplating applied for repair purposes seems to be more serious when the structure subjected simultaneously to static-fatigue loads.

The combination of corrosive environment and hydrogen charging operates in the metal with noticeable reduction of ultimate tensile strength.

All qualification destructive tests suggested to specifications for the assessment of hydrogen and corrosion effect after electroprocess on the high strength structure are time consumable and no so accurate for specific stress cases. These tests require static sustained load for the acceptance of structure after processing.

The present work leads to the conclusion that cyclic sustained loads should be incorporated in the qualification tests in order to be more accurate for the endurance limit and safer for the airworthiness of structure.

8. REFERENCES

1. Hydrogen-Damage Failures By the ASM committee on failure by mechanical environmental processes Metals Handbook pages 230-240

2. Corrosion Fatigue failures By the ASM committee on failure by mechanical environmental processes. Metals Handbook pages 230-240

3. B.F.Brown . A preface to the problem of stress corrosion cracking STP 518 page 3

4. A, A, Sheinker and J.D.Wood. Stress corrosion cracking of high strength steels STP 518 pages 16- 38

5. S.J.Ketcham. Testing Methods for Stress Corrosion Cracking STP 518 pages 79-86

6. H.E.Townsend, Jr. Resistance of high strength structural steel to environmental stress corrosion cracking. STP 518 pages 155-156

7. E.U.Lee, J.Kozol, J.B.Boodey, J.Waldman Corrosion of Landing Gear SteelsAgard CP565

8. Mil-Std-870. Cd Plating, Low Embrittlement, Electrodeposition

9. Mil-Std-870. Cd plating, low embrittlement, electrodeposition.

10. Air 3376. Instruction for electrolytic protective treatment on ferrous metals by cd and zn plating.

11. Messier-Hispano-Bugatti 32-09-01. Electrolytic cd plating (low embrittlement process) of high tensile strength steel parts heat treated to not less than 1450 Mpa

12. I.G.C. 04.73.106. Electrolytic cd plating

13. A/DET 0073. Electrolytic cd plating of non-stainless steels

14. FPS-1007. Cd plating for ferrous alloys, 180 to 240 ksi ultimate tensile strength

15. BAC 5718. Low hydrogen embrittlement Cd plating

16. BSS 7321. Hydrogen detection instrument test method

17. AMS 2401. Cd plating. Low embrittlement content deeposit

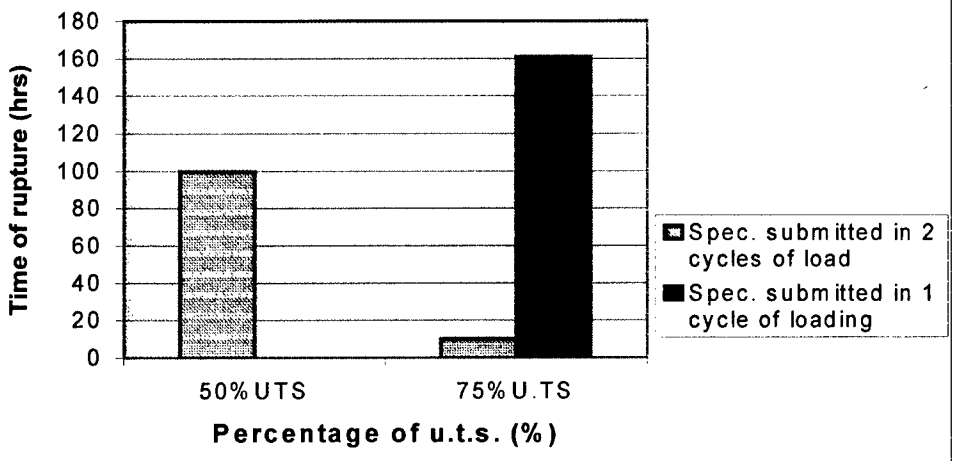

Fig.2: Influence of the Number of loading cycles in the rupture time

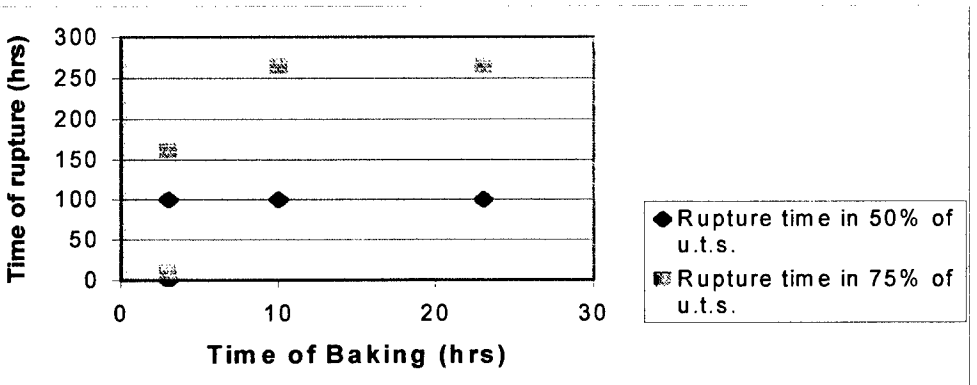

Fig.3: Influence of baking time in the rupture time for non corroded specimens

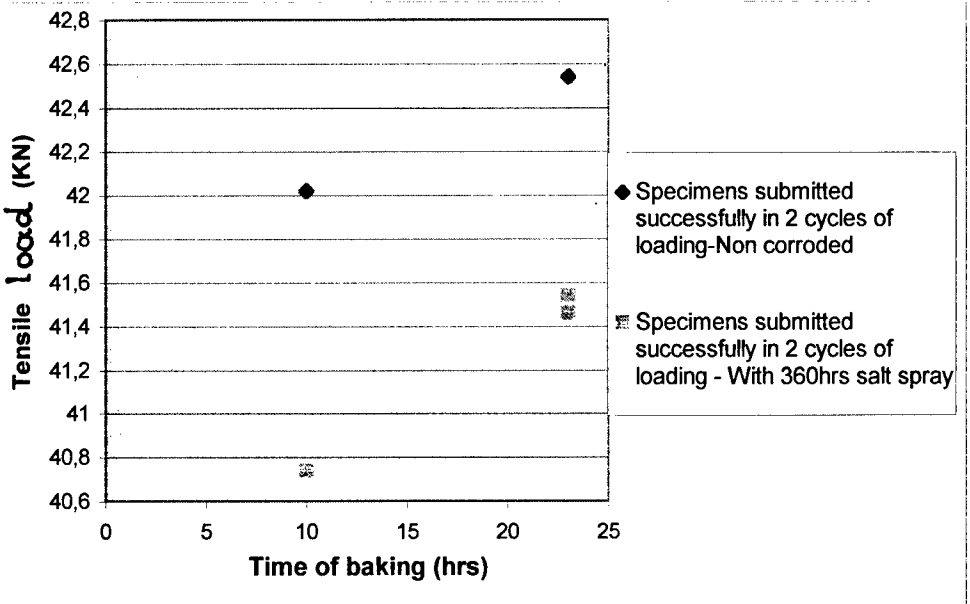

Fig. 4: Influence of baking and corrosion in tensile strength

Photo 1. Surface of specimen with hydrogen embrittlement (3 hrs baking) by SEM

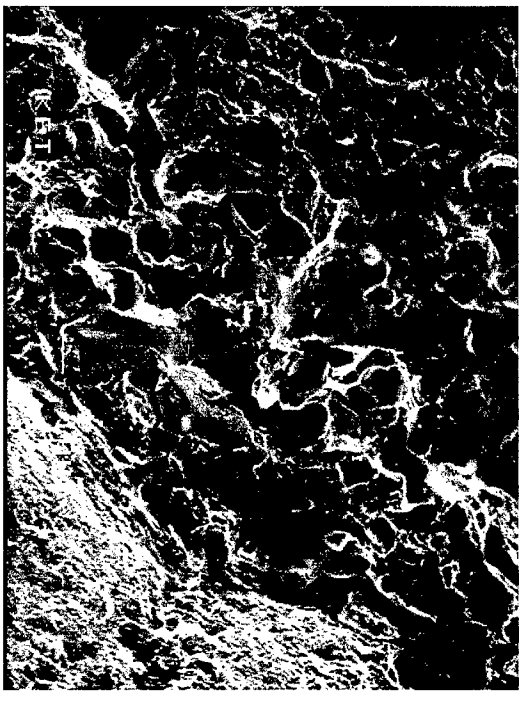

Photo 2. Surface of specimen with hydrogen embrittlement (3 hrs baking) and 2 cycles of loading by SEM

Photo 3. Fractured surfaces of specimen with 23 hrs baking and 0 hrs salt spray

Photo 4. Fractured surfaces of specimen with 10 hrs baking and 0 hrs salt spray.

Photo 5. Fractured surfaces of specimen with 10 hrs baking and 360 hrs salt spray

Photo 6. Fractured surfaces of specimen with 23 hrs baking and 360 hrs salt spray

Photo 7. Fractured surfaces of specimen with 23 hrs baking and 360 hrs salt spray, already passed a periodic qualification

Corrosion is a Structural and Economic Problem: Transforming Metrics to a Life Prediction Method

Craig L. Brooks, Scott Prost-Domasky, and Kyle Honeycutt
Analytical Processes / Engineered Solutions
3542 Oxford Avenue
St. Louis, Missouri, USA 63143

Summary

This paper advocates a basic engineering approach to compute the effects of corrosion on structural capability. The analyses use fracture mechanics methods and fundamental engineering principles. Engineering computations are combined with damage tolerance assessment concepts to formulate a model to approximate the life degradation effects of corrosion. The methods and assumptions used in the analyses are based on reasonable physical characteristics. Where scientific data is unknown, rational judgements are made and several options are explored to bracket the results in terms of the assumptions. Sensitivities of the parameters are examined to establish overall relevance of results. Although the life predictions are calculated using deterministic techniques, the scope of the problem and thus the life impacts computed should be considered as probabilistic. The results of this approach provide the analyst with numerical impacts of potential scenarios and a means for quantifying the effects of corrosion with fatigue. The results also provide a "benchmark" for methodology improvements as new data and information are obtained.

Crack growth life analyses of particular geometry configurations are used to show the relative life impact of corrosion metrics. For example, typical surface morphologies generated by corrosion in a lap joint are evaluated. The local stress amplification due to the corrosion roughness reduced the regional crack growth capability of a surface crack by 70%. The impact of sustained stress build-up caused by corrosion-induced pillowing in a lap joint degraded structural life 25 to 35% for a crack adjacent to a fastener hole. These results represent the level of potential life degradation that could be realized in the corroded regions. The individual models isolate the contribution of effects attributed to corrosion (i.e., pillowing, surface morphologies, etc.) and analysis results emphasize the need to include corrosion parameters in a component service life assessment. A simulation of a pressurized fuselage skin splice is used to illustrate the analytically derived impact to the life and safety of the joint in the presence of corrosion. The analysis includes time-dependent effects of corrosion into the structural life prediction for a multi-site damage (MSD) scenario. Twenty and fifty year corrosion assumptions are used based upon conditions found in existing aircraft. The results of this analysis indicate that corrosion is a potential structural problem for the particular aircraft locations that are experiencing this type of corrosion attack.

This paper presents the methodology for computing the effects of real time 'age degradation' on an aircraft structure. A companion paper, Reference 1, provides both substantiation and documents a process for incorporating these aspects into the existing infrastructure of the design, manufacturing, and maintenance of aircraft systems. The two papers thus provide a means of using the existing Structural Integrity process to meet the needs, opportunities and challenges being presented by the aging aircraft fleet.

Introduction

The demands for continued use of the Aging Aircraft Fleets around the world require methods and techniques for assessing the safety, readiness, and costs associated with corrosion. Fatigue, crack growth, and finite element modeling algorithms, each with corrosion interaction effects, are tools that can be readily adapted to provide adequate assessments to determine the magnitude of the corrosion problem. The results of USAF programs and several international research investigations justify the feasibility and practicality for using the concept proposed in this paper.

The fundamentals of the proposed approach are to:

- Determine the initial "as-built" quality condition of the structure and basic material for the initial starting condition,
- Model the effects of micro and macro surface morphology changes in time due to corrosion growth,
- Include the time dependence of any mechanically induced deflections due to corrosion by-products and effects of material loss, and
- Juxtapose and superimpose corrosion effects with cyclic fatigue crack growth using the appropriate environments.

The proposed procedure requires establishing the effective characteristics of material and structural quality states to provide an initial starting condition. Metrics include industry strain/stress "crack initiation" test data, surface morphology, local and global deflections and loads, crack growth rate data, corrosion growth rate data, related experimental data, field aircraft findings, and experience. Each state can contribute to crack extension in both the cyclic and time environment domains. Several transformations of metrics that represent damage mechanisms are simulated. There is much information to be gathered to demonstrate and validate the process—this paper presents a candidate for a collaborative focus.

This paper includes a description of each of the tools used. Procedures for determining the initial conditions, the finite element models used to characterize the surface morphology stress states, the stress analysis model for the multi-site damage (MSD) plate, crack growth simulations for different scenarios, and methods for combining the time dependent corrosion mechanisms with cyclic fatigue mechanisms are described. The results of scenarios show the structural impact of corrosion interaction with fatigue cycling. Structural life impacts in the multi-site damage scenario and residual strength computations with corrosion and fatigue interactions are shown.

By using the available state-of-the art fracture mechanics and structural analysis tools, an engineering method for integrating life impacts due to corrosion degradation can be incorporated into structural life assessments. With these tools and concepts it becomes feasible to determine the economic impact of corrosion, and to improve the structural airworthiness of all aircraft systems.

Paper presented at the RTO AVT Workshop on "Fatigue in the Presence of Corrosion", held in Corfu, Greece, 7-8 October 1998, and published in RTO MP-18.

Methodology

The engineering methodology used here has several attributes. First, the method allows flexibility so that as the technology evolves, individual parameters can be modeled into the life projection techniques. Second, the method uses established procedures that the aircraft community already understands and that work well. Third, the method provides a platform for including other degradation effects, in addition to surface corrosion, into an interactive prediction method that includes cyclic fatigue. Fourth, the method uses the existing structural integrity infrastructure for efficient implementation. And, fifth, the method provides an immediately accessible means for quantifying the impact of corrosion on the Aging Aircraft fleet.

1. The Basic Life Prediction Model

The following equation represents the basic conceptual formulation and analytical framework:

$$\Delta K_I = \beta_{pillowing}\beta_{corrosion}\beta_{FW}\beta_{K_I}\Delta\sigma_{cy}\sqrt{\frac{\pi a}{Q}} \quad \&$$

$$\beta_{corrosion}\beta_{TBD}\beta_{sustained}\Delta E_{time}\sqrt{\frac{\pi a}{Q}}$$

This equation includes the environment time domain (bottom) with the cyclic domain (top). Corrosion effects are both interdependent with and independent of the cyclic domain. The synergistic effects of the two are problem specific. The square root and π terms of the environmental component may be other functional forms. The corrosion rate equations have different forms than cyclic crack growth rate equations (da/dN curves). The particular form(s) of the equation are part of the evolving engineering process and solution development. It is anticipated that as corrosion rate models are determined, as corrosion effects are monitored and as cyclic stress influences are determined, the geometric correction factors (βs) and their relationships to crack length and effective stress intensities will become more refined.

For a lap splice problem, analytical approaches and techniques were developed to quantify the effects of corrosion on the structural integrity of the configuration. The effects of boundary conditions, fastener models, fastener bearing loads & through stresses, plasticity, local corrosion by-product pillowing, multiple site damage, load redistribution, surface morphology, and other influences were evaluated.

2. Initial Quality State (IQS)

As part of the analytical method, a "holistic" approach to fatigue life computations is used. The initial quality state (IQS) concept is similar to the equivalent initial flaw size (EIFS) concept, with the difference being that the IQS concept uses more stringent requirements in material crack growth rates, data correlation, and model qualifications. The restrictions placed on the IQS computations will be the subject of a future paper. Micro-porosity, inclusions, slip bands, non-homogeneity and variations in as-manufactured states are treated as initial flaw sizes with little regard for the flaws' sources. Distributions of flaw sizes extracted from the plethora of experimental data represent the number of cycles required to obtain known test termination events from the as manufactured condition of the material. The computed initial flaw sizes use test data conducted at many stress ratios and at several different constant amplitude peak stresses, and also represent several lots of the sheet material of interest. The results thus characterize the statistical nature of the flaw sizes by using crack growth analysis techniques, and model initial stages of crack formation and germination in the material's initial quality condition (or state). Figure 1a presents the analysis results for aluminum alloy 2024-T3 sheet (bare) material. Figure 1a shows the occurrences as a function of initial quality size for the different stress ratios. Results from the 2024-T3 sheet analysis are combined with 7075-T6 (bare) results in a Weibull distribution (Figure 1b) to show that the two materials have similarities in their IQS distributions. One test point calibration provided an extreme value of the distribution, Reference 2. This value was subsequently used as the effective 'holistic' rogue flaw. The specimens were smooth sections with low or no stress concentrations and thus represent bulk material behavior on a global scale (test data obtained using specimens with stress concentrations, preferably open holes of sizes typical of fasteners, might provide more representative distributions of flaw size distributions applicable to fastener hole regions). These IQS distributions represent the inherent condition of the as-manufactured material, and thus any corrosion attack as well the fatigue cycle crack extension will start from these initial conditions. These distributions control the Multi-site damage (MSD) flaw size distributions and result in more realistic MSD scenarios than currently used rogue or damage tolerant flaw scenarios.

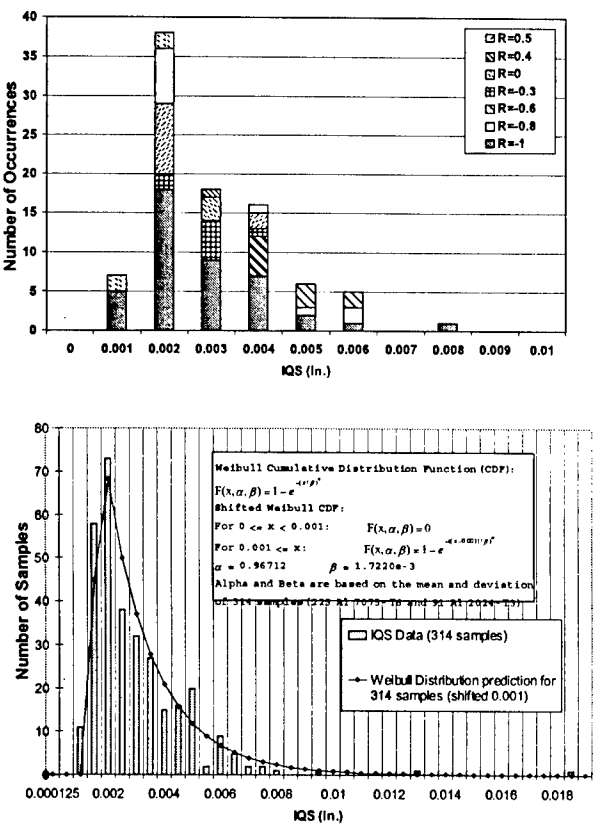

Figure 1 Spectrum of Initial Flaw Sizes Extracted from Test Data. Fig. 1a (top) is data for 2024-T3, and Fig. 1b (bottom) combines 7075-T6 and 2024-T3 data

3. Corroded Surface Morphology

Surfaces from both experimentally corroded and in-service corroded sheets were studied to evaluate surface morphology and material loss influences on damage tolerance of thin sheets typically found in lap joints. The life assessment tools model the local macro surface stress effects due to the morphology

produced by surface corrosion and pitting, affecting the stress intensity solutions. Results from analysis of typical splice joints are shown here. Corrosion causes pits, waviness and variable surface roughness that produce local stress risers and effective concentrations as shown in Figure 2a. The normal stress in the applied load direction is shown in Figure 2b. Some of the pit sizes were on the order of 25% of the corroded sheet thickness and some were as small as a few mils. In addition, the corrosion process results in more global surface decay or material thickness losses that result in additional stress variations.

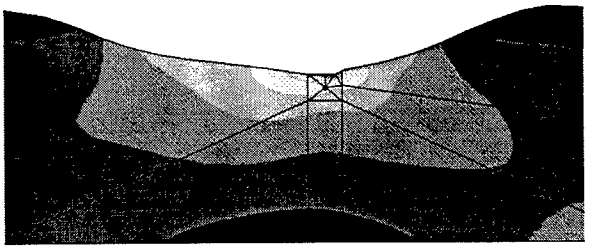

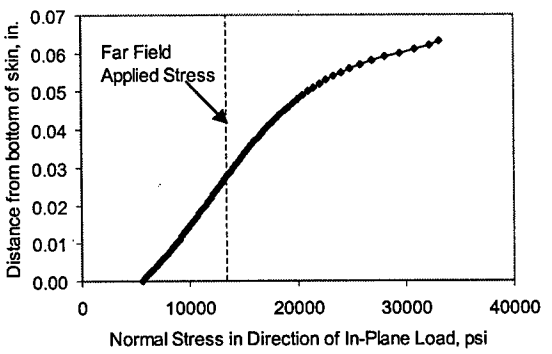

Figure 2 Stress Amplification Due to Corrosion Morphology
Fig. 2a (top) are von Mises stress contours, and Fig. 2b (bottom) are normal stresses at the thinnest part of the skin

Surface profiles were modeled using a sophisticated p-version finite element analysis code, "StressCheck," (Reference 3). A typical finite element model of a skin sample taken from a lap joint on an in-service aircraft is shown in Figure 3. The profile was obtained by a high-resolution optical scan and converted to a data file of x-y coordinates of the surface. Crack tip stress intensities computed in StressCheck were used to study the effects of different corrosion scenarios on several different profiles. Figure 4 shows the results of two types (Skin 1 was a profile similar to Figure 3, and Skin 2 was a single pit).

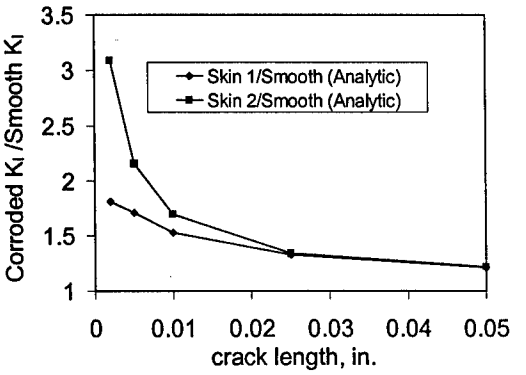

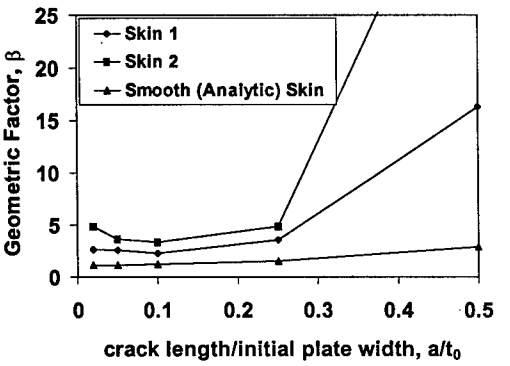

Figure 4 Stress Intensity and β Solutions for a Typical Corroded Surface Compared To Equivalent Crack in a Smooth Skin Surface

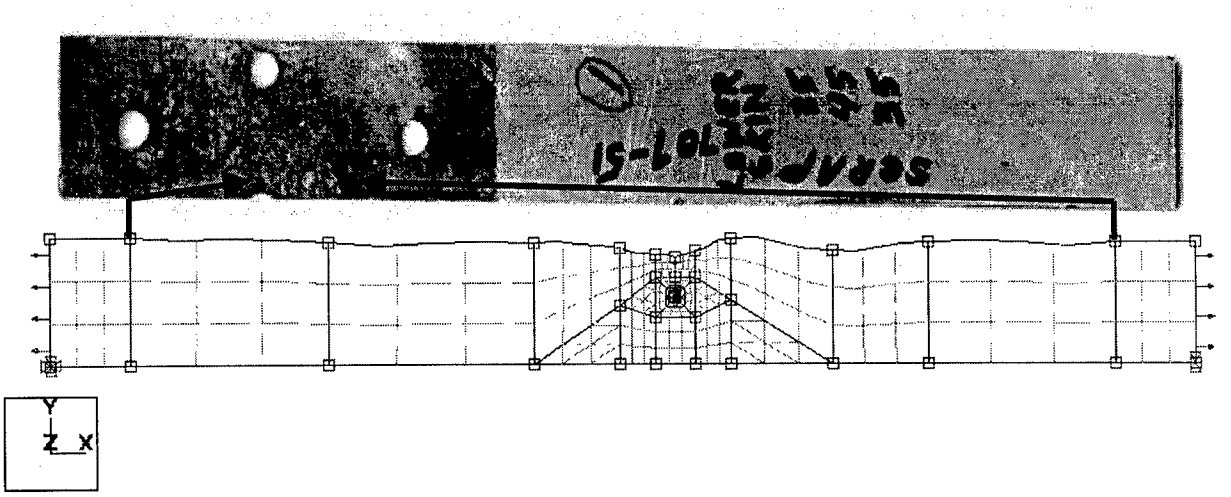

Figure 3 StressCheck Model of 10% Corroded Skin from Lap Joint. Fig. 3a (top) is Corroded Lap Joint Section from 707. Fig. 3b (bottom) is the StressCheck Finite Element Model. Arrows indicate section of skin analyzed.

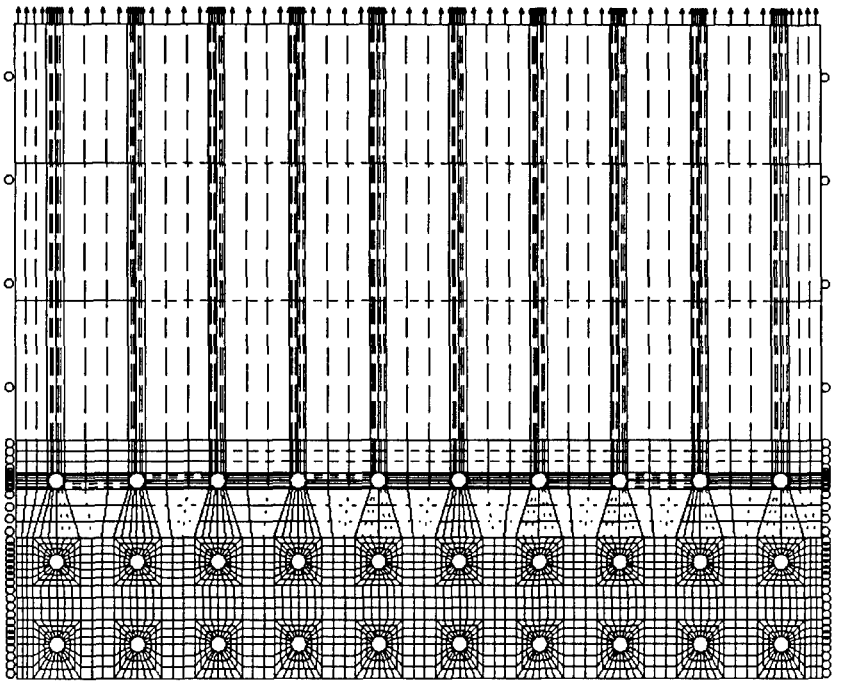

Figure 5 Multi-site Damage Model and Cracks Modeled at Any Combination of Holes

The first of the two figures show the normalized stress intensity effect due to the morphology as a function of crack length. The second shows the influence to the stress intensity solution due to backface amplifications that result from area and thickness loss. At this time, the fully corroded families have not been examined and thus future algorithms will evolve as these are investigated. StressCheck also provided a convenient platform for quick extraction of parametric variations in engineering quantities through its Handbook interface. Through cracks of varying lengths were introduced in the skins at the many locations but predominately at the highest stress locations.

4. Multi-site Damage (MSD)

A p-version finite model was constructed to represent some of the principal attributes of a 3-row, 60-fastener fuselage lap joint in typical cargo aircraft. The finite element simulations were in 2-D, since large transport fuselage panels have a relatively low curvature. Fuselage bulkheads that stiffen the lap joint were not modeled, so that the analysis focused on demonstrating the impact of corrosion without the influence of stiffening parameters. Symmetric boundaries and loads allowed the simplification of the two-skin lap joint to a finite element analysis of only the upper skin, Figure 5. The sides used symmetry constraints to represent additional bays, the edge closest to the bottom fastener row is free from constraint or load, and the back edge away from the holes is used for loading with an in-plane normal traction (representing fuselage pressurization). The interaction between the upper and lower skins was modeled with fastener connections on each hole, simulated as springs. This finite element model allowed us to study the effects of boundary conditions, fastener models, fastener bearing loads, through stresses, plasticity, multiple site damage, load redistribution, and other influences as required. The finite element models allow incorporation of any combination of size and location of cracks to be placed at any, some, or all fastener holes and at any preferred orientation. Flexibility in defining geometric and loading scenarios, efficient modeling of joint stiffness, load redistribution, elastic and plastic behavior, and many other features provide an ideal modeling environment in which to investigate MSD or corrosion scenarios.

Three types of fastener models were considered: distributed normal springs, applied bearing stress, and nonlinear pin connectors. The spring models consisted of elastic springs distributed over ½ of each of the hole circumferences, with stiffness equal to the stiffness of perfectly fitted fasteners. The bearing stress models consisted of a sinusoidal normal traction applied to ½ of each of the hole circumferences. The nonlinear pin models consisted of elastic pins with unknown contact regions between the pins and holes. StressCheck uses a nonlinear iteration procedure to determine the contact region location. Due to the nature of the load and constraints, which were relatively simple to describe, the stress intensity factors were rarely affected by the type of fastener model chosen; therefore, as the spring models were the easiest ones to implement, normal springs were used to model fastener connections.

Plasticity effects were evaluated using two pieces of information: size of plastic zone around crack tips, and comparison of J-integrals for elastic and nonlinear plastic finite element solutions. Plasticity effects in these models were found to be negligible until a crack tip was closer than one hole diameter from another crack tip or a region of high stress gradients. Perhaps not coincidentally, crack growth analyses described below indicated that the ligaments with the cracks would grow unstably when a crack tip was within approximately one hole diameter of another crack tip.

5. Corrosion Pillowing

In addition to the effects that corrosion has on lap joints in the form of thickness loss, early crack "initiation", stress corrosion cracking, and pitting; corrosion pillowing can occur. The National Research Council of Canada (NRCC) has investigated and documented this phenomenon extensively, Reference 4. Corrosion pillowing is caused by the additional volume that corrosion by-products require, over and above the material volume lost to corrosion—the volume of corrosion by-products

can be as much as 6 ½ times greater than the volume of parent material lost. Fastener constraints in the lap joint prevent uniform deformation of the skins—skins deform most in the middle of the ligaments between rivets, that is, the skins 'pillow.' The result is that the skins act much like plates fastened at 4 corners with a uniform out-of-plane pressure applied. Large bending stresses near the rivets result. As will be seen below, these large bending stresses have adverse effects on the structural integrity of lap joints. Three-dimensional finite element simulations (described in Reference 5) conducted by NRCC were used to estimate stress fields caused by corrosion pillowing. Figure 6 shows the individual stress state for a skin. The effects of this build-up of sustained stress in time are simulated to estimate the impact on the joint integrity. At this time, any crack extensions due to sustained stress mechanisms alone were not included. The model is capable of incorporating these mechanisms but additional data is desired prior to exercising this option.

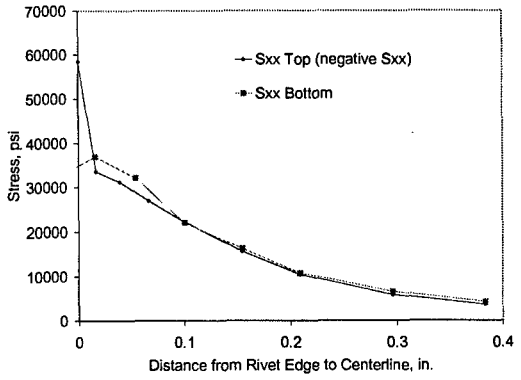

Figure 6 Sustained Stress Levels Due to Pillowing. Graph shows normal stress in direction of applied hoop stress, for top and bottom faces of the outer skin, in the region a countersunk fastener.

6. Crack Growth Analysis (CGA)

Corrosion is a time-dependent phenomenon while traditional fatigue is a cyclic stress-dependent one. The flexibility afforded by the crack growth analysis software AFGROW (produced by U.S. Air Force Wright Research Laboratory, Wright-Patterson Air Force Base, Ohio, USA, Reference 6) enabled step wise analyses to be performed. The analyses used superposition (when appropriate) and incremental spectrum loads to simulate time-dependent phenomenon such as corrosion along with crack growth increments due to stress cycles. Crack growth analyses (CGA) were performed with various load, geometry, and corrosion scenarios to explore the sensitivity of results to different scenarios and assumptions. Only constant amplitude stress ratio cycles of R=0, representative of fuselage pressurization, were used, in order to maintain a focus on the impact of the corrosion interaction. Several different fracture models were used to investigate scenarios and assumptions. For example, an elliptical surface flaw influenced only by surface morphology is used to determine the surface morphology influence. Runs were performed with and without the various influences, and often with several different assumptions. Corroded surface morphologies were assumed either to exist from the start of the analysis (consistent with a damage tolerance concept), or corrosion levels were increased gradually in the analysis to represent a simulation of time-varying corrosion. The following sections highlight some of the results of the studies performed to date. In each scenario, crack growth rates for Aluminum 7075-T6 are used to define material crack growth rates, Figure 7 (these curves were also used for determining the 7075-T6 IQS). A similar set of curves that fit 2024-T3 data were used for the 2024-T3 IQS. The crack growth models and scenarios have been selected to avoid debates about closure models, retardation, and other parameters.

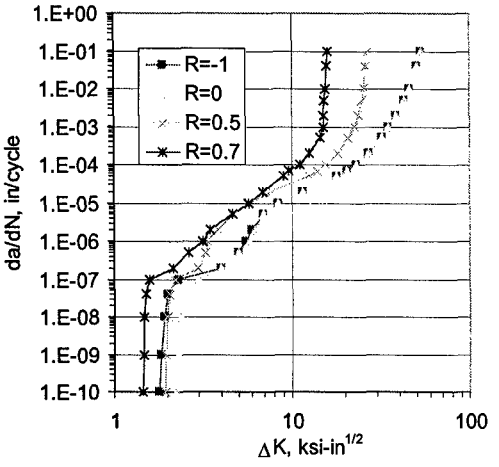

Figure 7 Aluminum 7075-T6 Alloy Crack Growth Rates (K_{max} plotted for R=-1)

Results

Crack growth analyses using potential scenarios (which take into account varying levels of corrosion, multi-site damage, etc.) are presented in this section.

1. **Scenario:** Multi-Site Damage Model with IQS Crack Distributions

The Multi-site Damage (MSD) finite element model described in Section 4 of the Methodology was modified so that initial crack lengths varied according to the initial quality states (IQSs) analysis described in Section 1 of the Methodology. In accordance with the IQS distribution, each fastener hole had a crack placed on both sides. A conservative ordering in which large cracks were placed together near other large cracks was used. A hoop stress of 15.5 ksi was applied to the far field boundary. Symmetry boundary conditions on the long vertical edges removed stiffener influences from the results. The crack growth analysis was done manually---a spectrum of crack lengths (20 total) was input to the StressCheck FEA model, stress intensity factors were extracted, crack growth rates for each crack tip were computed, and crack lengths were updated in the StressCheck model. The iterations continued until a specified event such as unstable crack growth occurred. For this crack length combination an interesting trend was observed—as the CGA progressed, stress intensity factors for the shortest cracks that were initially 50% lower than those of the longest cracks equilibrated to the stress intensities of the longest cracks. The implications of this observation are that MSD scenarios may become stable and the stress intensity solutions more simply computed, making the MSD crack growth solutions more readily obtainable. This equilibrium effect is further investigated in Scenario 2, the Section Finite Element Model. For the current scenario, stress intensity 'equilibrium' occurred within 2000 cycles. At 2000 cycles, the average of 20 total crack lengths was used as the initial crack length in an AFGROW crack growth analysis using the "Section Finite Element Model" described below, and the crack lengths adjusted uniformly until unstable fracture occurred. This much simpler model can be used because of the stress intensity

convergence or equilibrium noted above. The crack growth curves for the longest and shortest cracks in the MSD plate are displayed in Figure 8. The figure demonstrates that the cracks are growing at approximately the same 'speed' after 2000 cycles, and that there is little variation of number of cycles to unstable fracture across the spectrum of crack lengths analyzed.

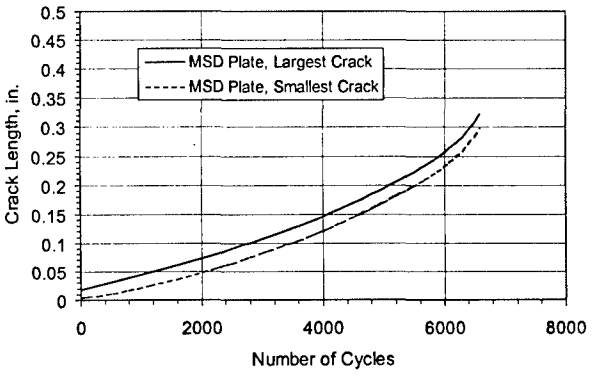

Figure 8 Crack Growth for Smallest and Largest Cracks

2. **Scenario:** Section Finite Element Model

A convenient method for quickly evaluating parametric variations in geometry, loads, materials, and fastener models is to construct a small finite element model which is a subset of the much larger and much more complicated MSD model described in the previous section. Some results from this model are discussed in this section. Symmetry boundary conditions were applied to each long edge, Figure 9. Two cracks of various lengths were introduced at the sides of the top hole. Crack growth analyses were carried out in two distinct crack scenarios: cracks of equal length, and cracks of two different lengths. Crack growth for the equal length cracks is easy to implement---simply extract stress intensity factors for a number of crack lengths, convert the stress intensities to geometric factors β and use as input to the User-defined Beta (β) model in AFGROW. We used this Scenario to investigate further the 'equilibrium' effect discovered in the CGA of the MSD Model with IQS distributions discussed in the previous section. Two cracks, one 0.0186 inch, the other 0.0045 inch, were introduced at the top fastener hole of the Section Finite Element Model. A hand CGA was done, with the result that crack tip stress intensities, though initially quite different, equilibrated quickly (by about 3200 cycles) to within 8%, Figure 10. Also shown in Figure 10 is the evolution of stress intensities for 3 cracks in the MSD scenario of the previous section: 1) the longest crack (0.0186"), 2) the shortest (0.0045") and 3) the mean (0.0062"). The stress intensities for these 3 cracks in the MSD scenario have 'equilibrated' by about 2000 cycles, therefore the results from the MSD plate scenario are used up to 2000 cycles and the results from the Section Finite Element Model are used to continue the analysis from 2000 cycles up to the last points shown.

3. **Scenario:** Corroded Surface Morphology

Crack growth simulations that accounted for surface morphology effects on stress intensity solutions are described in this section. Adjustments to the AFGROW "Center semi-elliptic surface flaw" model were made with stress intensity amplification information extracted from Section 3 of the Methodology. Only β_a, the geometric factor which controls crack growth into the interior (toward the back face), is adjusted with the Corroded Surface Morphology FEA results that included both corrosion profile stress amplifications and material loss effects. Surface βs were adjusted only for material loss effects due to corrosion. The number of cycles for the part-through elliptic crack to transition in to a through crack $N_{transition}$ is the figure of merit used to compare growth scenarios. Initial interior and surface crack lengths were the same for each crack simulation. Three scenarios were investigated: 1) No corrosion, 2) variable corrosion (1/2% per year, 400 cycles per year), and 3) 10% corrosion from the initial load cycle. Comparisons with the baseline case (No corrosion, 0.002 inch initial crack) indicate the relative factors of structural life degradation due to corrosion as a function of initial crack length: 0.002" cracks will transition up to 67% sooner than the 0.002" baseline case, and 0.01" cracks will transition 97% sooner than the 0.002" baseline case, Figure 11. This plot shows the importance of initial flaw size assumptions and how corrosion affected those assumptions. It is interesting to note that this level of corrosion for which the analysis was conducted used an aircraft lap joint corrosion profile that was **not** detected with standard NDI—the implications of this observation are serious for the structural integrity of the lap joint.

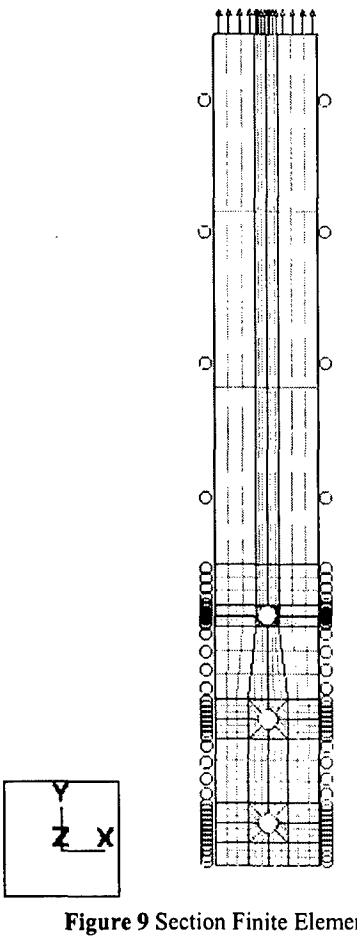

Figure 9 Section Finite Element Model

4. **Scenario:** Corrosion Pillowing

NRCC results of three-dimensional finite element models were used to estimate stress fields caused by corrosion pillowing. The 10% pillowing level from these simulations was considered a 'worst case'. The steady-state moments resulting from plate bending (discussed in Section 5 of the Methodology) must be combined with the cyclic loading due to normal aircraft usage.

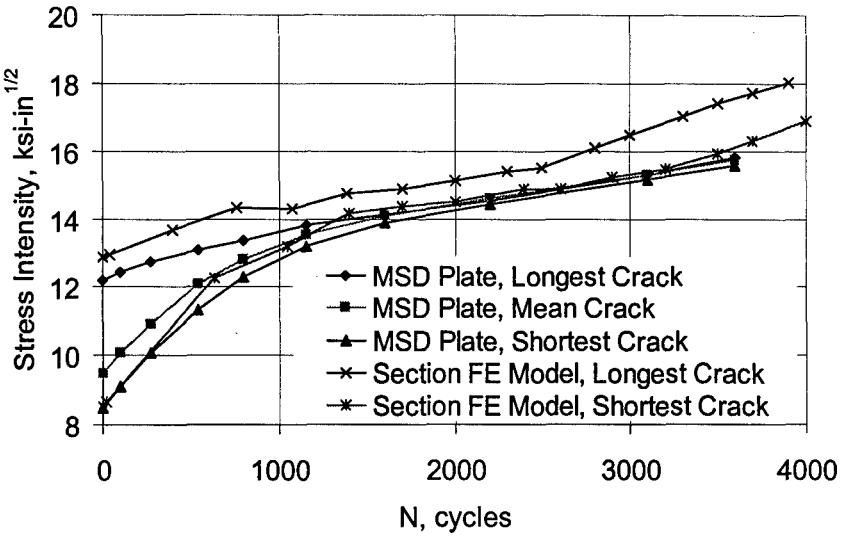

Figure 10 Crack Growth in MSD Plates, Variable Length Initial Crack. Shown are Results from the MSD Plate Scenario and the Section Finite Element Model Scenario

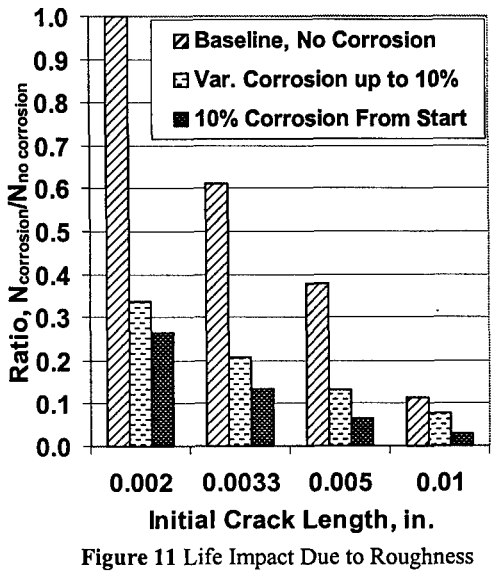

Figure 11 Life Impact Due to Roughness

As the corrosion level increases, the bending moment increases, thereby increasing the σ_{max} peak cyclic stress level while leaving the cyclic load range constant. However, as the crack grows towards the center (bending mid-plane) of the skin, the steady-state stress at the crack tip decreases due to the linear profile of the pillowing bending stress distribution. Two opposing influences are at work: the increase in steady state bending moment over time and the decrease of steady-state tensile stresses (due to bending moment) as the crack grows from the bottom towards the top of the skin. Geometry was based on Reference 5 geometry and included the following: a 0.1875" diameter fastener hole, a single 0.0033" by 0.0033" corner crack at the hole, and plate cross-sectional dimensions of 1.0" wide by 0.063" thick. The material properties used for crack growth were again the properties of Al 7075-T6. Two different corrosion rate scenarios were investigated. Both scenarios used corrosion that was increased over time: the first was up to 10% corrosion in 20 years and the second was up to 10% corrosion in 50 years, Figure 12.

Consistent with the assumptions used in the surface morphology scenario, a cyclic stress rate of 400 (R=0, 15.5 ksi maximum stress) cycles/year was assumed for mixing the environmental and cyclic domains. The combined environmental and cyclic spectrum for both scenarios is shown in Figure 13. Environmental degradation in the form of slowly increasing steady-state bending moment was applied at the end of each year of load cycles. In early crack stages, this degradation was manifested by an increase in σ_{max} along with an increase in effective R-ratio. As the crack tip crossed the mid-plane of the skin (the neutral axis of the pillowing stresses), the environmental effects might cease to degrade life as the crack tip becomes influenced by the compressive stresses due to the steady state bending moment, thus slowing through-thickness crack growth. In reality, however, a crack that is arrested from growing through the thickness will continue to propagate on the surface and find a path of least resistance. Long aspect ratio surface cracks and other multiple cracks might emanate from the skin bottom surface where the positive bending stress is at its peak—at this time, more advances in analytical approaches and more fleet data are needed to improve our prediction capabilities for pillowing effects.

The effect of corrosion pillowing on crack growth can be seen in Figure 14. It is difficult to make direct comparisons due to the compressive effects of pillowing cited earlier. For a conservative estimate of pillowing effects, the compressive stresses on the top half of the plate are ignored since a single crack arrested by these compressive stresses would probably be rerouted or develop into multiple cracks. For the initial 0.0033" x 0.0033" flaw, unstable internal crack growth to transition to through crack occurred 35% earlier than the no corrosion baseline in the 20-yr scenario, and 25% earlier than the no corrosion baseline in the 50-year scenario. From this limited data, the degradation in life does not appear to be overly sensitive to the assumed constant corrosion rate, but an important enough influence to early cracking. Thus, pillowing effects need to be included in computations of 'age degradation' effects. More realistic linear or nonlinear corrosion rates can easily be integrated into the prediction technique presented here as they are obtained.

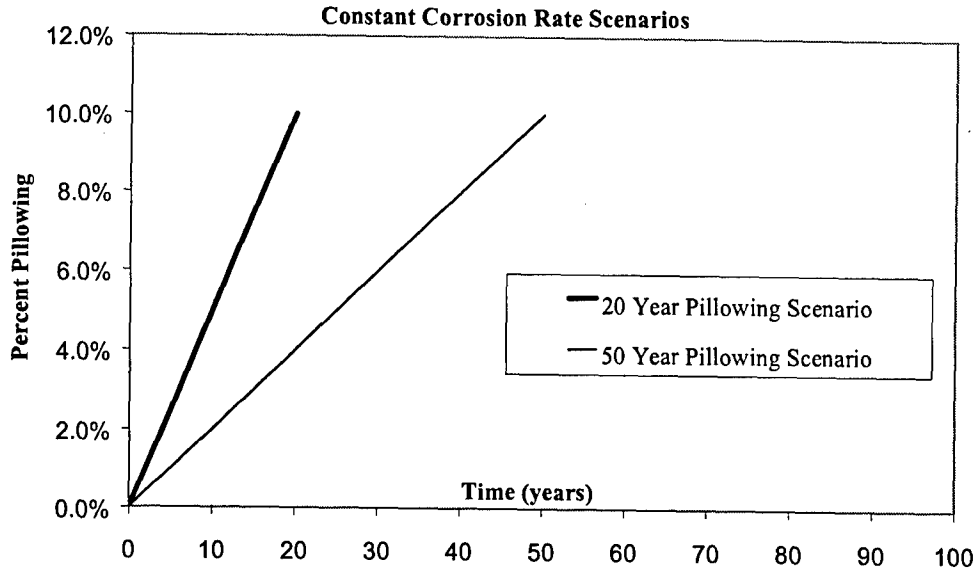

Figure 12 Constant Corrosion Growth Rate Scenarios

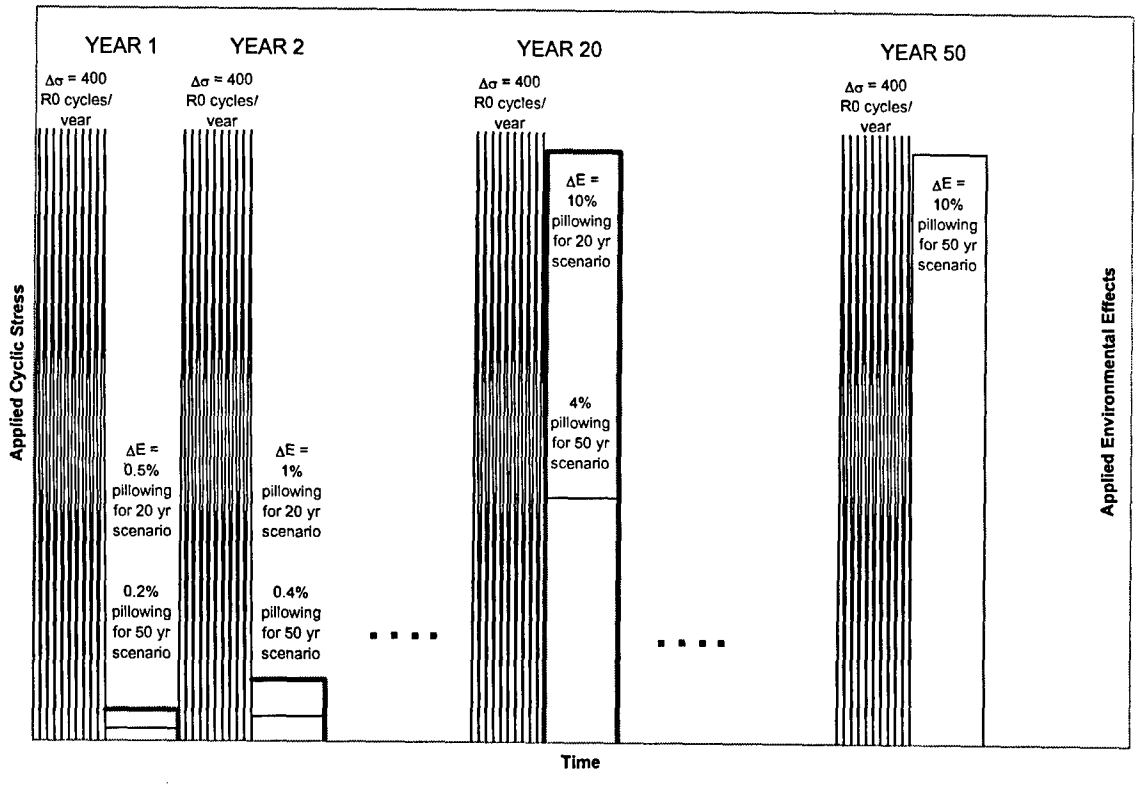

Figure 13 Cyclic and Pillowing Interaction Spectrum

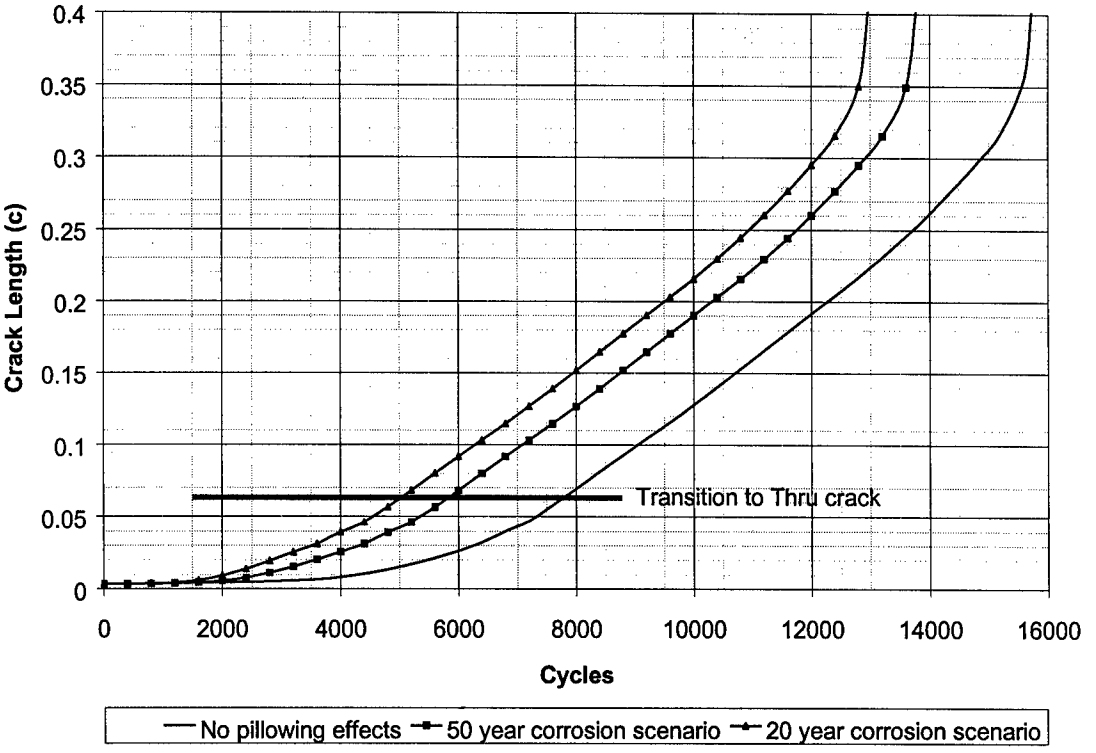

Figure 14 Corrosion Pillowing Rate Effects on Crack Growth Life

5. **Scenario:** The Whole Shebang

The last scenario investigated combined all the previously discussed effects: initial quality states, multi-site damage, corrosion pillowing, and surface morphology into one crack growth analysis. Each of these effects was modeled using the methods previously discussed. A 0.1875" fastener hole loaded with a bearing stress (estimated from StressCheck finite element simulations) was flawed with 2 0.0033" Initial Quality corner cracks. This value of 0.0033" is the mean of the IQS distribution of Figure 1. Results from the MSD scenario CGA above (Section 1) indicated that mean crack length was a good metric for adequately characterizing the global crack length distribution in the plates with MSD. The cracks were oriented perpendicular to the applied far field hoop stress of 15.5 ksi. Stress intensity solutions from the Section Finite Element Model Scenario were used to modify through crack β solutions in AFGROW. Surface morphology corrections from the FE simulations of Figure 3 above amplified AFGROW's internal crack β solution. In addition, material losses were accounted in the amplification of the surface crack β solutions. Corrosion pillowing stresses increased both R ratio and maximum stress. The 20-yr. 10% corrosion scenario was used to gradually increase surface morphology and pillowing amplifications. Figure 15 depicts the crack at a fastener hole. The bars and shading schematically represent the relative importance of the parameters to the two directions of crack growth. The dark shade indicates more impact and white indicates little or no impact. The result of combining all effects is synergistic, Figure 16. The degradation of structural life is calculated separately for each effect, and compared to AFGROW's simulation of the growth of one corner crack next to a hole, no corrosion. Surface morphology alone reduced structural life by 40%, MSD alone by 28%, and corrosion pillowing alone by 18%. Combined, however, all of the effects result in a 62% decrease in structural life—the whole is LESS than the sum of its parts.

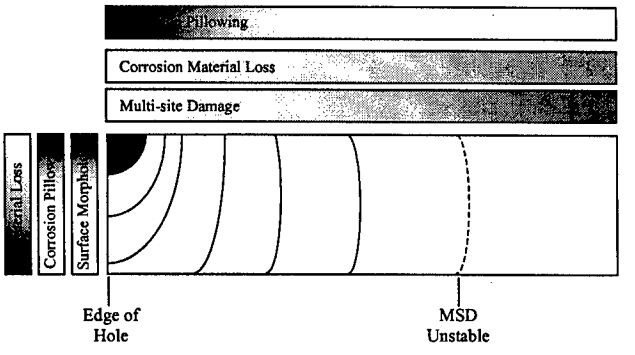

Figure 15 Schematic Representation of Effect of Parameters at Respective Crack Tip and Relative Position (Darker shades indicate more influence in the crack growth).

6. Evaluation of Fracture Criteria

There are many possible ways to predict a Fracture Event. Here we have investigated several of the better known criteria, and have determined the effect each criteria has on the predicted life of the Multi-site Damage (MSD) plate. Seven criteria were examined: 1) critical crack length determined by the fastener hole diameter, 2) Plane strain fracture K_{max}, 3) Plane stress fracture K_{max}, 4) plastic zone link-up, 5) Net section yield based on ligament area and material yield stress divided by 1.2, 6) AFGROW's net section yield criterion, and 7) AFGROW's K_{max} criterion. Each of these criteria was evaluated in the Section Finite Element Model scenario to determine sensitivity of the Fracture Criteria to predicted structural life. While crack lengths and stress intensities at Fracture varied, the cycles to

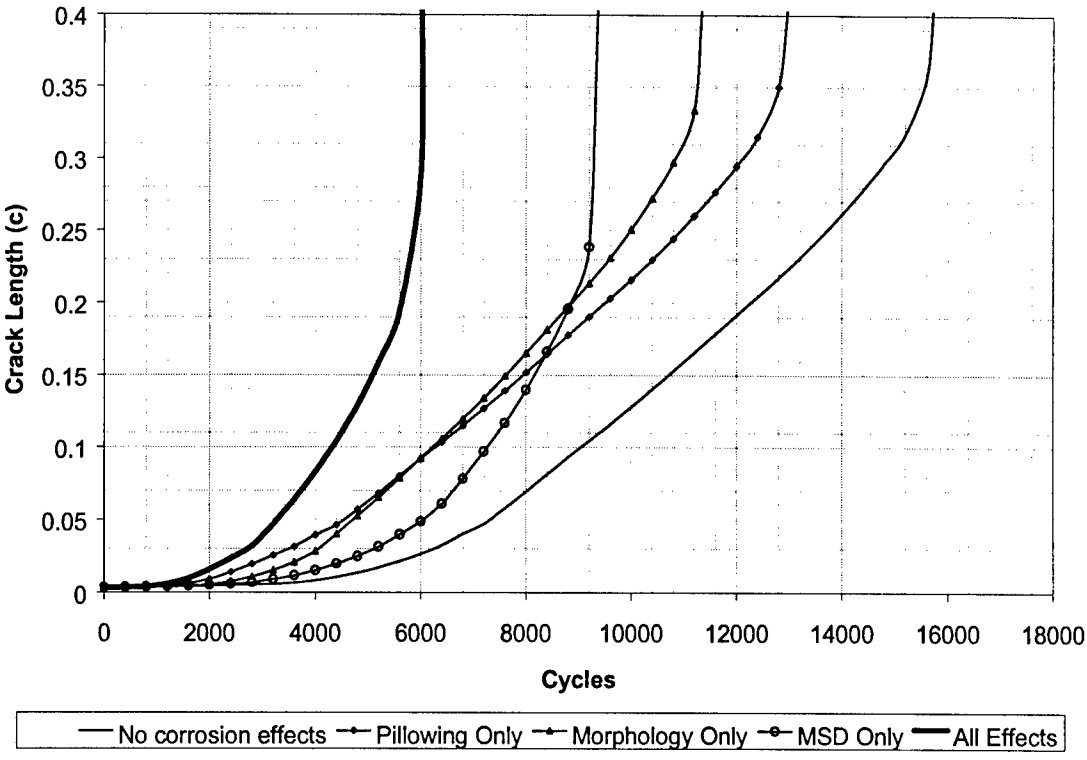

Figure 16 Combined Scenario—Corrosion Pillowing, Surface Morphology, Initial Quality States and Multi-site Damage

failure varied by only +/-4%, Figure 17, which we considered as statistically insignificant when compared to impacts computed for the early stages of cracking due to corrosion parameters.

7. Relation to the Current Structural Integrity Process

In order to establish inspection intervals and life limits of present field aircraft, traditional analyses in the current Structural Integrity Process often assume a single crack scenario with a damage tolerant flaw size of 0.05" growing to one or two bay failure, and predict a range of 30-50,000 cycles needed to reach critical crack lengths greater than 5". Recent attempts by some to include corrosion in this scenario assume a 10% material loss effect that elevates the applied hoop stress by 10%. With this assumption, the life is reduced to the 15-25,000 cycles needed to reach critical crack length greater than 5" in a corrosive environment. The results of the analysis presented in this paper indicate corrosion is a much more complicated phenomenon than just a material loss effect. Corrosion influences scenarios through Multi-site Damage, morphology (and thickness losses), and pillowing. Crack growth analysis results contained in this paper predict an impact of corrosion that is more substantial than traditional analyses predict. The Whole Shebang scenario described above accounts for Multi-site damage, surface morphology, material thickness losses, and corrosion pillowing. For constantly increasing corrosion (1/2% per year up to 20 years), the Whole Shebang results indicate that corrosion reduces the life of the lap to about 6000 cycles—a reduction of 80 to 90% in life relative to traditional analysis predictions. Figure 18 illustrates these differences and highlights the importance of initial flaw size and scenario assumptions to determine the appropriate inspection time and damage size to be detected.

8. Life Prediction Impact Summary

A methodology for including the effects of corrosion on fuselage lap joint structural life predictions has been proposed and exercised. Fracture mechanics and fundamental engineering principles, as well as state-of-the-art engineering analysis tools, have been integrated into a new damage tolerance approach which accounts for material initial quality states, multi-site damage, corroded surface morphologies, and corrosion mechanical effects. Corrosion pillowing has an adverse effect on crack growth and the ability of the structure to withstand high cycles, decreasing crack transition from part through to through 25% for the 50-yr. Scenario and 35% for the 20-yr. Scenario. Corrosion levels not detected by conventional NDI methods were shown to have severe impact on structural life of lap joints, decreasing life by 67% for a reasonable worst case, 10% corrosion Surface Morphology scenario. Multi-site damage was estimated to degrade structural life by 28%. In a 20-yr. gradually increasing corrosion scenario, pillowing alone degraded life by 18% and surface morphology alone by 40%—combined, the effects reduced the life of the structure by only 62%. These reductions indicate a life impact that is a concern for the lap splice scenario, and potentially for other aircraft locations.

Relatively simple, easy to construct FEA models were extremely useful for accurately modeling fastener connections, through stresses, plasticity, multiple site damage, load redistribution, surface morphology, and other phenomena as required. StressCheck (ESRD, Inc.) is an efficient engineering tool for obtaining reliable estimates of stress intensity factors for the scenarios examined. AFGROW was an enabling analytical tool that allowed us to quickly determine effects of different parameters and their variations on life estimates for the structures analyzed here.

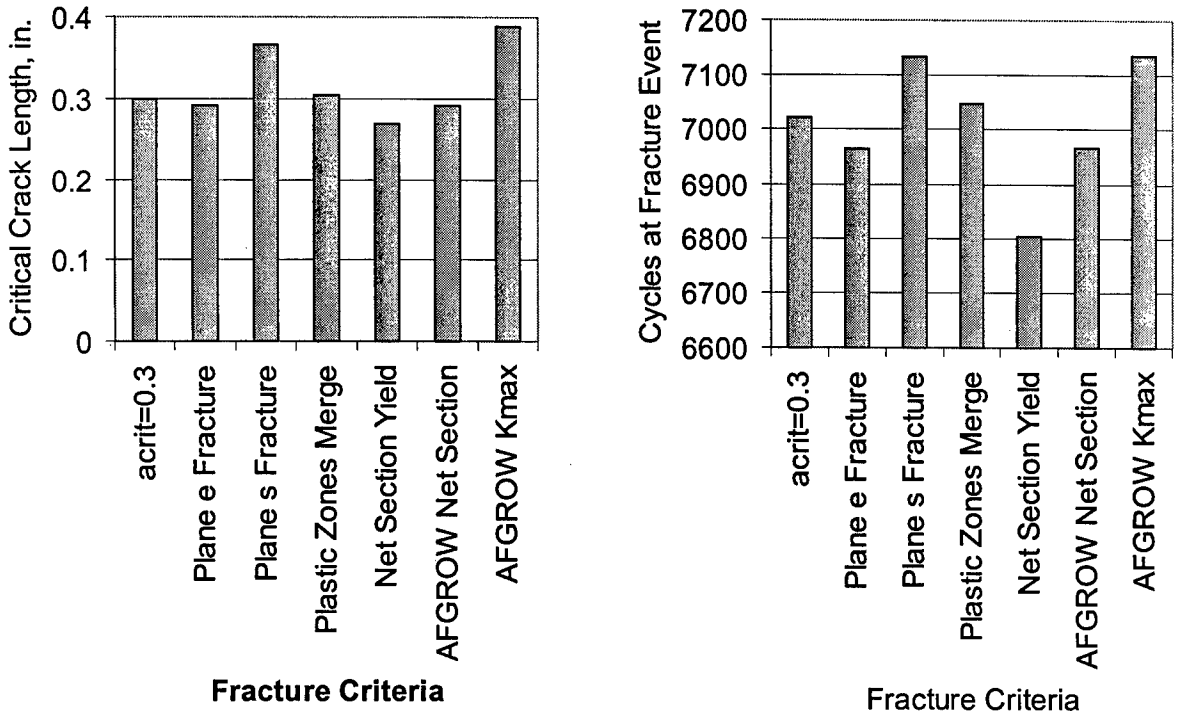

Figure 17 Though Fracture Criteria Were Divergent, Estimated Structural Life Did Not Vary Much

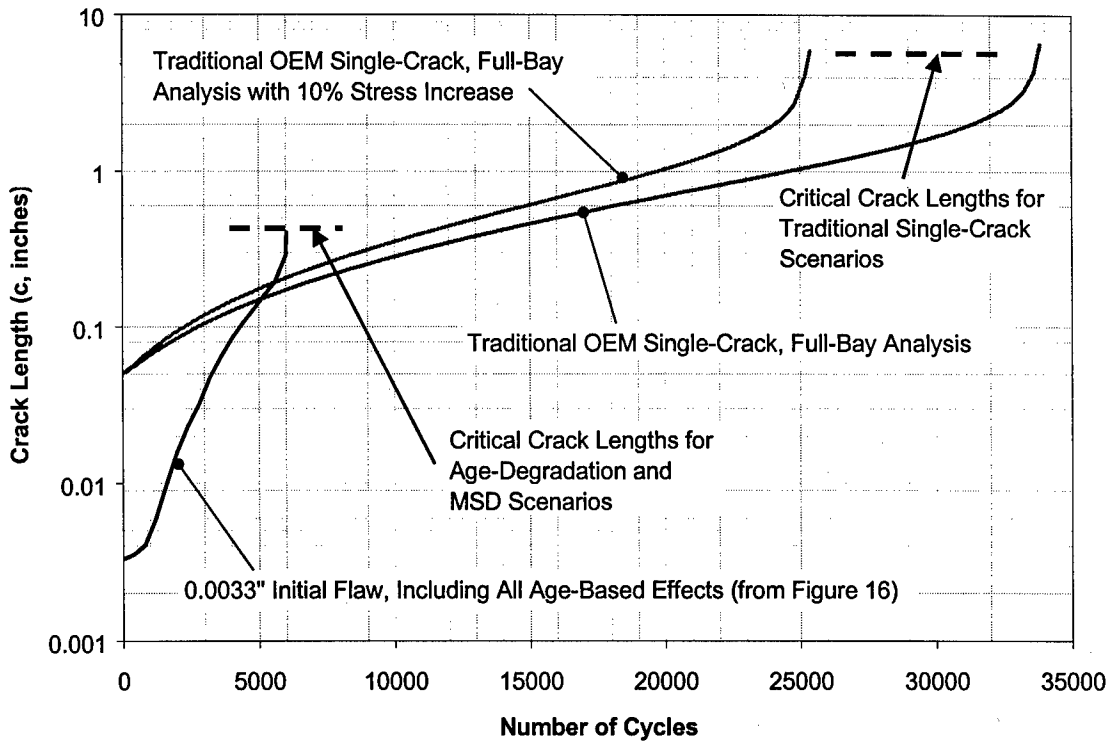

Figure 18 Ramifications of Using to Proposed Corrosion-Fatigue Interaction Model Relative to Traditional Damage Tolerance Analysis

Conclusions

- Corrosion degrades the structural life capability in the scenarios investigated here, to the point that corrosion is a structural problem, in addition to the already established position of corrosion as an economic problem.
- When combined with cyclic fatigue effects, the corrosion levels analyzed degraded structural life capability sufficiently such that corrosion should be a concern to the management of the existing 'Aging Aircraft Fleet'.
- The technology has matured enough to allow implementation of the described methodology. Though far from exact, the methodology of this paper provides a 'benchmark' and foundation for future development.
- Initial Quality States, surface morphologies, pillowing, material losses, and Multi-site damage (MSD) scenarios are important metrics that need to be taken into account and must be correlated with NDI techniques.
- Corrosion computations degraded structural life capability predominantly in the early stages of crack growth (for example, before a corner crack transitions to a through crack). Estimates of residual strength degradation due to corrosion do not sufficiently characterize corrosion effects on structural life capability.
- Acceptance and implementation of this concept can be used to ease the Economic burden of the Aging Fleet while ensuring safety and readiness.
- Future studies should address the effects of different corrosion rate models, alternative geometric and loading scenarios, and methods for transforming metrics so that maintenance depots can use this corrosion methodology to improve their maintenance decisions.
- An **Analytical Process** is available for applying structural life predictions that provides an **Engineered Solution** for modeling real time age degradation effects.

Acknowledgments

We are grateful for the financial support provided by the U.S. Air Force and NCI, Inc. through the subcontract NCI-USAF-9061-007, Dick Kinzie of AFRL/MLS-OLR, and Garth Cooke , Program Manager, NCI, Inc. This program has provided significant advances in corrosion prediction technologies. For additional information and supporting data on their program, you are invited to go to Reference 7.

We would like to acknowledge and thank Barna Szabo, Ricardo Actis, and support personnel at ESRD, Inc. for their on-going assistance and technical support of StressCheck. This finite element analysis code is the only known commercially available software that could have performed and solved some of these particular analyses. We would also like to thank Jim Harter at Wright Research Laboratories for his interactive development of AFGROW in support of this approach. We also thank Nick Bellinger and Jerzy Komorowski at National Research Council-Canada (NRCC) for their assistance, data, and analyses, for quantifying the corrosion pillowing influences. We also acknowledge Dave Simpson for his cooperative efforts with APES, Inc. in formulating the proposed integration concept for the Structural Integrity process, as provided in Reference 1.

References

1. Simpson, D. and C. Brooks, "Integrating Real Time Age Degradation Procedures Into the Structural Integrity Process", Proceedings of the NATO RTO's Workshop 2 on Fatigue in the Presence of Corrosion, October 1998, Corfu, Greece. To be published.
2. APES, Inc. internal document.
3. StressCheck, produced by Engineering Software Research and Development (ESRD, Inc.), St. Louis, Missouri, USA. Web address http://www.esrd.com.
4. Komorowski, J.P., N.C. Bellinger and R.W. Gould. "The Role of Corrosion Pillowing in NDI and in the Structural Integrity of Fuselage Joints", Proceedings of the 19th Symposium of the International Committee on Aeronautical Fatigue, 16-20 June 1997, Edinburgh.
5. Bellinger, N.C. and J.P. Komorowski. "Implications of Corrosion Pillowing on the Structural Integrity of Fuselage Lap Joints", Proceedings of the FAA-NASA Symposium on Continued Airworthiness of Aircraft Structures, 28-30 August 1996, Atlanta, Georgia, USA.
6. AFGROW, produced by AFRL/VASE, Wright-Patterson Air Force Base, Dayton, Ohio, USA. AFGROW's Web address is http://134.131.165.237/fibec/afgrow.html.
7. Internet document "Corrosion in USAF Aging Aircraft Fleets." U.S. Air Force Research Laboratory, AFRL/MLS-OLR and http://www.afcpo.com.

CORROSION IN USAF AGING AIRCRAFT FLEETS

Mr. Richard Kinzie
Mr. Garth Cooke
AFRL/MLS-OL2
420 2nd St.
Robins AFB, GA 31098 USA

1. SUMMARY

This paper summarizes the results of research projects undertaken by the United States Air Force Corrosion Program Office within the past year and a half. It reflects the cooperative results obtained from a team of almost 50 researchers that represented over a dozen different corporate entities. All were marching to a tune composed and conducted by the program office.

This paper covers work associated with environmental modeling, development of a revised corrosion maintenance concept, and development of a corrosion growth model that can be used by depot engineers to improve the maintenance of their aircraft.

2. BACKGROUND

Several of the USAF aircraft fleets are aging rapidly, and there is concern among the engineering authorities as to the effect of corrosion on these fleets as they continue to age. Unlike their commercial cousins that are experiencing the effects of fatigue as they age, USAF fleets commonly experience as little as 300- 400 hours a year. Consequently, they can come to the thirty-year point in their lives with only a small fraction of their fatigue lives used up. However, as these aircraft have commonly spent a good part of their lives sitting on the ground in some of the worst climates in the world, they may have experienced corrosion growth well in excess of that experienced by their commercial cousins. Certainly, as these fleets continue to age, we are spending more and more of our maintenance dollars on corrosion treatments. If we don't change the way we do business, that trend will continue to accelerate. What has been the effect of the corrosion on the safe life of these aircraft, and what can be done to ensure the continued safe operation of our aging fleets in a safe, economically sound manner?

In the past year, the US Air Force Corrosion Program Office (AFCPO) has initiated a number of efforts to examine these questions. The AFCPO characterized the extent of the problems faced by the corrosion community, developed a plan to re-orient the way we do corrosion maintenance, and began an effort to model growth of corrosion in Air Force aircraft.

3. PROCESS

The efforts initiated by the Air Force Corrosion Program Office can be broadly categorized in three areas: 1) characterize the corrosion problem, 2) develop a new way of doing business, and 3) develop models of corrosion growth.

3.1 Characterization of the Corrosion Problem

The characterization took place in two areas. A Study of the Role of Corrosion in ASIP looked at the joint effect of corrosion and fatigue on selected USAF fleets, and a "Cost of Corrosion" program examined the total cost of direct corrosion maintenance on USAF weapon systems and equipment.

3.1.1 Role of Corrosion in ASIP

Significant improvements in corrosion detection, treatment, prevention, and predictive modeling will be needed if corrosion maintenance is to continue to be effective on aging fleets. Toward this end, an assessment of the impact of corrosion on the structural integrity of USAF aircraft

Paper presented at the RTO AVT Workshop on "Fatigue in the Presence of Corrosion", held in Corfu, Greece, 7-8 October 1998, and published in RTO MP-18.

was conducted. This study provided an indication of the severity of the effect of corrosion on selected aircraft inventories. Corrosion damage encountered on selected USAF aircraft fleets was compared to their Durability and Damage Tolerance Assessments (DADTA). The Force Structural Maintenance Plans (FSMPs) were then evaluated to determine if they adequately addressed the inspections, repairs, or modifications required to assure continued fleet airworthiness in the face of continuing corrosion and fatigue damage.

The Study of the Role of Corrosion in ASIP was accomplished by selecting a representative Mission Design Series (MDS) from three of the four missions: Cargo, Trainer, Bomber, or Fighter. Criteria for selection of a fleet included: (a) age sufficient to provide significant exposure to the potentials for corrosion, (b) a reasonable level of DADTA documentation completed, (c) aging systems with a strong potential for continued utilization, and (d) sufficient numbers of aircraft going through depot level maintenance. The aircraft selected for detailed assessment during the study were the C-5 cargo aircraft, the F-15 fighter, and the T-38 trainer.

Structurally significant corrosion damage that has been encountered on the MDS was identified through discussions with maintenance engineers and technicians. The DADTA for that MDS was then examined to determine: (a) if the structural elements which were experiencing corrosion damage had been assessed during the DADTA, and (b) if the corrosion damage experience was consistent with the initial flaw assumptions of the DADTA. Then the structurally significant items affected by corrosion were compared to the FSMP to determine if corrosion damage was adequately addressed in long-range maintenance planning.

The results of this study offered the following conclusions:

- Corrosion damage in critical structure has resulted in an initial flaw size that dramatically reduced the predicted life of a critical component (and created a potential flight safety hazard).
- Corrosion damage in structural elements has rendered a structural analysis invalid and changed a component's status from non-critical to critical.
- Corrosion is a potential flight safety concern in a number of locations.
- Corrosion has led to premature cracking of major structural elements. With the sole exception of an aft pressure door actuator bracket, the cracks are all in built-up, redundant structures.
- DADTA models do not exist for most of the corrosion problems that were observed. Hence, corrosion inspection requirements cannot be derived through analysis, and inspection requirements derived through fatigue analysis may be in error by orders of magnitude.
- Multiple stress-corrosion crack sites occurred in a number of locations. Such multiple site damage is known to have a more serious effect on the damage tolerance and residual strength of the structure than the typical DADTA single crack models.
- The DADTA approach is generally assumed to be quite conservative in its damage model. The complexity of the corrosion attack experienced on all

three may significantly reduce ore remove this conservation.

- Most of the line experience on corrosion is inadequately reported in terms of location, type of corrosion, and severity of attack.
- Much of the corrosion engineering reporting is anecdotal and does not have a clear connection back to ongoing DTA modeling.
- Initial discovery of corrosion-induced damage to critical structural elements (whether ASIP critical or not) is generally fortuitous rather than the result of focused inspections driven by analytical processes.
- The corrosion experience to date on the three aircraft systems has been primarily economic in terms of the actual time and costs required for the inspections and repairs.
- The processes used in this study will not identify all the corrosion problems in the surveyed aircraft nor can the process identify corrosion in areas that are not otherwise inspected.

The following recommendations were offered:

- Incorporate a corrosion audit and updating process into every aircraft FSMP.
- Improve tracking and reporting of corrosion activity to provide the trigger for extensive fleet surveying.
- Improve models for identifying stress corrosion-prone locations and for predicting corrosion types and rates.

3.1.2 Cost of Corrosion

The Air Force Corrosion Program Office recently completed a study to determine the annual cost of direct corrosion maintenance to the United States Air Force. The study examined costs for FY97 and was a companion document to a similar study conducted in 1990.

The costs for all Air Force systems and equipment, including all unclassified systems/equipment except Real Property and Real Property Installed Equipment (RPIE) were examined. Corrosion maintenance was defined as all inspection for corrosion, all repair maintenance due to corrosion, washing, sealant application and removal, and all coating application and removal. Intangible or indirect costs were not addressed.

Costs were obtained through electronic searches of databases and interviews. The report presents the identified costs by Major Command, by Weapon System, by Base Location, by ALC, and by different relevant combinations. The report also compares the costs with a FY90 study. The cost comparisons are of particular interest in light of the extensive changes in the Air Force structure and the force structure reductions that have occurred in the intervening years.

The total annual cost of direct corrosion maintenance to the Air Force is $795,264,699; the elements that make up this cost are summarized in the table below. Depot maintenance accounts for 80 % of the total cost of corrosion maintenance. The number of aircraft in the fleet have decreased roughly 20%, but overall costs only declined 10%, and aircraft specific costs actually increased by 4%.

The charts on the following page provide cost breakdowns by fleet costs and by per aircraft costs.

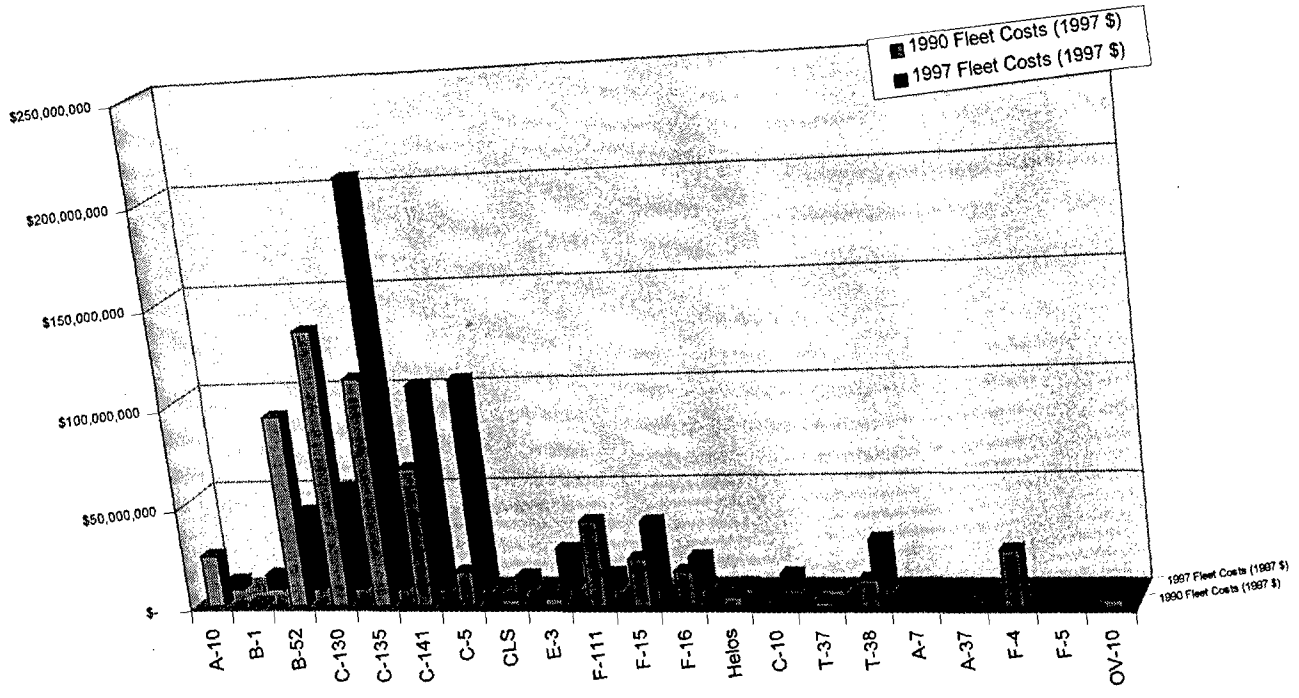

Chart 1: Fleet Cost

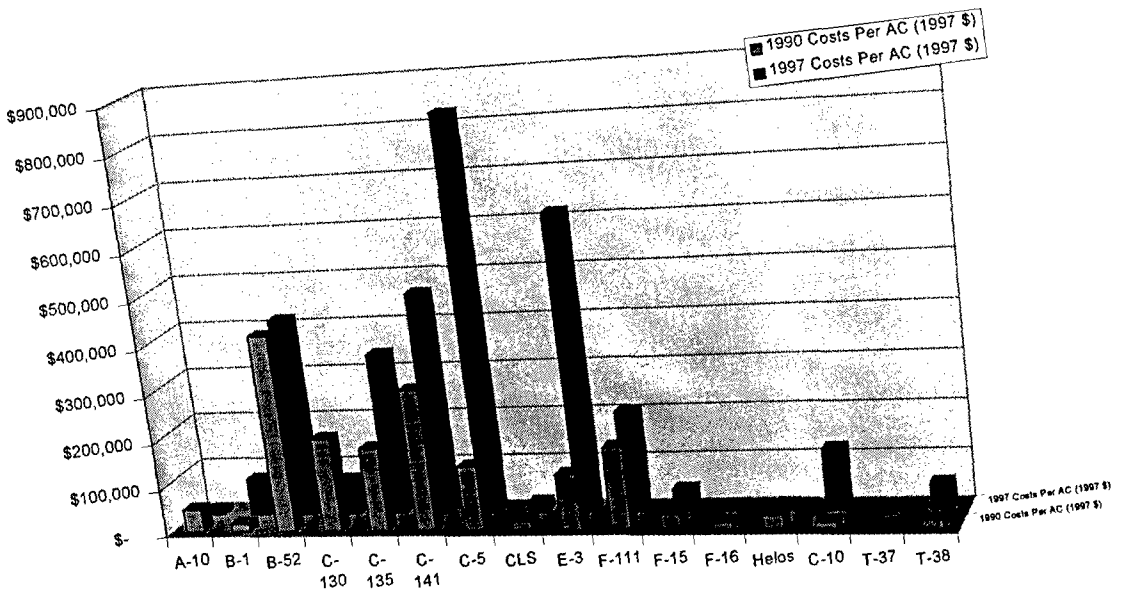

Chart 2: Per Aircraft Cost

Cost comparisons to the previous study focused on two main areas:

1. Changes in the overall corrosion maintenance costs and the contribution of different weapon system types, and
2. Changes in the per plane costs within weapon systems.

The aging effect is enumerated within the Cost of Corrosion Report. Each of the oldest fleets of aircraft is a high-dollar driver, and the difference in costs between these fleets is primarily a reflection of difference in size and slight differences in age. Three older fleets consume over half of all of the corrosion maintenance costs. In the older fleets, there is a simultaneous occurrence of new corrosion and recurrence of corrosion attack at sites that have been repaired in the past. This process will continue to accelerate as more and more sites experience breakdown of the as-built protection, and will continue to accelerate until the current maintenance process is no longer economically tolerable (or until corrosion-initiated damage becomes a mission limiting or safety-of-flight issue).

Some interesting observations on individual fleet costs:

1. The A-10, C-130, and F-16 fleets experienced a reduction in the cost of corrosion maintenance greater than the change in force structure. The decrease in A-10 costs is a reflection of the fact that early-life corrosion problems have been largely solved and force reductions have resulted in closing of two severe bases.
2. The decrease in C-130 corrosion maintenance costs is reflective of the completion of the very large wing modification on the C-130E fleet and continued delivery of C-130H models that are more corrosion resistant than earlier models.
3. B-1 and E-3 costs have increased. They have begun Programmed Depot Maintenance since the earlier study. As there were virtually no depot costs on these fleets in the earlier study, cost increases were expected.
4. The C-5 cost increases primarily reflect the C-5B change from ACI only to PDM.
5. The T-38 flow is unchanged despite reduction in fleet aircraft. Corrosion maintenance remains significant.

3.2 Identify and Manage

It has become clear over the past several years that simply continuing to perform corrosion maintenance as we have in the past will continue to consume huge parts of the aircraft maintenance budget, result in unsupportable depot flow times, and may not provide a safe and supportable aircraft out of our depot processes. In examining alternatives to the current way we do business, the USAF engineers came across the study performed Cole, Clark, and Sharp of the RAAF Defense Research Institute. That study provided the basis for what has become a new thrust for corrosion maintenance in the USAF. We have named it the "Identify and Manage" approach to corrosion maintenance as opposed to the current "Find and Fix" method of doing business.

3.2.1 Identify

The first step in corrosion maintenance is to Identify the places where corrosion attack has occurred. This is an area where additional research is needed to provide continuing ability to identify incidence of corrosion attack; however, currently available techniques and methods provide more evidence of corrosion attack than current maintenance practices can comfortably absorb. This was not a major area of research in our program.

3.2.2 Assess

Assessment of corrosion damage once it has been identified is a major thrust of the USAF program. This step in the process is what will make or break the new parts of the process. In this part of the program, we must provide the ability for engineers to determine:

- The immediate effect of each instance of corrosion attack on structural integrity
- The future effect of the corrosion damage if allowed to proceed unchecked
- The ability to define the best repair from among the available choices

3.2.3 Repair

The maintenance technician will then perform the defined repair. As every instance of corrosion damage will become an engineered repair, it is essential that each repair can be performed by the appropriate technician whether it is an abatement procedure, a standard corrosion repair, or a remove and replace action.

3.2.4 Document

As the options for maintenance expand, it is clear that all of the decisions and actions must become part of the permanent record for the aircraft involved. A complete history from damage discovery through completion of the repairs will be necessary so that an appropriate decision can be made the next time the aircraft visits the depot. This will be accomplished through automated record keeping.

3.2.5 Research Required

The above activities require a coordinated research effort to accomplish. Some of them are underway as described later in this paper. Others are programmed over the next couple of years, while still others depend on research initiatives that are beyond the control of the Air Force Corrosion Program Office.

- Research initiated:
  - Corrosion Growth Rates in Crevice Corrosion
  - Corrosion Growth Modeling
  - Corrosion Severity Modeling
- Research Programmed
  - Corrosion Abatement Technologies
  - Exfoliation Corrosion Growth Rates
- Research Needing Programming
  - Growth rates for other forms of corrosion (Pitting, Uniform, Intergranular)

3.3. Corrosion Modeling

This section summarizes the results of our modeling effort to date. Our model integrates the results of environmental modeling, susceptibility modeling, condition modeling, corrosion growth rate modeling, and structural effects modeling. All have been completed and integrated. A combining model has been developed that results in a corrosion prediction that permits determination of present corrosion damage and predicts the effects of future

corrosion damage. An economic effect model has been joined to the structural model that permits the examination of cost effectiveness of various maintenance actions.

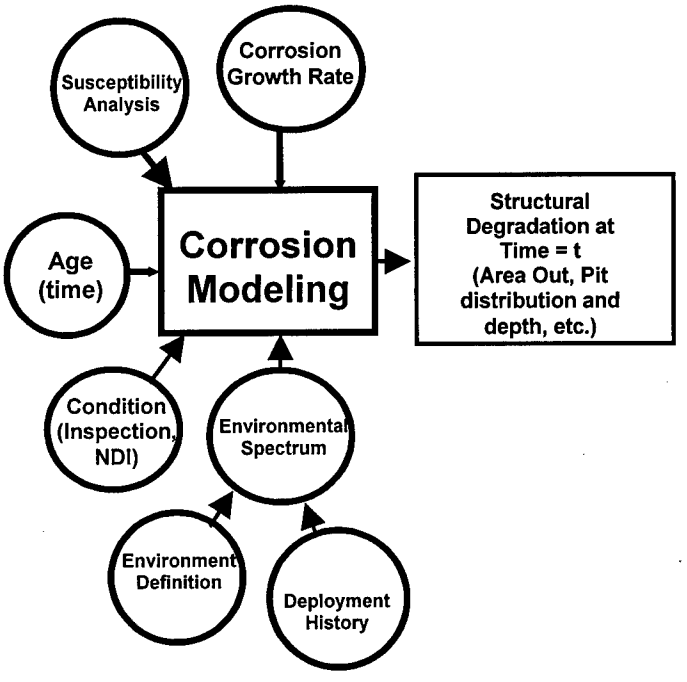

Figure 3.3: Corrosion Modeling

3.3.1 Environmental Modeling

In the mid-90's, it became apparent that the base level corrosive environments that had been established in the mid-70's was no longer sufficient. The qualitative ratings from an earlier time had been sufficient to establish base-level maintenance actions; however, they were inadequate for the current needs. What was needed was a quantitative environmental severity rating that would establish differences between base level environments. This would allow engineering managers to use the severity ratings as an aid in determining the probable corrosion damage that could be expected at the next depot visit for an aircraft stationed at a particular base. In 1997, the Air Force Corrosion Program Office set out to accomplish this for all Active, National Guard, and Reserve bases both within the United States and overseas.

The effort was greatly aided by the results of the National Acid Precipitation Assessment Program. In that effort there were a number of regressions established which reliably correlate the weight loss on a number of metals with variations in the environment. In addition, the program gathered a great deal of environmental data at a large number of sites throughout the United States which in many instances correlate with the local base. Air quality data were harder to come by. In general, the number of air quality recording sites has been greatly reduced over the past few years, and a great deal of interpolation is required in order to define the pollution levels at a base. One thing that can be said however is that within the United States the quality of the atmosphere is greatly improved over the last 20 years. Insofar as overseas bases are concerned, the amount and quality of climatic data are certainly adequate to support the program; however, the air quality data are almost non-existant.

That having been said, it was possible to establish the quantitative measures demanded. The values range from a high of 64 for Diego Garcia to a low of 4 for Tabuk, Saudi Arabia.

There was some question about the validity of the values stemming from the correlations provided. To this end, the correlations were re-accomplished with values for Chloride accretion provided for a limited number of bases using a different method of data collection. The correlation proved to be much better using this data. This leads us to the conclusion that the method used to estimate Chloride accretion for our initial values might have

been in error. We will be using Chloride sensors provided by Dr. William Abbott of Battelle Columbus Laboratories to gather more Chloride data during the coming year.

In the mean time the values provided by the original estimates is adequate to calculate the Corrosion Severity Code (CSC) for the corrosion prediction capabilities.

3.3.2 Susceptibility Modeling

Whereas the base environmental severity coefficients were determined for "typical" aerospace structural materials, no aircraft is actually built from "typical" materials. In this effort, actual materials of construction were determined for ten different fleets of aircraft. The environmental severity of each base was adjusted based upon the actual aircraft stationed at that base. That is, while Kadena AB, Japan has a generalized coefficient of 58; the value for F-15s stationed there is 50 based upon the amount of titanium used in construction. Conversely, the value is 64 for KC-135s stationed there because of the high corrosion susceptibility of the aluminum alloys used in its construction, 2024-T3/T4, and 7075-T6

3.3.3 Condition Modeling

Eddy current technique is commonly used as an NDI (Non Destructive Inspection) for detection of hidden cracks and corrosion in commercial aircraft structures. This technique detects variations in the specimen's ability to generate eddy current in the presence of the time varying magnetic field. Therefore, it is sensitive to any changes in the material which affect the conductance of the material such as cracks or variations in thickness. An output of eddy current technique was provided in the form of a scanned image of the hidden corrosion within the hidden layers of the lap joint specimen. Different colors of the image represent different magnitudes of induced voltage. Special calibration standards are used to transform the different values of induced voltages to the corresponding values of corrosion depths throughout the corroded area. Those values of the thickness variation characterize the As-Is condition of the lap joint.

The "Engineering Corrosion Growth Model" then takes these data and performs the following tasks:

- Select or calculate the CSC for the planned basing.
- Look up the relevant distribution of corrosion rates from the database using the CSC.

The next step in the model would be to apply the corrosion rate distribution selected to the initial pit depth distribution from NDI and to calculate:

- The final pits depths distribution, and;
- How long it would be before the tail of the distribution would hit the specified defect size (for fatigue) or thickness loss (for residual strength).

To feed this model, the values of the thickness loss or pit depths throughout the lap joint area must be presented in the form of a Probability Distribution Function. A Two-parameter Weibull Probability Function has been chosen because it is one of the very few probability functions that is non-symmetrical and is determined only for positive values.

Measured values of different thickness losses for the 707 lap joint have been processed with the ReliaSoft Weibull 5++

Software to obtain the Weibull Probability Density Function. The resulting parameters of the corresponding Weibull Probability Density Function are used in the probability data analysis to make the corrosion status predictions.

3.3.4 Corrosion Growth Rate Modeling

Corrosion rates of lap joints under different CSC conditions are obtained from SQUID (Superconducting Quantum Interference Device) measurements performed by the group headed by Dr. John Wikswo (Vanderbilt University). The main principle of this technique is measurement of the magnetic fields distribution associated with the corrosion currents within the lap joint after it had been subjected to the corrosive environment.

At the present time SQUID is the only available technique to image the hidden corrosion in situ. The sensitivity of SQUIDs operating at 4 K in liquid helium is such that corrosion can be detected for salt concentrations as low as one part per million. Because of the unparalleled sensitivity of 5-20 $fT/Hz^{1/2}$ spatial resolution, and dc-to-10 kHz bandwidth, hidden corrosion in 4% NaCl can be detected through 1.4 cm of aluminum.

A model has been developed that allows to transform the magnetic fields' images to corrosion rates. The basic idea of this model is that total double integral of the magnetic field distribution over the surface of the specimen and over time of corrosion is proportional to the total mass loss of the specimen. Based on this model, the experimental procedure that allows to obtain the correlation function between the magnetic fields and mass loss has been designed and performed successfully.

Following this approach, NCI has mathematically proven the procedure of mapping the magnetic fields over the specimen to the corrosion rates in each point of the specimen at the specified time frame.

To feed the corrosion growth model, corrosion rates must be presented in the form of a Weibull Probability Distribution Function.

Resulting parameters of the Weibull PDF, β and η, were used in the corrosion growth model to predict the final distribution of the depth values of corrosion attack at time $t = t_o + t$ under the various corrosion conditions established by the CSC.

3.3.5 Corrosion Growth Modeling

From NDI modeling and corrosion growth rate modeling, NCI has developed a corrosion growth model to predict further corrosion damage (pit or corrosion depth in lap joint sheets) in the future (generally, one depot cycle – approximately 4-5 years). Because both corrosion damage depths from NDI and corrosion rates from SQUID measurements are expressed in frequency distributions, a probability approach has been used to develop the model for lap joint corrosion prediction. Data required in developing the model are as follows:

(1) Aircraft deployment plan (base name and station time),

(2) AF base CSCs and time-of-wetness,

(3) Distribution of initial corrosion damage depths, from NDI measurements, at time t_0 for a lap joint of interest for corrosion damage prediction,

(4) Distribution of corrosion growth rates from SQUID measurements for a lap joint in a given CSC.

The mathematical treatment involved in developing the probability model is briefly described as follows. Initial corrosion damage depths are described by number of sites of given depth (NSD). Corrosion growth rates are described by frequency of occurrence rate (FOR) in a given CSC. Both NSD and FOR are normalized distributions. A new distribution of corrosion damage depths, called predicted number of sites of given depth (PNSD), is generated in a given time $t_0 + \Delta t$. At t_0, the number of corrosion damage depths from h_0 to h_0+dh is given by $NSD(h_0) \bullet dh$. The probability of corrosion growth rates in a range of r to r+dr is $FOR(r) \bullet dr$. The number of corrosion damage depths from h_t to h_t+dh_t at $t_0+\Delta t$ is given by:

$$\text{Probability}(h_t \le h \le h_t + dh) = \int_{h=0}^{h=h_t} NSD(h) * d(h) * FOR(r) * dr \quad (1)$$

because any initial corrosion damage depth h_0 can grow into corrosion damage depth h_t ($\ge h_0$) after a given time Δt at rate $r = (h_t - h_0)/\Delta t$. Equation (2) below can be derived from Equation (1).

$$PNSD(h_t) = \int_{r=0}^{r=\frac{h_t}{\Delta t}} NSD(h_t - r * \Delta t) * FOR(r) * dr \quad (2)$$

Equation (2) usually cannot be solved analytically because of mathematical complication of distribution functions. A user-friendly computer program, called lap joint corrosion prediction, has been developed to solve Equation (2) mathematically. A Weibull distribution function was chosen for both NSD and FOR in the computer program for example calculation. The computer program model consists of two parts: (1) a database of Air Force base CSCs, time-of-wetness and corrosion growth rates associated with CSCs, and (2) Visual Basic (VB) program interfaced with the database for solving Equation (2). The contents and functionality of the computer program model include:

(1) Database building: a database comprised of Air Force base names, CSCs, and time-of-wetness associated with each base,

(2) Data input: a user enters aircraft tail number, MDS number, location of a lap joint used for prediction, and deployment plan,

(3) Corrosion parameter selection: the computer program selects: AF base CSCs, time-of-wetness and parameters of corrosion growth rate distribution functions associated with the CSCs from the database,

(4) PNSD calculation: the VB program will solve Equation (2) numerically, and for multi-CSCs (multi-AF base deployment plan), the calculated PNSD from a previous CSC is treated as NSD for the current calculation,

(5) Result expression: final PNSD and cumulative distribution of PNSD are tabulated and graphically expressed,

(6) Important parameters of distributions: characteristic parameters for both initial and predicted corrosion damage depth distributions (means, medians and modes) and their changes are calculated and listed in a table,

(7) Reliability calculation: the VB program can calculate a critical depth when a user provides the maximum probability of corrosion

failure which the user can withstand,

(8) Output: the results can be printed and/or saved for records or future use.

By using the computer program model, distribution of corrosion damage depths of a lap joint of interest can be calculated. The calculated distribution will be provided to structural integrity assessment, as described in the following section, for a reliable life prediction of lap joints due to combined effect of fatigue and corrosion.

3.3.6 Structural Effects Modeling

Simply stating the amount of corrosion that has taken place or predicting the amount that will take place in the future is of little use to the engineers responsible for maintaining the safe life of an aircraft. We must provide corrosion damage descriptions in terms that mean something to the structural community. Two different aspects of this problem were attacked in the past year.

Boeing Aerospace and a group of consultants showed that the existing codes could be used in new ways to calculate the effects of corrosion as long as the corrosion community can provide them with the amount of material lost due to corrosion attack. They showed that it is possible to provide a risk assessment based on the loss due to corrosion and the residual strength.

As part of this project, APES, Inc. showed that it is possible to use finite element analysis and the surface roughness resulting from different amounts of corrosion to calculate the resulting fatigue crack performance.

These results indicate that both the corrosion community and the fatigue analysts need to communicate better if we are to successfully battle the effects of corrosion.

3.3.7 Cost Effects Modeling

Modeling corrosion activity and the maintenance activities employed to control it, is fraught with difficulties. However, the benefits to be derived from such an effort make the daunting task indispensable to an efficient Air Force. An important element of efforts to model corrosion attack on aircraft, is the impact of corrosion maintenance on aircraft serviceability. Obviously, the final goal of corrosion modeling efforts is to improve the operation and service of the aircraft fleet. A model to evaluate the most efficient maintenance alternative to arrest corrosion attack is essential to optimizing maintenance decisions. The AFCPO has begun to develop a model to perform this maintenance optimization.

The first step to successfully developing effective models of corrosion itself and corrosion maintenance alternatives, was to attack a problem sufficiently limited to allow a detailed model not hopelessly lost in its own complexity and details. For that purpose, current efforts are focused on lap-joint corrosion and rivet and lap joint maintenance options.

The first element to a Cost Model of corrosion maintenance, is an actual model of corrosion attack itself. Only recently has technology advanced sufficiently to promise the ability to develop corrosion growth rate models. Corrosion is not uniform and precisely predictable. However, distributions of corrosion rates can be used to develop statistical models of corrosion attack which yield corrosion attack probabilities.

A Markov Decision Model is the basic structure of the maintenance optimization model. The founding principle of Markov

mathematics is that future states are dependent on current states and independent of past states. That assumption is valid for corrosion attack. The model requires determining from the rate distribution functions the transition probability from one state to all others in some time period (envisioned to be one depot cycle). The states can be mathematical (0.03 vs. 0.04 mm mass loss) or definitions (Moderate vs. Severe). The next step in the modeling process is to determine the costs associated with each state. Through discussions with former maintainers and telephone confirmation, simple costs for single rivet repairs have been estimated, and (short of acquiring complete actual costs) can be extrapolated. For example, the costs could range from $1600 to $2000 for a grind-out repair, to $3200 to $4000 for a sheet metal repair, with a high cost assumed for failure. The transition probability matrix can then be transformed into a series of simultaneous equations and solved for steady state probabilities (the probability after time of being in each state). The probability distributions can also be adjusted to determine the impact of different maintenance policies, which, when combined with the cost matrix yields cost optimization.

4. CONCLUSION

In early 1997, the Air Force Corrosion Program Office set out to show that the problems associated with corrosion and its effect on the ultimate airworthiness of aircraft was both serious and capable of being modeled sufficiently to allow its inclusion in maintenance planning. In less than a year, we have made remarkable strides toward achieving those two goals. The progress, while not spectacular, has consistently shown that imaginative application of science and engineering can yield useful results in a reasonable time frame.

ENVIRONMENTAL EFFECTS ON FATIGUE CRACK INITIATION AND GROWTH

A. K. Vasudevan
Office of Naval Research
800 N. Quincy Street
Arlington, VA 22217-5660, USA

K. Sadananda
Naval Research Labs.
Washington, D. C. 20375, USA

ABSTRACT

This article discusses briefly the relative effects of the role of environment on the fatigue crack initiation and growth at ambient temperatures. Emphasis is given to describe the crack tip driving forces required to understand the basic physics. It is observed that the fatigue damage requires two driving force parameters (ΔK and K_{max}) over the entire range and that the relative role of each parameter depends strongly on the role of deformation slip and environment. The environmental effects fall into four categories that depend on the synergistic role of the environmental kinetics and deformation. The study points out that one needs the correct parameters to develop a life prediction model. The overall topics are focussed to the near threshold behavior and the concepts can be extended to higher growth rates.

BACKGROUND

The phenomena of crack initiation and growth kinetics in structural materials under service loading conditions are in general due to the combination of environment, stress and alloy microstructure. Thus the performance of a material can be degraded by the interactions of environment with cyclic loading. The environment can be either chemical or temperature or both. Fig. 1 (crack length variation with fatigue cycles) illustrates the possible sequence of degradation of a material subjected to aqueous environments from an inert (like a good vacuum) environment. Below the service inspection limit (NDE), where the crack is undergoing subcritical crack growth, the environment can impact the early stages of cracking by the introduction of pit initiation and growth to crack initiation and growth to microcrack coalescence to macroscopic crack growth. There is a high probability of environmentally assisted crack initiation sites developing during the early stages of a component life. The problem of life prediction then devolves to the understanding and quantification of the growth of these small cracks from the initiation sites prior to the formation of a macroscopically large crack. Hence the attempts in developing a reliable analytical life prediction methodology must unify the crack initiation to small cracks to large cracks to final failure.

In the last several decades there has been several dozens of empirical life prediction models proposed. To date, quantitatively reliable prediction modeling is still lacking. The existing models do not have any terms in them to include the environmental effects. As a result, they are unable to predict the shapes and magnitude of **a** vs **N** curve when some unforeseen effects from the corrosion are introduced during service loading conditions. To overcome these limitations, safety factors are commonly introduced in practice to incorporate the possible effects from the load-environmental interactions that can degrade the life severely. Interestingly, even after the safety factors are included at the design stage, cracks are often observed much earlier than the scheduled inspection intervals. Due to

Paper presented at the RTO AVT Workshop on "Fatigue in the Presence of Corrosion", held in Corfu, Greece, 7-8 October 1998, and published in RTO MP-18.

such observations, components are fatigue tested using actual simulating service loads and environments and the damage life is then estimated. Generally, these procedures are expensive, statistically limited and are not applicable to other load-environmental conditions that the component can experience.

Major uncertainties in the life prediction methods arise due to a lack of understanding and quantifying the load-load interactions and the role of environment on the overall damage. A short-term approach to this problem is the crack inspection methods that are in place at many of the maintenance depots. Fig. 2 shows the generic approach in the maintenance field. A sensor (NDE) is used to detect a crack on a component. After detection the operator makes some decision as to whether the component should be repaired or replaced. This is along the Path-1. Along Path-1 lies some uncertainties that can make the operators decision undependable. These uncertainties can span from the unknown loads and environment to the hidden cracks to material inhomogenieties. Given such a case, one should take the Path-2 where the same NDE inspection data is integrated with a reliable life prediction model that can be used by the operator to make a better judgement on his outcome.

In general the environment can affect the fatigue crack growth characteristics either at the near threshold region or at some higher crack growth rates. Corrosion assisted fatigue crack growth resistance in materials has been schematically classified into three types [1]. Fig. 3 schematically shows the three variations of the mechanical fatigue and environmentally assisted crack growth dependence on K_{max}. Fig. 3a illustrates the true corrosion-fatigue coming from the synergistic effects of fatigue loads and environment. Here the environment alone, in the absence of fatigue, is taken to have no affect on crack growth resistance. Instead, the environment accelerates the crack growth rates only under the fatigue conditions by degrading the material by the time-dependent process. This true corrosion-fatigue influences the cyclic fracture behavior even at the maximum stress intensity factor values $K_{max} < K_{Iscc}$, where K_{Iscc} is the stress corrosion threshold under sustained load conditions. Fig. 3b shows the case when stress corrosion-fatigue process can occur by a superposition of stress corrosion and mechanical fatigue mechanisms. Here the stress corrosion occurs when $K_{max} > K_{Iscc}$. The combination of true corrosion-fatigue (Fig.3a) and stress corrosion – fatigue (Fig.3b) leads to a mixed corrosion behavior shown in Fig.3c. In the following discussion we restrict our topical discussion to the first case shown in Fig. 3a. The discussion can be extended to the other cases. For a given environment, the effects vary with the alloy microstructure, its strength and ductility. The effects can be observed to vary with load ratio and frequency. In addition, we shall attempt to describe the corrosion assisted fatigue damage behavior from the crack initiation to long crack growth region. They can be classified into four types.

Current explanation of the corrosion – fatigue under aqueous environments can be summarized into the following items [2]:

- corrosion pits that serve as crack nucleation sites,
- enhanced slip reversibility due to slip-step oxidation process,
- preferential electrochemical attack at slip bands where deformation is localized,
- preferential electrochemical attack at sites where the oxide film has ruptured,
- surface energy reduction due to adsorption of chemical species with an attendant increase in crack growth.

Thus the rates of chemical attack and their subsequent influence on fatigue damage lives are strongly affected by the electrochemistry of the environment as well as by the type of mechanical loading pattern. The damage process falls into two main mechanisms namely; anodic slip dissolution and hydrogen embrittlement. This makes the corrosion –

fatigue analysis difficult to understand and quantify into a parameter that can be used in a life prediction model. In general, the overall influence of the corrosion chemistry is a complex competition between the kinetics of the passive oxide layer formation, its dissolution and fracture with respect to the rate of crack growth in that medium.

There seems to be no single model, which quantitatively accounts for the key features of corrosion assisted fatigue for a broad class of materials. A simple model [3,4] has been proposed that assumes that the overall crack growth rate (da/dN) of a material can be determined by a linear superposition of the crack extension rates mainly due to mechanical fatigue $(da/dN)_f$ determined in vacuum and stress corrosion rate $(da/dt)_{sc}$. These models have included frequency and waveforms. Such a model implies that there are no synergistic effects between the mechanical and corrosion components of corrosion – fatigue. The model applies to cases when $K_{max} > K_{Iscc}$. The model also tacitly assumes that the mechanisms of stress corrosion and corrosion - fatigue are the same. These two assumptions run counter to the experimental observations, particularly for lower strength materials where there is large plasticity. These superposition models have been modified [5, 6] by others to include $K_{max} < K_{Iscc}$.

In order to account for these limitations in the corrosion – fatigue analysis crack closure models were introduced [7, 8]. It was suggested that there is an increasing amount of crack closure due to the formation of corrosion deposits within the cracks, at near threshold ΔK regions that can reduce the rate of crack growth at $K_{max} < K_{Iscc}$ (as in Fig. 3). Such a model is considered where the results are usually compared with dry nitrogen or hydrogen or helium results (considered as inert environment) and not to a good vacuum. Environmental results must be compared to that in a good vacuum, since vacuum results are truly the condition in which there should only be contribution from mechanical fatigue and not corrosion. If closure effects from environment persists then the crack growth data from the environment should lie to the right of the vacuum (or inert) data and not to its left, see Fig. 3. To date, the authors are not aware of any environment that promoted a beneficial effect on fatigue crack initiation or growth behavior.

We have critically examined the crack closure concepts and find the following salient issues [9 – 11]:

- plasticity induced closure is not possible,
- complete closure is possible if the crack volume can be filled with oxide or a corrosion product, which is rarely observed,
- asperities occur randomly and as a result asperity – induced closed closure cannot explain the systematic deterministic behavior of ΔK_{th} with R,
- partial closure is possible locally at the asperity sites, but their effects are nominal on the crack- tip stress fields.

Thus, in most aqueous environmental fatigue cases, closure levels are small to affect the near threshold crack growth.

NEW CONCEPTS - TWO PARAMETRIC DRIVING FORCE FOR FATIGUE

We restrict our discussion to the near threshold crack growth region where $K_{max} < K_{Iscc}$. In this region the corrosion effects can degrade the fatigue resistance of a material significantly depending on the type of slip deformation, environmental aggressiveness and the loading conditions. The role of frequency and waveform can affect depending on the crack tip environmental reactions. The frequency effects are commonly observed at higher crack growth rates than at near thresholds.

Assuming that closure is not a major factor for crack advance, we have analyzed the

fatigue data of many different materials from the literature and arrived at the following conclusions [10, 12]:

- to completely describe a fatigue damage, one needs two independent loading parameters ΔK and K_{max} and not one like ΔK,
- these two parameters must to be satisfied simultaneously for a crack advance,
- this leads to two critical thresholds ΔK^*_{th} and K^*_{max} that are directly related to the alloy microstructure, slip mode and environment,
- this concept is independent of closure, testing methods and is applicable over all crack growth rates.

Fig. 4a shows a ΔK_{th}-R plot for a Ti-6Al-4V alloy [13] in moist air environment for R varying from –2.0 to 0.9, where ΔK_{th} decreases linearly with R . Since R is a driving force parameter, Fig. 4a can be replotted in terms of ΔK_{th} -K_{max}, as in Fig. 4b. This plot gives two asymptotic values in ΔK and K_{max}, namely $\Delta K^*_{th} \sim 1.6 Mpa\sqrt{m}$ and $K^*_{max} \sim 3.5 Mpa\sqrt{m}$, which represent the two minimum values for the threshold crack growth rates. One can extend such plots to higher growth rates to obtain the corresponding minimums in the two parameters. This form reflects the intrinsic behavior of fatigue of a given alloy. Such a method is applicable to various types of materials, ranging from monolithic to composites [12,14,15].

The stress intensities, ΔK and K_{max}, depend strongly on the microstructure and environment [10, 12]. The degree of this effect depends on the slip mode of the material and the level of aggressiveness of the environment. For a planar slip alloy both ΔK and K_{max} can vary; while in a wavy slip alloy, either ΔK or K_{max} can vary depending on the environment. To illustrate the first case, one can look at an example from a 7075 aluminum alloy [10], heat treated to give constant yield strengths in the underaged condition (UA, planar slip, σ_{ys} ~456 MPa) and an overaged alloy (OA, wavy slip, σ_{ys} ~470 MPa). Such tailored microstructures in vacuum (absence of environment) causes a downward shift in both ΔK_{th} and K_{max} values from UA to OA condition, as shown in Fig. 5. For comparison, pure aluminum data is included, for air. For the same constant yield strength alloy microstructures (UA vs OA) the aqueous environment (moist air) shows a marked effect for the planar slip alloy compared to the wavy slip, as in Fig. 6. The crack tip environmental interaction affects the crack growth process depending on the kinetics of formation of the passive film and its fracture. The relative variations in the K_{max} with environment due to differences in the slip mode could be due to the relative ease to fracture the passive film at the crack tip. Thinner films can be easily fractured at a lower K_{max} than thicker ones. Details of the mechanisms of the crack tip environmental interactions are still at its infancy.

Early investigators like Erdogan [16], Smidt and Paris [17] have noted indirectly the two driving forces ΔK and K_{max}. Unfortunately, they did not pursue to examine the concepts further. Table – 1 gives a list of the key contributors [16-26] to the ΔK and K_{max}. The ΔK - K_{max} plot was first introduced by Doker and Marci [13]. First semi-empirical model of crack growth was given by Erdogan [16] in the form: $(da/dN)=B\, f(\Delta K, K_{max})$. Recently, Wilkinson and Roberts [26] were first to correctly predict the ΔK -K_{max} curve for copper using computer simulation of dislocation motion near a crack-tip.

CRACK INITIATION, SHORT CRACKS & LONG CRACKS

The overall fatigue damage consists of four main stages: crack nucleation, a short and a

long crack growth and final failure. The three main stages were first graphically related by Kitagawa and Takahashi [27]. The two parametric descriptions can be extended to the short crack growth region as well as the endurance limit. In order to do this we redefine the similitude concept (that is assumed to be an issue in the short cracks)as: **equal crack tip driving forces lead to equal crack growth rates for the same governing crack growth mechanisms if all the forces are included** [28,29]. By this definition, we can ignore the anomalous difference between the long and short crack behavior. Fig. 7 compares the behavior of long and short crack growth behavior in terms of K_{max}. The contrasting behavior of these two crack can be summarized as follows:

- there are no unique thresholds associated with short cracks,
- short cracks grow at stress intensities below long crack threshold,
- lack of similitude at the same K_{max} does not result in the same crack growth rates,
- short cracks can accelerate, decelerate and in some cases come to an arrest,
- at high growth rates the short crack converge with long cracks,
- excessive data scatter is observed experimentally in short cracks,
- in contrast, long cracks show only crack growth with less experimental scatter with a unique threshold.

Based on the experimental results and analysis, we consider that the long crack growth behavior under constant amplitude is the fundamental material behavior. The same two thresholds must be satisfied by both long and short cracks. Deviations from the long crack behavior (Fig. 7) are considered as due to the presence of **internal stresses**. One can note that irrespective of the nature of the short cracks, all short cracks grow from pre-existing notches or initiated at free surfaces and their behaviors are similar. The generalities that contribute to the deviations from the long crack behavior (Fig. 7) can be considered from introducing a concept of **internal stress** that can help or hinder the crack growth. Examples of internal stresses are: residual stresses, thermal stresses etc. In the case of a notch, the internal stress is the notch stress gradient. Thus a crack growing from a root of notch is experiencing the stresses from the notch stress gradient. The total stress at the crack tip is then a sum of the applied stress and the internal stress. Thus, crack growth is permitted if the total stress is greater than the K^*_{max} threshold of the long crack [28,29].

Stress amplitude fatigue limit in a S-N fatigue test and the corresponding threshold data for long and short cracks can be combined into a single curve called the Kitagawa-Takahashi [27] diagram. This is shown (Fig. 8) for a 13Cr-steel data from Usami [30] at different R-ratios. Linear portion at long crack lengths with the slope of half is related to the square root singularity under LEFM considerations. At smaller crack lengths the curve levels off to different fatigue limits for different R-ratios. Linear portion of the long crack data intersects the horizontal portion from fatigue limits at different critical crack lengths, a^*_R; which signifies the partition between long and short crack region. The extrapolation of the linear portion of the long crack region to the short crack region indicates that the actual stress required to sustain a crack that is less than a^*_R is significantly higher than the fatigue limit stress. The difference between the fatigue limit and the back-extrapolated stress is the required internal stress that is helping the short cracks to grow at lower stresses. Thus, the short crack anomaly is mainly due to the lack of recognition of the two long crack thresholds and the role of internal stress [31]. Thus the two driving force parameters provides a unified framework for the overall characterization of fatigue damage. Detailed analyses of the short cracks are given in references [28, 29, 31].

These concepts can be considered to the cases where the environment affects are superimposed on the mechanical fatigue. Fig. 9 schematically illustrates the corrosion-fatigue behavior with reference to an inert environment. The figure is a modified version of Kitagawa-Takahashi diagram connecting the crack initiation region to the long crack growth. Here σ_{max} and K_{max} versus crack length are used instead of $\Delta\sigma$ and ΔK. There appears to be four class of behavior due to the role of corrosion on mechanical fatigue. Each case differs whether the effects are in the initiation region or in the propagation region or both. The reasons for each case can be obtained from the summary diagram given in Fig. 10. The slip mode, microstructure (like grain size), relative ductility and the aggressiveness of the environment affect each region of the figure. The mechanisms are only known qualitatively, but lack the quantification. This is due to the lack of systematic experimental data in both environments (vacuum and corrosion) in the nucleation and growth regions.

These descriptions of the environmental-fatigue interactions give some basic understanding from which quantitative methods may be derived for an application to a model. For a given case in Fig. 8, the internal stresses can be quantified by taking the algebraic difference between the inert and corrosion data. Knowing the long crack thresholds data from the ΔK-K_{max} curves and analytically computing the internal stress gradient for a given design load, one can estimate when a crack can nucleate from a stress concentration site. Details of the mechanisms will be given elsewhere [32].

SUMMARY

- Description of fatigue damage must include two deriving forces: ΔK and K_{max}; these two parameters have to be met by long and short cracks.
- Constant amplitude fatigue is the fundamental material behavior.
- All the deviations from the steady state constant amplitude behavior are due to the presence of **internal stresses** introduced during service loads.
- Understanding and quantifying the role of **internal stress** gradients is fundamental to the development of a reliable life prediction model.
- Life prediction models must integrate damage over the entire range from crack nucleation to short crack to long crack to final failure. The model must also incorporate results from NDE.

CONCERNING ISSUES

- Need systematic base constant amplitude fatigue data, both S-N and (da/dN)-ΔK, at all load ratios $0<R>0$ in inert and environmental conditions. This would give the major differences in the two behaviors that are basic inputs to developing a model.
- Need an accurate quantitative description of service loads, like load-load interactions.
- Need an accurate quantitative description of crack-tip environment.
- Need an analytical method to describe the **internal stress** gradient, as it is difficult to measure experimentally.

REFERENCES

1. McEvily, A. J. and Wei, R. P., "Corrosion - Fatigue: Chemistry, Mechanics and Microstructure", vol. NACE-2, pp.381-395, 1972, Houston, National Association of Corrosion Engineers.
2. Suresh, S., "Fatigue of Materials", Cambridge University Press, 1998.
3. Bucci, R. J., Ph. D Thesis, Lehigh University, Bethlehem, 1970.
4. Wei, R. P. and Landes, J., Materials Research and Standards, vol.9, pp.25-27, and 44-46, 1970.
5. Wei, R. P. and Simmons, G. W., Int. J. of Fracture, vol. 17, pp.235-247, 1981.

6. Austen, I. M and McIntyre, P., Metal Science, vol. 13, pp.420-428, 1979.
7. Suresh, S., Zaminski, G. F. and Ritchie, R. O., Metall. Trans., vol. 12A, pp.1435-1443, 1981.
8. Vasudevan, A. K. and Suresh, S., Metall. Trans., vol. 13A, pp.2271-2280, 1982.
9. Vasudevan, A. K., K. Sadananda, K. and Louat, N., Scripta Metall. et Materialia, vol. 27, pp. 1673- 1678, 1992.
10. Vasudevan, A. K., K. Sadananda, K. and Louat, N., Mater. Science & Eng., vol. A 188, pp. 1-22, 1994.
11. Louat, N., K. Sadananda, K., Duesbery, M. S. and Vasudevan, A. K., Metall. Trans., vol. 24A, pp. 2225-2232, 1993.
12. Vasudevan, A. K., K. Sadananda, K. and Louat, N., Scripta Metall. et Materialia, vol. 28, pp. 6
13. Doker, H and Marci, G., Int. J. of Fatigue, vol. 5, pp.187, 1983.
14. Vasudevan, A. K. and Sadananda, K., Metall. Trans., vol.26A, pp. 1221, 1995.
15. Vasudevan, A. K., K. Sadananda, K. and Louat, N., Scripta Metall. et Materialia, vol. 28, pp. 837-843, 1993.
16. Erdogan, F., "Crack Propagation Theories of Fracture-an Advanced Treatise", Academic Press, New York, 1968.
17. Schmidt , R. A. and Paris, P. C., ASTM STP-536, pp.79-94, 1973.
18. Robinson, J. L. and Beevers, C. J., Metal Sc. J., vol.7, pp. 153-159, 1973.
19. Doker,H. and Marci, G., Int. J. of Fatigue, vol. 5, pp.187, 1983.
20. Doker, H., Int. J. of Fatigue, vol.19, pp. S 145, 1997.
21. Priddle, E. K.,"Fatigue Thresholds", Stockholm, Sweden, pp. 581-600, Warley, EMAS Publ.,1981.
22. Lal, D. N and Namboodhiri, T. K. G., Mater. Sci. Engg., 1990, vol. A130, pp.37, 1990.
23. Lal, D. N., Fat. Fract. Engg. Mater. Struct., vol.15, 793, 1992.
24. Lal, D. N., Int. J. Fat., vol. 15, pp.109, 1993.
25. Xu-dong Li, Engg. Fract. Mech., 1998, in presss.
26. Wilkinson, A. J. and Roberts, S. G., Scripta Metall. et Matl., vol. 35, pp. 1365, 1996.
27. Kitagawa, H. and Takahashi, S., "Second International Conference on Mechanical Behaivior of Materials", American Society of Metals, pp. 627-631, 1976.
28. Sadananda, K and Vasudevan, A. K., ASTM STP-1296, pp. 301-316, 1997.
29. Sadananda, K and Vasudevan, A. K., Int. J. of Fatigue, vol. 19, pp. S99-S108, 1997.
30. Usami, S., "Short Crack Fatigue Properties – Current Research on Fatigue Cracks", Elsevier Publn., vol. 1, pp. 117-147, 1987.
31. Sadananda, K and Vasudevan, A. K., "Fatigue 96", Pergamon Press, vol.1, pp 375-380, 1996
32. Ricker, R. E, Vasudevan, A. K. and Sadananda, K., In. J. of Fatigue, 1999, in press.

Table 1. Key Papers on the Topic of Kmax and DK

YEAR	AUTHORS	ALLOY	REMARKS
1968	Erdogan	Model	Empirical model that related rate of crack propagation to the size of two plastic zones- one on alternating plastic zone that depended on ΔK and the pulsating zone based on Kmax: da/dN= B f(Kmax, ΔK)
1973	Schmidt & Paris	Aluminum alloy	Explained the experimentally determined ΔKth-R-ratio using closure concept; but plotted ΔKth and Kmax thresholds seperately with R-ratio; indicated that Kmax was constant when Kmin<Kcl and when Kmin>Kcl ΔKth was constant; did not plot ΔK vs Kmax, nor recognize the two necessary driving forces for fatigue crack growth
1973	Robinson & Beevers	Alpha-Titanium	Explained the vacuum vs lab air data of ΔKth -R similar to Schmidt & Paris; pointed that in vacuum the fatigue is controlled by ΔK where there is no closure, vs the air where the closure plays an important role; did not plot ΔK vs Kmax, nor recognize the needed two driving forces
1981	Priddle	Mild steels	Similar explanation to Schmidt & Paris, plotted data in the form of ΔKth -Kmax curves but interpreted the results to be consistent with the concept of oxide induced closure; did not recognize the importance of two driving forces ΔK & Kmax for fatigue
1981 1983 1997	Doker, Bachman &Marci; Doker & Marci; Doker	Titanium & Aluminum alloys	First to plot their systematic data in the form of ΔKth vs Kmax; but explained the experimental results using closure concepts; later implied that there are two critical thresholds for crack growth
1990 1992 1993	Lal & Namboodhiri; Lal	Aluminum and Steels	Analyzed fatigue thresholds without invoking crack closure on the basis that for R>0.6 the crack growth is ΔK-controlled and for R<0.6 it is Kmax controlled; but did not plot the ΔK vs Kmax; nor recognized the two driving forces needed for crack growth
1993 1997	Vasudevan & Sadananda	All materials	Explicit statements that two independent driving forces ΔK and Kmax are required for crack growth dependent on microstructure & environment, independent of crack closure and test methods; applicable to the entire crack growth region and to variety of materials; applies to both long and short cracks.
1998	Xu-Dong Li	Aluminum alloys	Prediction model using ΔK and Kmax parameters explicitely to predict ΔK vs Kmax curve
1996	Wilkinson & Roberts	Copper	First dislocation model using ΔK &Kmax for threshold fatigue predicts the need for the two parameters and gives a fundamental reason for their occurence; predicts correctly da/dN vs ΔK and ΔK vs Kmax trends

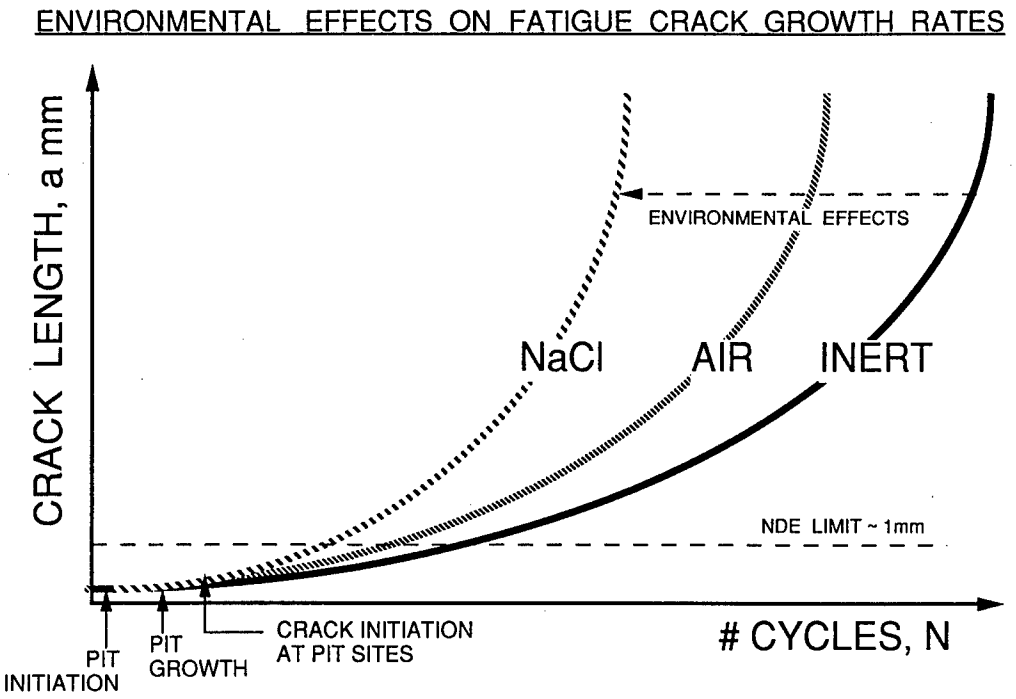

Figure 1. Schematic illustration of the role of environment on the crack growth from the early stages, with reference to the inert environment such as vacuum.

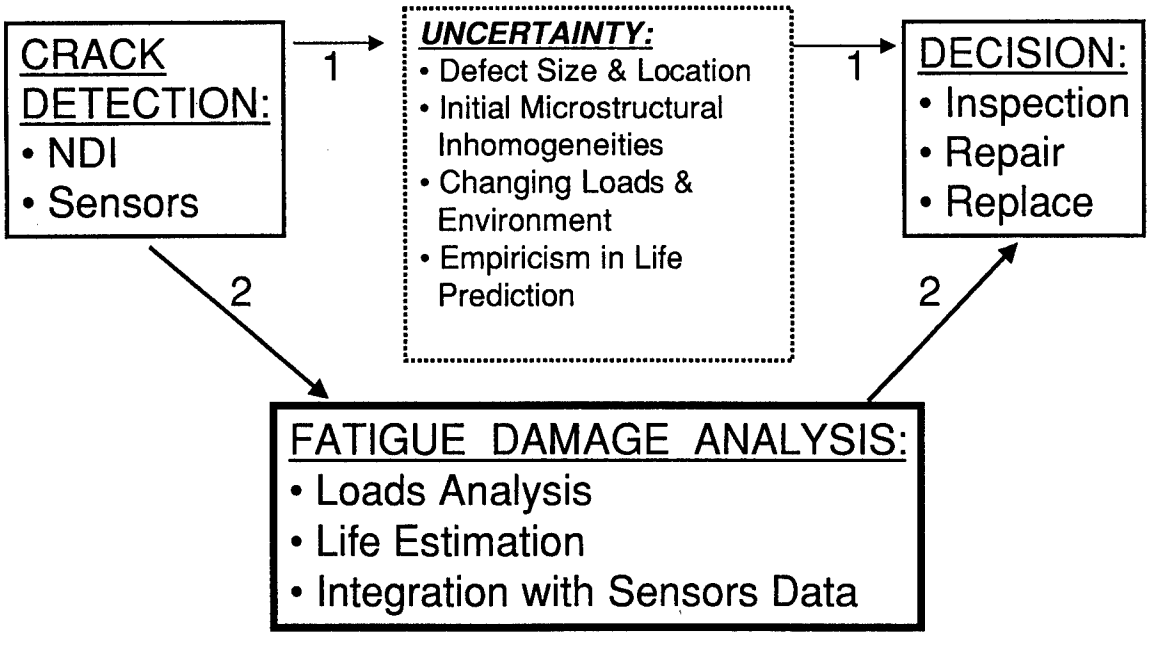

Figure 2. Schematic representation of the fatigue damage analysis.

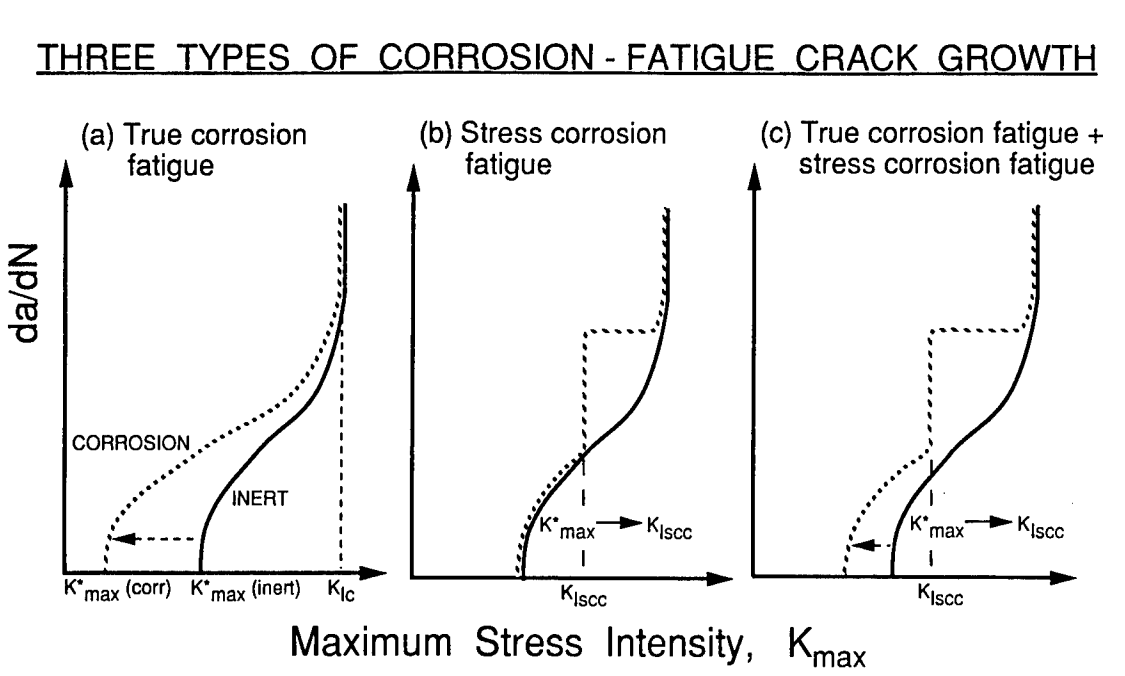

Figure 3. Schematic illustration of the three types of corrosion - fatigue mechanisms in terms of crack growth rate versus K_{max}

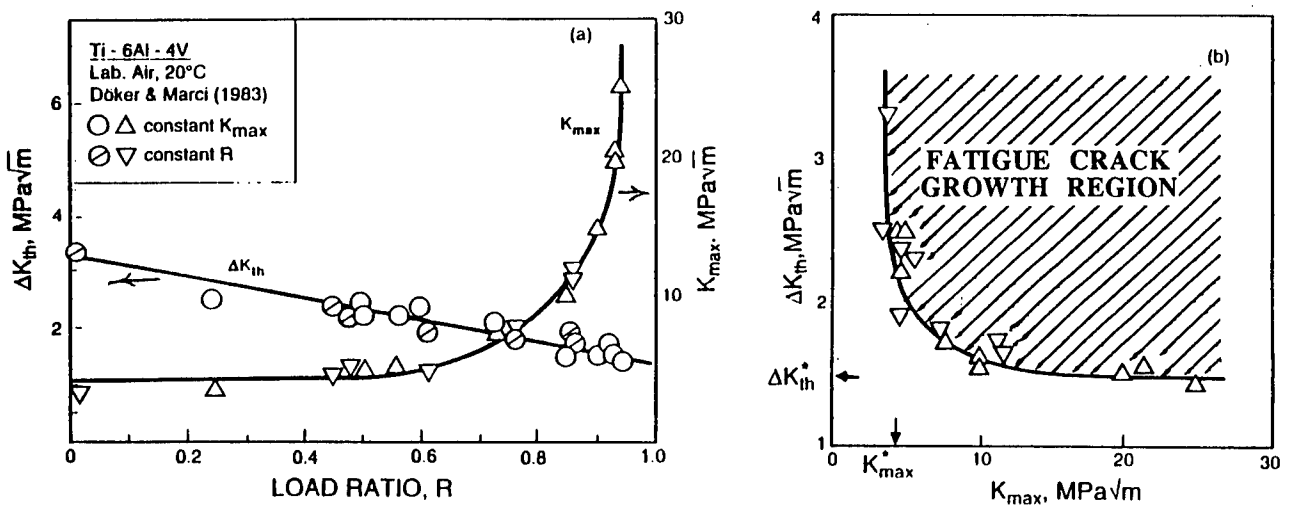

Figure 4. Near threshold fatigue crack growth results on Ti-6Al-4V alloy in lab air: (a) variation in ΔK_{th} and K_{max} with R, and (b) a replot of (a) in the form of ΔK_{th} - K_{max}, as a fatigue map.

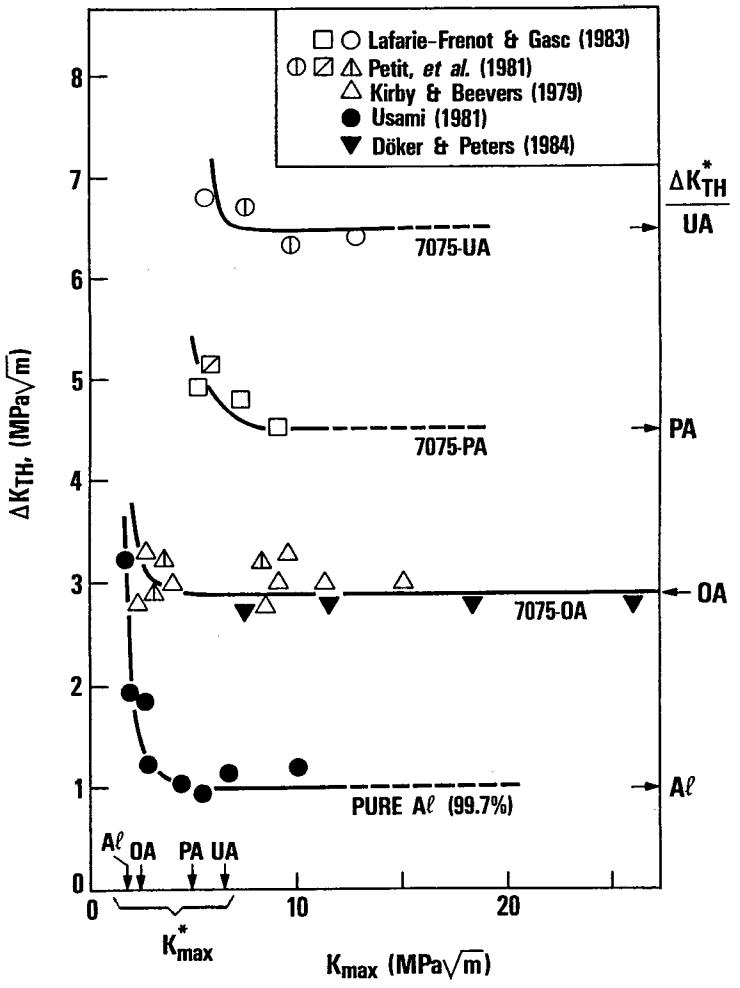

Figure 5. Microstructural effects shown in terms of ΔK_{th} - K_{max} for under (UA), peak (PA) and overaged (OA) heat treatments in a 7075 alloy.

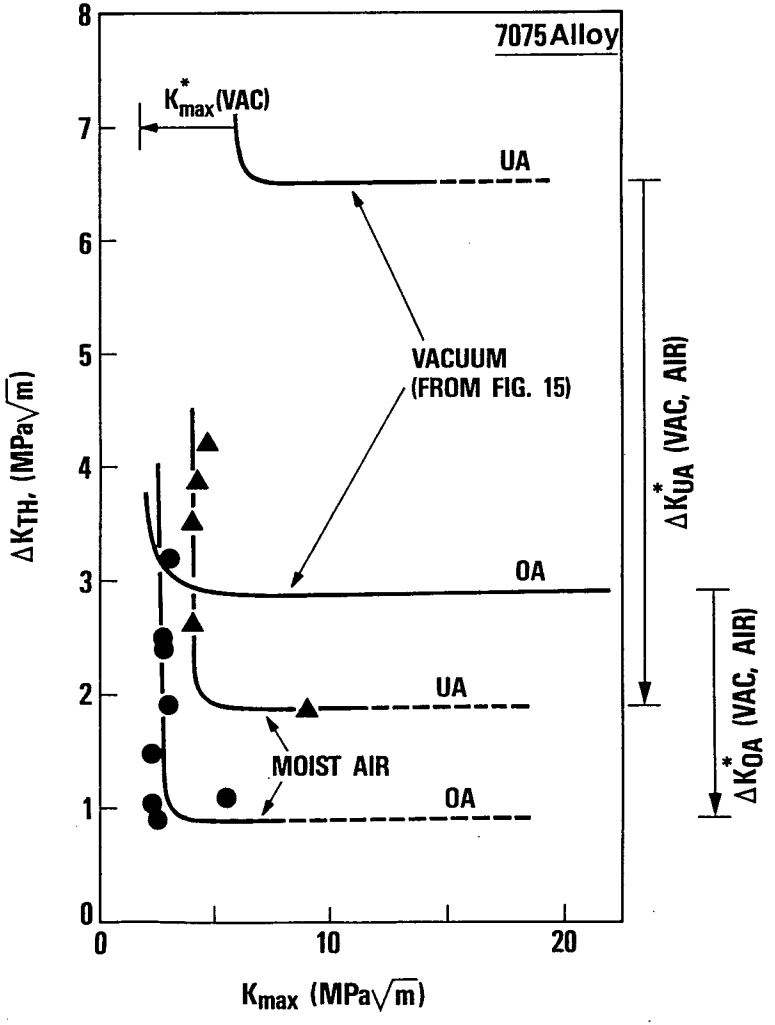

Figure 6. Effect of slip mode on ΔK_{th} - K_{max} due to aqueous environments (moist air & vacuum) in a 7075; for planar slip in UA vs wavy slip in OA conditions.

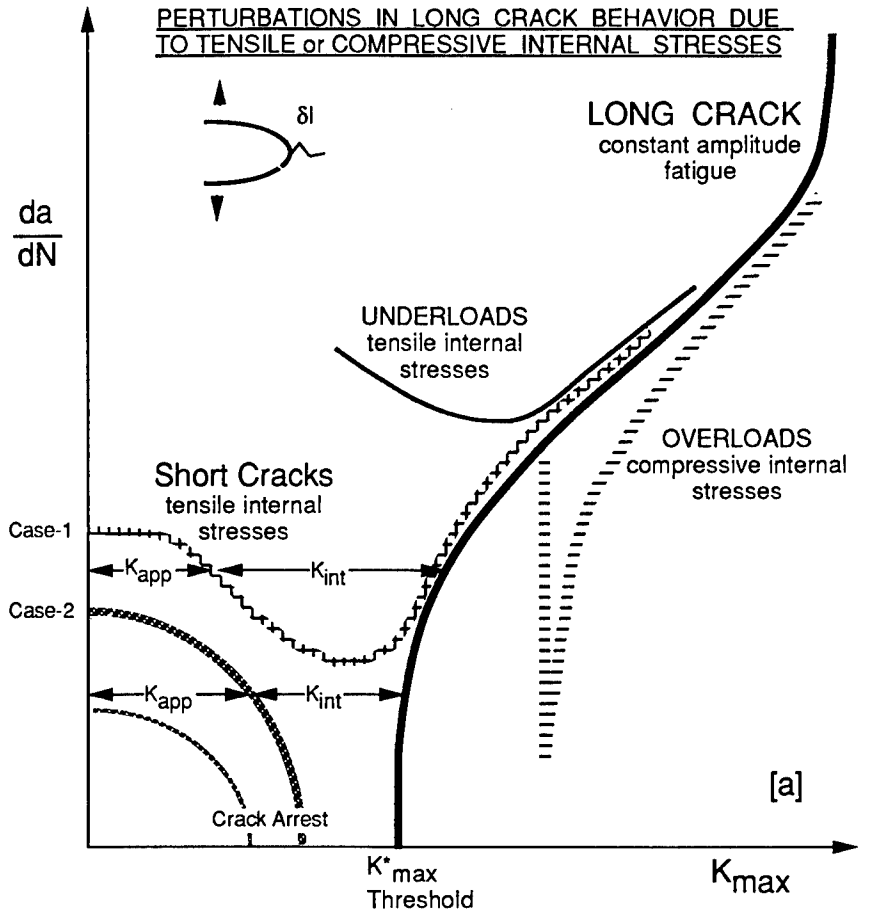

Figure 7. Schematic illustration of short crack growth in relation to long crack growth behavior; and the role of internal stresses in short cracks, under and overloads. Long crack growth is the fundamental property of the material.

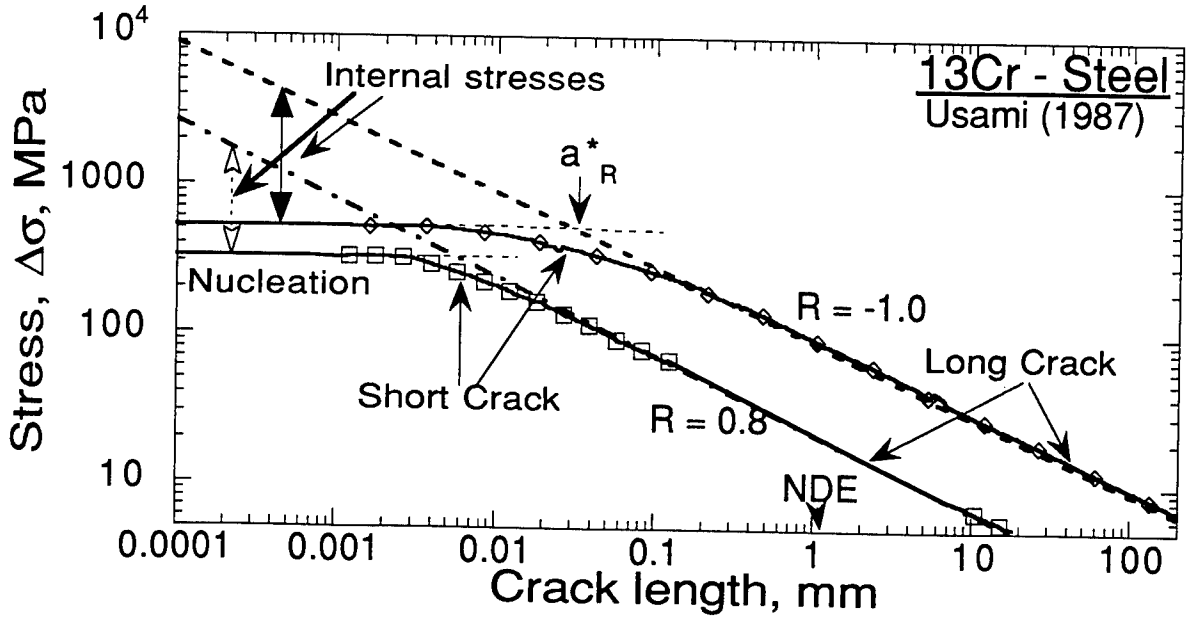

Figure 8. Kitagawa-Takahashi diagram for 13Cr-steel alloy connecting the Fatigue limit and thresholds for long and short crack at R=-1, 0.8.

FOUR CLASSIFICATION OF FATIGUE DAMAGE AFFECTED BY THE ENVIRONMENT

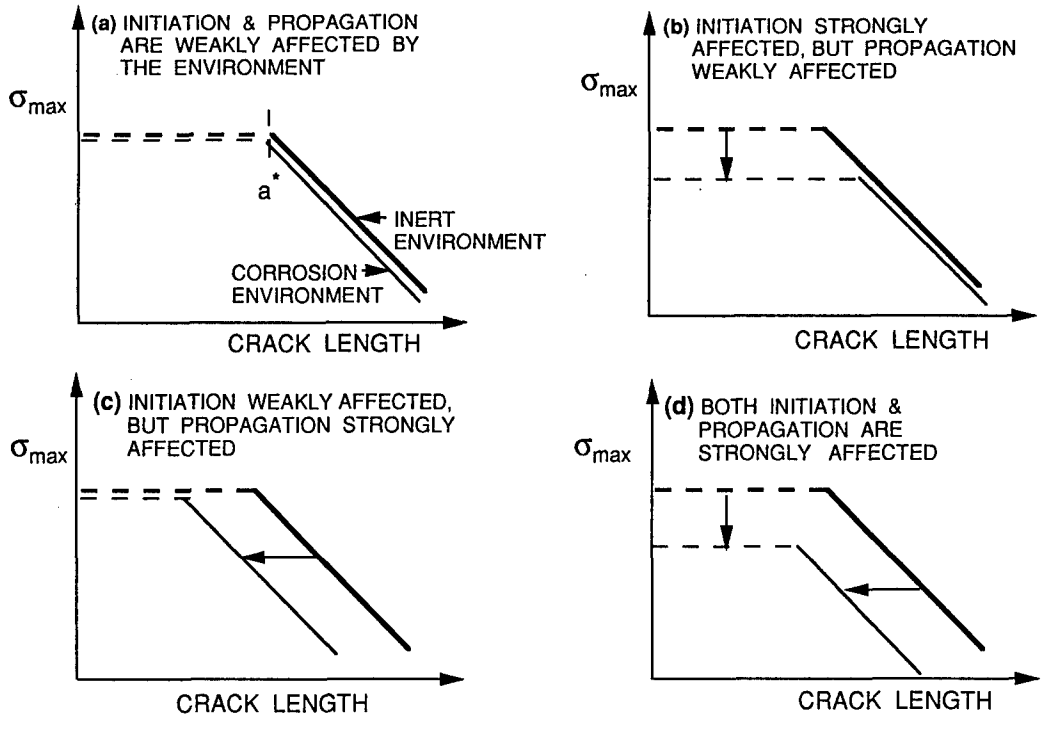

Figure 9. Four classification of corrosion-fatigue in the form of Kitagawa-Takahashi diagram at near threshold conditions, at R ~ 0.

POSSIBLE EFFECTS OF MICROSTRUCTURE & ENVIRONMENT ON THE CRACK NUCLAEATION AND GROWTH STAGES OF FATIGUE DAMAGE

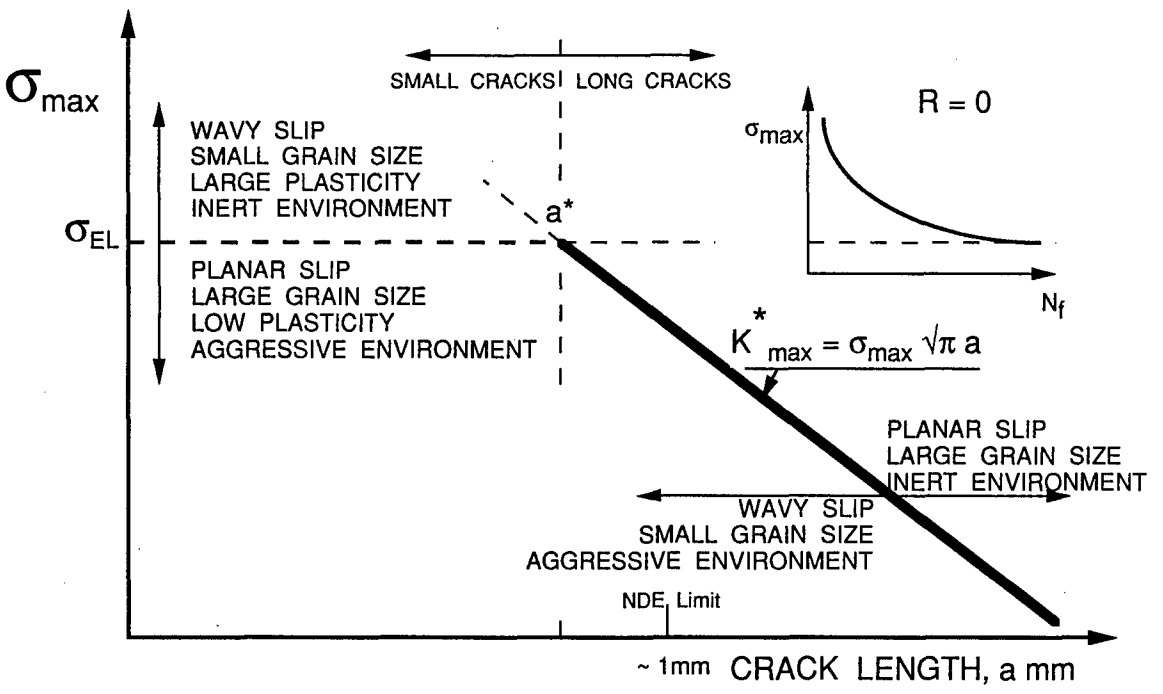

Figure 10. Schematic illustration of the possible effects of microstructure and plasticity on the overall corrosion fatigue explaining the trends in Fig. 9.

Role of Surface Pitting Corrosion on Effectiveness of Hole Cold Expansion

R. Cook *
N. Glinos +
P. Wagstaff +

* Structural Materials Centre, DERA, Farnborough, Hants, GU14 OLX, UK
+ University of Kingston, Roehampton Vale, London, SW15 3DW, UK

SUMMARY

Fatigue tests have been carried out on open hole specimens which have been cold expanded prior to or subsequent to exposure to corrosive environments. The results show that the effectiveness of hole cold expansion in enhancing fatigue endurance can be significantly reduced when cold expansion is carried out after exposure to corrosive environments. The reduction in effectiveness is associated with a change in failure location. In specimens cold expanded after exposure to corrosion, failures initiate from pits remote from the hole in an area of tensile residual stresses. Analytical models have been developed to predict the rate of crack growth from these corrosion pits which correlate well with experimental data. Models have also been developed to predict the rate of growth of cracks from cold expanded holes which show reasonable correlation with experimental data. The findings have important implications to the aircraft industry where corrosion problems can be serious and where hole cold expansion is frequently employed in repair schemes.

NOTATION

AT-CX: Atmospheric corrosion prior to cold expansion
AT-PL: Atmospheric corrosion with no cold expansion (plain hole)
COR-CX: High corrosion severity prior to cold expansion
COR-PL: High corrosion severity with no cold expansion (plain hole)
CX: Cold expansion with no corrosion exposure
CX-COR: Cold expansion prior to high severity corrosion
CX-LCOR: Cold expansion prior to low severity corrosion
LCOR-CX: Low corrosion severity prior to cold expansion
LCOR-PL: Low corrosion severity with no cold expansion (plain hole)
PL: No cold expansion (plain hole) with no corrosion

1. INTRODUCTION

The cold expansion of fastener holes in aircraft structures is frequently employed both at build and in subsequent repair schemes to enhance fatigue endurance. In the UK, civil aircraft designers utilise cold expansion at build and in repair but in military aircraft cold expansion is usually limited to fatigue life enhancement/repair schemes. The benefits of cold expansion are to increase the fatigue endurance of a component which results primarily from a reduction in fatigue crack growth rates in the early stages of life [1]. This reduction in growth rate arises because cracks have to grow through compressive residual stress fields created by the hole cold expansion process. The residual stresses are compressive in an annulus of material around the hole which extends for a few millimetres from the hole. This compressive residual stress region is balanced by a region of tensile residual stresses which extend for tens of millimetres away from the hole. Although the tensile residual stress region extends over a much greater area than the compressive region, the magnitude of the residual stresses are much smaller than the compressive stresses [2]. However, there remains the possibility that any defect present in this tensile residual stress region could result in crack initiation and growth under subsequent fatigue loading. In other words the cold expansion process may in itself cause a crack to grow, when subjected to fatigue loading, if a defect was located in the tensile residual stress region. There are many possible sources of such damage, particularly in joints where fretting of the faying surfaces for example could initiate a crack especially in dry assembled joints. Other possible causes are manufacturing defects or damage caused during assembly, but of particular concern is the damage created by corrosion. This concern arises because if corrosion were present, it could create large pits over a wide area and hence there would be a high probability that a damage source would be present in the region of peak tensile residual stress. This potentially damaging situation was the subject of an investigation carried out at Kingston University under contract from the Defence Evaluation and Research Agency (DERA)[3-5].

Two scenarios were examined in the investigation, representing cold expansion at build (cold expansion followed by exposure to corrosion) and cold expansion as part of a repair process (exposure to corrosion followed by cold expansion). The primary reason for examining both scenarios is that in addition to corrosion offering potential sites for premature failure, the residual stresses formed by cold expansion could provide sites for stress-corrosion cracking. The interactions could therefore become quite complex. The main aims of the investigation are to determine the effects of these interactions on the crack nucleation period and position, on the growth rates of fatigue cracks and hence on the fatigue endurance of components containing plain and cold expanded holes. These have been investigated in an experimental programme described in 2 below. An analytical study has also been made to determine the stress distribution in the components tested and hence the most likely sites for crack nucleation. Attempts have also been made to predict the rates of growth of these cracks and comparisons made with experimental observations. This work is described in 3 below. A metallographic study was undertaken to determine the extent of corrosion damage formed and to examine typical

Paper presented at the RTO AVT Workshop on "Fatigue in the Presence of Corrosion", held in Corfu, Greece, 7-8 October 1998, and published in RTO MP-18.

corrosion pits to determine their shape and size. This work is described in 4.

2. EXPERIMENTAL PROGRAMME

Test pieces were manufactured from a batch of 7050-T76 aluminium alloy supplied by USAF at Wright Patterson Air Force Base. The material has been used in previous AGARD investigations [6-8] during which the mechanical and chemical properties were determined and are presented in tables 1 and 2 below. A number of plates were supplied, some of which were protected by plastic coating and some were unprotected. Due to a delivery problem, the material was stored temporarily on an airfield site where the unprotected sheets became severely corroded. This material is described as being subjected to atmospheric corrosion (AT-CX). The protected plates of material did not suffer significant corrosion and tests conducted on specimens manufactured directly from these plates are referred to as non-corroded (CX and PL). In addition, some specimens manufactured from the protected material were subjected to artificial corrosive environments of 3.5%NaCl (COR- high corrosion severity) and 0.35%NaCl (LCOR-low corrosion severity). After exposure, the specimens were washed in distilled water, dried and stored in a dessicator.

	Cu	Mg	Si	Fe	Mn	Zn	Ti	Zr	Cr
%Min	2.0	1.9	-	-	-	5.7	-	0.08	-
%Max	2.6	2.6	0.12	0.15	0.1	6.7	0.06	0.15	0.04

Table 1. Chemical composition of 7050-T76

	Min	Max
0.2% Proof stress	521	552
Ultimate tensile strength	573	592
Elongation % (Gauge length 50 mm)	12	12.5

Table 2. Mechanical properties of 7050-T76

Test pieces were manufactured to the dimensions shown in figure 1. Plain holes were manufactured by drilling and reaming to a diameter of 6.35mm. Cold expanded holes were prepared firstly by drilling and reaming to the required start dimensions. Specimens to be subjected to artificial corrosion prior to cold expansion were then put in salt solution for the required period and then cold expanded and finally reamed to a diameter of 6.3 mm. Hole preparation and cold expansion was carried out using FTI standard tooling and recommended procedures to specification 8-0-N [9].

Fatigue testing was carried out using a servo-hydraulic test machine with computer control. Tests were performed at a frequency of 10 Hz. with a stress ratio of R=0. 1 and a gross section peak stress of 175 MPa. Tests were stopped periodically and a load equal to 80% of the maximum applied whilst acetate replicas were made of the specimen surface. Crack lengths were measured from the replicas after completion of the test using a shadowgraph projector.

Baseline tests were performed on plain (PL) and cold expanded (CX) hole specimens manufactured from non-corroded material; to determine the effectiveness of cold expansion in extending the crack nucleation and crack growth phases. A similar series of tests were performed on specimens manufactured from the material which had been inadvertently exposed to atmospheric corrosion with plain (AT-PL) and cold expanded holes (AT-CX). In order to expose specimens to a controlled corrosive environment, specimens were immersed in a solution of 3.5%NaCl solution for periods of between 1 and 720 hours. Specimens were exposed to this environment prior to cold expansion (COR-CX) or after cold expansion (CX-COR).

The test results showed this to be a particularly aggressive environment which produced severe pitting corrosion after even the shortest exposure times, and a significant reduction in fatigue endurance. As a consequence a further set of tests were performed using a less severe environment of 0.35% NaCl solution. Tests were performed only on specimens which were cold expanded after exposure (LCOR-CX).

3. ANALYTICAL PROGRAMME

Initial tests on specimens subjected to corrosive environments showed that cracks frequently initiated from corrosion pits remote from the cold expanded hole [3]. This was not observed in tests with plain holes, and it was concluded that these occurrences must result, therefore, from the residual stresses created by the hole cold expansion process. The first part of the analytical programme was addressed at defining the residual and alternating stresses in the component to determine the most probable location of cracking which would cause component failure.

The residual stresses had been measured in previous DERA investigations [1,2,10] using experimental and analytical techniques. It was shown that the residual stress distribution was complex and stresses varied around the hole, away from the hole and through the thickness of the material. The experimental techniques included X-ray diffraction [2] and Sachs boring methods [1], whilst a 2-D Boundary Element method [10]was the analytical technique employed. Each method has advantages and disadvantages, and there are areas where each is expected to perform more accurately. For example X-ray diffraction gives accurate surface measurements at most locations, but measurements are not possible close to the hole. This is because the irradiated volume must not include any part of the hole, hence measurement close to the hole is limited by the surface area irradiated by the X-rays. Similarly the Sachs method measures an average stress across the specimen thickness and data cannot be used to describe the surface stresses. A combined residual stress distribution was defined which utilises data from each method where it is expected to be the most appropriate. The distributions for the surfaces at the mandrel inlet and outlet locations are shown in figure 2. In order to determine the applied stresses, a Finite Element model was made of one quarter of the test specimen and the stresses resulting from the applied loads calculated. The applied and residual stresses were simply added at each node and the resultant stresses acting to open the crack were calculated.

It has been observed in previous investigations at DERA [1,2], that cold expansion has little effect on the crack nucleation period, but a significant effect on the crack propagation period. It was decided therefore that analytical examination should concentrate on fatigue crack growth and that a fracture mechanics approach should be used. The approach used was to consider a corrosion pit located at the 'hot spots' defined from the above analysis. The corrosion pit dimensions were selected

from preliminary metallographic studies and a semi-hemispherical defect was assumed. The stresses calculated above were utilised and the stress ratio at each point of interest also calculated. It was observed from this analysis that stresses in most regions of concern were fairly constant in the immediate vicinity of the pit and, therefore, uniform stress distributions could be assumed.

The only 'hot-spot' location where stresses were not uniform was at the edge of the hole and consequently a uniform stress approach was not valid. A Green's function method was applied at this location following a method developed at DERA [12] which utilises a solution developed by Shivakumar and Forman [13] for a through crack at a hole in an infinite sheet subjected to an arbitrary stress field. The method was modified to allow corrections to be made for the expected crack shape and the finite specimen width. Crack growth rates were estimated using the stress intensity factor distributions calculated for pits remote from the hole and for cracks at the hole. These were calculated using material crack growth rate data measured at a range of stress ratios.

4. METALLOGRAPHIC STUDIES

These studies were undertaken to determine the size and distribution of corrosion pits formed in each of the test series, for different times of exposure to the various corrosive environments. It is also required to determine from the fracture surfaces, the dimensions of pits formed, particularly those from which crack growth occurred, and how cracks grew and coalesced. The programme essentially comprised three different phases, as described below.

In the first phase of the work the microstructure of the material was examined in a scanning electron microscope (SEM) to determine the typical grain dimensions, and the extent to which these were deformed by the cold expansion process. This was performed on material which had not been exposed to any corrosive environment, and had not been subjected to fatigue loading.

In the second phase of the investigation, examinations were made in a SEM of specimen surfaces which had been exposed to low and high corrosion severities for a range of times to determine the size and density of corrosion pits which had formed. This involved sectioning of corroded specimens (across the minimum section) to determine the shape and size of the corrosion pits which had formed on the surface and in the depth of the material. This included specimens which had been cold expanded prior to or subsequent to exposure to the corrosive environment. In this part of the investigation the location of corrosion pits was examined in detail to determine whether corrosion pits in the plastically deformed region were similar to those located elsewhere.

The final part of the metallographic study involved an examination of the fracture surfaces to study the formation and growth of fatigue cracks which led to specimen failure

5. RESULTS

5.1 Experimental Programme

5.1.1 Crack nucleation sites

Crack nucleation in all plain hole specimens originated from the edge of the hole. This was independent of the corrosive environment or period of exposure (LCOR-PL, COR-PL and PL). Specimens which were cold expanded (CX) and had no exposure to atmospheric or artificial corrosive environments also failed from cracks initiating at the edge of the hole.

Specimens which had been subjected to atmospheric corrosion and subsequently cold expanded (AT-CX) all failed from cracks nucleating at corrosion pits remote from the hole. In the majority of cases (82%), the crack nucleation site from which the main crack developed was on the mandrel outlet face of the specimen. Similarly in the majority of cases (80%), the crack nucleation site from which the main crack developed was in the tensile residual stress region. Extensive cracking was observed in all tests from corrosion pits predominantly located (92%) in the tensile residual stress region. The location of all cracks from pits was approximately equally distributed on the mandrel inlet and outlet faces. In all cases, cracks also initiated at the hole but crack growth rates soon slowed and only small cracks were present at the time of failure. A typical failure pattern for AT-CX specimens was therefore extensive crack formation at corrosion pits in the tensile residual stress region and at the hole on both sides of the specimen with the main crack forming in the tensile residual stress region on the mandrel outlet face.

Specimens which were cold expanded after exposure to high severity corrosion (COR-CX) exhibited a similar failure pattern to the AT-CX specimens. The notable difference, however, was that the cracks which caused failure still nucleated at corrosion pits in the tensile residual stress region but were located with equal probability on the mandrel inlet and outlet faces.

Failure patterns in specimens which were cold expanded after exposure to low severity corrosion (LCOR-CX) exhibited different failure patterns which were dependent on the period of exposure. For low exposure times (less than 5 hours), all cracks which caused failure nucleated from the edge of the hole. As exposure times increased, the probability of failure from a location remote from the hole increased. For exposure times of less than 5 hours the probability of failure from a remote location was zero, between 8 and 48 hours exposure the probability increased to 33% and for exposure times greater than 120 hours, the probability was 64%. Secondary cracking at pit locations in the tensile residual stress region was again observed with equal probability on the mandrel inlet and outlet faces.

In tests where the cold expansion was carried out prior to exposure to corrosive environment (CX-COR) the majority of crack locations which caused failure (70%) were at the hole edge. This is in direct contrast to tests which were exposed to high severity corrosion prior to cold expansion (COR-CX) in which all tests failed from cracks at locations remote from the hole.

A summary of crack locations which caused failure is given in table 3 below.

	Hole	Pit Inlet	Pit Outlet
	%	%	%
PL	100		
AT-PL	100		
COR-PL	100		
CX	100		
AT-CX	0	18	82
COR-CX	0	50	50
LCOR-CX	67	24	9
CX-COR	70	?	?

Table 3 Location of cracks causing failure

5.1.2 Crack nucleation and growth

The average number of cycles to nucleate a crack (0.1 mm surface length) and to propagate to failure are presented in Table 4 below.

Test type	Nucleation period	Growth period	Total
PL	13,666	8,760	22,426
COR-PL	15,874	5,411	21,285
LCOR-PL	13,490	6,313	19,803
AT-CX(R)	41,156	76,435	117,591
COR-CX(R)	52,597	62,862	115,469
LCOR-CX(R)	96,375	62,250	168,736
CX-COR(R)	90,735	64,856	155,591
CX (H)	54,936	120,074	175,010
LCOR-CX(H)	59,921	117,851	177,772
CX-COR(H)	56,104	108,023	164,127

Note:
(R) denotes that crack causing failure initiated remote from the hole
(H) denotes that crack causing failure initiated from the hole

Table 4 Crack nucleation and growth periods

It can be seen from table 4 that the nucleation and growth periods for all plain hole specimens (COR-PL, LCOR-PL and PL) were similar and it appeared that there was no effect of corrosion on the fatigue performance of plain hole specimens. In general, the fatigue endurance will depend on the severity of corrosion, (i.e. on the probability of a corrosion pit being present at a critical location at the edge of the fastener hole), and the magnitude of the applied stress. At relatively low stresses the presence of corrosion pits usually reduce the crack nucleation period.

In all tests where cold expansion was used, regardless of failure location, cracks formed at the hole and all had similar nucleation periods. This is to be expected as crack formation at the hole will not be affected by corrosion but will be dominated by the local stress conditions. This observation is supported by the results of the plain hole tests where exposure to corrosive environments had no effect on the nucleation or growth periods.

The effectiveness of cold expansion as a repair technique, i.e. after exposure to corrosive environments, can also be studied from an examination of table 4. The effects on fatigue behaviour of the various corrosive environments, can be examined by comparing nucleation and growth periods of tests in which specimens were exposed to atmospheric corrosion (AT-CX), controlled corrosion of low severity (LCOR-CX) and controlled corrosion of high severity (COR-CX) prior to expansion. It was observed in the previous section that all specimens exposed to atmospheric and high severity corrosion failed from initiation sites remote from the hole, as did some specimens exposed to low severity corrosion for extended periods. Comparing the fatigue behaviour of these specimens, it can be seen that the nucleation periods are longest for LCOR-CX (96,375) and shortest for AT-CX (41,156), confirming that for cold expanded holes, the severity of prior corrosion affects the nucleation period in tests where failure occurs from origins remote from the hole. The results suggest that the greatest corrosion damage was formed by atmospheric corrosion (nucleation period of 41,156), similar or slightly less damage by the severe corrosion environment (nucleation period of 52,597) and the least damage was created by the low corrosion severity (nucleation period of 96,375). This is in line with what is expected based on the exposure times and the severity of corrosive environment.

The crack growth periods were similar for the two artificial corrosion types, COR-CX and LCOR-CX (62,862 and 62,250 cycles respectively) but slightly longer for the atmospheric corrosion tests (76,435). It was expected that the growth periods would be similar as they are controlled primarily by the residual and applied stress fields which are similar in all test types. The slightly longer growth period in the atmospheric corrosion tests could result from shielding of the main crack by the large number of secondary cracks associated with more widespread corrosion. It can be concluded that corrosion prior to cold expansion has a significant influence on the location of the crack causing fatigue failure and that the nucleation periods of cracks forming at pits remote from the hole are affected by the severity of the different corrosive environments and exposure times, but the crack growth period is little affected.

Test specimens which were exposed to low corrosion severity for short periods failed from cracks initiating at the edge of the hole. Fatigue endurances of these specimens (177,772) were considerably greater than those of specimens exposed to corrosive environments prior to cold expansion (described above) which failed from remote locations (117,591, 115,469 and 168,736 for atmospheric, high and low corrosion severities respectively). Specimens which failed from cracks nucleating at the hole were exposed to low severity corrosion for short periods (less than 8 hours). It is possible that corrosion pits of sufficient size had not developed making the hole the most critical region. This is supported by the metallographic work which showed that pits were shallow and had a rounded shape following these short exposure times.

The crack growth periods in tests with short exposure times to low severity corrosion (LCOR-CX), in which cracks which cause failure nucleated at the hole (117,851), are much greater than those for tests in which failures initiate from corrosion pits (62,250 to 76,435). This is because of the different stress fields through which the cracks had to grow. The stress field in the region adjacent to a cold expanded hole has high compressive residual stresses, which extend for several millimetres, but

alternating stresses due to the stress concentration. This resulted in a smaller crack driving force compared with that around a corrosion pit which has moderate tensile residual stresses and low alternating stresses. The effective stresses at the two locations were derived in previous work [3]. It can be concluded that the total fatigue endurances of specimens which fail from pit origins are shorter than those of specimens which fail from cracks initiating at the hole.

In the majority of CX-COR tests, in which cold expansion was carried out prior to high corrosion severity exposure, the majority of failures were from cracks which nucleated at the hole. From previous discussions of plain hole data, it is expected that the nucleation and growth periods of cracks from cold expanded holes will not be affected by the corrosive environment or exposure times. An examination of table 4 shows this to be the case; the nucleation and growth periods for CX-COR being similar to those of CX and LCOR-CX tests which also failed from cracks originating at the hole.

Similarly, from the foregoing discussions, it is expected that the nucleation periods in CX-COR specimens which failed from pit origins remote from the hole will be dependent on the corrosion severity and should, therefore, be similar to those observed in the COR-CX tests. This was not the case, as can be seen from table 4, where the nucleation periods were 90,735 and 52,597 for the CX-COR and COR-CX tests respectively. This suggests that the effect of corrosion severity is not the same when applied before and after cold expansion.

The growth periods for CX-COR tests in which failure occurred from cracks initiating remote from the hole were similar to those for the other test series in which remote failures occurred, as expected from the above discussions. This can be seen from table 4, where the growth period for the CX-COR tests was 64,856 compared with 62,250 to 76,435 for the other test series.

The main questions deriving from the CX-COR tests are why do the majority of failures occur from the hole when in COR-CX tests all failures occur remote from the hole, and why is the effect of similar exposure to corrosive environment not the same for tests in which cold expansion was performed prior to corrosion compared with those in which cold expansion was performed subsequent to corrosion. These issues will be addressed in the discussion.

5.2 METALLOGRAPHIC OBSERVATIONS

5.2.1 Microstructure

The microstructure consists of long pancake shaped grains, however, near to the mid-thickness of the material, an unrecrystallised structure was observed with much smaller grains present (see figure 3). The recrystallised grain structure near to the specimen surfaces is typical of those found in aluminium alloys where large deformations occur as a result of rolling. By comparison, the deformation caused by hole cold expansion is small and no significant differences in microstructure were detected by micro-texture analyses in regions close to the hole and remote from it.

5.2.2 Corrosion pits

Examination of corroded specimens showed a wide variety of corrosion pit shapes and sizes within each specimen but an attempt was made to categorise typical pit dimensions and locations in artificially corroded specimens; this study is presented below.

Exposure to low corrosion severity (0.35% NaCl solution) prior to cold expansion resulted in the formation of corrosion pits even after the shortest exposure time of one hour. Pits were found on all specimen surfaces, which included the hole surface and the specimen sides and edges. Typical pits after exposure for 1 hour had surface areas of between $1.6.10^{-5}$ and 9.10^{-4} mm^2, depths of between 3 and 7μm and a density of about 2.10^5 pits per m^2. After 24 hours exposure, typical pit sizes had increased in size to between 1.10^{-4} and 9.10^{-3} mm^2 with depths of up to 9μm and about the same density. After 20 days the density had reached about 10^6 pits/m^2 and some pit depths had reached 72μm.

A similar analysis was performed for specimens subjected to high severity corrosion (3.5% NaCl) prior to cold expansion. The pit areas, depths and densities were generally greater than for the low severity corrosion at comparable exposure periods. After one hour, typical pit areas were between 1.10^{-4} and 2.10^{-3} mm^2, with depths of 3 to 8 μm and a density of about 5.10^5 pits/m^2. The pit sizes and densities increased with exposure time and after 15 days, two pit groups could be identified; small pits with an area typically of about 10^{-4} mm^2 and a depth of 7-25 μm and large pits with an area of 3.10^{-3} to 4.10^{-3} with a depth of up to 22μm.

Recent analyses have commenced examining pits in specimens which were cold expanded prior to exposure to high severity corrosion (CX-COR). The distribution of pits remote from the hole needs to be analysed in the same way as described above, but initial indications are that pits are much smaller than in COR-CX tests after the same exposure times. It can be seen for example in figure 5 that at a location of about 3mm from the hole edge, a typical pit in the CX-COR programme is much smaller (surface length about 10μm) than a typical pit in the COR-CX programme (surface length about 50μm) despite the fact that the exposure time was greater in the CX-COR test (4 days compared to 1 day). It was also observed that no pits had formed in the vicinity of the hole (within about 2mm from the hole edge) and that the majority of significant pits were found in the tensile residual stress region (between 2 and 8 mm from the hole edge). Further work is in progress to establish whether this is a consistent effect.

5.2.3 Crack initiation sites

The final phase of the metallographic analysis was an examination of crack nucleation sites remote from the hole. Nucleation sites of cracks which caused failure were examined and their locations recorded as described in 5.1.1. The corrosion pits associated with these nucleation sites were also examined and their details recorded. A typical example of a corrosion pit from which a crack nucleated and caused specimen failure is presented in figure 6. In this case, the specimen was corroded at low corrosion severity for 7 days. The pits shown were located 8.6 mm from the edge of the hole and 1.2 mm from the

specimen centre-line where the applied hoop and radial stresses were respectively 180 and 0 MPa. The left hand corrosion pit was 150 μm in diameter and 70 μm deep while the right hand corrosion pit was 75 μm in diameter and 50 μm deep.

Observations were also made, using acetate replicas, of specimen surfaces after exposure to the corrosive environment followed by cold expansion, but prior to fatigue loading. There was no evidence of cracking from the corrosion pits. Cracking was only observed after a period of fatigue cycling.

5.3 Analytical programme

The nucleation positions of cracks causing failure in all tests were measured and have been grouped based on the local stress amplitude and stress ratio prevailing at the nucleation site. Nine groups were identified with stress ratios ranging from -0.9 to 0.3. Two typical examples of predicted crack growth rates are presented in figures 7 and 8 for two such groups. Figure 7 shows the predicted and measured growth rates from a corrosion pit located in the compressive residual stress region where the local stress ratio was calculated to be R=-0.45. This was the most compressive stress ratio at which critical cracking was found and only one test result was found in this group. The data presented in figure 8 are for crack nucleation sites located in the tensile residual stress region where the local stress ratio was calculated to be R=0.25. The experimental measurements are from seven tests and this represents the highest stress ratio at which critical cracking was found. Similar predictions were made for seven other groups of pit locations and the general conclusion was that reasonable correlation was found between experimental and predicted growth rates in the elastic region, but that agreement was poor in the plastic region. In the plastic zone, the experimental crack growth rates were always faster than predicted.

Measured crack growth rates are presented in figure 9 for all of the tests in which failure occurred remote from the hole. Also shown in this figure are crack growth data for 7050-T76 material tested at a stress ratio of R=0. 1 (the test stress ratio). It can be seen that there is very little scatter in the test data measured in the current test programme. This is surprising since the location of the pits from which crack growth occurred covered a wide area where the stress ratios varied from -0.45 to 0.25. However, it can be seen that the predictions indicate that a single stress ratio slightly greater than R=0.1 would result in good correlation with the experimental data at stress intensity factors greater than about 3MPa.$m^{0.5}$. At stress intensity factors below this value, the experimental growth rates are much faster than predicted and do not appear to have an obvious threshold. There are a number of possible reasons for this as described below.

The first is that cracks are very short in this low stress intensity region and short cracks have been shown to grow much faster than long cracks at the same calculated stress intensity factor, and also to grow at stress intensity factors smaller than the long crack threshold [14]. The second possible reason is that the stress intensity factor distribution does not adequately describe the region around a corrosion pit. This is quite likely since the solution used is for a hemispherical defect whereas corrosion pits are very complex in shape and will have larger stress concentrations than a hemispherical defect. The third possible reason is that there are residual stresses associated with the corrosion pit resulting from the cold expansion process. The final reason is that cracks could initiate subsurface in the region where intergranular cracking was observed and that cracks could be growing quite rapidly when they break the specimen surface and are measured by the surface replication technique.

6. DISCUSSION

Cold expansion of fastener holes is a process widely used in the aircraft industry to enhance fatigue performance. Life enhancement occurs as a result of the compressive residual stresses formed during the cold expansion process which increases the crack nucleation period, but more importantly retards the rate of growth of cracks. The compressive residual stress region, in an annulus of material surrounding the hole, is constrained by a larger annulus of material surrounding it in which the residual stresses are tensile. The compressive residual stress region is deep acting (several millimetres from the hole) and contains residual stresses close to the compressive yield stress of the material. The tensile residual stress region is expansive (tens of millimetres) but contains only moderate stresses (less than 100MPa) which maintains stress equilibrium. It is of concern that cracks could nucleate and grow in these tensile residual stress regions and negate or reduce the benefits of the cold expansion process. This would require stress concentrating features in the tensile residual stress region to initiate such cracks. These could result from various sources but in this investigation stress concentrations occurring at corrosion pits were studied as corrosion is extremely common in aircraft structures.

Cold expansion of open hole specimens manufactured from 7050-T76 material was found in previous investigations [1,2] to enhance the fatigue endurance and the degree of life enhancement was found to be dependent on the applied stress range. A stress ratio of R=0. 1 with a peak nett section stress of 175MPa was selected for this investigation as it resulted in fatigue endurances close to the fatigue limit of cold expanded specimens which might be typical of stresses used in aircraft wing structures.

Two specific areas of relevance to aircraft structures were simulated in this programme; the use of cold expansion during manufacture and the use of cold expansion as a repair process. Two test series were defined to examine the effect of corrosion prior to cold expansion (cold expansion as a repair) and after cold expansion (cold expansion at build). The effectiveness of cold expansion in the absence of corrosion was also examined for comparison, and consisted of tests with plain or cold expanded hole samples manufactured from uncorroded material.

Tests performed on plain non-expanded hole specimens showed that corrosion did not affect the location of failure, as all tests irrespective of corrosion severity or exposure times failed from cracking at the hole; the fatigue nucleation periods and fatigue endurances were also similar in all tests.

The first test series on cold expanded holes involved material which had been subjected to atmospheric corrosion for a period of about two years (AT-CX). The main conclusion from this series of tests was that fatigue endurances were shorter (by about 33%) than cold expanded specimens manufactured from non-corroded material. The reason for this reduction in fatigue endurance was attributed to crack nucleation from pits in the

tensile residual stress region which caused premature failure of the specimens from cracking remote from the hole. A stress analysis of the component was carried out which showed that although the effective stresses were largest close to the hole, the effective stresses decreased rapidly with distance away from the hole. Effective stresses of slightly smaller magnitude than those at the hole were present in the tensile residual stress region, and remained fairly constant over a large area. It follows that cracks nucleating in the tensile residual stress region will grow faster than cracks emanating from the hole. It was concluded that corrosion pits were the nucleation sites for cracking and that the tensile residual stresses resulted in premature failure of the specimens due to an effective stress distribution greater than that at the hole.

The second investigation examined controlled corrosion prior to cold expansion (COR-CX) to determine the degree of corrosion required to nucleate cracks in the tensile residual stress region. Specimens were exposed to 3.5% NaCl solution (a corrosive environment widely used in the aerospace industry to accelerate corrosion in laboratory investigations) for various lengths of time. Even with relatively short exposure times (5 minutes), premature failures occurred from cracks nucleating at corrosion pits remote from the hole. The nucleation and growth periods were similar to those observed in tests with atmospheric corrosion, indicating that the stress concentrations at the pits were also similar. Cracks also formed at the holes in both test series but they decreased in growth rate as they grew into the increasingly compressive residual stress field.

The corrosion severity was clearly too great in the above test series to examine the transition in failure location from the hole to a remote site. Accordingly a third test series was performed in which the corrosion severity was reduced by using a 0.35% NaCl solution (LCOR-CX). This resulted in failures from the hole at low exposure times (less than 5 hours), the majority of failures from the hole (66%) at intermediate exposure times (8 to 48 hours), and the majority of failures from remote locations (64%) at longer exposure times (greater than 120 hours).

Good correlation was found between corrosion pit surface area, depth and density with increasing exposure time despite the variability in pit dimensions measured on each specimen. From these measurements it is possible to correlate failure crack location as a function of pit size. Cracks initiated from the hole when typical pit surface areas were in the region of 10^{-5} to 10^{-4} mm^2 and depths of less than 10 μm. Cracks initiated from pits remote from the hole when typical pit surface areas were in the range 10^{-4} to 10^{-3} mm^2 with depths greater than about 15 μm. The pit areas required to cause remote failure agree well with those observed in the high severity corrosion tests which were all greater than 10^{-4} to 10^{-3} mm^2 and hence all failures for high corrosion severity were from remote locations. Pit size is not the only important parameter. Pit density may also be important as it increases the probability of a pit of sufficient size occurring at a critical location. The critical pit density was estimated as $5.10^5/m^2$.

The deleterious effects of corrosion can be observed from these test results where specimens in which failure occurred from remote cracking had shorter endurances than those in which failure occurred from the hole. An examination was made of crack nucleation periods at the hole in each of the above test series and it was found that nucleation periods were independent of exposure times to atmospheric, low severity or high severity corrosion. This is in line with the results from the plain hole tests described above. A similar examination was made of crack nucleation periods for cracks forming remote from the hole. In this case the nucleation period was dependent on the corrosive environment and was longest for low severity corrosion and greatest for high severity corrosion. Crack growth periods were also examined for remote failure tests and it was found that the growth periods were similar for all corrosion types. This was expected as the stress fields which determine fatigue crack growth rates were similar in all tests.

Having established the effect of corrosion severity on crack nucleation and growth periods at the two possible initiation sites for specimens cold expanded after exposure to corrosion, test results were examined where cold expansion was carried out prior to exposure (CX-COR). Markedly different behaviour was found in CX-COR tests from that observed in COR-CX tests. 82% of specimens failed from cracks emanating from the hole in CX-COR tests but all failed from remote locations in COR-CX tests. Since the corrosive environment, exposure times, and fatigue loading were identical in CX-COR and COR-CX tests, it was concluded that either the cold expansion process affects the corrosion pits which had already formed in the COR-CX tests or that the residual stresses formed by cold expansion affect the formation of corrosion pits in CX-COR tests.

The observed behaviour has implications to the aircraft industry where cold expansion is utilised. It should be borne in mind that despite the deleterious effects of corrosion described in this paper, cold expansion still provides significant life enhancements. The results of this work do not suggest that cold expansion should not be used on potentially corroded structure, rather that the methods used to qualify the repair should account for the possible presence of corrosion and that inspections should include areas remote from the hole in cold expanded structures.

7. CONCLUSIONS

7.1 The corrosive environments and exposure times did not affect the fatigue endurance of tests with plain holes.

7.2 Corrosion prior to cold expansion can cause premature fatigue failures from locations remote from the hole and thereby reduce the effectiveness of cold expansion.

7.3 The reduction in effectiveness of cold expansion is dependent on the severity of corrosion.

7.4 The remote locations causing premature failure were predominantly located in the tensile residual stress region.

7.5 Exposure to corrosive environments after cold expansion had little effect on fatigue endurances.

7.6 Pits forming in regions adjacent to in holes specimens corroded prior to cold expansion were much bigger than pits in specimens corroded after cold expansion.

8. REFERENCES

1. AT Ozdemir, R Cook and L Edwards, *Residual stress distributions around cold expanded holes* in: Estimation enhancement and control of aircraft fatigue performance. Vol 2, Pub EMAS, 1995.

2. R Cook and P Holdway, *Residual stresses induced by hole cold expansion* in: Computer Methods and Experimental Measurements for Surface Treatment Effects. Pub. CMP, Southampton, UK, 1993.

3. N Glinos, PG Wagstaff and R Cook, *The effects of surface corrosion on the fatigue behaviour of aluminium alloy specimens containing cold expanded holes (II)* Proceedings of the 20th ICAS Congress, Sorrento, 1996.

4. N Glinos, PG Wagstaff and R Cook, *The effects of surface corrosion on the fatigue behaviour of aluminium alloy specimens containing cold expanded holes (I)* in: CMT 96. Pub. CMP, Southampton, UK, 1996.

5. N Glinos, PG Wagstaff and R Cook, *The influence of corrosion on the fatigue and fracture behaviour of 7050-T76 aluminium alloy specimens containing cold expanded holes* in: Proceedings of the 21st ICAS Congress, Melbourne, 1998.

6. T Coombe and RB Urzi, *Critically Loaded Hole Technology Pilot Collaborative Test Programme* Final Technical Report, AGARD Report No 678, 1980.

7. HH van der Linden, *Fatigue Rated Fastener Systems - An AGARD Coordinated Testing Programme* AGARD Report No 721, 1985.

8. R Cook, *Standard Fatigue Test Specimens for Fastener Evaluation* AGARDograph No 304, 1987.

9. *FTI Standard Tooling Catalogue.*

10. R Cook *Effect of cold expansion on fatigue crack growth from fastener holes* DRA Customer Report DRA/SMC/CR942021.

11. VMA Leitao *Boundary elements in nonlinear fracture mechanics* Topics in Engineering Vol. 21, Pub. CMP, Southampton, UK, 1994.

12. R Cook, DP Rooke, A Smith and RI Bowles, *Residual stress fields at notches: Effect on fatigue crack growth* RAE Technical Report TR 85049, 1985.

13. V Shivakumar and RG Forman *Green's function for a crack emanating from a circular hole in an infinite sheet* Int. J. Fracture, Vol 16, pp305-316, 1980.

14. PR Edwards and JC Newman Jr., *The behaviour of short cracks under constant amplitude and aircraft spectrum loading* AGARD Report No 767, 1990.

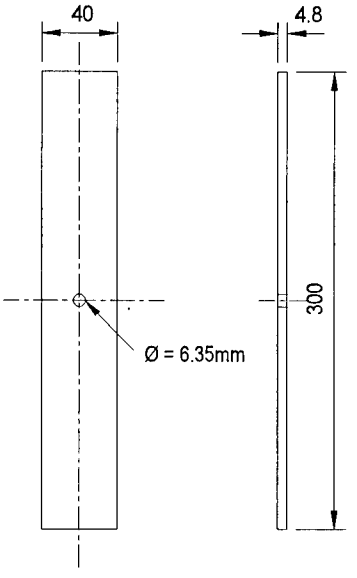

Figure 1 Fatigue test specimen

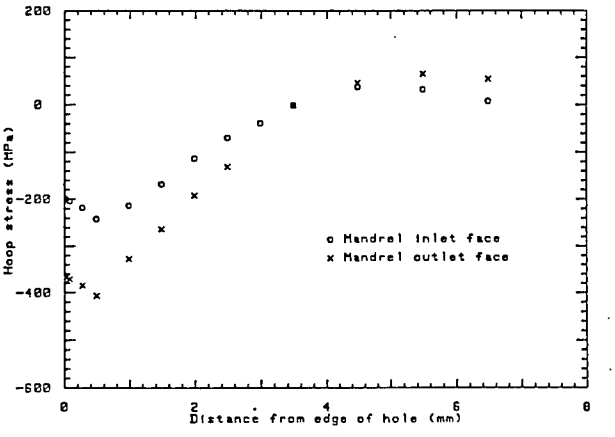

Figure 2 Residual stress distribution

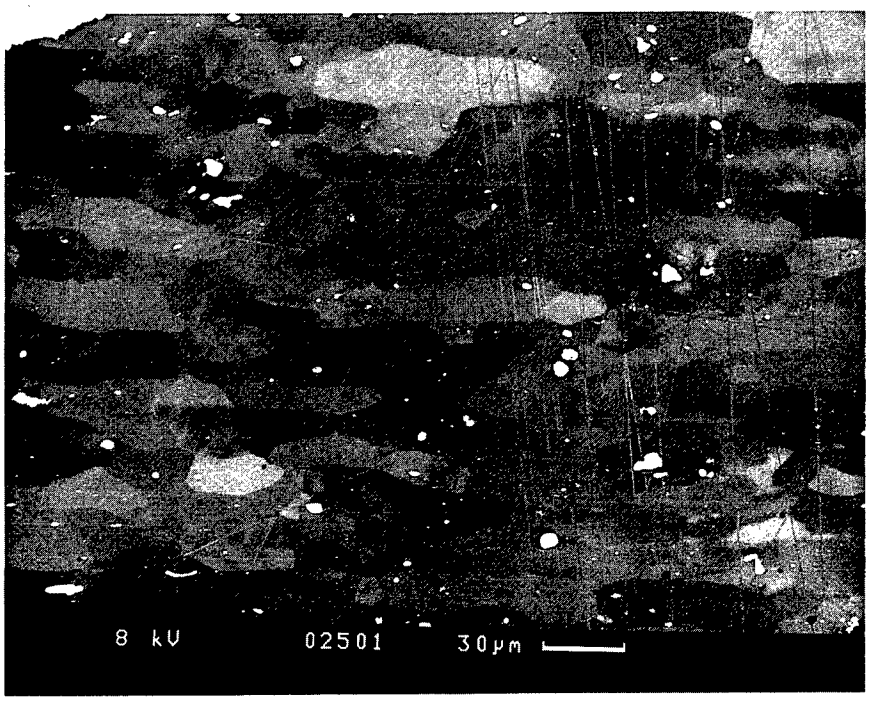

a. Near surface

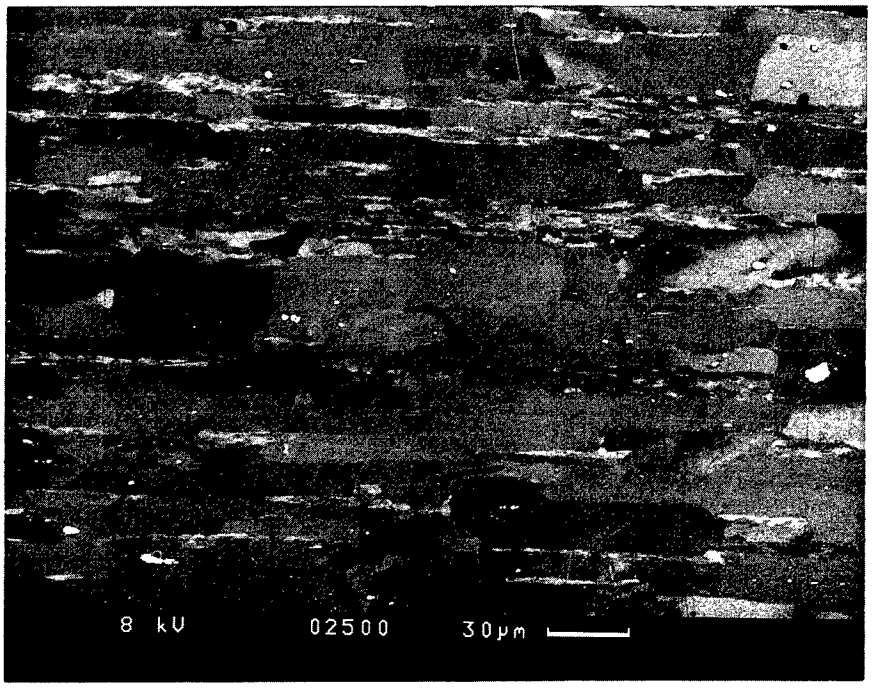

b. Near mid thickness

Figure 3 Microstructure 7050-T76 aluminium alloy

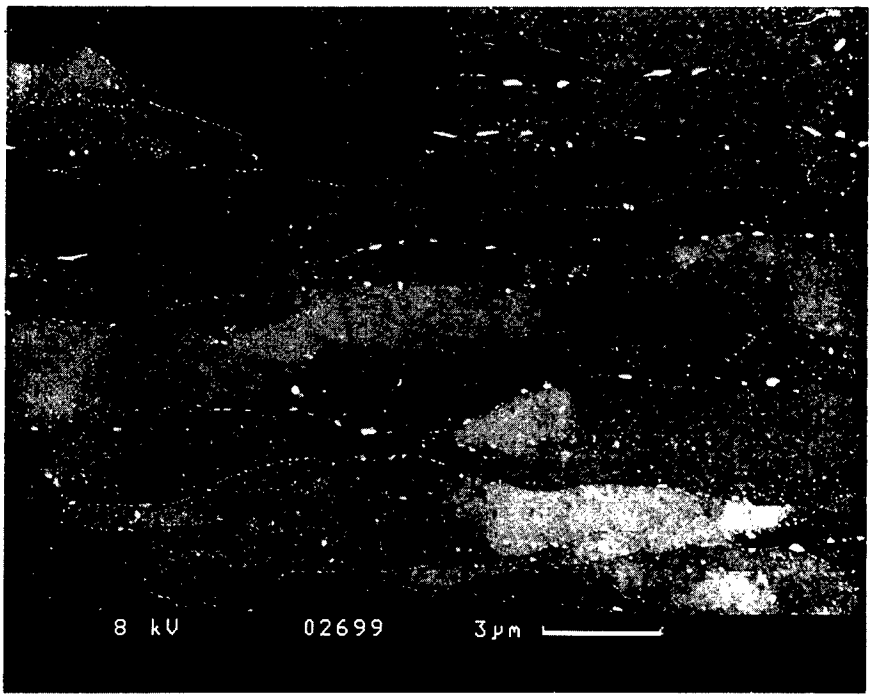

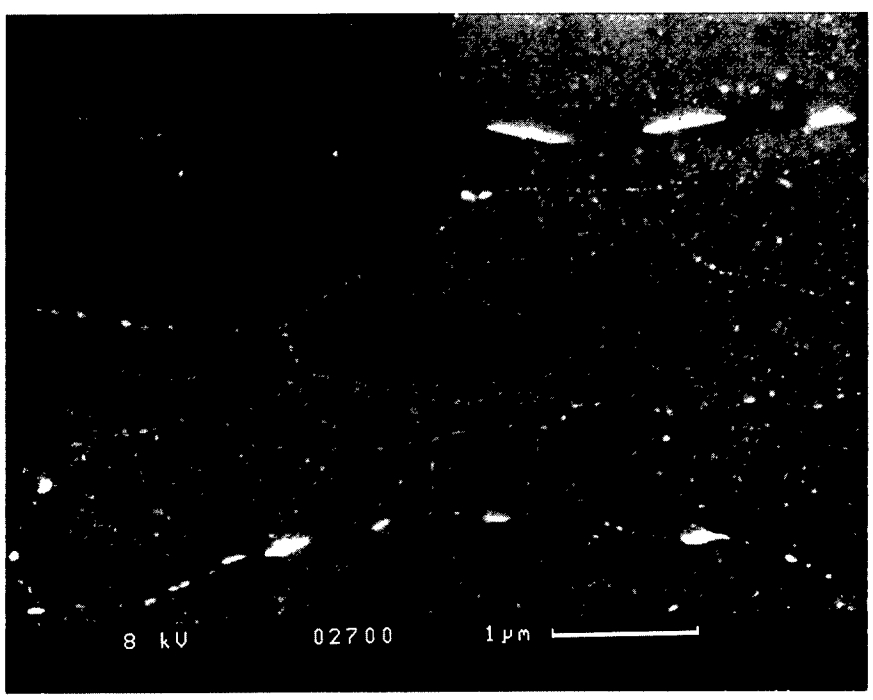

Figure 4 Precipitates at grain and subgrain boundaries

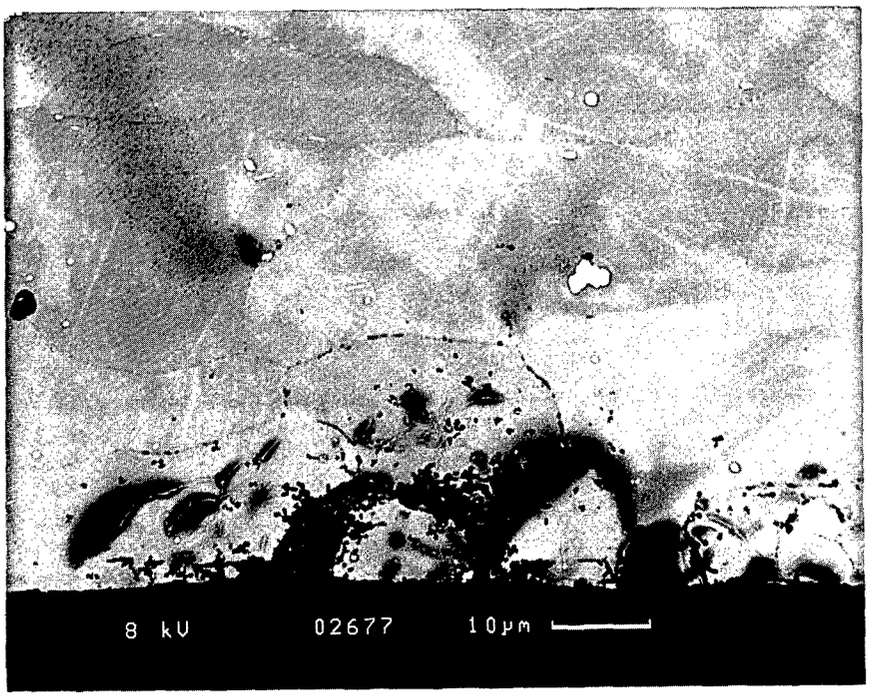

a. COR-CX test

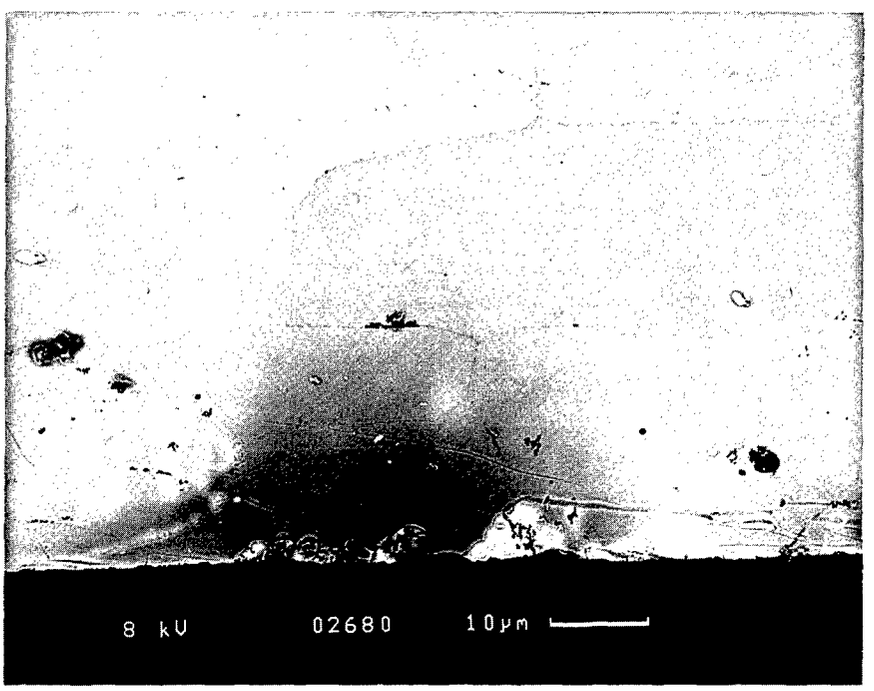

b. CX-COR test

Figure 5 Pits in COR-CX and CX-COR tests at 3mm from the hole edge

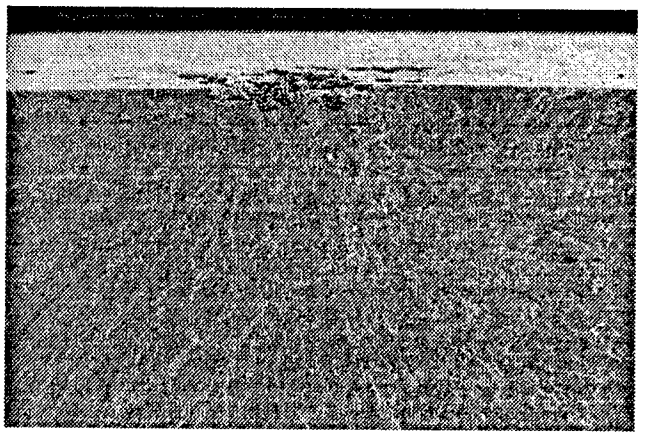

Figure 6 Typical crack initiation site at corrosion pit

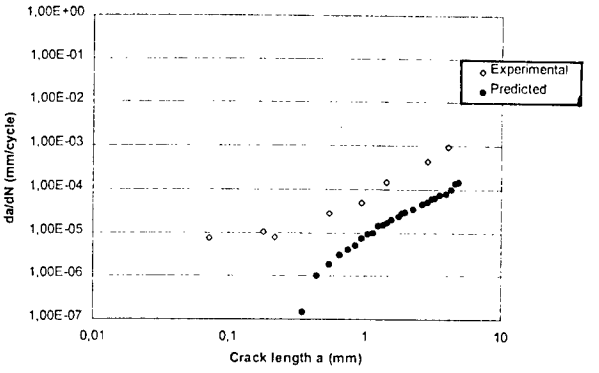

Figure 7 Measured and predicted crack growth rate R = -0.45

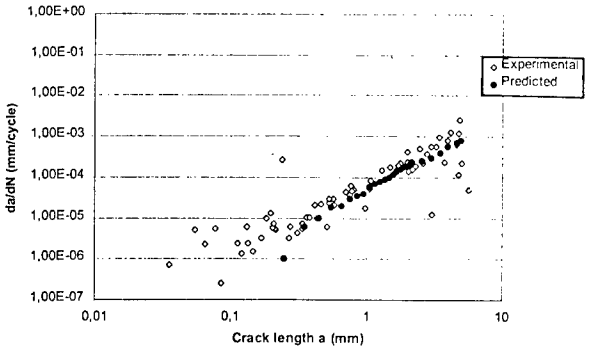

Figure 8 Measured and predicted crack growth rates R = 0.25

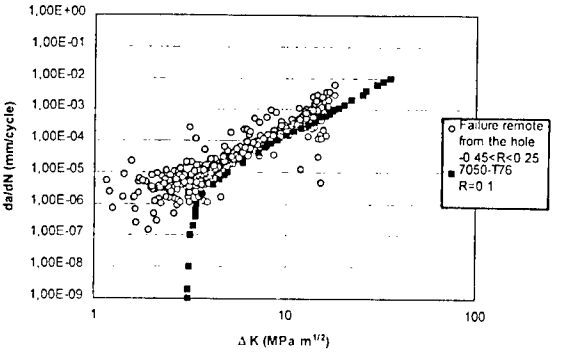

Figure 9 Measured and predicted crack growth rates, all pit locations

© British Crown Copyright 1998/DERA
Published with the permission of the Controller of Her Brittanic Majesty's Stationery Office

AN EXPERIMENTAL STUDY OF CORROSION/FATIGUE INTERACTION IN THE DEVELOPMENT OF MULTIPLE SITE DAMAGE IN LONGITUDINAL FUSELAGE SKIN SPLICES

Graeme F. Eastaugh, Ali A. Merati, and David L. Simpson
Structures Materials and Propulsion Laboratory, Institute for Aerospace Research,
National Research Council, Montreal Road, Ottawa, Ontario, Canada K1A 0R6

Paul V. Straznicky, Jason P. Scott, R. Brett Wakeman, and David V. Krizan
Department of Mechanical and Aerospace Engineering, Carleton University,
1125 Colonel By Drive, Ottawa, Ontario, Canada K1S 5B6

SUMMARY

It is difficult and costly to study either the fatigue or the corrosion/fatigue behaviour of longitudinal fuselage splices using in-service aircraft or full-scale structural test articles. These studies are further complicated by variations in splice designs in different types of aircraft. Therefore, a means of performing representative experimental studies cost-effectively for different aircraft has been devised. A special uniaxial specimen developed earlier has been used to simulate the stress environment of an aircraft splice. This specimen is capable of providing representative fatigue crack initiation, growth, and link-up data for the typical multiple site damage (MSD) failure mode and for other crack scenarios. In-service corrosion has been simulated by applying an accelerated corrosion process to the interior of the splice without damaging other areas of the specimen. Combined exposure to both corrosion and fatigue has so far been simulated by pre-corroding, drying and then fatigue testing the specimen. The accelerated corrosion damage in MSD specimens has been compared with natural corrosion damage in aircraft splices and the overall experimental approach is considered to be adequately representative for an initial study of the effects of corrosion on the durability and damage tolerance characteristics of fuselage splices. The preliminary results of an exploratory test programme indicate that corrosion at levels found in some aircraft could significantly reduce the fatigue life of longitudinal fuselage splices and could cause important changes in failure modes.

1. INTRODUCTION

There is little quantitative data from in-service aircraft or laboratory experiments on the effects of corrosion on the durability and damage tolerance characteristics of rivetted sheet structure such as the fuselage skin splices in pressurized transport aircraft. Since maintenance of corroded splices is costly, such in-service and experimental data is important for the definition of cost-effective policies and analytical approaches for design, inspection, corrective action, and fleet management. For example, data on fatigue crack initiation sites and crack growth, interaction and link-up characteristics are needed to assess failure modes and probabilities, develop cost-effective analytical methods, and determine inspection thresholds and repeat intervals both with and without the presence of corrosion. Teardown examination of cracked splices is needed to provide additional data on the first order mechanisms of corrosion/fatigue interaction in the aircraft in question and thereby also help in the development of cost-effective analytical methods and maintenance policies.

It is difficult and costly to study either the fatigue or the corrosion/fatigue behaviour of fuselage splices using in-service aircraft or full-scale structural test articles. These studies are futher complicated by variations in splice designs in different types of aircraft. Therefore, a means of performing representative experimental studies cost-effectively for different aircraft has been devised. This paper reviews the characteristics of fatigue and corrosion in fuselage splices and describes the experimental approach. Some preliminary conclusions are presented on corrosion/fatigue interaction and possible analytical approaches.

2. FATIGUE IN FUSELAGE SKIN SPLICES

The material traditionally used for the fuselage skin of pressurized transport aircraft has been 2024-T3 clad aluminium alloy. 2024-T3 combines high strength with good fracture toughness. It should be noted that in some new designs it is being substituted by 2524-T3, an aluminium alloy with better damage tolerance characteristics and improved resistance to corrosion **[1]**.

The primary fatigue load on longitudinal skin splices is hoop stress due to fuselage pressurization. Design nominal hoop stresses are typically 25-30% of yield stress, but stress concentrations and out of plane bending result in much higher stresses near rivet holes.

There is an increased risk of fatigue cracks occurring as aircraft approach or exceed their original design lives. These cracks typically develop in several rivet holes at approximately the same time and, when visible, appear like those in **Figure 1**. In the lap splice configuration shown, the cracks tend to occur in the upper rivet row of the outer (countersunk) sheet, as viewed from outside the aircraft. Such cracks are a well known form of multiple site damage or MSD, which is a term used to

Paper presented at the RTO AVT Workshop on "Fatigue in the Presence of Corrosion", held in Corfu, Greece, 7-8 October 1998, and published in RTO MP-18.

define any situation where interactive multiple cracks exist in the same structural element. In this case, the structural element is the portion of a splice within a frame-bay.

One serious concern with MSD in splices is that the cracks are difficult to detect individually and can link-up relatively quickly to form a long lead crack like the one in **Figure 2**. Another serious concern with MSD in fuselage splices is that when it exists ahead of a long crack it can reduce the fail-safe qualities of the fuselage. It can do this in two ways:

- by reducing the effectiveness of crack containment at frames and tear straps;
- by promoting potentially catastrophic longitudinal crack growth instead of fail-safe flap formation.

3. CORROSION IN FUSELAGE SKIN SPLICES

Aluminium alloy in contact with air rapidly develops a thin, compact, barrier film of aluminium oxide. In the presence of moisture this film thickens, and is believed to include aluminium hydroxide and hydrated (crystalline) forms of aluminium oxide. Its growth and composition are complex and are influenced by the temperature, the ions present, and the duration of immersion. When the film is breached physically or chemically, pitting or intergranular corrosion may occur, depending on the circumstances. The corrosion product usually consists of amorphous aluminium hydroxide $Al(OH)_3$ and various forms of hydrated aluminium oxide – one common form is Bayerite, $Al_2O_3.3H_2O$ **[2]**.

As part of this work, a study has been made of natural corrosion in the longitudinal fuselage splices of retired 727 and 747 aircraft from the NRC/IAR Aircraft Specimen Library (http://www.nrc.ca). The 727 had flown 48,655 flights over 24 years. The 747 had flown 16,612 flights over 24 years. The samples are three-row bonded lap splices in Alclad 2024-T3 with rivets in 2017-T4 alloy and with a stringer at the central row. The spliced sheets in the 727 and 747 were 1 mm (0.040 in) and 1.6 mm (0.065 in) thick respectively, including approximately 55 μm (0.002 in) of cladding per side in the 727 and 65 μm (0.003 in) in the 747. There were no doublers or changes of thickness at the splice. Corrosion was widespread on both faying metal surfaces (**Figures 3 and 4**), but the distribution of the corrosion indicates that corrosion developed primarily in the inner (driven head) sheet and that the main source of moisture was the interior of the aircraft.

The corrosion product had caused pillowing of the skin between rivets (**Figure 5**). One rivet in the central row of the 727 splice had been replaced. Since it was in a location of relatively high corrosion, the original rivet may have failed as a result of corrosion in combination with tensile stress due to product build-up at the faying surfaces around the rivet. The section in **Figure 6** shows another rivet in the same splice with a large fissure under the head.

To study the corrosion damage, the corrosion product was removed chemically using a modified ASTM procedure. At low magnification a variety of surface morphologies are apparent. These suggest that corrosion in cladding starts as isolated pit colonies **(Figure 7)** which generally broaden and join together to form a network pattern of ridges and hollows, giving the surface a scalloped appearance (**Figure 8**). Eventually, the ridges are corroded away, leaving a smoother surface. At high magnification, the surfaces of pits and scalloped regions in cladding have a terraced appearance typical of etching along preferred crystallographic planes (**Figure 9**). A perfect crystallographic shape is a characteristic feature of chloride induced pitting in aluminium alloy.

In several locations in corroded cladding in the 727 and 747 samples there are small fissures (**Figure 10**). These occur throughout the splices, including at the edges of rivet holes. They all run in directions roughly perpendicular to the direction of hoop stress. The origins and causes of the small fissures are still under investigation.

In the 747 sample there was no attack into the core 2024-T3 alloy. In the 727 sample, corrosion attack in the core 2024-T3 alloy was more localised than in the cladding, but appears to have progressed laterally by means of pitting and intergranular attack as well as through the thickness. Some of the pits tunnel laterally, possibly along grain boundaries, to produce a porous, layered structure within the damage zone (**Figures 11 and 12**). Several thin fissures run laterally from the pit colonies in the form of early exfoliation corrosion. Several well-developed regions of corrosion damage in the core material similar to the one in the figures were found.

Corrosion attack at the faying surfaces close to rivet holes was limited to the cladding in both the 727 and 747 samples, but extended to the edges of the holes in all cases. The depth of attack was generally less than the depth of attack elsewhere in the splice. Under magnification, there was evidence of light fretting around some of the rivet holes.

Chemical analysis indicates that the corrosion products in the 727 splice consist of aluminium hydroxide and various hydrated forms of aluminium oxide, together with traces of chlorine and sulphur. An earlier chemical analysis of corrosion product in a different 727 splice by Krishnakumar et al of the NRC **[3]** also identified

aluminium hydroxide and hydrated forms of aluminium oxide as the major constituents.

Well-developed radial cracks have recently been found by Bellinger et al. of the NRC at the faying surface around rivet holes in several splices from retired 727 and 1011 aircraft, including a nearby portion of the 727 splice described above. The details of this corrosion-related failure mode have been reported separately **[4]**. Circumstantial and fractographic evidence and finite element modelling indicate that the cracks initiated due to a combination of corrosion and pillowing stress. Residual stress from rivet installation may also have played a role.

4. SIMULATION OF FATIGUE IN SPLICES

In 1992 the international Industry Committee on Widespread Fatigue Damage (WFD) noted that available coupon test specimens did not represent MSD in splices properly, because net section stress, and hence crack growth rates, increased atypically as cracks grew. This gap in test capability has meant that all damage tolerance testing of splices has had to be done using full-scale structure. For this reason, the NRC and Carleton University are developing inexpensive, uniaxial coupon test technology for preliminary durability and damage tolerance testing of skin splices and for general parametric studies.

The resulting inexpensive uniaxial fatigue test specimen for fuselage skin splices is illustrated in **Figure 13**. The key feature of the concept is the use of bonded side straps to simulate the load transfer from cracked areas to surrounding structure that occurs on aircraft. This allows MSD cracks to develop and link-up in a typical manner, with typical crack growth rates, and without premature failure of the specimen. The specimen shown is a 10-inch wide version designed to be roughly representative of the longitudinal fuselage splices in some narrow-body transport aircraft. The design concept and early proof of concept testing are described in **[5]**.

Examples of multiple crack growth curves from four fatigue tests are shown in **Figure 15**. The format used allows all data to be seen for all cracks simultaneously and in the same sense that the crack growth is observed on the specimen. The format also allows the visible crack growth characteristics of different specimens to be compared easily, including initiation pattern, crack interaction, link-up, and associated individual and aggregate growth rates. These are important splice characteristics, since they can affect the frequency of inspection needed to comply with damage tolerance regulations.

The concept can be tailored to a particular aircraft by designing the MSD specimen to simulate the distribution of hoop stress and out-of-plane bending stress experienced on the aircraft. The side straps must also be designed to simulate the load transfer from cracked regions to the surrounding fuselage structure. The general methodology is explained in **[5]** and is currently being implemented by the NRC on Canadian Forces CC-144 Challenger aircraft to investigate whether military mission profiles might increase the risk of MSD. It involves constructing finite element models of an aircraft frame-bay with splice and using finite element modelling to design the MSD specimen to match the fuselage stresses in the cracked as well as the non-cracked condition. A strain survey is needed to validate the finite element models.

Efficient rivet idealisations that give accurate membrane and out-of-plane bending stresses within and around the splice are needed for this scale of modelling. **Figure 14** illustrates a finite element model that uses an idealisation developed by Bedair and Xiong of the NRC. It shows the inner and outer surface hoop stress distribution in the current generic MSD specimen and has been verified using strain gauge and photoelastic coating measurements. The idealisation will be used for the modelling of fuselages and for MSD specimen design. Related research is discussed in **[6]**. The photoelastic coating measurements were made using an automated technique being developed by Sparling and Komorowski of the NRC **[7]**. It can be used in aircraft strain surveys as well as on laboratory specimens and yields a full-field contour distribution of maximum shear strain, as shown for the current MSD specimen in **Figure 16.** This together with stress line profiles can be used to verify a FE model, as illustrated in **Figure 17.**

Since 60% to 80% of the useful fatigue life of a splice involves crack development under the rivet head, new techniques have been developed for monitoring this crack growth period. Surface wave ultrasonics and specially placed strain gauges (**Figure 18**) provide early detection, while acoustic emission monitoring techniques developed in collaboration with AEMS Inc., Kingston **[8]**, provide early detection and hidden crack growth curves (**Figures 19 and 20**).

5. SIMULATION OF CORROSION/FATIGUE IN SPLICES

It is considered impractical to assess the effect of corrosion on the fatigue durability and MSD crack growth characteristics of splices from service data, and so it is necessary to simulate in-service corrosion/fatigue interaction in the laboratory.

Laboratory tests need to be representative if they are to be of any value in assessing corrosion/fatigue interaction and predicting general aircraft behaviour. The use of full

scale testing of fuselage sections to compare the fatigue and corrosion/fatigue performance of a particular splice would probably be costly, since many tests would be required for a proper parametric study. Another approach is needed.

To be cost-effective, the experimental technology should contain the following elements:

- a splice specimen and fatigue test procedure capable of simulating adequately the fatigue failure modes and durability and damage tolerance characteristics of the splices in a particular aircraft of interest in a relatively inexpensive manner compared to full-scale testing;

- a rapid and inexpensive means of creating corrosion inside the splice that adequately simulates in-service corrosion for fatigue test purposes;

- an inexpensive procedure for combining corrosion exposure and fatigue loading to adequately represent operational conditions;

- better non-destructive means than are currently available for measuring the level of corrosion in an intact splice, so that the accelerated corrosion process can be controlled and so that NDI-based corrosion metrics can be correlated with observed changes in durability and damage tolerance characteristics;

To attempt to meet these requirements, the NRC and Carleton University have developed MSD specimen technology that includes an accelerated corrosion process and new corrosion NDE techniques. Over two dozen MSD specimens have been manufactured and tested in small batches over several years as part of this development process. Recently a single batch of over twenty MSD specimens has been manufactured in an attempt to reduce variability and obtain a more statistically significant comparison of fatigue and corrosion/fatigue performance. A higher level of corrosion involving 5% to 6% average thickness loss is being used. So far two corroded and two non-corroded specimens from the new batch have been tested and three more specimens have been pre-corroded to the required level. Preliminary conclusions are included in this paper.

The basic accelerated corrosion process was developed several years ago by Krishnakumar and Komorowski of the NRC from the ASTM B368 Copper Accelerated Acetic Acid Salt Spray (CASS) test. In the process developed for MSD specimens special measures are taken to protect the specimens against external corrosion. Only the interior of the splice is allowed to corrode.

The accelerated corrosion process has been found to produce physical effects in a splice made from clad 2024-T3 that are generally similar to those of natural corrosion. **Figures 21 to 28** show a MSD specimen from the new batch corroded throughout the splice to an average thickness loss of between 5% and 6%, which has undergone fatigue testing. At this level of corrosion, which requires an exposure of 5 to 6 months, most of the cladding has been consumed and there are regions of substantial attack into the core 2024-T3. This level of corrosion permits a direct comparison with the 727 splice sample discussed earlier, except for the mechanical details of the rivet installations.

The physical effects of corrosion on the two splices are generally similar. Both splices displayed substantial corrosion pillowing, and the appearance of the corrosion product after disassembly was similar. Chemical testing of the corrosion product in these specimens is incomplete. With the product removed, the general distribution of corrosion damage appears random in both specimens except for some bias towards the upper regions – possibly related to the source of the corrodent. In both specimens the corrosion damage extends up to the edges of most of the rivet holes, but is generally lighter around the rivet holes than elsewhere. The general appearance and microscopic topography of the damage in cladding is similar, except that the crystallographic features are less clearly defined in the MSD specimen at high magnification. The attack into the core 2024-T3 leaves porous, layered pit colonies in both cases (**Figures 11, 12, 27 and 28**). The MSD specimen lacks the thin lines of intergranular attack running laterally from the pit colonies. This difference may be due to the much more aggressive nature of the corrodent in the MSD specimen.

It will not be known until the new test batch has been completed whether the slight physical differences between the accelerated and natural damage might be significant from a fatigue standpoint. If testing shows the microscopic morphology of the cladding to be a potentially important factor in crack nucleation in splices, specific experimental investigation of this parameter might be warranted. The lack of thin, lateral intergranular fissures at pit colonies in the core material does not seem significant in view of their orientation. The structure of the pitting attack seems more important in the present context, and these structures are quite similar in the accelerated and natural samples examined so far. Therefore, it appears that the current accelerated corrosion process is adequate for an initial study of corrosion/fatigue in splices.

An average service load cycle involves pressurization of the fuselage for one or more hours under cold/dry exterior conditions and warm/humid interior conditions,

followed by dwells of hours or days without load under ground-level atmospheric conditions. A full representation of this environment is impractical, and so for initial research a simple combination of full pre-corrosion followed by drying and fatigue testing has been used in most MSD corrosion/fatigue tests. Fatigue testing has been done using constant amplitude loading at a load ratio of 0.02 and a frequency of 8 Hz. A frequency of 4Hz is being used in the new batch. This combination of corrosion and fatigue assumes that corrosion/fatigue interaction occurs only in the context of pre-existing corrosion and in a dry splice. This is a reasonable approximation for two reasons. First, teardown of aircraft splices and anecdotal evidence indicates that substantial corrosion often exists without any associated fatigue cracking. Second, the high in-service loads occur when any moisture in the splice is likely to have frozen. Nevertheless, this approximation may be too simple, particularly with respect to possible interaction between corrosion and fretting, and so a procedure that involves alternating periods of corrosion exposure and fatigue loading is being considered for future batches.

6. CORROSION/FATIGUE INTERACTION

The current MSD test programme is intended to help identify the first order effects of corrosion on the fatigue characteristics of fuselage skin splices. Since a rivetted splice in thin sheet material is a complex system whose performance can vary greatly depending on detailed mechanical design, observations on corrosion/fatigue interaction may vary from one splice design to another. The splice design used in this test programme is a generic narrow-body aircraft lap splice configuration with knife-edge countersinks and no adhesive or interfaying treatments (apart from cladding). The accelerated corrosion process produces corrosion products and damage in the cladding and core 2024-T3 alloy that are similar to those of natural corrosion. Therefore, while the specimen and test procedure do not fully simulate the design and environment of a particular aircraft splice, observations of failure modes, fatigue endurance, and other symptoms of corrosion/fatigue interaction can be expected to have potential relevance to splices on a number of ageing aircraft types.

Until recently, MSD specimens have been manufactured and tested in small batches. The corrosion level used in the corrosion/fatigue tests has been in the range of 2% to 4% average thickness loss per sheet. Statistical analysis of sixteen relevant tests based on a log normal distribution indicates with an 80% level of confidence that corrosion reduced the mean visual initiation life (the number of load cycles before the first crack is visually detected). However, the apparent reduction – from 190,000 cycles to 157,000 cycles (17 %) – is of the same order as the variability in the data. While the variability measured as log standard deviation has been fairly large, it has been within the range typical of fabricated structure. Therefore, larger samples would be needed at these corrosion levels to confirm a significant change in fatigue characteristics.

As mentioned earlier, the new test batch is relatively large and the level of corrosion has been increased to an average thickness loss of 5% to 6%. This level is not generally regarded as severe, but the fatigue testing on the first two pairs of corroded and non-corroded specimens show a 34% reduction in mean visual initiation life and a change in failure mode.

Several potentially useful observations regarding corrosion fatigue/interaction can be made from the work done so far with MSD specimens and from the examination of naturally corroded aircraft splices. These are outlined in the following paragraphs. These observations should be regarded as preliminary, since the new test programme has only just started and the teardown examination of previous specimens is not yet complete.

6.1 Changes in Failure Mode

In non-corroded specimens the failure mode has invariably been MSD at rivet holes in the upper rivet row of the countersunk sheet. The cracks have usually initiated at one or both of two general locations – either near the top of the hole, or at an intermediate location above the centreline of the rivet row. Both types of crack can be seen in **Figure 29** and in the sketch in **Figure 19.** Heavy fretting occurs around the upper half of the rivet hole (**Figure 30**). Cracks usually initiate in or at the outer edge of the fretted area and grow into as well as away from the hole. The upper crack location is clearly associated with high out-of-plane bending stress, while the lower location may be associated with high hole-edge stress concentration.

In corroded MSD specimens, three main failure modes have been observed:

- MSD at the rivet holes in the upper row;
- fatigue cracking in the inner (driven) sheet below the lower rivet row;
- tensile failure of one or more rivets before any external load has been applied.

The first failure mode is associated with average thickness losses of up to 4% per sheet. At this level of corrosion, there is unlikely to be any attack into the core 2024-T3. The additional two failure modes are associated with an average thickness loss of 5% to 6%. As mentioned earlier, well-developed localised attack into the core metal has been observed at this level of corrosion.

The second failure mode – cracking in the inner sheet below the lower rivet row – has occurred in two of five MSD specimens corroded to the 5% - 6% level. Teardown examination of one of these has shown that the crack initiated in a pit colony in the core metal. **Figure 27 and 31** show the crack initiation site at different magnifications. The third failure mode – rivet failure – is apparent in the other three specimens corroded to the 5% - 6% level. The locations vary, and in one case the rivet head is not yet detached. These specimens have not yet been fatigue tested and so their full failure characteristics are not yet known.

6.2 Reduced Fretting

Pre-corrosion clearly reduces fretting around rivet holes in corroded MSD specimens. Above 5% average thickness loss there is almost no fretting damage, while in non-corroded specimens there is invariably substantial fretting damage (**Figure 30**). The mechanism of this reduction is not clear and may be complex. Since corrosion extends to the edges of the holes, the product build-up is believed to be exerting strong pressure at this location. It is also intervening between the faying surfaces and may be allowing relative shear movement without fretting of the metal surfaces. Alternatively, the product might be preventing any shearing movement at the rivet hole. The build-up of product elsewhere in the splice may also be increasing friction load transfer generally and reducing load transfer at or near the rivet holes. This would also help to reduce fretting near the holes. Other evidence of this possibility is given in Section 6.8 below. Since fretting plays a role in initiating cracks at rivet holes, a reduction of fretting in corroded splices would tend to offset any adverse effects of corrosion damage around rivet holes. These observations highlight that the combination of corrosion and fatigue exposure in laboratory testing might be important.

6.3 General Thickness Loss

As described earlier, corrosion in cladding is equivalent to a general area attack, and so there will be an associated increase in alternating stress over wide areas of the splice.

6.4 Local Change in Geometry and Compounded Stress Concentration in Core 2024-T3

When the average thickness loss exceeds the depth of the cladding, there is likely to be substantial attack into the core metal. The damage in core metal consists of porous, layered pit colonies, whose effect on local stress is probably equivalent to a substantial local change in geometry, such as a hemispherical notch. Thus the stress at the tip of a small pit at the edge of the damage zone can be regarded as the compounded value of the area stress increase due to cladding loss, the stress concentration due to the damage zone in the core material, and the superimposed stress concentration due to the small pit itself.

6.5 Potential Variability in Crack Initiation Site in Core 2024-T3

The cracking 0.5 cm below the lower rivet row in two MSD specimens corroded to an average thickness loss of 5% to 6% (**Figures 27 and 31** show one of these cases) was due to a combination of core metal attack and high membrane and secondary bending stress at the location in question. Similar corrosion damage was found in the naturally corroded 727 specimen (**Figures 11 and 12**), and so the same mechanism could occur in an aircraft splice. This possibility creates maintenance and safety concerns, because the cracked location cannot be inspected visually without removing interior trim, and because large hidden cracks could develop.

The stress distribution in a rivetted splice is complex (**Figures 14 and 16**) and so the presence of core metal attack does not guarantee crack initiation at that site. There are other high stress locations in any splice that could combine with core attack to create a crack initiation site. The region in the countersunk sheet above the upper rivet row is a prime candidate. Some regions around the rivets contain the highest stresses in the splice; however, these show a tendency to escape the severest corrosion.

6.6 Increase in Local Static Stress due to Pillowing

Corrosion pillowing is present in all corroded splices. The high volumetric ratio of corrosion product to lost metal (**Figure 32**) adds high static stresses at the faying surface at certain locations around a rivet hole that are also subject to high alternating stress [9]. Consequently, corrosion pillowing is likely to reduce the fatigue endurance of splices, particularly when MSD at rivet holes is the failure mode.

Evidence of the faying surface radial cracks from rivet holes mentioned earlier and reported in [4] have not yet been found in corroded MSD specimens.

6.7 Failure of Rivets

The tensile failure of rivets in three of five MSD specimens corroded to an average thickness loss of 5% - 6% and in the 727 splice described earlier appears to be due to a combination of corrosion of the rivets and tensile stress in the rivets due to a local build up of corrosion products. The rivets have not yet been examined. Rivet failures have occurred in aircraft in service and have been observed in other aircraft specimens at the NRC. They are not a new

phenomenon, but the evidence from MSD specimens and the 727 specimen seems to indicate that such failures can occur at average corrosion levels not hitherto considered severe.

6.8 Increase in Nominal Membrane and Secondary Bending Stresses

The MSD specimen fatigue tests are conducted using a constant amplitude load. Strain gauges placed on both sides of the countersunk sheet 2.54 cm from the centre of the upper rivet row, which is outside the spliced region, indicate that the membrane and bending stresses at this location are slightly higher in corroded specimens. The net effect is an average increase of 6% (about 6.9 MPa, 1 ksi) in the stress at the inner surface of the countersunk sheet in corroded specimens. This can be expected to translate into a similar increase in the faying surface stress at the rivet holes. There could be a significant reduction in fatigue crack visual initiation life at the rivet holes due this phenomenon alone.

An increase in membrane stress outside the splice could be caused by a general increase in the apparent tensile stiffness of the spliced region. An increase in secondary bending stress could be caused by a reduction in the tendency of the rivets to "tilt" under the shearing action of the two spliced sheets. Plausible explanations can be offered as to why corrosion product build-up might cause both of these effects. For example, product build-up could be transferring some friction load transfer away from the regions around rivets while also generally increasing shear resistance between the sheets. This is a complex phenomenon and further investigation is warranted.

7. CORROSION METRICS

One important objective of the test programme is to identify corrosion metrics, i.e., direct or indirect measurements of the level of corrosion that bear some relationship to changes in fatigue characteristics. If such metrics can be found, it should be possible to model corrosion/fatigue interaction in durability and damage tolerance analysis and determine operationally acceptable, safe, and cost-effective maintenance action for corrosion found in service.

The information needed to derive the desired metrics includes an accurate assessment of:

- the thickness loss distribution for both sheets of an intact splice;
- the extent and depth of local damage zones in the core metal;
- the pillowing profile of the splice.

Unfortunately, sufficiently accurate thickness measurements for both sheets of an *intact* splice are not yet obtainable. Single frequency eddy current measurements cannot be accurately calibrated and may be indicating sheet separation due to corrosion product rather than thickness loss. Pulsed eddy current offers some promise and the NRC NDE Group and Canadian Forces are collaborating in research in this technique. Ultrasonic thickness measurement using Novascan 3000 equipment and hand-held probes provides accurate measurement of cleaned corrosion damage in single sheets, but the accuracy is uncertain with intact splices. Digitized x-ray using techniques developed by Chapman et al. of the NRC **[10]** provides efficient and accurate thickness maps of single sheets that have been cleaned of corrosion product, but research is still needed into the interpretation of x-ray images of intact corroded splices. This work is proceeding at the NRC. Maps of a MSD specimen created using the various techniques mentioned above are in **Figure 34**.

Currently, the most practical and accurate method for estimating thickness loss in intact splices is considered to be the direct measurement of the out-of-plane distortion (pillowing) of the skin due to corrosion product. This can be performed using a deep-throw micrometer gauge or dial gauge. A less direct but more efficient technique is to use laser 3-D imaging. To estimate the average thickness loss in an intact MSD specimen, micrometer gauge or laser measurements of **pillowing** distortion in previous specimens are calibrated against digitized x-ray maps of thickness loss in the same specimens, obtained from single sheets after disassembly and cleaning. The transfer functions derived in this manner have shown some variability with specimen and location, and so development is continuing. Current general purpose laser imaging equipment offered by Canadian companies such as Vitana Corporation of Ottawa can be used to obtain surface profiles of pillowing that can be interpreted to an accuracy better than 50 microns (**Figure 33**). Vitana's equipment is portable and relatively inexpensive and could be adapted for use on aircraft.

Corrosion metrics based on measurements made after teardown are also of interest in this research. Measurements of thickness loss, specific damage and surface morphology are being made with x-ray, SEM, metallography, and other techniques. While they may not be of direct use to aircraft operators, they are potentially useful in obtaining an understanding of corrosion/fatigue interaction for modelling purposes. Also, it may be possible and useful to relate important microscopic features to NDE measurements of corrosion in an intact splice.

8. MODELLING AND PROBABILISTIC ANALYSIS

The immediate objective in MSD specimen testing is to obtain representative data to perform a durability and damage tolerance analysis, which in turn is required to certify the design of the fuselage/splice and determine safe and economic inspection methods and frequencies. The number of stochastic variables involved in analysing MSD data, particularly if corrosion is considered, indicates that a probabilistic approach to presenting and using the multiple crack initiation, growth and link-up data would be beneficial.

Berens et al **[11]** have used MSD test data provided by the NRC to analyse multiple crack scenarios, reverse-grow cracks to obtain an equivalent initial flaw size (EIFS) distribution, and thereby estimate a probability of failure curve using an adaptation of established USAF durability and damage tolerance analysis procedures.

Another approach being investigated by Xiong and Shi at the NRC **[12]** is to analyse aggregate crack growth data stochastically using the process illustrated in **Figure 35.** The first step is to obtain a series of aggregate crack growth rates and associated crack lengths for each specimen by local curve fitting to the experimental data. These data are then plotted on a log-log graph and a straight line fit is made. The linear parameters read from this graph are used to define the values of parameters in a stochastic equation that predicts aggregate crack length at any time. If "failure" is defined as the exceedence of a given aggregate crack length, a curve representing the cumulative probability of failure of the splice after a given number of load cycles can be constructed.

Figure 35 shows the cumulative probability of failure of non-corroded MSD specimens derived from a group of nine tests for an aggregate crack length of 10.2 cm (4 in). This is an arbitrary failure criterion selected for illustrative purposes. The critical crack length in transport aircraft fuselage skin is actually in the range 50 to 100 cm. The approach proposed by Xiong and Shi is an adaptation of one used by Yang et al. of the USAF for single cracks **[13]**. It is simple, includes all stochastic variables, including any corrosion/fatigue interaction, and does not require the use of expensive finite element analysis for the estimation of stress intensity factors.

9. CONCLUSIONS

A representative and cost-effective method of performing laboratory fatigue and corrosion/fatigue testing of longitudinal fuselage splices has been described. It uses a special MSD test specimen and provides data that can be used for durability and damage tolerance analysis.

Comparisons of corrosion damage from MSD specimens and naturally corroded aircraft splices indicate that the accelerated corrosion process currently used is adequate for an initial corrosion/fatigue study. It is applied as full pre-corrosion, after which specimens are dried and then fatigue-tested. Alternating corrosion and fatigue exposures are being considered for future batches.

A generic MSD specimen design roughly representative of lap splices in some ageing aircraft is being used for an exploratory test programme. The corrosion level used in early corrosion/fatigue tests was in the range of 2% to 4% average thickness loss per sheet. Corrosion reduced the mean visual initiation life by 17%, but statistical analysis indicates that larger sample sizes would be needed at these lower corrosion levels to confirm a significant change in fatigue characteristics.

Recently, over twenty more of these MSD specimens were manufactured in a single batch to help minimize manufacturing variability. These are being corroded to an average thickness loss of 5% to 6%. So far two pairs of corroded and non-corroded specimens have been fatigue tested. These early tests indicate a 34% reduction in mean visual initiation life.

Also, two new failure modes have emerged. First, cracking initiated in the inner (driven head) sheet below the lower rivet row in the two corrosion/fatigue tests performed so far. Second, complete or partial tensile failures of rivets have occurred in three other specimens that have completed pre-corrosion.

The inner-sheet cracking is particularly worrisome, because visual inspection is only possible from inside the aircraft and large hidden cracks could develop.

The failure of rivets is not a new phenomenon on in-service aircraft, but the data from MSD specimens and the examination of a 727 specimen indicate that it can occur at a corrosion level of only 5% - 6% average thickness loss in 1mm sheet.

Teardown examinations of MSD specimens and naturally corroded aircraft splices manufactured from 2024-T3 Alclad indicate that when the average thickness loss in a corroded region is less than the nominal thickness of undamaged cladding, the corrosion is likely to be confined to the cladding and to be equivalent to general area attack. When the average level of thickness loss exceeds this value there is likely to be several zones of porous, layered pitting attack into the core 2024-T3.

Based on the work done so far, several other observations have been made with regard to

corrosion/fatigue interaction in splices: reduced fretting; general thickness loss; compounded stress concentrations in core 2024-T3; potential variability in crack initiation site; increase in static stress due to pillowing; and an increase in nominal membrane and secondary bending stress. Future work will continue the investigation of these interactions.

Current NDE techniques for the measurement of corrosion in splices are not sufficiently accurate to provide good corrosion metrics that can be related to changes in durability and damage tolerance characteristics. Some new techniques are under development for laboratory and service use.

Several useful laboratory techniques for monitoring hidden MSD cracks under rivet heads have been developed. These include acoustic emission monitoring, which can provide hidden crack growth curves.

The analysis and presentation of MSD fatigue and corrosion/fatigue test data for use in durability and damage tolerance studies could benefit from the use of probabilistic techniques. A technique based on aggregate crack length that is simple to apply has been outlined and a graph of cumulative probability of structural failure vs. load cycles based on nine tests of non-corroded specimens has been presented.

ACKNOWLEDGEMENTS

Funding for this work was provided by the National Research Council, the Department of National Defence, and Carleton University. The substantial advice and support of other researchers and technical staff at the NRC, DND, AEMS Inc., and Vitana Corporation is gratefully acknowledged.

REFERENCES

1. R.J.Bucci and C.J. Warren, "Material Substitutions for Aging Aircraft", The First DoD/FAA/NASA Conference on Aging Aircraft, Ogden, Utah, July 1997.

2. H.P.Godard, W.B.Jepson and M.R.Bothwell, and R.K.Lane, "The Corrosion of Light Metals", John Wiley and Sons Inc., 1967.

3. S.Krishnakumar, J.P.Komorowski and I.Sproule, "Chemical Characterization of Corrosion Products in Fuselage Lap Joints", National Research Council Canada LTR-ST-1952, November 1993.

4. N. C. Bellinger, J. P. Komorowski and R. W. Gould (NRC Canada), "Corrosion Pillowing Cracks in Fuselage Joints", paper to be published in the proceedings of the Second Joint NASA/FAA/DoD Conference on Aging Aircraft, Williamsburg, Virginia, 31 August - 3 September, 1998.

5. G.F.Eastaugh and D.L.Simpson (NRC Canada), P.V.Straznicky and R.B.Wakeman (Carleton University), "A Special Uniaxial Coupon Test Specimen for the Simulation of Multiple Site Fatigue Crack Growth and Link-up in Fuselage Splices", AGARD-CP-568, December 1995.

6. Y.Xiong and O.K.Bedair (NRC Canada), "Analytical and finite element modelling of riveted lap joints in aircraft structure", paper to appear in the AIAA Journal.

7. S.A.Sparling, J. Gagnon, and J.P. Komorowski (NRC Canada), "Photoelastic Analysis by 6-image Phase Stepping with RGB Input", National Research Council report LTR-ST-2154, 1998.

8. S.L.McBride (AEMS Inc.), J.P.Scott (Carleton University), and G.F.Eastaugh (NRC), "Use of Acoustic Emission Monitoring to Detect, Locate and Measure Multiple Site Damage (MSD) Fatigue Crack Growth Underneath Rivet Heads", paper to be published in the proceedings of Second Joint NASA/FAA/DOD Conference on Aging Aircraft, Williamsburg, Virginia, 31 August - 3 September 1998.

9. N.C. Bellinger and J.P Komorowski (NRC Canada), "Implications of Corrosion Pillowing on the Structural Integrity of Fuselage Lap Joints", Proceedings of FAA-NASA Symposium on Continued Airworthiness of Aircraft Structures, 28-30 August 1996.

10. C.E.Chapman (NRC Canada), "Corrosion detection and thickness mapping of aging aircraft lap joint specimens using conventional radiographic techniques and digital imaging", proceedings of the 43rd Annual Conference of the Canadian Aeronautical and Space Institute, Ottawa, May 1996.

11. A.P.Berens, (University of Dayton Research Institute), A.Trego, and J.D.West, (Boeing), "Risk assessment of fatigue cracks in corroded lap joints", paper to be presented at NATO-RTO Air Vehicle Technology Panel Workshop on Fatigue in the Presence of Corrosion, Corfu, 7-8 October 1998.

12. Y.Xiong and G.Shi, "Prediction of failure probability for fuselage splice joints with MSD using a stochastic crack growth model", National Research Council report LTR-ST-2152 (not yet released).

13. J.N.Yang, S.D.Manning, W.H.Hsi and J.L.Rudd (USAF), "Stochastic crack growth models for application to aircraft structures", paper in Probabilistic Fracture Mechanics and Reliability, J.W.Provan (Editor), Martinus Nijhoff, 1987.

Figure 1 - MSD cracks in a 737 aircraft.

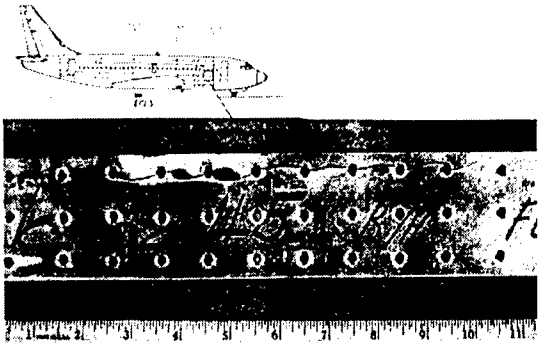

Figure 2 - MSD cracks which have linked to form a long lead crack. (courtesy T.Swift, FAA)

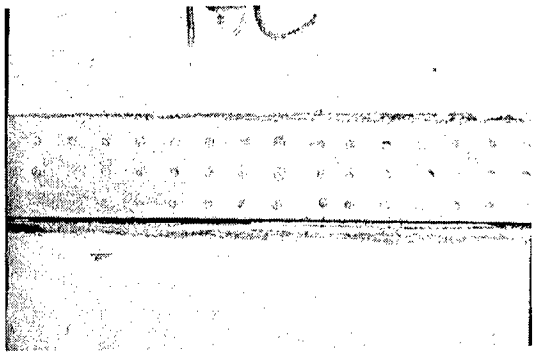

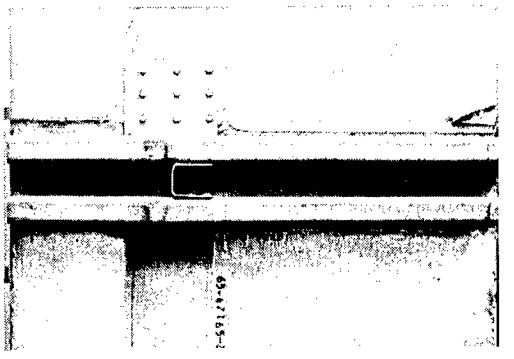

Figure 3 - Boeing 727 splice used for study of natural corrosion.

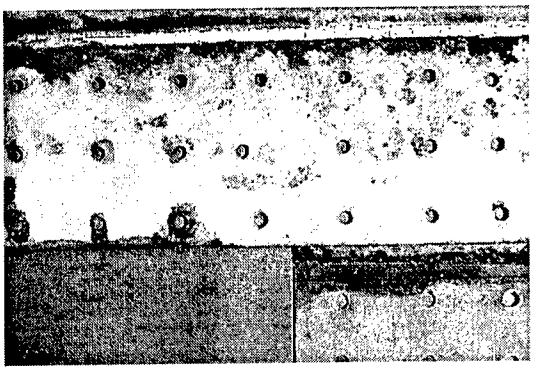

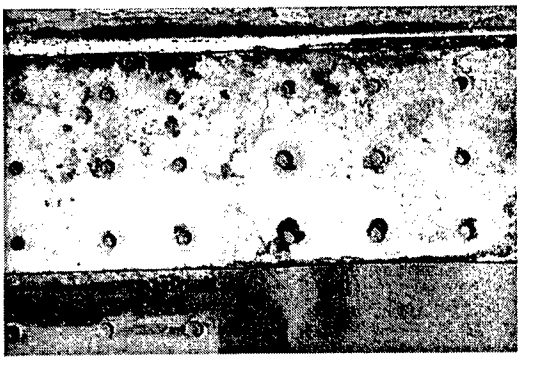

Figure 4 - Adjoining sections of the faying surface of the inner sheet of 727 splice showing corrosion product.

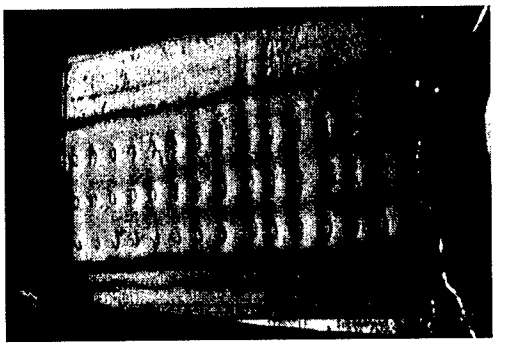

Figure 5 - D Sight image of pillowing in 727 specimen. (R.Gould)

Figure 6 - Montage of section through pillowed 727 splice showing corrosion in cladding and crack in rivet. Dark region contains corrosion product and adhesive.

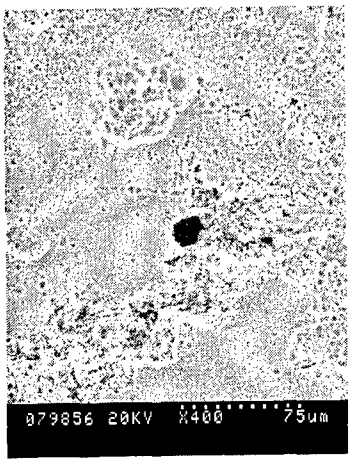

Figure 7 – Light pitting in cladding of 727.

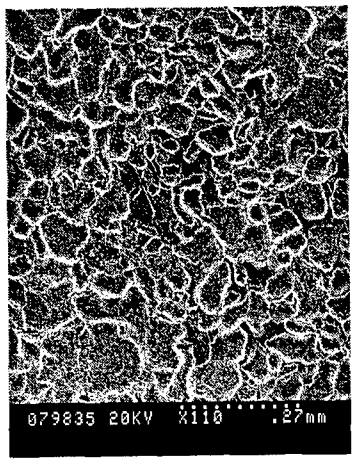

Figure 8 - Scalloped appearance of developed corrosion in cladding of 727.

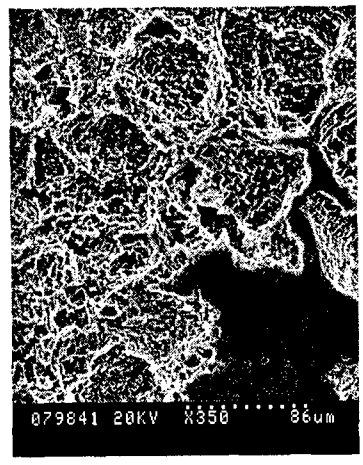

Figure 9 - Closer view of scalloped region showing crystallographic etching.

Figure 10 - Small fissures in cladding of 727.

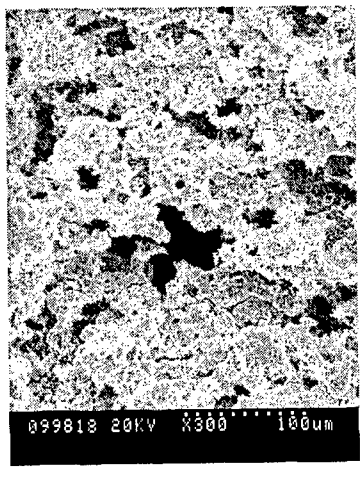

Figure 11 - Typical porous, layered pit colony in core 2024-T3 of 727.

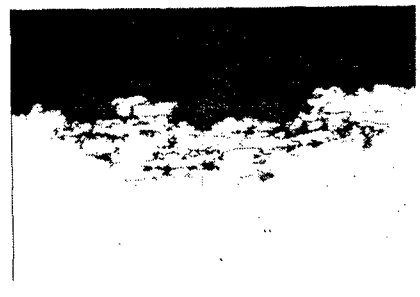

Figure 12 - Section through pit colony in core 2024-T3 of 727 showing porous, layered structure.

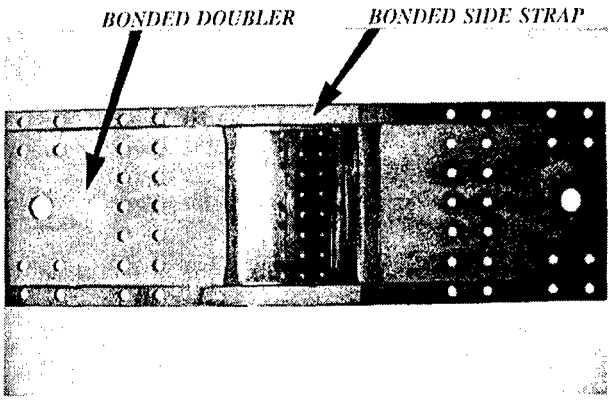

Figure 13 - Generic version of MSD test specimen.

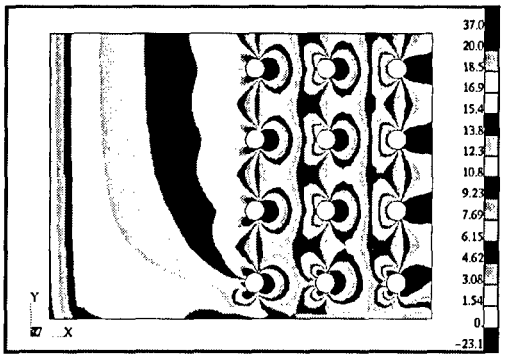

Figure 14 - Finite element (half) model of MSD specimen showing hoop stress at inner surface of countersunk sheet. (O.Bedair).

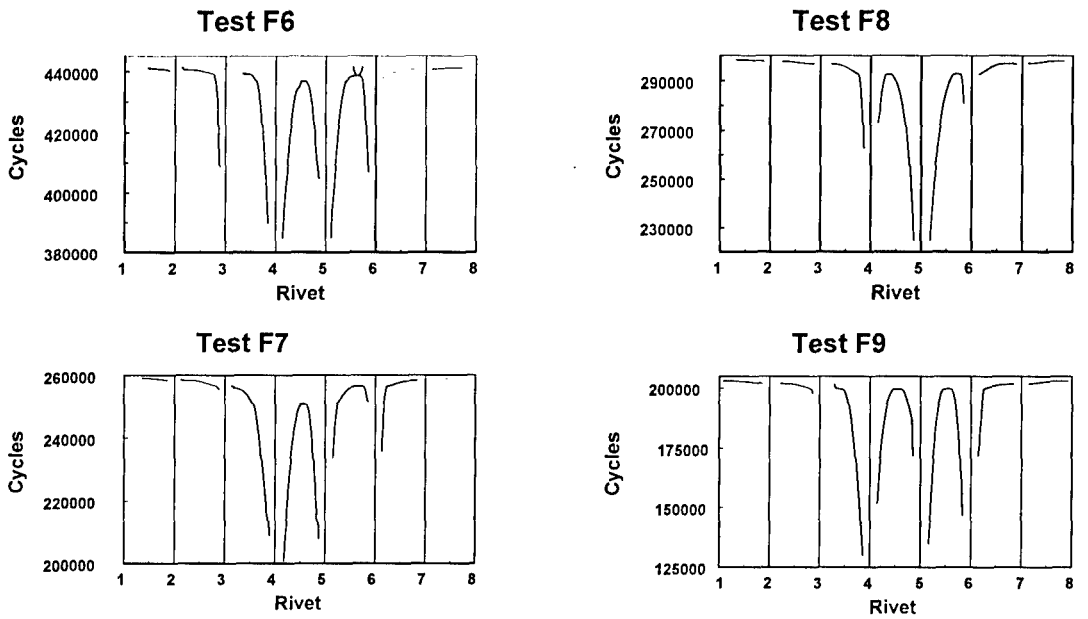

Figure 15 - Multiple crack growth curves from fatigue tests of four MSD specimens.

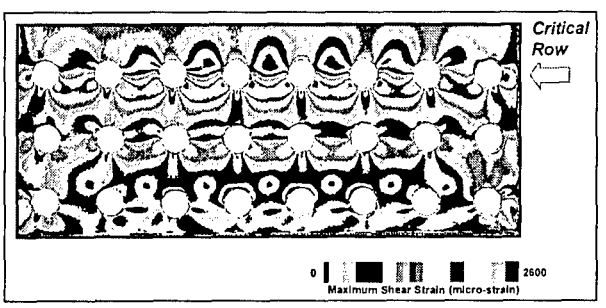

Figure 16 - Maximum shear strain distribution in MSD specimen using NRC's automated photoelasticity system. (S.Sparling and D.V.Krizan)

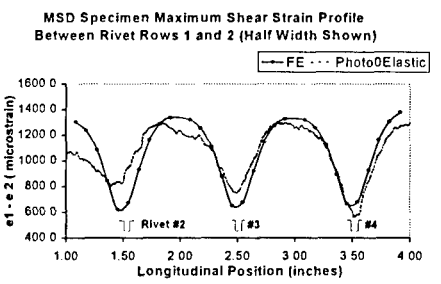

Figure 17 - Line profile comparison between photoelastic measurements and FE model of MSD specimen. (S.Sparling, O.Bedair and D.V.Krizan)

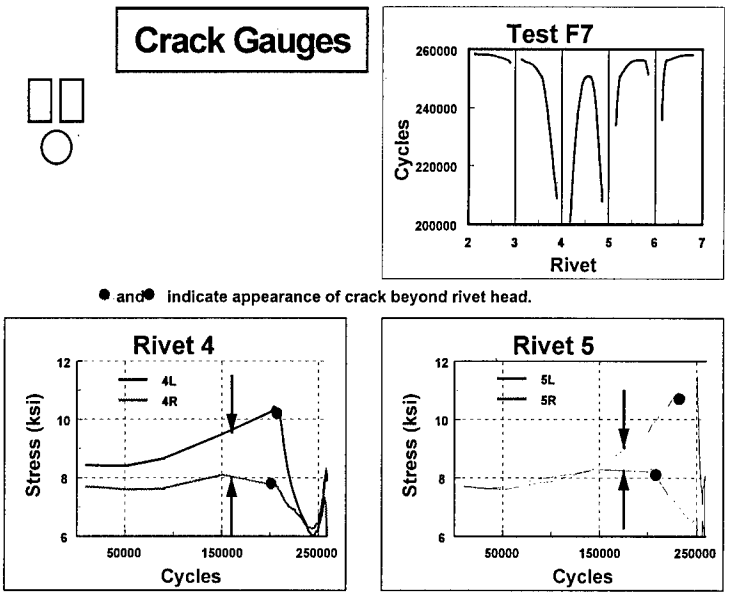

Figure 18 - Use of strain gauges to obtain early detection of hidden cracks under two rivet heads in a MSD specimen. Divergence or other features of the strain curves indicate the presence of a crack. Arrows indicate cycles at which there is first clear evidence of a crack. Visible crack growth for the full test shown in top graph.

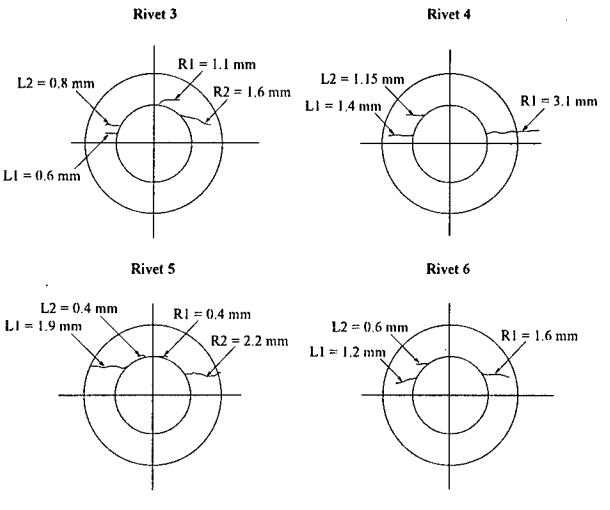

Figure 19 - Hidden fatigue cracks under the heads of the four central rivets in the critical row of a MSD specimen – test terminated after first visual initiation.

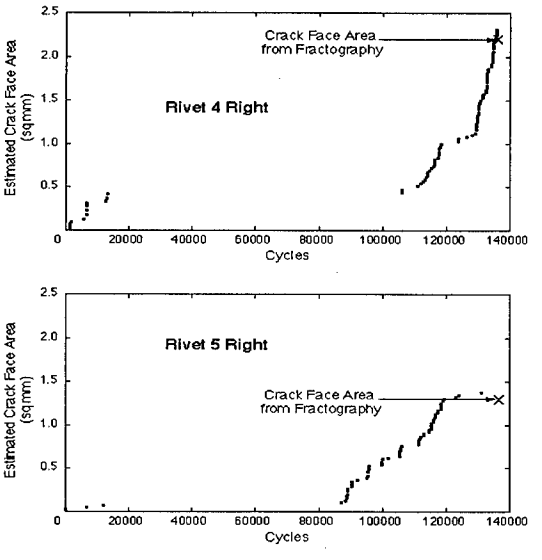

Figure 20 - Crack growth curves for two of the hidden cracks in a MSD specimen obtained using acoustic emission monitoring – same test as shown in previous Figure. Visual initiation 130,000 cycles. (S.L.McBride, AEMS Inc.)

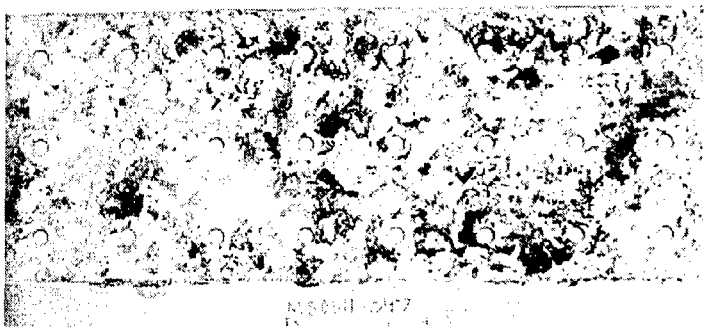

Figure 21 - Faying surface of driven head sheet of a MSD specimen after corrosion/fatigue testing. Crack 2.6 cm long runs longitudinally mid-way between rivet hole number 5 (from left) in the lower row and the lower edge of the corroded region. Average thickness loss throughout splice 5%-6%.

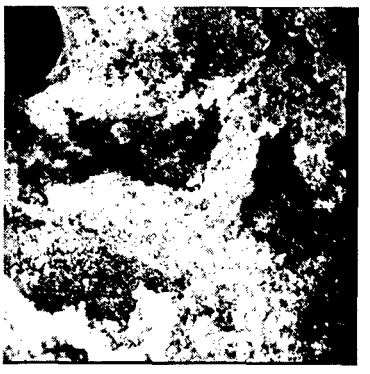

Figure 22 - Closer view of MSD specimen in previous Figure.

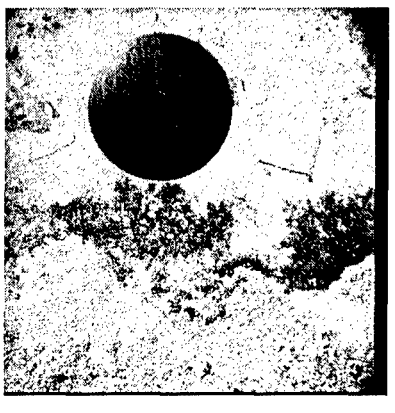

Figure 23 - Closer view of MSD specimen with corrosion product removed.

Figure 24 - Corrosion in cladding with product removed, showing 'scalloped' appearance.

Figure 25 - Etching along preferred crystallographic planes in cladding.

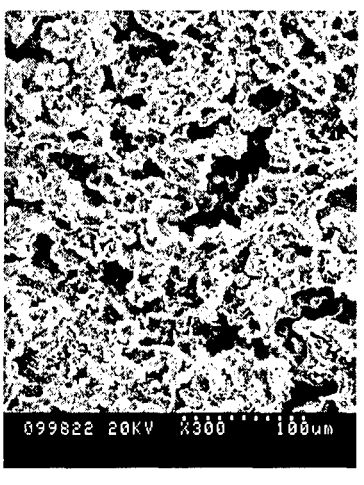

Figure 26 - Typical porous, layered pit colony in core 2024-T3 in MSD specimen.

Figure 27 - Crack face showing porous, layered pit colony in core 2024-T3 in MSD specimen.

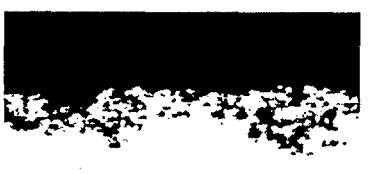

Figure 28 - Section through pit colony in core 2024-T3 of MSD specimen showing porous, layered structure.

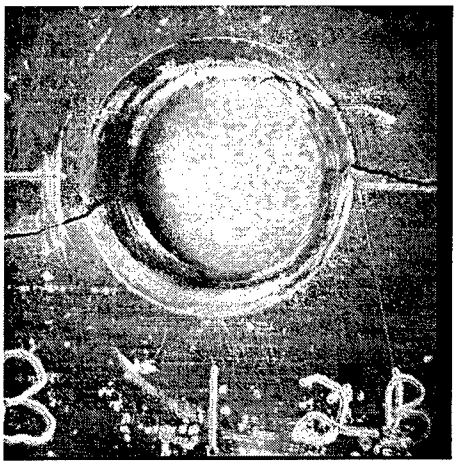

Figure 29 - Countersunk rivet hole in non-corroded MSD specimen with typical fatigue cracks

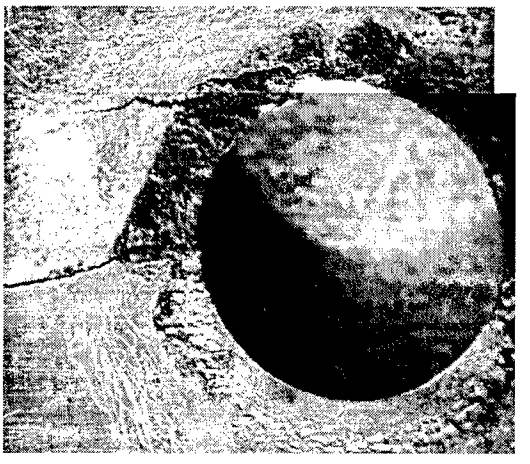

Figure 30 - Faying surface of same rivet hole as in previous Figure (montage).

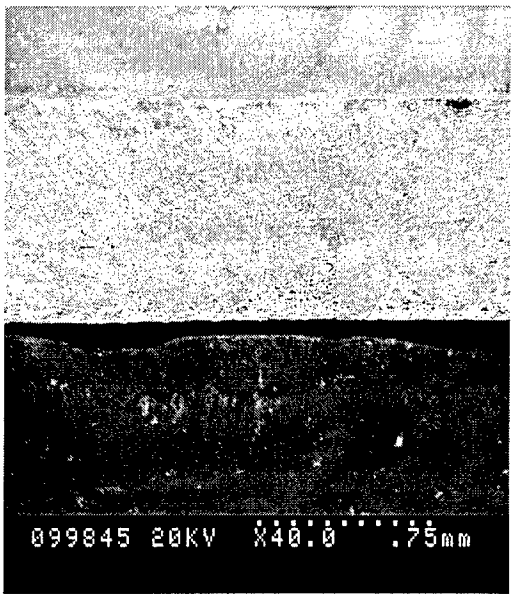

Figure 31 - Crack initiation at pit colony in core 2024-T3 in corroded MSD specimen.

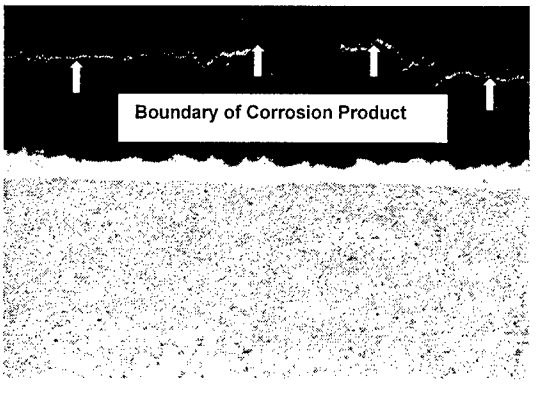

Figure 32 - Section of typical corrosion in cladding of 727 showing high volume ratio of corrosion product to thickness loss.

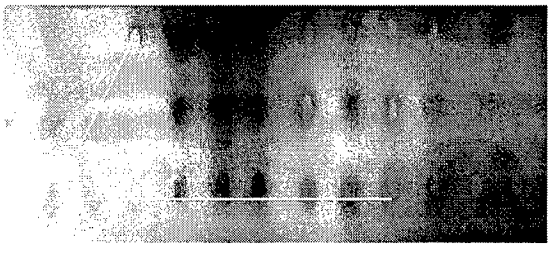

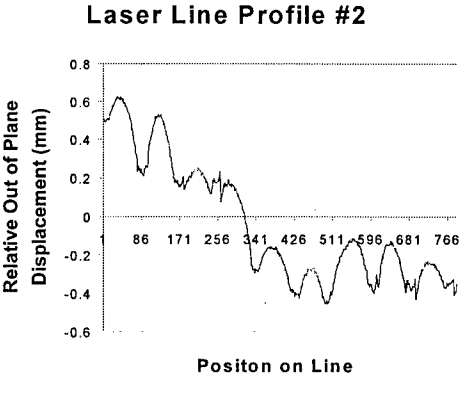

Figure 33 - Density plot derived from laser 3D image of pillowing in 727. Opposite is an accurate pillowing line profile along line #2, also derived from laser scan. (Original scan courtesy of T.Schoenhoffer, Vitana Inc.)

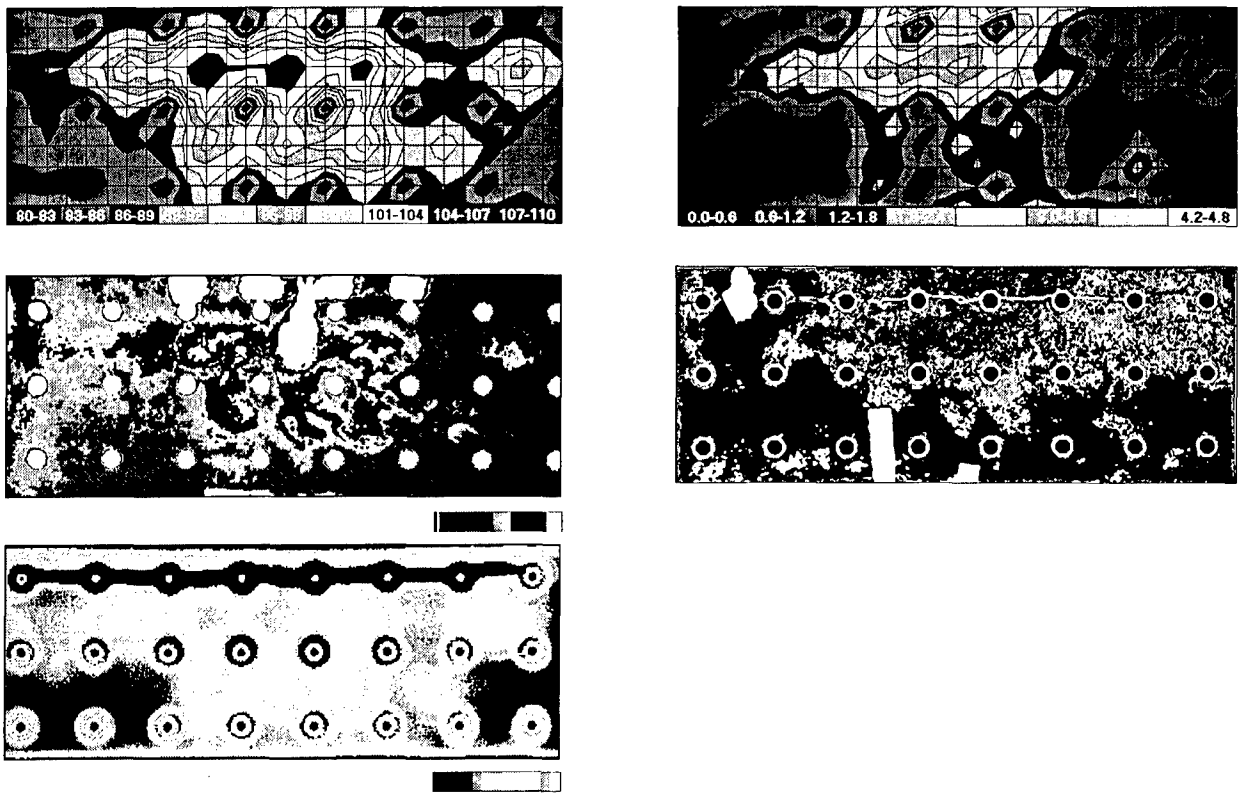

Figure 34 - Illustration of aggregate NDE maps of corrosion in both sheets of a MSD specimen – corrosion less than 4% average thickness loss. In column order: (1) pillowing amplitude measured on an intact splice with a micrometer; (2) x-ray density map of an intact splice; (3) single frequency eddy current C scan; (4) hand-held ultrasonic thickness (loss) measurements; (5) x-ray density map of splice after teardown and removal of corrosion product – can be accurately calibrated to give a thickness loss map. (J.P.Scott and C.E.Chapman)

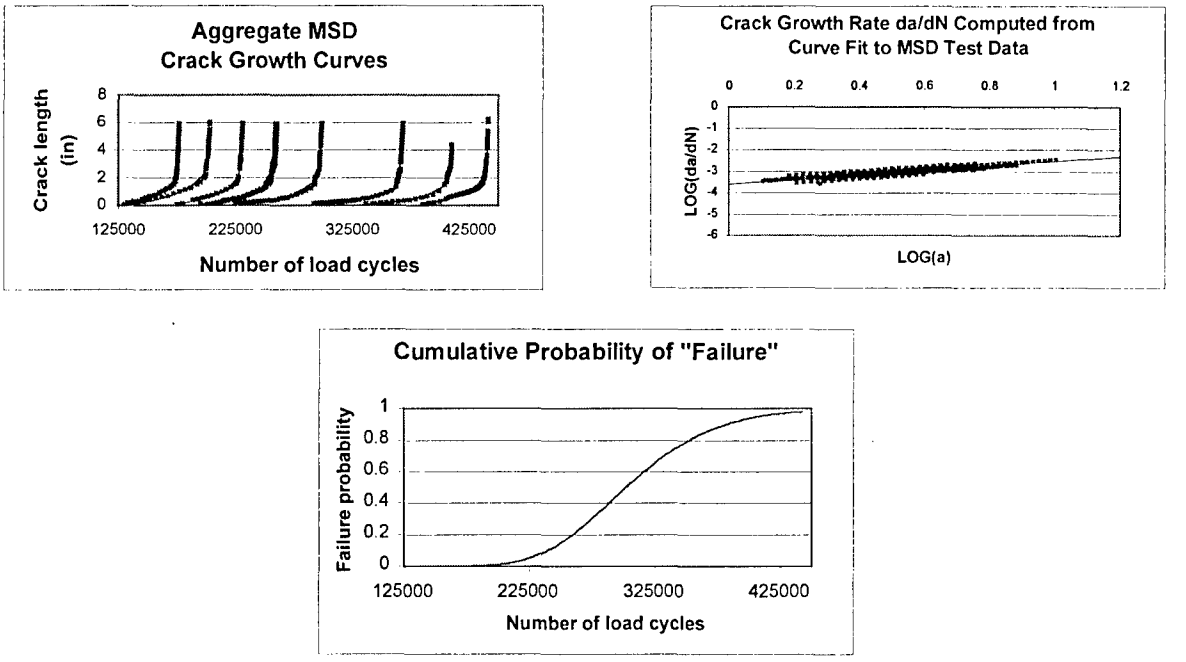

Figure 35 - Illustration of stochastic MSD crack growth model based on aggregate crack growth. Failure arbitrarily taken as exceedence of an aggregate crack length of 10.2 cm (4"). (Y.Xiong and G.Shi)

Risk Assessment of Fatigue Cracks in Corroded Lap Joints

Alan P. Berens
University of Dayton Research Institute
Dayton, Ohio 45469-0120 USA

J. Doug West and Angela Trego
Boeing Defense & Space Group
P.O. Box 7730 MS K86-74
Wichita, Kansas 67277-7730 USA

1. SUMMARY

As part of a program to develop analytical tools for predicting and validating the effects of corrosion on fatigue life assessments, deterministic crack growth predictions were made for a test specimen that is representative of a transport fuselage lap joint. Fatigue tests had been performed using this specimen and the results were made available by the National Research Council of Canada. The test data provided the necessary information to define boundary conditions, cracking scenarios, and initiating crack size distributions as well as to validate predictions. In addition to corrosion severity, which was modeled by the metric of uniform material thinning, the crack growth predictions also had to account for multiple site damage.

This paper uses the lap joint specimen test data and the deterministic crack growth predictions to demonstrate a risk analysis approach for quantifying random effects of factors associated with corrosion damage. Stress intensity factors and crack growth are calculated for selected percentiles of assumed distributions of corrosive thinning. Output from these deterministic analyses are then used in the risk analysis program Probability Of Fracture (PROF) to calculate conditional failure probability as a function of experienced cycles for the multiple sets of defined conditions. The results are interpreted by a comparison of risks for the various degrees of thinning and by an implied distribution of hours to reach a fixed failure probability for the assumed distributions of corrosive thinning.

2. INTRODUCTION

Fatigue crack growth predictions are at the core of damage tolerance analyses of metallic structures. To date, these predictions have been based on design geometries and material properties and do not account for the degradation associated with corrosion. Modeling tools and data are now being developed that will permit deterministic predictions of fatigue crack initiation and crack growth life in corroded structure. However, the severity and extent of corrosion and the unknown state of fatigue damage in aging aircraft are stochastic effects that must somehow be accounted for in the planning of inspections, repairs, and replacements. The traditional approach to accounting for random variation in life influencing factors is to make conservative assumptions that cover the expected scatter. In recent years, risk analysis has seen increasing use as an additional fleet management tool that directly addresses the stochastic nature of structural integrity [1, 2, 3].

Structural risk analysis is based on the probability of failure in a defined population of structurally significant details. In a fatigue environment, this probabilistic evaluation of strength versus stress is dynamic since strength degrades as fatigue cracks initiate and grow. Fracture mechanics provides deterministic tools that predict the growth of cracks for fixed stress sequences from an initial size to critical size. By introducing probabilistic descriptions of the factors that produce different initiating conditions and crack growth in the population, the results from deterministic tools can be extended to quantify the degree of safety during an operating period by calculating the probability of failure of a structural element as a function of time.

The objective of this paper is to demonstrate that risk analyses can also include a probabilistic description of corrosion severity. Failure probabilities are calculated using the computer program PRobability Of Fracture (PROF) which is based on deterministic damage tolerance analysis data and an initiating distribution of crack sizes in the population of details. The demonstration uses crack growth predictions and

Paper presented at the RTO AVT Workshop on "Fatigue in the Presence of Corrosion", held in Corfu, Greece, 7-8 October 1998, and published in RTO MP-18.

initiating data from a test program on a lap joint specimen that is representative of a cargo/transport airframe. A simple probabilistic description of multiple site damage (MSD) is also included in the example.

3. RISK METHODOLOGY

The risk analysis methodology of this paper uses a fracture mechanics based program, PROF, that was formulated for United States Air Force applications. The program uses the stress and crack growth data that are known to be available for all critical locations of structurally significant details because of the USAF Aircraft Structural Integrity Program. In PROF, the distribution of crack sizes at a critical location is grown by projecting the percentiles of the distribution in accordance with the calculated crack size versus flight time history for the anticipated stresses. Provision is made for updating the crack size distribution at inspection and repair intervals. A single run of PROF calculates the probability of failure as a function of flight hours from the joint distribution of crack sizes, maximum stress per flight, and fracture toughness. PROF input and output is presented in schematic form in Figure 1. See [4] for a complete description of the program and [3, 5, 6] for example applications.

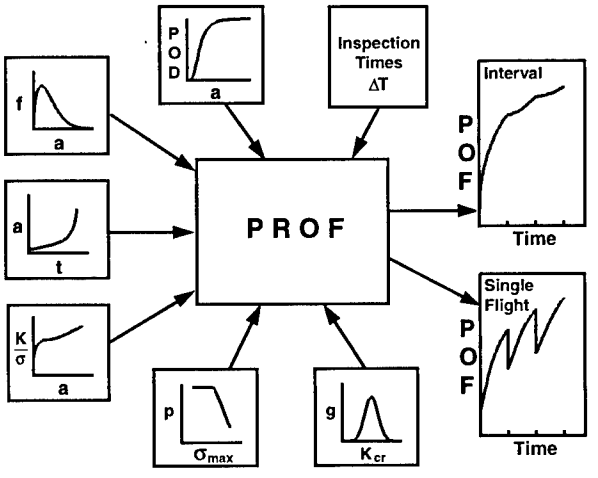

Figure 1. Schematic of PROF Calculation of Failure Probability

A single run of PROF produces failure probabilities for the specific population of details being modeled by the geometry and anticipated stresses of the deterministic crack growth model. For example, regions of equivalent stress and geometries are often identified for stress raisers in a fleet of aircraft. When the initiating crack size distribution is representative of all cracks that are present in the stress raisers in the fleet, the failure probabilities would be applicable to a randomly selected airframe from the fleet. There are many structural details for which this calculation is directly relevant and, in fact, decisions to change inspection schedules have been influenced by such risk calculations. However, there are also many structural details for which the conditions are not constant across an entire fleet and the effect of these conditions can be modeled through multiple runs of PROF.

The total population of details is divided into sub-populations of equivalent stresses and geometries. Conditional failure probabilities are calculated for each sub-population. The conditional probabilities can be directly interpreted in terms of the sub-population represented by the conditions. When the relative frequencies (probabilities) of the conditions are also known, the conditional fracture probabilities can be combined to provide an overall fracture probability as a function of time. This calculation is given by

$$POF(T) = \sum POF(T/C_i) \bullet P(C_i) \qquad (1)$$

where $POF(T/C_i)$ is the probability of failure at T given that condition C_i was used to determine the crack life of the structure and $P(C_i)$ is the probability that condition C_i applies and $\sum P(C_i) = 1$.

To illustrate this concept, consider the lap joint risk analysis that will be demonstrated in this paper. The population of lap joint specimens to be analyzed will be divided into sub-populations based on combinations of MSD scenarios and corrosion severity levels. Cracking occurred in dominant MSD scenarios whose influence on crack growth was exhibited through the stress intensity factor. Corrosion severity was characterized by the metric of uniform thickness loss whose influence on crack growth is exhibited through the experienced stress levels. Each combination of MSD scenario and thickness loss produces a different crack growth analysis so that each combination must be individually analyzed in the risk analysis. In this paper, two dominant MSD scenarios were judged sufficient to model the life determining lead cracks in the lapjoint. Five degrees of uniform thickness loss were assumed to represent degrees of corrosion severity.

		Dominant MSD		
Corrosion Severity	**Proportion of Joints**	**Scenario 1 p_1**	**Scenario 2 p_2**	**Composite over MSD**
Thickness Loss 1	q_1	$POF_{11}(T)$	$POF_{21}(T)$	$p_1POF_{11}(T)+p_2POF_{21}(T)$
Thickness Loss 2	q_2	$POF_{12}(T)$	$POF_{22}(T)$	$p_1POF_{12}(T)+p_2POF_{22}(T)$
Thickness Loss 3	q_3	$POF_{13}(T)$	$POF_{23}(T)$	$p_1POF_{13}(T)+p_2POF_{23}(T)$
Thickness Loss 4	q_4	$POF_{14}(T)$	$POF_{24}(T)$	$p_1POF_{14}(T)+p_2POF_{24}(T)$
Thickness Loss 5	q_5	$POF_{15}(T)$	$POF_{25}(T)$	$p_1POF_{15}(T)+p_2POF_{25}(T)$

$POF_{ij}(T)= POF(T/S_i,L_j)$ = Probability of failure for Scenario i, Thickness Loss j
p_i = Proportion of lap joints with crack initiating under Scenario i
q_j = Proportion of lap joints with uniform thickness loss at level j

Figure 2. Conditional Failure Probabilities for 2 MSD Scenarios and 5 Levels of Uniform Thickness Loss

Figure 2 illustrates the partitioning of the total population of the lap joints into the ten sub populations. Every lap joint must fit into one of the sets of conditions defined by MSD scenario and thickness loss. The probability that cracks will initiate under Scenarios 1 and 2 are p_1 and p_2, respectively. The probability that a randomly selected lap joint will have uniform thickness loss level j is q_j. $POF(T/S_i,L_j) = POF_{ij}(T)$ is the probability of fracture as a function of time for the combination of MSD Scenario i and Thickness Loss j. The calculation of the unconditional probability of failure for a random lap joint in the fleet for each corrosion severity level is shown in the last column. An analogous calculation could be performed across severity levels to obtain composite failure probabilities for each MSD scenario.

An interpretation of the corrosion effects can be made directly from the PROF output. If an estimate of the distribution of thickness loss in the fleet is also available, the results of the individual runs of PROF can be combined using Equation (1) to provide an overall fracture probability for a randomly selected detail. Further, the distribution of time to reach a fixed fracture probability can be inferred from the percentiles associated with the corrosion severity levels. These analyses will be demonstrated for corrosion in a representative lap joint.

It is realized that the risk analysis reported herein does not account for the stress levels increasing as a result of increasing corrosion over the analysis period. At present, there are no accepted models for the corrosion damage growth (thickness loss) as a function of time so that the crack growth calculations are based on the state of corrosion at the beginning of the analysis interval. In reality, the stresses in the spectrum should be slowly increasing. If this effect could be accounted for in the deterministic analysis, the crack growth data input to PROF would reflect the change. However, the peak stress distribution would need to be made more severe at discrete increments. This added complexity could be performed by performing multiple PROF runs. It might be noted that in the lap joint example of this paper, the peak stress distribution had no effect on the failure probability. The failure of the joint specimen was determined by reaching an unstable crack growth state when the lead crack reached a fixed size that was far below the critical crack size for the applied far field stress.

4. LAP JOINT CORROSION EXAMPLE

As part of a program to develop an analytical corrosion damage assessment framework [7], crack life predictions were made for a lap joint specimen to verify the prediction methodology. The lap joint specimens had been used in a fatigue test program by Carleton University and the National Research Council (NRC) of Canada [8,9]. The specimen, Figure 3, is constructed of two 1mm sheets of 2024-T3 clad aluminum with three rows of 4mm 2117-T4 rivets (MS20426AD5-5). The rivet pattern has 25.4mm pitch and row spacing with an edge margin of 9.1mm. The test specimens were 25.4cm wide with 8 fasteners in each row across the width.

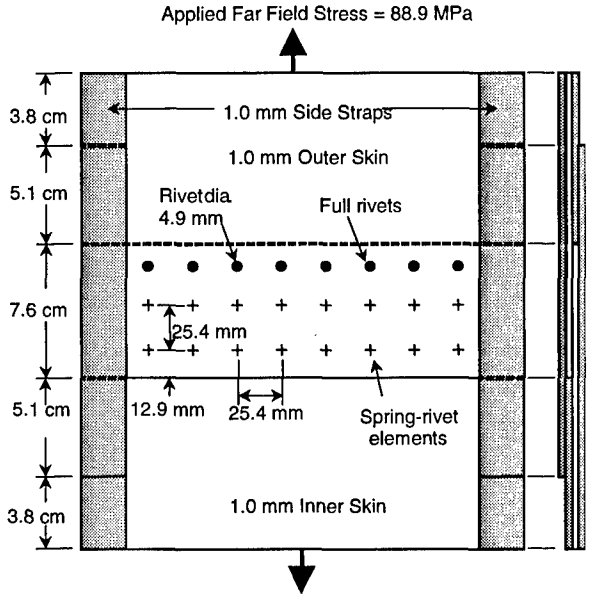

Figure 3. Schematic of Lap Joint Specimen

Constant amplitude fatigue tests had been conducted at Carleton University on the lap joint specimens in non-corroded and corroded conditions with a constant amplitude far field stress of 88.9 MPa with R = 0.2. Details of the test procedure and resulting fatigue crack growth data are presented in [8]. Nine non-corroded specimens were tested to failure to provide baseline data for comparison with corrosion specimens. Only data from these non-corroded baseline specimen tests are used in this paper. Histories of crack size versus cycles for all cracks that initiated in the top row of rivet holes were available for analysis. Examination of the histories showed that 95 percent or more of the joint life was expended when the lead crack reached about 9mm and crack growth became unstable. Further, lead cracks initiated in accordance with two dominant scenarios. In Scenario 1, a single crack originated from one side of a central hole. In Scenario 2, approximately simultaneous, diametric cracks originated from both sides of a central hole. Subsequent analysis showed significantly shorter lives for the double initial cracks. Analysis also showed that assuming both cracks were of equal size produced only 5 percent shorter lives than assuming one crack was twice the size of the second. Consequently, the assumptions were made that: a) joint life is determined by the initiation and growth of lead cracks that originate by one of two scenarios; b) the cracks are of equal size in the double crack scenario, and, c) the panel is essentially failed when the lead crack reaches 9mm.

Because first cracks were simultaneously discovered in different holes in four of the nine data sets, there were a total of 13 lead cracks. Eight were from Scenario 1 and five were from Scenario 2. For this population of structural elements, it was assumed that probability of a randomly selected lap joint having a Scenario 1 lead crack was 8/13 and the probability of a randomly selected lap joint having a Scenario 2 lead crack was 5/13.

Crack growth analyses were performed for both scenarios [10]. Stress analysis was performed using FRANC2D/L, a finite element, fracture mechanics analysis code with crack propagation capability [11, 12]. The resulting crack tip stress intensity factor values as a function of crack size were then input to the crack growth code AFGROW [13] for selected degrees of corrosion severity. The no corrosion, constant amplitude peak stress of the baseline fatigue tests and crack growth analyses was 88.9 MPa with an R ratio of 0.2. Predicted cyclic life from 0.25mm to 9mm averaged about 30 percent more than the test data.

Corrosion severity was modeled in terms of percent of thinning with the attendant increase in stress. To reflect corrosion severity, crack growth predictions were made for the somewhat arbitrarily selected levels of 2, 5, 8, and 10 percent corrosive thinning by proportionate adjustments of the stress levels.

5. RISK ANALYSIS (PROF) INPUT

The risk analysis for the lap joint corrosion example requires ten individual runs of PROF – two MSD scenarios and five stress levels for each of the MSD scenarios. The most significant inputs for the runs of this lap joint example are the crack growth projections and the initial crack size distribution. The other PROF inputs that reflect the changes between runs are the table of stress intensity factor divided by stress (K/σ) as a function of crack size and the distribution of peak stresses. These were changed between runs even though they had no affect on the results. K/σ came from the FRANC2D/L analysis. The peak stress distribution was estimated by a Gumbel extreme value distribution that had a mean at the appropriate constant amplitude level and a very small standard deviation to reflect the constant amplitude nature of the tests. Fracture toughness for the specimen was assumed to be normally distributed with a mean and standard deviation of 152 and 11.4 Mpa$\sqrt{m}$, respectively. Because the example being modeled does not include inspection and repair

cycles, reasonable, but arbitrary, data were used to define the inspection capability and the equivalent repair flaw size distributions.

The AFGROW crack growth curves for Scenarios 1 and 2 are presented in Figures 4 and 5, respectively. Each figure contains five crack growth curves reflecting the five levels of corrosion severity. The shorter crack growth lives from Scenario 2 are apparent from a comparison of these figures.

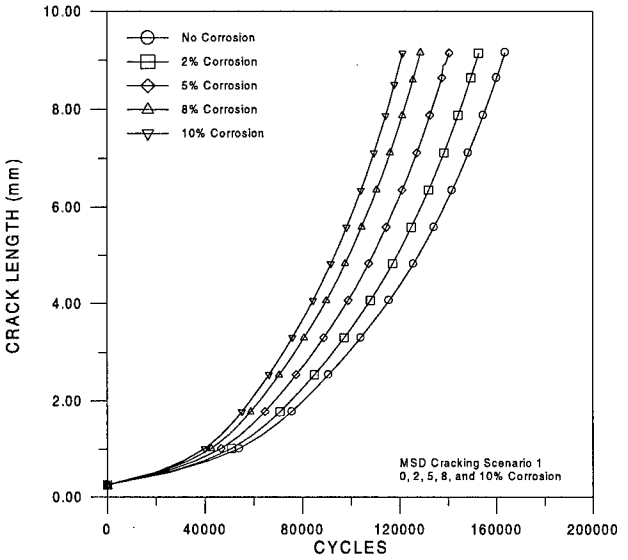

Figure 4. Crack Size versus Cycles for Scenario 1

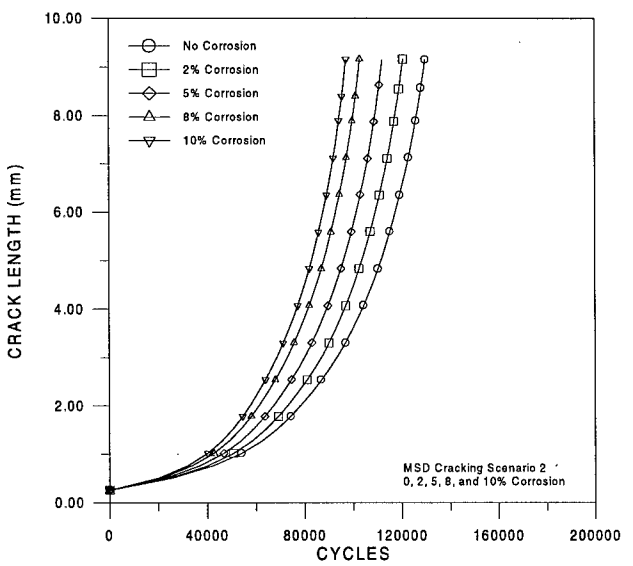

Figure 5. Crack Size versus Cycles for Scenario 2

The initiating flaw size distribution was generated by back calculating from the sizes of the first observed lead cracks and their corresponding ages in the specimen test data. The back calculation was performed in two steps. First the no corrosion crack size versus cycles data of Figures 4 and 5 were used to determine the time at which each lead crack would have reached 0.25mm. An exponential growth model was then fit to each lead crack to estimate an equivalent crack size at 50,000 cycles. The extrapolation process for the lead crack sizes is shown in Table 1. Note that the inverse of this process returns each of the observed lead cracks to its original size and cycles.

Table 1. Extrapolation for Initiating Flaw Size Distribution

Scenario 1 - Single Crack on Side of Rivet Hole					
ID	Size at 1st Obs.	Cycles at 1st Obs.	Cycles at c=0.25mm*	B=2.76e-05 A**	Size at 50000***
F1-4R	2.49	291955	202297	9.60E-04	3.81E-03
F1-3R	0.74	291955	251938	2.45E-04	9.70E-04
F3-5L	1.45	175000	107493	1.31E-02	5.20E-02
F4-4L	2.74	195000	100638	1.58E-02	6.29E-02
F6-4L	0.46	385000	364914	1.08E-05	4.31E-05
F7-4R	0.89	208006	160214	3.07E-03	1.22E-02
F9-5R	1.09	130103	73559	3.35E-02	1.33E-01
F9-4L	1.80	135000	58939	5.00E-02	1.99E-01
Scenario 2 - Double Cracks of Equal Lengths at Rivet Hole					
ID	Size at 1st Obs.	Cycles at 1st Obs.	Cycles at c=0.25mm*	B=2.70e-05 A**	Size at 50000***
F6-5L/R	1.40	385000	319467	4.60E-05	1.77E-04
F0-6L/R	1.98	336563	258737	2.37E-04	9.12E-04
F5-6L/R	2.41	133000	48075	6.93E-02	2.67E-01
F7-5L/R	2.06	201003	121787	9.53E-03	3.67E-02
F8-4L/R	2.31	225000	141641	5.56E-03	2.15E-02

* Translation from calculated c versus Cycles

** A = 0.25/exp(Cycles at 0.25 * B), B from 1st two points of calculated c versus Cycles

*** c = A exp(B*Cycles)

The times to reach 0.25mm for the cracks from the two MSD scenarios were statistically indistinguishable. Similarly, there was no statistical difference between the equivalent lead crack sizes from the two MSD scenarios at 50,000 cycles. The two sets of data were pooled to obtained the initiating flaw size distribution. The equivalent crack sizes at 50,000 cycles were fit with a mixture of two Weibulls as shown in Figure 6. Also indicated in Figure 6 are the MSD scenarios of origin of the lead cracks.

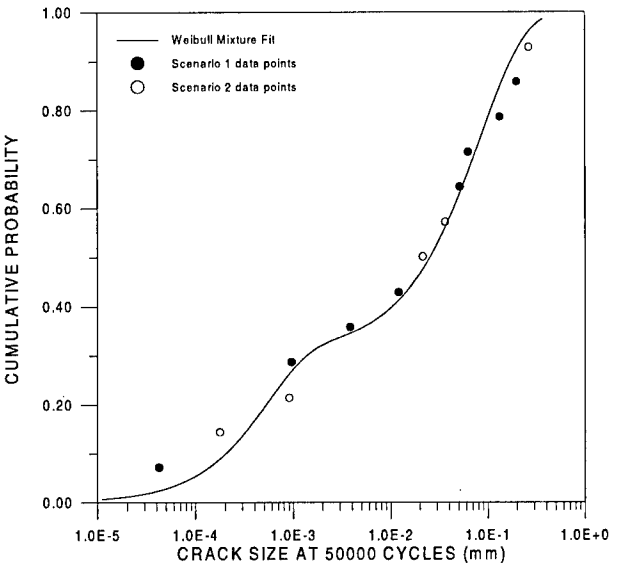

Figure 6. Weibull Mixture of Initial Crack Sizes

6. RISK ANALSYSIS RESULTS

Probability of failure as a function of cycles was calculated for each of the ten combinations of cracking scenario and corrosion severity. Failure of the lap joint specimens was defined as the lead crack exceeding 9mm, as previously discussed. Figures 7 and 8 present the failure probabilities as a function of experienced cycles for Scenarios 1 and 2, respectively. The failure probabilities behave as expected with increased risk of failure at a fixed age for Scenario 2 as compared to Scenario 1 and increasing risk of failure as the stress level increases due to corrosion material loss. These calculations do not account for any additional corrosive thinning after the start of the analysis.

As a gross check on the capability of the risk analysis methodology, Figure 9 compares the calculated probability of failure as a function of cycles for 0% corrosion for Scenarios 1 and 2 to the observed distributions of failure times. Superimposed on the predicted failure probabilities are the observed cumulative distributions of the cycles to failure from the lap joints that were the basis of the analysis. The observed cumulative distribution function was obtained by ordering the cycles to failure and dividing the ranks of the ordered times by the sample size plus one. That is,

$$F(T_i) = i/(n+1) \qquad (2)$$

where i is the rank for T_i, the time at which the i^{th} crack exceeded 9mm and n is the number of observed cracks that met the definition for the scenario. Sample sizes for Scenarios 1 and 2 were eight and five, as noted earlier. The differences between the observed and predicted probabilities of failure are most likely due to the conservative deterministic life predictions or the extrapolation of the crack size versus cycles relation that was required to obtain the initiating distribution of crack sizes.

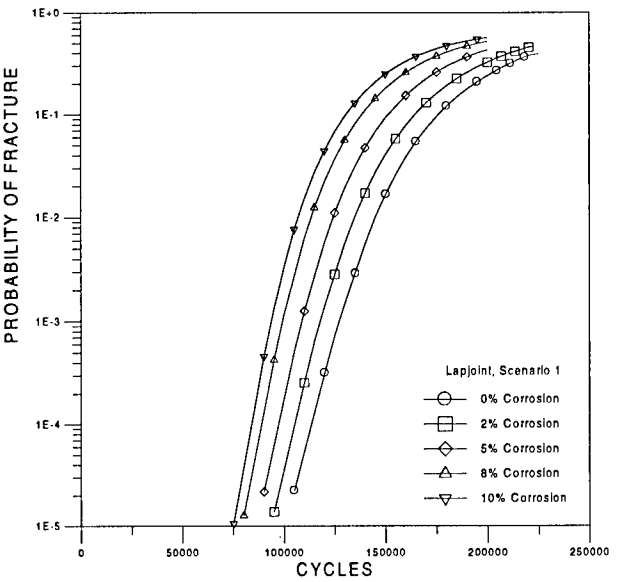

Figure 7. POF versus Cycles for Scenario 1

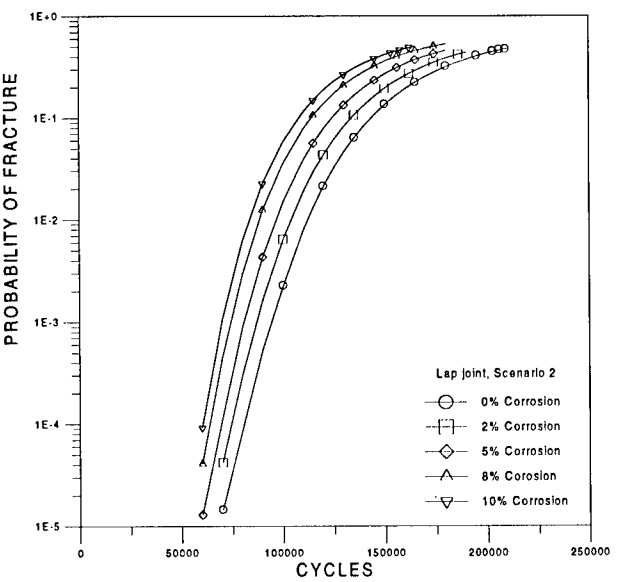

Figure 8. POF versus Cycles for Scenario 2

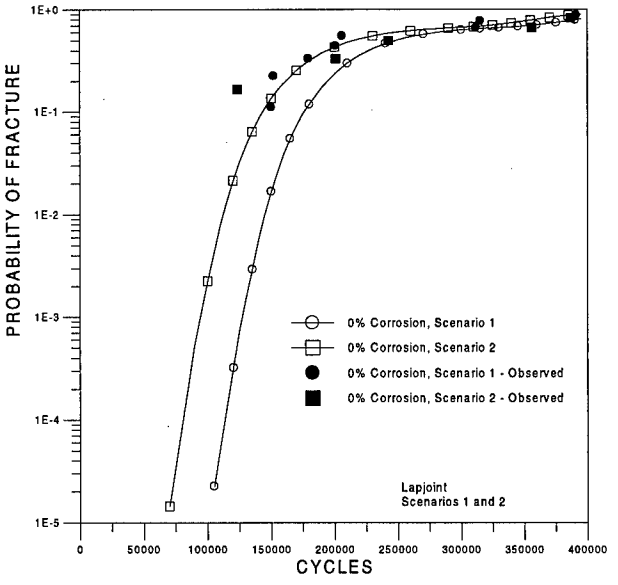

Figure 9. POF versus Cycles for Scenarios 1 and 2 Showing Comparison with Observed Data

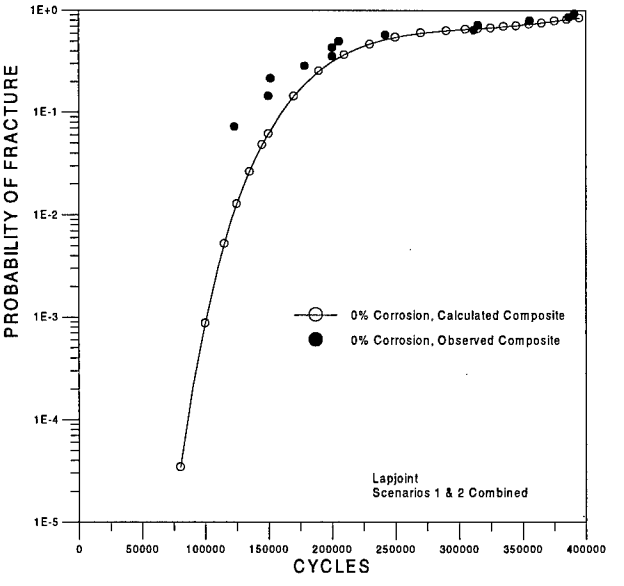

Figure 10. POF versus Cycles for Composite of Scenarios 1 and 2 Showing Comparison with Observed Data

Figures 7 and 8 present the conditional failure probabilities given the respective cracking scenario. The unconditional failure probability for a lap joint chosen at random from the population being analyzed is calculated as a weighted average of the conditional probabilities where the weighting factors are the proportion of specimens which will initiate cracks in the two scenarios. See Equation (1) and Figure 2. The weighting factors were estimated from the lap joint data in which 8 of the 13 lead cracks were from Scenario 1 (initial lead crack from one side of the hole) and 5 of the 13 were from Scenario 2 (initial lead crack from diametrically opposite sides of the hole). Using these factors, a comparison of the observed and predicted cycles to failure for the composite of the two scenarios without corrosion is shown in Figure 10. Again the difference between the predicted and observed distributions of cycles to failure displays the somewhat non-conservative risks of the predicted failure probabilities.

Figure 11 summarizes the probabilities of failure for a randomly selected lap joint that can have either MSD scenario and is subject to the expected stress history for five levels of corrosion severity. These results will be interpreted both in terms of the times to reach a defined probability of fracture (POF) and in terms of the relative differences in POF at a fixed number of cycles.

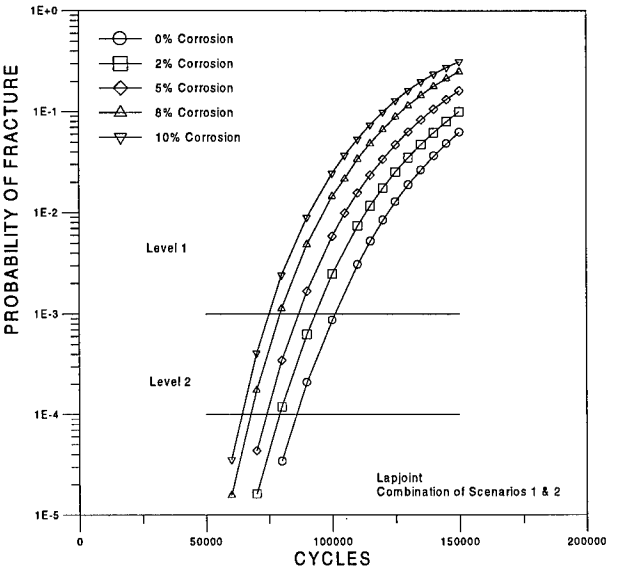

Figure 11. POF versus Cycles for Scenario Composites

The cycles to reach a fixed POF for the different degrees of corrosion severity can be read from Figure 11 as indicated, for example, at POF equal to 0.001 and 0.0001. Assume that the proportion of lap joints in the population that contain each of the five degrees of corrosion is known. Then the distribution of the

time to reach the POF levels can also be inferred. To illustrate, three representative distributions of corrosion damage were assumed, as given in Table 2. Mix 1 is symmetric about a five percent material loss. Mix 2 is representative of a more severely corroded population. Mix 3 is representative of a less severely corroded population and is considered to be more representative of the corrosion that would be expected in aircraft. Figure 12 presents a histogram of Mix 3. The corresponding percentage of lap joints would be expected to reach the selected POF level in the indicated number of cycles. The histogram for cycles to reach POF = 0.0001 for severity Mix 3 is shown in Figure 13. The cumulative distribution of time to reach the two POF levels for the three distributions of corrosion severity are shown in Figure 14.

Table 2. Representative Corrosion Level Damage Distributions

% Joints with Corrosion Severity			
Severity	**Mix 1**	**Mix 2**	**Mix 3**
0%	5	5	15
2%	20	15	40
5%	40	35	25
8%	25	35	15
10%	5	10	5

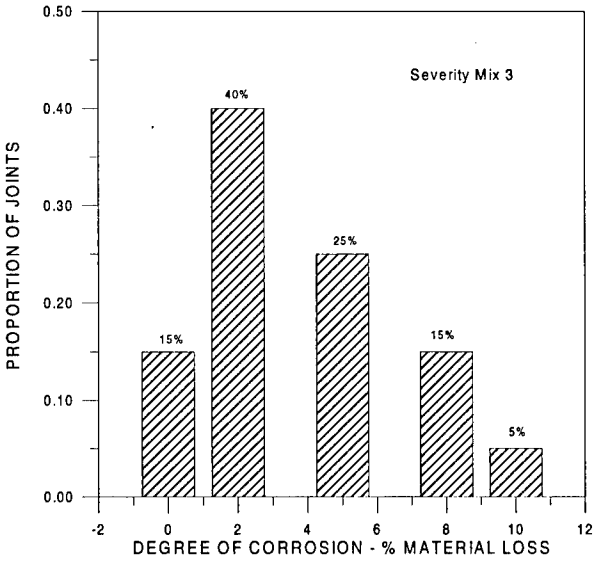

Figure 12. Example Histogram of Levels of Corrosion Damage – Severity Mix 3

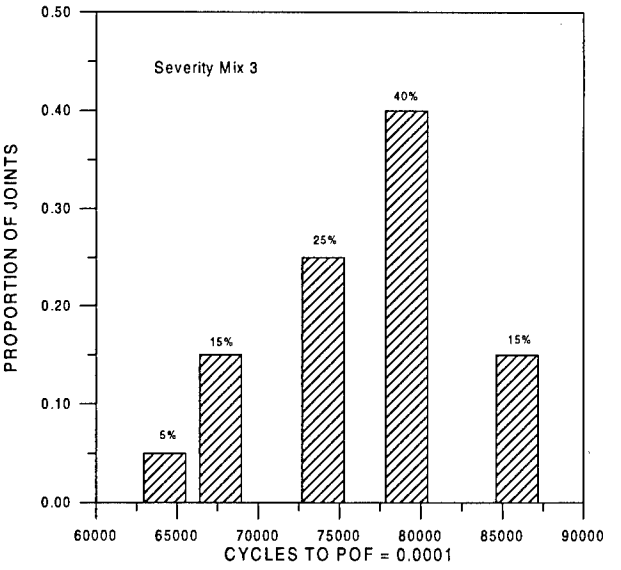

Figure 13. Example Histogram of Cycles to POF = 0.0001 – Severity Mix 3

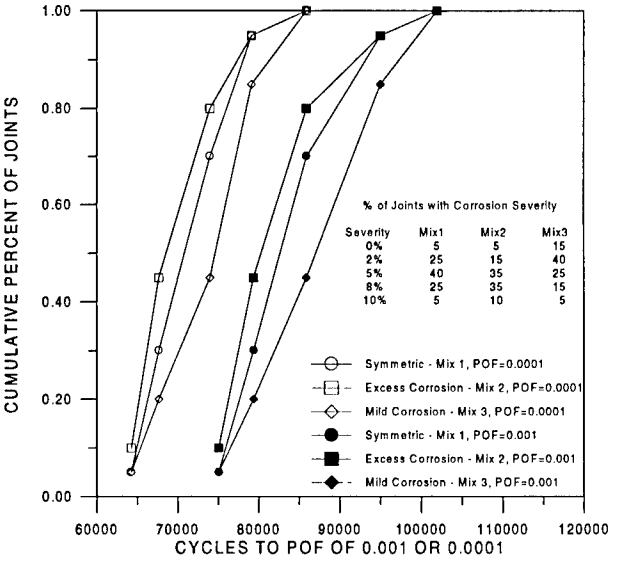

Figure 14. Cumulative Distributions of Cycles to Selected POF – 3 Corrosion Severities

At a fixed number of cycles, the failure risk of a corroded lap joint can significantly exceed that of a non-corroded lap joint. To illustrate this difference, Figure 15 presents the ratio of failure probabilities for each of the four degrees of corrosion severity to that of the non corroded lap joints. The ratios are presented as a function of the failure probability of the non corroded lap joint. The lap joint failure

probability for the severity characterized by ten percent thinning can be 70 times greater than that of a non corroded lap joint. If maintenance scheduling were based on keeping the failure probability below about 0.0001 to 0.001, a lap joint with ten percent corrosion thinning would have a 25 to 50 times greater chance of resulting in fracture.

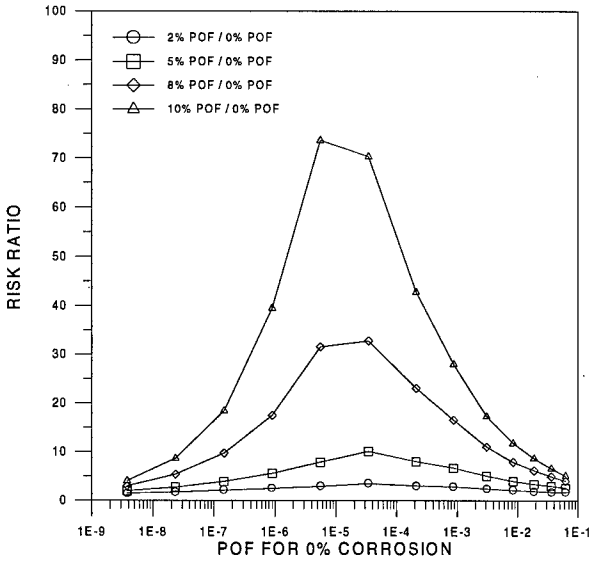

Figure 15. Risk Ratios Normalized to No Corrosion Condition

7. CONCLUSIONS

The use of risk analysis in structural maintenance planning recognizes that many life influencing factors may be unknown, and possibly unknowable, for all equivalent details in an entire fleet. When acceptable conservative bounds cannot be determined for the condition of the higher order of importance factors, uncertainty in the characterization of the factors can be introduced in the form of distributions of severity. The risk analysis approach quantifies the degree of safety in terms of the likelihood of failure of the detail. The timing of maintenance actions can then be planned on the basis of keeping the probability of failure acceptably low or on the basis of minimizing ownership costs that also include the costs that are the result of unlikely, but possible, failures.

This paper demonstrates that it is possible to extend deterministic fracture mechanics crack growth results to include probabilistic descriptions of the factors which influence fatigue life. In particular, a risk analysis was performed for fatigue failures in a representative lap joint in which the crack growth calculation was influenced by corrosion thickness loss and two scenarios of MSD. The basic approach to the analysis is to use deterministic crack growth calculations for different percentiles of the influencing factors in the probability of failure calculations, yielding conditional probabilities of failure. The full use of the analysis assumes that estimates of the distribution of the influencing factors are available so that the conditional failure probabilities can be combined or otherwise interpreted.

In the lap joint example of this paper, the relative frequency of the two dominant MSD scenarios was estimated from data from a test program of the modeled specimen. Example distributions of thickness loss were assumed to demonstrate the calculations and interpretation. For this example, a ten percent thickness loss increased the failure probability by a factor of as much as 70 over the no corrosion condition. Depending on the consequences of failure, inspection intervals based on the no corrosion stress levels could pose a safety issue to corroded joints. The results were also used to demonstrate the generation of the distribution of time to a fixed risk.

The risk analysis calculations of this study are dependent on the quality of the deterministic crack growth analysis and the quality of the crack size data that characterize the damage state of the structural element. At present, crack growth modeling techniques which account for all of the complexities of corrosion damage are under development. Further, data for characterizing the crack size distribution in a population is generally sparse.

8. REFERENCES

1. Lincoln, J.W., "Risk Assessments – USAF Experience," Proceedings of the International Workshop on Structural Integrity of Aging Airplanes, Atlanta, GA, 31 March – 2 April 1992.
2. Manning, S.D., Yang, J.N., and Welch, K.M., "Aircraft Structural Maintenance Scheduling Based on risk and Individual Aircraft Tracking," Theoretical Concepts and Numerical Analysis of Fatigue, A.F. Blom and C.J. Beevers, Eds., Engineering Materials Advisory Services, LTD, London, 1992, pp. 401-420.

3. Berens, A.P., "Applications of Risk Analysis to Aging Military Aircraft," SAMPE Journal, Vol. 32, No. 5, September/October 1996, pp. 40-45.
4. Berens, A.P., Hovey, P.W., and Skinn, D.A., "Risk Analysis for Aging Aircraft, Volume 1 – Analysis," WL-TR-91-3066, Air Force Research Laboratory, Wright-Patterson Air Force Base, Ohio, October, 1991.
5. Berens, A.P., "Risk Analysis Input for Fleet Maintenance Planning," Structural Safety and Reliability, Schueller, Shinozuka, and Yao (eds.), Balkema, Rotterdam, 1994.
6. Berens, A.P. and Burns, J.G., "Risk Analysis in the Presence of Corrosion Damage," AGARD - CP- 568, Widespread Fatigue Damage in Military Aircraft, NATO, Advisory Group for Aeronautical Research and Development (AGARD), Neuilly-Sur-Seine, France, December, 1995.
7. D500-13008-1 (1998). "Corrosion Damage Assessment Framework". The Boeing Company, Seattle, WA. Release date August 5, 1998.
8. Scott, J.P., "Corrosion and Multiple Site Damage in Riveted Fuselage Lap Joints," Master's Thesis, Carleton University, March 1997.
9. Eastaugh, G.F., Simpson, D.L., Straznicky, P.V., and Wakeman, R.B., "A Special Uniaxial Coupon Test Specimen for the Simulation of Multiple Site Fatigue Crack Growth and Link-Up in Fuselage Skin Splices," National Research Council of Canada and Carleton University, AGARD-CP-568, December 1995.
10. Trego, A., Cope, D., Johnson, P., and West, D., "Analytical Methodology for Assessing Corrosion and Fatigue in Fuselage Lap Joints," 1998 Air Force Corrosion Program Conference Proceedings, April 1998, Macon, Georgia.
11. Wawrzynek, P.A., and Ingraffea, A.R., "FRANC2D: A Two-Dimensional Crack Propagation Simulator, Version 2.7, User's Guide," NASA CR-4572, March 1994.
12. Swenson, D. and James, M., "FRANC2D/L: A Crack Propagation Simulator for Plane Layered Structures", Version 1.4 User's Guide, Kansas State University, December 1997.
13. Boyd, K., Harter, J.A., and Krishnan "AFGROW User's Manual Version 3.1.1," WL-TR-97-3053, Air Force Research Laboratory, Wright-Patterson Air Force Base, Ohio, February, 1998.

Integrating Real Time Age Degradation Into the Structural Integrity Process

Craig L. Brooks*
Analytical Processes/Engineered Solutions Inc.
3542 Oxford Avenue
St. Louis, MO, USA 63143

David Simpson**
National Research Council of Canada
Ottawa, Ontario, Canada
K1A 0R6

Abstract

The principal focus of this paper is to describe a process for incorporating the "age degradation" aspects of aircraft into the existing infrastructure of the design, manufacturing, and maintenance of aircraft systems. The tailoring of the structural integrity process enables the industry and the user communities to meet the needs, opportunities, and challenges being presented by the Aging Aircraft Fleet. The economic and safety impact of the continued use of some aircraft necessitates an enhancement to the existing system. This paper describes the rationale, approaches, and techniques to evolve the structural integrity process to include the effects of corrosion, sustained stress corrosion cracking, and other age related degradation effects. A viable method of utilizing the proposed approach is presented in a fashion to realize benefits throughout the full life cycle of aircraft systems.

Introduction

The demands for extended use of the aging aircraft fleets around the world are providing new challenges to the aerospace community to ensure continued safety, readiness, and reduced costs. Integrity can be built into a product with the existing processes, but can not be proclaimed into an existing aircraft system. For an existing fleet, the challenge is to maintain safety and readiness while keeping control of operating and maintenance costs.

The responsibility for ensuring continued safety and readiness for the aging fleets lies primarily with the end users. Design decisions made, however, by the Original Equipment Manufacturer (OEM) heavily influence the operators' ability to maintain appropriate levels of safety and readiness in a cost-effective manner. Current structural integrity processes focus on usage related degradation such as static strength, fatigue and damage tolerance but do not fully address real time related degradation phenomena such as corrosion. There are cost and safety benefits to integrating consideration of real time based degradation mechanisms with the current structural integrity processes.

Modifications to the existing structural integrity processes are required to:

- include technical issues associated with actual use and effects of the field environment;
- consider maintenance practices and information gained from maintenance programs that were not included in the design criteria or covered in the in-service maintenance plans;
- provide the end users with the appropriate technical information and engineering tools to effectively manage aging aircraft;
- ensure that all disciplines adequately interact during the design phase to address the issues of degradation of the assembled aircraft in the field environment;
- incorporate recent advances in corrosion assessment and prediction technologies that are not included in conventional practices and procedures.

The objective of this paper is to establish the case that it makes both safety and economic sense to be proactive in managing the durability and structural integrity impact of corrosion. This can be achieved by entrenching quantitative consideration of real time degradation processes in the design requirements for new aircraft and by providing the engineering processes and data to support the maintenance, inspection, repair and life extension of existing aircraft.

Situation

The term "aging aircraft" is relatively new and was introduced to describe the circumstance whereby a large number of the world's aircraft fleets were operating in regimes beyond their initial design goals. The implication of this predicament is that the aircraft are venturing into operating regimes and potential risk areas that were not evaluated by the design certification processes. New failure modes such as multiple-site damage and loss of fail-safety have been identified. Higher risks and costs associated with time related phenomena such as corrosion, stress corrosion, and general wear are also being encountered.

Aircraft can "age" in a variety of ways. There is the real time scale that is a simple measure of how old the aircraft is. Another is the usage scale that is a measure of how far the aircraft has progressed towards its fatigue design life. Finally, there is the operational capability scale that is a measure of how capable and efficient the aircraft is in performing its assigned role in its current operational environment. Figure 1 illustrates this situation.

The optimum, from an economic viewpoint, is to ensure that the aircraft proceeds along these scales in a relatively parallel fashion such that the aircraft just reaches its full certification life limits at the time of operational obsolescence and at a real time that is maximized. A more practical concern is to avoid costly life extension and operational upgrade programs on aircraft that are life limited or uneconomical due to real time process degradation.

---

* President and Chief Engineer, Analytical Processes/Engineered Solutions
** Director, Institute for Aerospace Research, Structures Materials & Propulsion Laboratory

Paper presented at the RTO AVT Workshop on "Fatigue in the Presence of Corrosion", held in Corfu, Greece, 7-8 October 1998, and published in RTO MP-18.

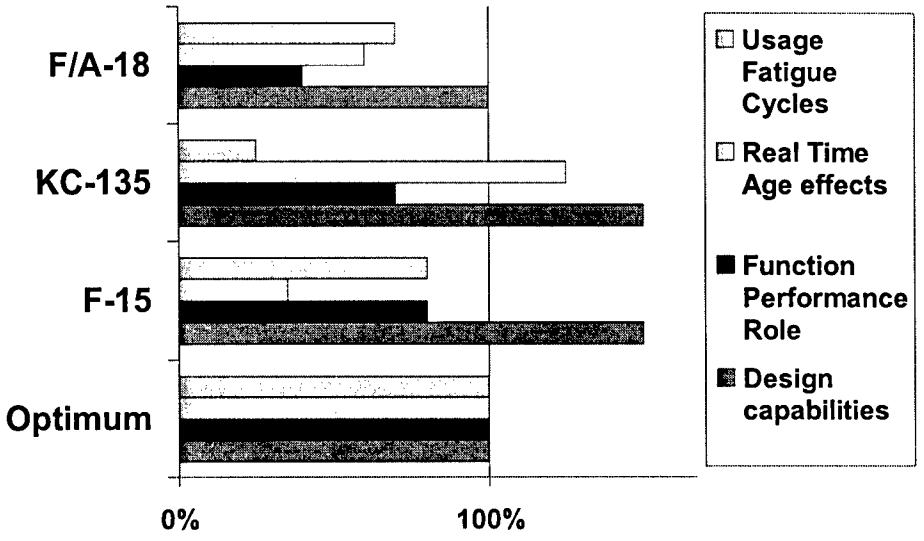

Figure 1 Aging Processes

The goal of both the designer and the life cycle manager should be to ensure this happens. The designer should evaluate the intended role(s) and performance goals of the aircraft and then formulate technical specifications to ensure that the aircraft will meet these goals and also satisfy the regulatory requirements. The life cycle manager has several tools that can be used to modify the rate at which an aircraft ages along any of these scales. These include repair and overhaul of the airframe at selected times to address time-related issues such as corrosion, aggressive fatigue life management programs that modify the rate of usage damage accumulation, mid-life structural modification programs, operational or performance enhancing modification programs and life extension programs.

Historically, aircraft have been retired from service for reasons of technical or economic obsolescence (no longer proficient at performing its role), changes in strategic scenarios, or because the usage (fatigue) life has been expended. Rarely have they been retired because of real time processes such as corrosion.

Economic considerations have become more dominant. For the military, reduced capital budgets and more attention to the bottom line as well as a perceived reduction in military threat have resulted in a new paradigm whereby it is more cost effective to pursue life extension programs for existing aircraft than it is to introduce new aircraft. Civil operators have had similar constraints. In terms of usage, fatigue life enhancement technologies, advanced repair technologies and major re-builds supported by modern analysis and test programs have been successful. Operationally, major equipment upgrades, particularly to the avionics and engines, have resulted in improved performance. These programs have been successful because they are reacting to known structural deficiencies (from the certification process, as a result of secondary analytical reviews or mid-life structural testing or from in-service experience) or quantified operational deficiencies.

More challenging is how to address the real time degradation processes or more specifically, how to address influence of corrosion. Schutz[1] raises serious concern regarding prediction capabilities for residual life of corroded structure. Lincoln[2] expressed some concern that though the highly successful United States Air Force (USAF) Aircraft Structural Integrity Program[3] (ASIP) maintains a structural failure rate of less than 1 in 10 million flying hours, this may not be adequate in the future if aircraft are operated beyond their design service life. He cites the influence of corrosion on crack growth acceleration and the early onset of wide spread fatigue damage as major concerns. Mar[4] comments that the synergy between corrosion and crack initiation is not well understood and is not considered during the design phase and that corrosion must therefore be controlled to prevent excessive material loss or undetected crack initiation.

The issue is not only the immediate problem of the current fleets of "aging" aircraft but also the future fleets of "aging" aircraft. Aircraft currently operating within their design service life boundaries will, without doubt, be extended beyond these boundaries. The "aging" aircraft situation is not short term in nature but rather represents a fundamental shift in the way aircraft will be operated and extended in the future. It is therefore axiomatic that this fundamental shift be addressed fully through process changes to the design and manufacturing stages and to the in-service life cycle management practices. Engineering tools and data to efficiently address these issues are required for both safety and economic reasons.

Potential Economic and Safety Impacts

The essential issue of whether or not the current corrosion preventative programs and current approaches to managing the impact of corrosion on airworthiness is "sufficient". A review of the available data indicates that these programs are not sufficient for determining impact of corrosion on the economic and flight safety aspects of aircraft life cycle management.

Economic Impacts

The economic impact of corrosion is well recognized and substantiated by estimates of corrosion related costs from many sources[5,6,7]. For example, a United States National

Research Council report[8] identified corrosion as the "most costly maintenance problem in the USAF," and it has been estimated that corrosion costs the USAF in excess of $1 billion and the United States about $13 billion annually[5,9]. The Canadian Forces, which operate a number of "aging" aircraft, have also identified corrosion-related costs as their highest maintenance expenditure.

A comprehensive US Air Force study into costs of corrosion maintenance[10] confirms the intuitive conclusion that aircraft related costs are increasing at an accelerating rate as the continued operation of aging aircraft expands. This extended operation results in new corrosion sites and re-occurrences of corrosion in previously repaired sites that leads directly to increased costs and downtime. This upward trend will continue as more aircraft reach the aging category, although the rate of increase may diminish due to the more corrosion resistant materials and design/manufacturing processes used in the more recently designed aircraft. Even for these aircraft, corrosion cannot be eliminated. Another potential influence on the long-term corrosion performance of today's aircraft is the elimination of some of the most effective corrosion inhibitors, such as chromic acids, due to environmental considerations. It is not known how well the replacement processes will perform under real conditions over 20 to 50 years?

The economic situation exists, therefore, where even incremental improvements in corrosion prevention and in-service management can result in substantial cost avoidance. There are opportunities for improvements in how corrosion is addressed both in the design/manufacturing process and during in-service management that will reduce costs and provide important returns on technology investment.

For in-service management, substantive efforts are underway world-wide to develop better corrosion detection and quantification techniques, particularly for hidden corrosion or corrosion in second and deeper layers. In parallel, there are several programs currently in progress at the National Research Council of Canada (NRCC) and in the US and Europe that are attempting to develop analytical capabilities to support corrosion damage assessments of aircraft structures. These analytical models will require, as input, quantified corrosion damage data from non-destructive inspections. The outputs from the corrosion damage assessments will allow the planning of maintenance actions depending on the current state of corrosion, its influence on structural integrity and its projected growth.

The intent of such programs is to move away from the current *"find it-fix it"* philosophy of dealing with corrosion to managed proactive maintenance that considers both safety requirements and economic issues. One suggested approach for the future is *"find it sooner-evaluate-plan-fix"*. Advances in NDI allow earlier identification of corrosion[11]. To take full economic advantage of this earlier detection, the operators must be allowed increased repair scheduling flexibility if they can demonstrate that structural integrity is not compromised. Regulatory mandated inspections must be based on a real consideration of the impact of the corrosion on structural integrity, not set by arbitrary and conservative assumptions. The corrosion damage assessment process can be used to plan repair actions for the corrosion such that down time and repair costs are minimised and the risk of incurring additional damage is reduced. The operator can choose between early resolution or a later resolution by accepting the penalties of an inspection burden and potentially a more complicated and costly repair.

As will be discussed later in the document, the methods used for engineering disposition of in-service corrosion can also be used during the design phase to evaluate the sensitivity of critical structure to the onset of corrosion. This evaluation can lead to improved corrosion resistant structure and to more efficient inspection programs. In the same way that damage tolerant assessments can identify fracture critical structure, corrosion sensitivity analysis can identify corrosion critical structure. Economic gains can be realised.

Safety Impacts

Hoeppner[12] has provided the most recent and comprehensive review of United States engine and airframe failure statistics involving corrosion and fretting. Using a Campbell and Lahey[13] report that contained a major world-wide review of fixed wing and rotary wing aircraft accident statistics, Hoeppner concluded that corrosion and fretting contributed to 13% of the 449 fixed wing cases and 23% of the 125 rotary wing cases.

Recent studies of corrosion in transport aircraft fuselage lap joints also indicate that corrosion may have safety implications[14]. Corrosion at the faying surface of riveted sheets produces the well-known pillowing effect, and multiple, hard-to-detect surface cracks. The effects of these cracks on residual strength and residual life due to the interaction between corrosion and fatigue raises concerns for the safety of continued operation of corroded fuselages. Because the cracks are not detectable on the surface by visual inspection or by high frequency eddy current, this is a particularly nasty form of multiple site damage.

Reference[16] cites recent examples of corrosion problems in three USAF aircraft that raised safety concerns. The major conclusions of this study were:

- Corrosion damage in critical structure has resulted in an initial flaw size that dramatically reduced the predicted life of a critical component;
- Corrosion damage in structural elements has changed a component's status from non-critical to critical;
- Durability Assessment and Damage Tolerance Analysis (DADTA) studies do not provide inspection locations and intervals for the observed corrosion problems;
- Corrosion damage has led to flight safety concerns for a number of locations on the C-5 and prompted changes to inspection procedures;
- Corrosion has led to premature cracking of major structural elements, significantly earlier than DADTA predictions.

Berens and Burns[17] performed a risk analysis of a representative wing lower front spar structure with and without corrosion using assumptions that the only real effect of the corrosion was thinning. No pitting or stress redistribution was assumed. The fracture risks increased by more than an order of magnitude over that of the uncorroded baseline structure. The authors' basic conclusion was that if the inspection intervals are set by the fracture performance of the pristine structure, the accelerated damage effects of corrosion would be a safety issue.

Corrosion, particularly undetected or hidden corrosion, can and most likely will become a safety issue. The two ways to address this problem are to ensure that corrosion is detected in flight critical structure at a demonstrated confidence level or to generate inspection requirements based on degraded structural performance assuming the presence of corrosion.

Structural Integrity Process

Regulatory agencies, both civil and military, have similar goals: maintenance of an appropriate level of safety throughout the full economic life of the structure without undue restrictions on availability and cost. The USAF Aircraft Structural Integrity Program[3] (ASIP) was defined in the early 70's and has been adopted or adapted by the regulatory agencies of many countries. It is organized into 5 tasks (Figure 2) and addresses not only structural airworthiness but also offers a more holistic management plan covering all aspects of the integrity process from technology development, technology implementation, compliance demonstration and in-service management. This paper will use the ASIP model as a way of organizing the discussion of where the current ASIP process requires augmentation to address corrosion more comprehensively. Tasks 1 through 3 provide the engineering foundation for Tasks 4 and 5. If not all aspects of the degradation of structural integrity are addressed during the first three tasks, Tasks 4 and 5, which are essential for continued safety and durability, will be incomplete. This leads to unplanned actions resulting in higher costs, reduced availability and reduced safety. The success of the ASIP program is that current failure rates due to structural causes are less than one in ten million flying hours.

The implementation of the ASIP process was costly and time consuming and involved organized Durability and Damage Tolerance Reviews of the existing USAF fleets. Similarly, the civil regulatory agencies introduced a form of ASIP reviews in defining the Supplementary Inspection Documents for the aging airliner fleet. Current design requirements incorporate durability and damage tolerance assessments as part of the design process. As will be discussed in the following sections, there are significant benefits to integrating quantitative considerations of the safety and durability impacts of corrosion early in the design process.

Welburn stated that up to 90% of life-cycle costs are determined as a result of design and manufacturing decisions[18]. As corrosion related activities have been identified as one of the most costly items, it is important that it be appropriately integrated technically into the design/manufacturing decision processes. ASIP, like other structural airworthiness requirements, does not ignore corrosion and states explicitly: Design analyses and development tests must account for "the environments in which the airframe must operate" in designing and sizing the airframe. The requirements do not state that corrosion degradation of the structure must be assumed which means that this environmental degradation requirement can be met through corrosion prevention and inspection programs leading to the design assumption that corrosion does not need to be considered quantitatively.

In reality, corrosion does occur and, as previously discussed, occurs with increasing frequency as the aircraft ages and is therefore a prime concern for aging aircraft. The current approach to corrosion as something that can be prevented has a parallel in the early approach to managing fatigue cracks as something that can be prevented through safe life design. Ignoring the potential occurrence of fatigue cracks lead to highly fatigue resistant but non-damage tolerant component designs and material choices. Similarly, ignoring the potential occurrence of corrosion can lead to design configurations and material choices that result in early crack initiation and accelerated crack growth if corrosion does occur. There is a requirement to quantify the structural performance of selected critical areas with assumed corrosion present.

TASK I	TASK II	TASK III	TASK IV	TASK V
DESIGN INFORMATION	DESIGN ANALYSES & DEVELOPMENT TESTS	COMPONENT & FULL SCALE TESTING	FORCE MANAGEMENT DATA PACKAGE	FORCE MANAGEMENT DATA PACKAGE
Integrity Master Plan Structural Design Criteria Damage Tolerance & Durability Control Plan Selection of Mat'ls & Processes Design Service Life and Design Usage	Materials & Joint Allowables Loads, Sonic, Vibration & Flutter Analysis Design Service Loads Spectra Design Chem./Therm. Environment Spectra Stress Analysis Durability & Damage Tolerance Analysis Design Development Testing	Static, Durability & Damage Tolerance Tests Flight & Ground Operations Tests Sonic, Flight Vibrations, and Flutter Tests Interpretation & Evaluation of Test Results	Final Design Analyses Strength Summary Force Structural Maintenance Plan Loads/Environment Spectra Survey A/C Tracking Program	Loads/Environment Spectra Survey A/C Tracking Data A/C Maintenance Times Structural Maintenance Records

Figure 2 Aircraft Structural Integrity Program Tasks

There are significant benefits to integrating quantitative considerations of the safety and durability impacts of corrosion early in the design process. Initially, this would allow more realistic consideration of cost-benefits of design and manufacturing decisions. Minor modifications to reduce costs during these initial phases can have extraordinary influences on the cost of operation. Also, re-evaluation of current fleets using enhanced processes for evaluating both the likelihood of corrosion occurring and the impact of the corrosion on the structural integrity and durability of the aircraft, would result in economic and safety benefits through more educated fleet management.

Aspects of the Present Design

The most cost-effective time to incorporate structural integrity into an aircraft system is during the design/manufacturing phase. Although re-manufacturing, retrofits, depot repairs, and modifications can be effective post design improvements with long range benefits, they are more costly to implement. The evolution of the integrity processes for all systems has captured lessons learned resulting in improved vehicle performance and service life capability. The challenge is to capture "Lessons Learned" for implementation into the design process prior to a costly and life threatening catastrophic event. This section of the paper discusses some aspects of the present design process and identifies some shortcomings pertinent to the consideration of corrosion and sustained stress effects on the integrity of the system. Current design processes used by the OEMs can be modified to address potential future corrosion and sustained stress issues in new designs. These same enhanced processes can be used to support the aging fleet.

The Design Process

The design procedures within OEMs require consideration of static strength, form, fit, function, ease of manufacture, and weight. Two other major influences are cost and schedule. Design for a service life capability is another amongst the list of requirements. Competing design requirements necessitate general guidelines and simple methods which designers and stress analysts can use to develop the necessary aspects of a good design. Most design and strength engineers have limited experience using life prediction methods and a limited understanding of material behavior beyond mechanical properties. Although, most manufactures have supporting specialists, (such as metallurgists, fatigue and fracture engineers, test engineers, and others), their numbers are below optimum for comprehensive considerations and influence. The information thus provided to the designers for service life considerations during the design phase usually consists of a maximum local stress allowable relative to a particular design condition, standard material and design handbook data, and historic company typical design practices.

Damage Tolerance in the Design Phase

The implementation of damage tolerance has continued to evolve into the design process, and has been applied to some of the recent aircraft systems. In most cases, damage tolerance analyses and assessments are essentially post-design verification analyses with secondary impact on the design itself. Even as currently applied, major improvements in the structural integrity of aircraft are apparent. The use of damage tolerance analyses in design has only recently begun to influence design decisions. Damage tolerance considerations have provided improved toughness materials, more redundancy in load path, and more thorough evaluations of single load path structure. Although not part of the design phase, damage tolerance assessments have allowed the establishment of a "safety by inspection" concept in the maintenance of the structural integrity of aircraft. This effectively modifies the concept of an established design life to one of retirement-for-cause. Since damage tolerance assessments and the resulting inspection programs are the primary mechanisms for maintaining flight safety, it is critical that these assessments consider all variables that may affect residual strength, crack initiation and crack growth.

Most recently, "affordability" has influenced designs through the use of monolithic structures and reduced part counts, therefore new aircraft have more single load path critical structure with less forgiveness. Damage tolerance and time degradation analyses therefore may become even more important in new designs.

Corrosion in the Design Phase

The presence of corrosion can affect damage tolerance performance, however, the methods for addressing corrosion in the design phase are presently limited. The method of choice when considering corrosion issues in aircraft has been and continues to be to protect and prevent. This approach is considerably more effective if implemented in the design phase. Material manufacturers have improved their metallic products in terms of their resistance to corrosion, but are far from developing corrosion proof alloys. The lessons learned with alloys such as 7075-T6 and 7079-T6 have been captured by the material manufacturers, OEMs and operators. They no longer appear in modern designs and are frequently being replaced in existing aircraft during maintenance and overhaul programs. The reliance on corrosion prevention as a design assumption and the unarguable fact that aircraft are corroding has resulted in a requirement for OEMs to use extensive and often multi-redundant sealing and surface protection to help retard corrosion ("Affordability" initiatives have also discovered these redundant practices). The other means of addressing corrosion in the design phase consist of:

- access to newest alloys (often not known to designers);
- handbook information of qualitative ratings of material corrosion susceptibility;
- general cautions related to use of dissimilar metals;
- use of basic material properties such as K_{ISCC} (without a defined method of using the values quantitatively in the design process).

This general information does not contain the systematic engineering procedures needed to influence the design for potential corrosion effects and thus are ineffective. The evolution of the integrity process must consider a means of providing quantitative information for design decisions. This implies that any methods or procedures for these inputs will need to fit within the existing design and certification systems and be understood by designers.

Sustained Stress in the Design Phase

The method for designing in consideration of sustained stress is another area of technology deserving mention. Sustained stress limits by alloy are provided in the manuals and handbooks, such as the Mil-HDBK-5G, and are expressed as "the sustained stress level should not exceed a particular

percentage of the yield strength". Sustained stress computations are usually only performed for designed in clamp-up stress for bolts, and the several techniques used for the computations provide a wide range of answers. Often the joint or clevis deflections are not considered. The major considerations for sustained stresses in design are in applications where they are perceived and considered beneficial, such as interference fasteners and cold-worked holes. Although few procedures are used to quantify the actual stress mechanisms, the process of building in beneficial local stresses permits "life improvement factors" to be used in computing the service life capability.

For damage tolerance assessments, the benefits from the interference levels are approximated by smaller initial flaw size assumptions. Relatively few analytical checks are performed in consideration of potential assembly induced clamp up, mismatch, alignment, or dimension variability. Most locations and details are analyzed assuming the components are produced within typical dimensional tolerances and that during manufacturing and fabrication, the part will fit as designed. Most manufacturers have found that assembly is complicated by distortions, variability in machining, and artifacts that have not been defined or quantified in the manufacturing techniques. For example, all surfaces of holes are assumed to be flat and smooth, and all mating surfaces precisely aligned throughout fabrication. Future aircraft designs should have fewer locations subject to potential sustained stress cracking events, as automated design procedures and automated manufacturing should alleviate some of the unanticipated sustained stress locations.

Full Scale Test to Support Design

A heavy reliance for design verification is placed upon the results of full-scale static and fatigue tests. These tests are performed most often using early production test articles to capture the deficiencies early enough for changes to be incorporated for most of the production runs. More frequently, mid-life full-scale fatigue tests are being conducted to capture the effects of actual versus design usage differences and untested production changes to the design. Seldom are these full-scale tests able to simulate the time dependent influences of environment, and the airframe to airframe variation during production runs. The definition of the usable service life of the aircraft system thus depends on the outcome of full-scale fatigue tests that do not address all the degradation mechanisms. In addition to demonstrating a service life capability, the full-scale fatigue tests provide indications of critical locations and a database of cracking locations. Unfortunately, the tests do not indicate "hot spots" or critical locations that will result from time dependent degradations.

The high costs associated with this empirical approach could be readily and beneficially supplemented with advances in analytical technologies and the implementation of additional considerations in the integrity process. Full-scale fatigue test results need to be augmented with analytical evaluations to account for the degradation of the structure due to real time environmental processes that the aircraft will encounter in service.

Life Cycle Cost in Design

Since Life Cycle Cost (LCC) has not historically been perceived as a critical requirement by the military customer in their aircraft specifications, no priority level considerations of LCC have existed in the design phase. Civil aircraft OEMs have placed more emphasis on LCC because of the competitive commercial environment, but it is still not a priority design parameter. In general, weight, schedule, and manufacturing costs have been the significant parameters for OEMs. This is rapidly changing. As discussed by Welburn[18], acquisition programs are emphasizing consideration of LCC early in the program when tradeoffs are still viable. Dobbs et al.[19] go even further and discuss how LCC is included in the Rockwell Affordable Systems Optimization Process as a design variable along with other engineering, manufacturing, operational and support variables. There is a trend that although accurate cost data is difficult to obtain, it will increasingly become an integral part of multiple-disciplinary design optimization.

Corrosion considerations, as a high cost item, must be quantitatively integrated into LCC optimization programs and into design trade-off studies.

AUGMENTATION OF THE STRUCTURAL INTEGRITY PROCESS TO ACCOUNT FOR CORROSION AND SUSTAINED STRESS CORROSION CRACKING

The following describes some procedures and concepts to assist the evolution of the structural integrity process to improve the design, manufacturing, and support of aircraft systems in consideration of real time degradation effects. To maximize the benefits of considering corrosion and sustained stress corrosion in the structural integrity process requires the modifications to be compatible with the existing process by using practical metrics that ensure a strategic implementation. These modifications can be achieved using a systematic approach to integration based on sound engineering principles and existing structural integrity processes.

Process

To be effective, implementation must be built on the existing structural integrity process. The five Tasks in the integrity process (Figure 2) provide an ideal format for integrating corrosion and sustained stress analyses into the structural evaluations. Equally important to real time degradation effects, is the inclusion of LCC as part of the Task requirements. Figure 3 highlights the recommended items to be added to the Structural Integrity Tasks to include lessons learned from aging fleets and to incorporate the recent advances in corrosion assessment technology. This approach benefits both the design and maintenance communities by including corrosion and Sustained Stress Corrosion Cracking (SSCC) as structural design issues as well as in-service safety and service life issues. The implementation plan results in minimal disruption of the current processes while bringing the issues forward to the disciplines that can readily apply new methods with the most significant impact.

The aircraft engineering community worldwide is increasingly becoming more familiar with the concepts and terminology of damage tolerance and the structural integrity process. Terminology and nomenclature consistent with the present requirements and direct extensions of concepts are utilized to assist in the implementation. To compliment Damage Tolerance Assessments (DTA), Corrosion Tolerance Assessments (CTA) would be introduced. These assessments would emulate the DTA process, and would include provisions to compute the effects of corrosion scenarios with and without interaction with cyclic fatigue. In like fashion, a

TASK I	TASK II	TASK III	TASK IV	TASK V
DESIGN INFORMATION	DESIGN ANALYSES & DEVELOPMENT TESTS	COMPONENT & FULL SCALE TESTING	FORCE MANAGEMENT DATA PACKAGE	FORCE MANAGEMENT DATA PACKAGE
Structural Design Criteria and Design Usage including Corrosion and SSC Corrosion Tolerance Control Plan Material/Cost Trade Studies including Corrosion and SSC Critical Component Selection Process Definition Methodology and Analysis Approval Plan	Design Chem./Therm. Environment Spectra Corrosion Tolerance Analysis LCC Assessment	Assembly Process Verification Test (with revisions and updates) Analytical Process Verification Test	Force Structural Maintenance Plan including Corrosion Tolerance Operational Database including Corrosion, Cracking, Repairs, Cost Loads/Stress Database including Corrosion, SSCc, FEA, Models, Files and Geometry Durability, Damage Tolerance & Corrosion Summary	Cost Assessment Process Repair Tracking Systematic Feedback Documentation of Lessons Learned

Figure 3 Additions to the Aircraft Structural Integrity Program Tasks

Corrosion Critical Component (CC) classification would be recognized along with Fracture Critical Components (FC), Mission Critical Components (MC), and Durability Critical Components (DC). Corrosion Critical Components are those components for which the corrosion attack, if undetected, could result in the loss of the aircraft. Some fatigue critical locations are identified by the full-scale fatigue tests, but aging aircraft experience has revealed multi-site damage and corrosion damage modes of failure that were not identified by full-scale fatigue tests.

The inclusion of corrosion and SSCC with the Integrity Program forces design and maintenance consideration of real time degradation processes and their potential structural and life cycle cost impacts. For efficiency, a means of assessing component criticality is required similar to that used for identifying durability and fracture critical components. Continuing to build on established procedures, a formal and systematic approach[20] leading to a documented "Criticality Assessment", was first used as part of a Federal Aviation Administration certification and then subsequently used for several fighter aircraft assessments. The systematic nature of the process enables corrosion and SSCC to be addressed and identified as potential critical elements of the structure and thus the first level evaluations are performed and documented in a prioritized fashion.

Criticality Assessment Details: Ten general categories are recommended to characterize a component. These key categories are: 1) operational stress level, 2) limit strength and residual strength, 3) fail-safe aspects, 4) load distribution characteristics, 5) susceptibility to sustained stress corrosion cracking, 6) susceptibility to corrosion, 7) susceptibility to accidental damage, 9) inspectibility, and 10) cost to repair or replace. Each component or location from an extensive "candidate list": is evaluated under each category. Within each category, detailed descriptions and attributes are described for multiple subgroups or characteristics that discriminate the conditions of the component being evaluated. The matrix of options that describe the component provide a means to rate the item using a common set of criteria across the broad realm of scenarios. Each of which has been pre-established with associated levels of severity or importance. Specific numerical rating values are thus associated for each of the categories and sub-categories in terms of relative severity. The resulting qualitative and quantitative rankings determine the components' criticality level and prioritize subsequent evaluations. This disciplined process forces consistent and logic steps to be applied to all structure and provides a well understood documentation trail. This type of criticality assessment was developed to be readily adapted to any type aircraft system. The recent technology developments for quantifying the effects of corrosion can be incorporated into this established procedure. This would permit evaluations of potential corrosion scenarios to be included in the process with direct identification of critical components (including those becoming critical due to the real time degradations).

The schematic shown on Figure 4 illustrates the aircraft component screening and nomenclature process with the incorporation of Corrosion into the "Criticality Assessment" requirements. The revisions to the criticality classifications include structure that is safety, mission, or durability critical: 1) due only to corrosion or SSCC degradation; and 2) due to interaction between corrosion or SSCC and cyclic fatigue mechanisms. These new critical locations would be added to the Critical Parts Lists that previously only had been identified by considering cyclic fatigue mechanisms and failure modes.

The results of this evaluation during the design process can assist the operators in their corrosion disposition decisions and could potentially result in significant cost reductions and reduced aircraft maintenance down time. This evaluation would also benefit any re-assessments of aircraft during updated Damage and Corrosion Tolerance Assessments, thus transitioning the lessons learned to date of corrosion interaction to provide immediate impact. Under the new process, the ASIP defined Force Management Data Package and the Force Management package would contain information and direction on effective life cycle management

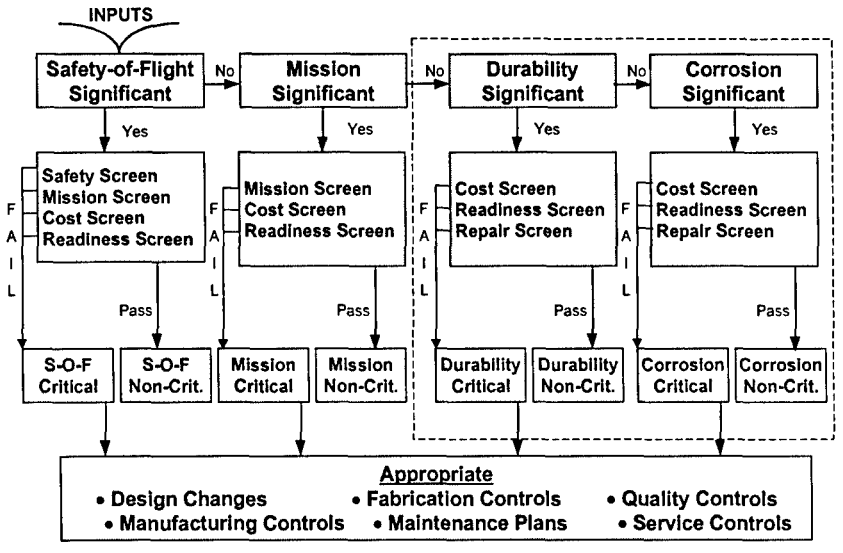

Figure 3 Component Criticality Assessment

practices for corrosion critical and sustained stress corrosion critical areas.

Practical Corrosion Metrics

Brooks[21,22] and others have shown that there is a reasonable engineering correlation between surface topographies and the fatigue nucleation process. The reduced life differences observed with increased surface roughness of a chemically milled specimen correlated well with analytical predictions when the local surface stress amplification due to the roughness were included. In addition, reduced lives for test specimens with rough surface holes were predicted when the stress intensities for these macro effects were considered in the crack growth analyses. The empirical connection of the fatigue process linking the behavior and results of strain/stress life coupon tests from pristine material to specimen failure using fracture mechanics techniques allows the use of a large database of historic lab test data to characterize the as-produced condition of the basic material. The observations indicate that crack growth analysis from the initial quality state inherent in basic materials are viable predictors of initial cracking and durability when the local macro states of stress are included. Subsequently, quantification of the as-manufactured condition of a component then produces a modified state that can be accounted for. The effects of age degradation processes also produce a change in the topography, and thus provide a means to transition the physical characteristic in life prediction methods from the as-built condition or state to a future state.

Finite element analysis of corroded surfaces is presently being used to develop algorithms to model level of corrosion effects and their interaction with the fatigue cracking process. Two and three-dimensional surface profiles of corroded aircraft panels are mapped to establish their characteristic shapes and classify attributes which can be related to levels or stages of corrosion.

The volume content and build-up of corrosion by-products at lap splice faying surfaces can be determined and used to compute lap joint deflection levels, induced bending stress, and relative material area loss[14,15]. Multiple techniques are being developed to reliably detect corrosion in hidden areas including pulsed eddy current and enhanced optical techniques. Accelerated corrosion tests are being conducted at the NRCC and elsewhere to relate corrosion growth rate with some of the above elements. Corrosion rate models are being developed through the use of "SQUID" experiments[23] at Vanderbilt University using measurements of the magnetic fields during corrosion and relating those fields to physical characteristics of the corrosion profiles on time degraded pieces of field aircraft. The above items describe only a relative few metrics and measurable physical characteristics associated with corrosion. These technology areas are being pursued by the USAF Corrosion Program Office through NCI Information Systems and their subcontractors[24,25]. The concurrent engineering approach used for this research is resulting in a reasonable engineering framework for including corrosion effects in structural strength and life predictions. An important aspect of this concept is the establishment of a series of metrics that can be used with confidence.

Corrosion metrics must transition across the disciplines in quantitative terms that are pertinent to static, fatigue and damage tolerance analyses, and then transition into terms that are related to NDI capabilities. The final transitions must be through a series of tools and guidelines for the end users. The depot engineers need access to engineering methods to assess the structural impact of corrosion in order to facilitate a cost-effective approach to decision making regarding disposition. The aircraft life cycle manager needs information that can be used to assess the global influence of the aging process in terms of the cost, availability, and safety of the aircraft fleet. The transformation of metrics is significantly improved when a physical or measurable attribute can be readily associated with the metric. Although it is not necessary for each

discipline within the process to understand the intimate details of all metrics, it is imperative that the importance and implications of the metrics translate coherently across disciplines. Figure 5 presents the conceptual flow across the disciplines for appropriate integration into the integrity process.

Strategic Implementation

Strategic implementation implies that the concept and procedures can be readily integrated to provide an immediate, effective, and efficient improvement to the safety, readiness, and cost of aircraft systems. The following provides an illustrative example using the "Criticality Assessment" and the components classification along with the transformed metrics to formulate the strategic implementation.

The advantage to an operator of having a useable corrosion and fatigue damage classification matrix based on real corrosion metrics is that contrary to present practice, immediate repair may not be necessary and may be deferred to a more convenient time. The classification of the damage directs the additional analysis, actions, reactions, and or dispositions for the structure based upon the potential durability or damage tolerance impact.

As an example, areas where mild forms of corrosion are found during maintenance presently require extensive grinding and multi-fastened patches. Now assume the criticality assessment provided a classification of non-critical, indicating the analytical evaluation of the location during design or during re-assessment showed an adequate service life with the corrosion degradation included. Then instead of repair, a simple pacification or monitoring of this "nuisance" corrosion would be an acceptable solution. Alternately, the repair could be delayed to a convenient time. The classification of component criticality allows field technical analyses or specific dispositions to be focused on important components, thus supporting the depot personnel with the selection of maintenance actions. This idea is illustrated by Figure 6.

Under Task 4 of Table 3, Force Management Data Package, structure would be identified relative to these types of structure. Corrosion Criticality would be provided with NDI techniques, limits, and support data. For Type 1, no action is needed as the structure continues to perform as designed. For Type 2, specialized analysis techniques are required for the assessment. This type structure is the biggest concern for it has the most severe safety implications. Detailed special analyses would be required to address this scenario, and is one of the prime focuses of the authors' present work. For Type 3, the acceptable damage levels and extent of damage need to be quantified. Corrosion damage indications that are within specific limits for the location would open several options to the maintenance engineer. For some items, corrosion will not affect safety, but if found, the engineer may want to implement an early repair before it reaches some pre-defined corrosion limits that means either a more extensive repair or would cause the part to be reclassified as Type 2 safety critical. The engineering assessment tools required to make these decisions are similar to those for Type 2. For Type 4 structure, the choice is simply to repair or replace as directed in the structural repair manual.

The "nuisance" type corrosion associated with a Type 3 location, for the above example, could be rectified during maintenance actions with corrosion protection compounds, thus avoiding unnecessary costly repairs.

Analytical Life Assessments

The basis of this proposal is that life prediction methods can be adapted to accept corrosion and sustained stress parameters to simulate their degradation effects in both independent and interdependent interactions with the fatigue process. The analytical approximations, using a spectrum for stress cycles and a spectrum for environmental cycles, relate corrosion to fatigue through fracture mechanics parameters of crack lengths and stress intensity. This approach allows evaluations to be conducted utilizing damage tolerance

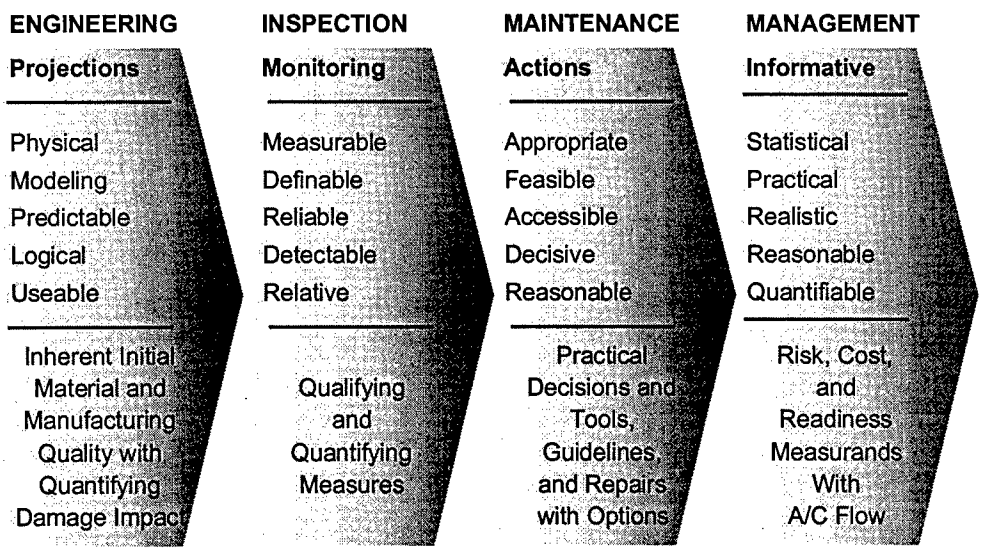

Figure 4 Transition of Metrics Across Disciplines

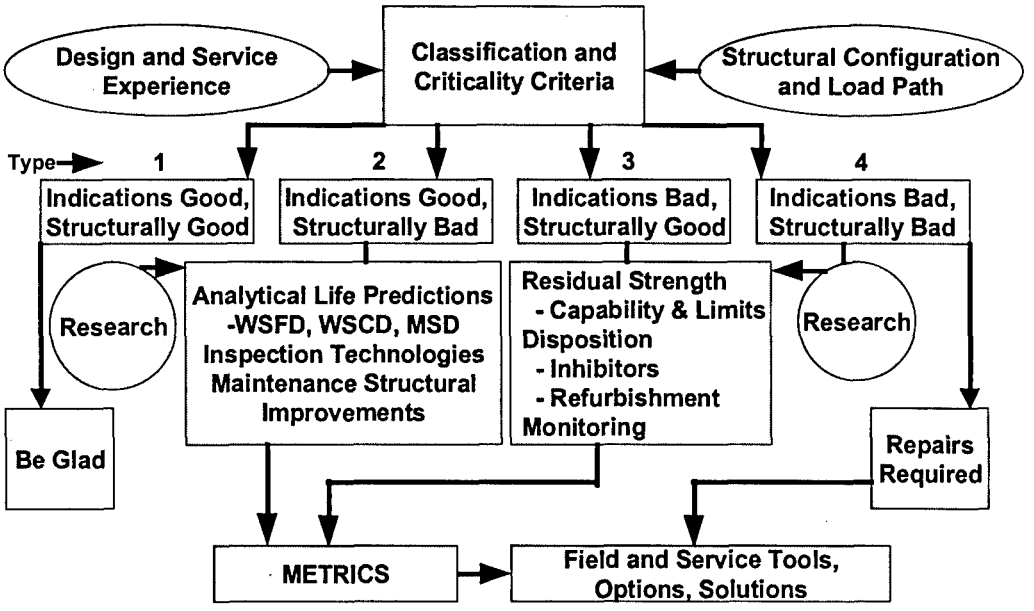

Type 1	Structure where there is No visual or NDI damage indication AND the structure has more than adequate service life margins
Type 2	Structure where there is No visual or NDI damage indication BUT the structure has a potential corrosion scenario that would NOT meet service life needs nor safety requirements
Type 3	Structure where there is visual or NDI detectable damage, BUT the structure has more than adequate service life margins
Type 4	Structure where there is visual or NDI damage indication, AND the structure has a potential corrosion scenario that would NOT meet service life needs nor safety requirements

Figure 6 Field Based Applications for Decision-Making

computations that interact both cycle and real time domains. An example of a basic conceptual formulation, based upon the analytical framework discussed in References 21 and 22, is shown on Figure 7. Reference 24 presents examples of the impact of corrosion on a lap joint and provides a demonstration of the application, even though real time corrosion rates are unknown. The analysis computations will utilize scenarios synonymous with a corrosion rogue flaw, minimum detectable corrosion level, and effective stress intensity modifications to account for surface profiles and pillowing induced deflections. Existing stress analysis tools, crack growth tools, repair analysis programs, and other supporting computer codes will readily accept the concept with minimal impact to their perceived use. Modifications to the process, simply stated, include corrosion in the integrity process as an additional effect that interacts with fatigue crack growth computations and damage tolerance techniques. The corrosion aspect will require consideration for the environment spectrum, will impact particular component criticality, will require NDI techniques and detectable limits to be established, and will have analytical tolerance analysis assuming corrosion states below detectable limits. The effects on structural capability will be examined both independently of and interdependently with fatigue from the cyclic environment as appropriate. For example, multi-site damage scenarios would be evaluated considering scenarios such as: a varying number of defect probabilities and sizes; with and without corrosion pillowing; and variations in surface topography degradation as a function of time.

Assessments to address corrosion, SSCC, and age degradation can be integrated into the integrity program by applying many of the same rules, guidelines, concepts, philosophies, procedures, and approaches presently used for Durability and Damage Tolerance Assessments. Some examples of new terms that would come into use are: minimum detectable corrosion limits (Cd), probability of detecting corrosion (PODC), initial corrosion assumptions (aco), corrosion/SSCC failure modes and effects, multi-site corrosion damage (MSCD), wide spread corrosion damage (WSCD), and corroded residual strength (CR/S). Since the corrosion process appears to be variable in nature, assuming high levels of corrosion at all locations from day zero is unrealistic. The probabilistic nature of corrosion can, however, be approximated. This approximation technology has parallel requirements to the statistical techniques being developed to address multi-site damage and wide spread fatigue damage and will benefit from developments in these areas.

Maturity of Technology and Processes:

Integration of corrosion and other age degradations into the structural integrity process have been described by this paper

$$\Delta K_I = \beta_{pillowing}\beta_{corrosion}\beta_{FW}\beta_{K_t}\Delta\sigma_{cy}\sqrt{\frac{\pi a}{Q}} \quad \&$$

traditional stress induced analysis

$$\beta_{corrosion}\beta_{TBD}\beta_{sustained}\Delta E_{time}\sqrt{\frac{\pi a}{Q}}$$

corrosion time/environment interaction

Assumption: An active fatigue crack is present in the 'As-Built' configuration. This Initial Quality condition has crack extensions due to cyclic load mechanisms $(\Delta\sigma_{cy})$ and from environmental time mechanisms (ΔE_{time}). The growth is independent as well as interdependent through common measurands, the Crack Tip Stress Intensity (K),crack size (a), and β solutions.

Figure 7 Conceptual Analytical Fatigue with Corrosion Interaction Model

and supported by details of referenced papers. The authors perceive the maturity of the engineering technology and maturity of existing processes is at a point that it would be beneficial to begin the integration. The authors also believe that significant returns on investments could be realized almost immediately relative to the cost to implement. The integration process is evolutionary and thus savings would come concurrently, and continue long into the Aging Aircraft era.

Figures 8 and 9 are attempts to portray the perceived levels of maturity. Although, they may readily be debated, an acceptance of the approach and cooperative support would provide a considerable catalyst for the success of the proposed Integration Plan.

Summary

Whilst significant progress has been made in technology related to corrosion and structural integrity; better understanding of basic material behavior, improvements in NDI corrosion detection, and use of analytical tools for predicting residual strength and residual life, the benefits from this technology development have not been fully realized. The state of the technology is that it is mature enough to be used but requires real applications to advance and to prove its potential. Improvements in new designs and solutions for the aging fleet require a strategic implementation into the life cycle management processes from the OEM designer through to the field level and depot level maintenance engineers, and then followed by aircraft structural integrity managers. It also requires focussed developmental programs to increase the capability of the analytic and experimental tools and to develop effective corrosion measurement and classification tools and processes. This paper has proposed that by integrating corrosion and sustained stress corrosion into the existing integrity framework of tools and concepts, this concurrent engineering approach will provide the most strategic incorporation and rapid application of new solution techniques.

Conclusions

- Aging aircraft issues are not short-term phenomena that will disappear with the retirement of the present fleets of aircraft that are being operating beyond their design service life. Rather, extended term operation of aircraft beyond initially defined service lives is likely to be the norm of the future.

- Corrosion, corrosion-fatigue interactions and sustained stress corrosion are major influences on the Life Cycle Costs of an aircraft. Effective means of reducing these costs through design considerations and through effective in-service management practices are required.

- Corrosion, corrosion-fatigue interactions and sustained stress corrosion affect flight safety by introducing additional failure modes and by compromising analytical and test evaluations based on no-corrosion assumptions.

- Real time degradation effects are threats to both the economic viability and the safety of aircraft that must be addressed directly through enhancements to the aircraft design and certification regulations and processes. The modifications to the process, simply stated, consist of integrating corrosion considerations into the integrity process as an additional terms and extensions of fatigue and damage tolerance. The corrosion aspect will require consideration for the environmental spectrum, will impact particular component criticality, will require NDI techniques and detectable limits to be established, and will have analytical tolerance analysis assuming corrosion states below detectable limits. The effects of structure will be looked at as independent influences and also as interdependent influences with fatigue from the cyclic environment, as appropriate. For example multi-site damage scenarios would have evaluations considering an increased defect probability and size due to corrosion or sustained stress attach.

- The recommendations advanced in this paper include a systematic and disciplined process, based on the present integrity processes, to identify and classify critical components accounting for corrosion influences. The corrosion damage tolerance analysis concepts include computations addressing the inspection intervals based on corrosion-fatigue interaction. Also, inspection intervals for locations that primarily degrade due to corrosion can be determined. These two types of analyses will consider both NDI crack and NDI corrosion detectable limits.

- The approach and modifications to the structural integrity process proposed in this paper compliment the findings of the "Aging of the U.S. Air Force Aircraft"[8] report by the United States National Research Council. The methods and procedures proposed enable reasonable engineering approximations to be performed that will improve the life cycle management decision process for aging fleets and will allow evaluation of new designs for sensitivity to corrosion degradation. The use of corrosion damage rates and interaction with fatigue crack growth provides a tool that overcomes shortcomings of the original damage tolerance assessments related to real time processes.

- The technology infrastructure, related to corrosion detection and quantification, structural analysis, testing and life prediction technologies, has reached sufficient maturity whereby applications can be initiated.

- Implementation of the process on selected components of existing aging aircraft could proceed with positive results both to the structural integrity of the selected components and to the development and refinement of the databases and engineering processes.

REFERENCES

1. Schultz, W., "Corrosion Fatigue – The Forgotten Factor in Assessing Durability", 15th Plantema Memorial Lecture, Fatigue in New and Aging Aircraft – Proceedings of the 18th Symposium of the International Committee on Aeronautical Fatigue, Melbourne, Australia, May 1995, pp1-51, EMAS Publishing 1995.

2. Lincoln, J. W., "Aging Aircraft – USAF Experience and Actions", 16th Plantema Memorial Lecture, Fatigue in New and Aging Aircraft – Proceedings of the 19th Symposium of the International Committee on Aeronautical Fatigue Edinburgh, 16-20, June 1997, pp1-38 EMAS Publishing 1997.

3. Department of the Air Force, "Aircraft Structural Integrity Program, Airplane Requirements", MIL-STD-1530A, 1975

4. Mar, J.W., "Preserving Aging Aircraft", Aerospace America, January 1996 pp 38-43

5. Internet document: "http: //www.afcpo.com/cost.html", US Air Force Corrosion Program Office, June 1998

6. Internet document: http://www.finishing.com/icorr/index.html, Institute of Corrosion, Bedfordshire, UK.

7. Agarwala, V.S., "Corrosion and Aging Aircraft", Canadian Aeronautics and Space Journal, Volume 42, No. 2, June 1996

8. "Aging of U.S. Air Force Aircraft", Final Report of the Committee on Aging of U.S. Air Force Aircraft, National Materials Advisory Board, Commission on Engineering and Technical Systems, National Research Council, Publication NMAB-488-2 National Academy Press, 1997

9. Groner, D.J., Nieser, D.E., "U.S. Air Force Aging Aircraft Corrosion", Canadian Aeronautics and Space Journal, Volume 42, No. 2, June 1996

10. "A Study to Determine the Cost of Corrosion Maintenance for Weapon Systems and Equipment in the United States Air Force", Final Report, Contract #F09603-95-D-0053, February 1998, pp39-40

11. Komorowski, J.P., Forsyth, D.S., Simpson, D.L., Gould, R. W., "Probability Of Detection Of Corrosion In Aircraft Structures", NATO Research and Technology Organization Conference Proceedings MP-1, To be published

12. Hoeppner, D. W., Grimes, L., Hoeppner, A., Ledesma, J., Mills, T, Shah, A, "Corrosion and Fretting as Critical Aviation Safety Issues", Estimation, Enhancement and Control of Aircraft Fatigue Performance – Proceedings of the 18th Symposium of the International Committee on Aeronautical Fatigue, Melbourne Australia, May 1995, pp87-106, EMAS Publishing 1995.

13. Campbell, G.S., Lahey, R., International Journal of Fatigue, Vol. 6, No. 1, 1984, pp.25-30

14. Komorowski, J.P., Bellinger N.C. and Gould, R.W., "The Role of Corrosion Pillowing in NDI and in the Structural Integrity of Fuselage Joints", Fatigue in New and Aging Aircraft – Proceedings of the 19th Symposium of the International Committee on Aeronautical Fatigue Edinburgh, 16-20, June 1997, pp251-266, EMAS Publishing 1997.

15. Bellinger, N.C. and Komorowski, J.P., "Damage Tolerance Implications of Corrosion Pillowing on Fuselage Lap Joints", Proceedings of the 1996 USAF Aircraft Structural Integrity Program Conference, 3-5 December 1996. Vol.1 pp. 383-410, WL-TR-97-4050, June 1997.

16. Kinzie, D, "Corrosion Snapshot", Proceedings 1998 Corrosion Program Conference, www.afcpo.com/Archives/Conf_proceed/98_AF_CPC/

17. Berens, A.P., and Burns, J.G., "Risk Analysis in the Presence of Corrosion Damage", AGARD Conference Proceedings, Widespread Fatigue Damage in Military Aircraft 10-11 May 1995, AGARD-CP-568, pp 8-1 to 8-9, December 1995

18. Welburn, S, "Maintenance Free Aircraft", AGARD Advisory Report 360, Volume III, pp 126-127, September 1997

19. Dobbs, S.K., Schwanz, R. C., Abdi, F., "Automated Structural Analysis Process At Rockwell", AGARD Report 814, pp 8-1 to 8-12, October 1996

20. Brooks, C.L., "An Engineering Procedure to Select and Prioritize Component Evaluations Under USAF Structural Integrity Requirements", Proceedings of the 1990 USAF Structural Integrity Conference, also WWW.APESolutions.com

21. Brooks, C.L., "The Impact on Total Life of Corrosion/Fatigue Interaction – An Engineering Approach", Proceedings USAF 4th Aging Aircraft Conference, 1996

22. Brooks, C.L., "Corrosion is a Structural and Economic Problem: Transforming Metrics to a Life Prediction Method", Proceedings AGARD Workshop on Fatigue in the Presence of Corrosion, in October 1998 at Corfu, Greece, to be published.

23. Cooke, G., "Corrosion/Fatigue Effects on Aging Aircraft", Proceedings USAF Technical Interchange Meeting, December 1997.

24. Kinzie, R. and G. Cooke, "Corrosion in USAF Aging Aircraft Fleets," Proceedings AGARD Workshop on Fatigue in the Presence of Corrosion, in October 1998 at Corfu, Greece, to be published.

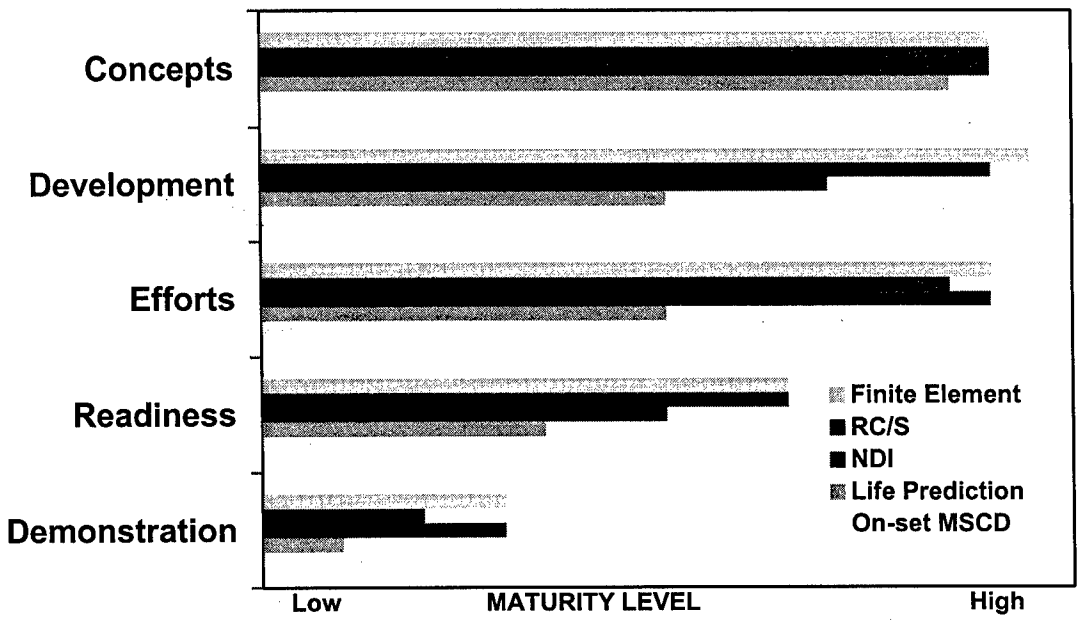

Figure 8 Engineering Technology Maturity Levels

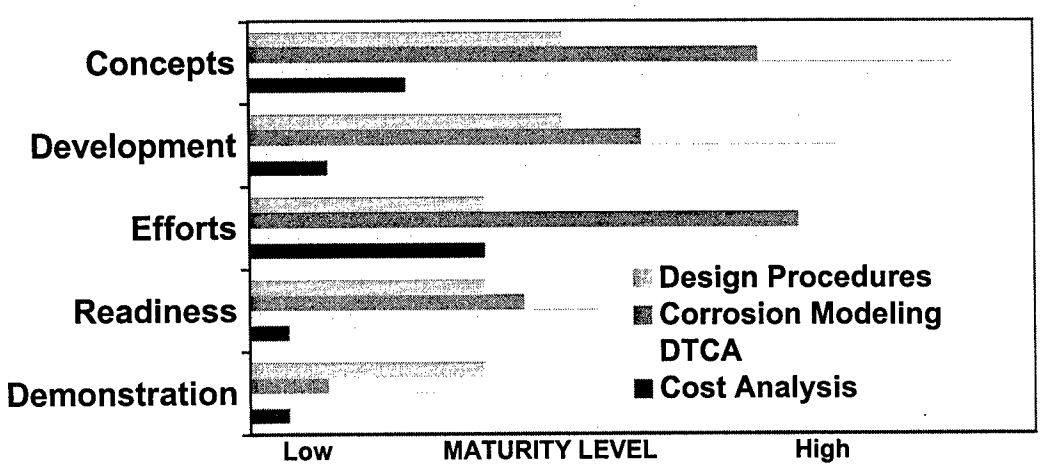

Figure 9 Engineering Processes Maturity Level

REPORT DOCUMENTATION PAGE

1. Recipient's Reference	2. Originator's References	3. Further Reference	4. Security Classification of Document
	RTO-MP-18 AC/323(AVT)TP/8	ISBN 92-837-1011-8	UNCLASSIFIED/ UNLIMITED

5. Originator Research and Technology Organization
North Atlantic Treaty Organization
BP 25, 7 rue Ancelle, F-92201 Neuilly-sur-Seine Cedex, France

6. Title

Fatigue in the Presence of Corrosion

7. Presented at/sponsored by

the Workshop of the RTO Applied Vehicle Technology (AVT) Panel (organised by the former AGARD Structures and Materials Panel) held in Corfu, Greece, 7-8 October 1998.

8. Author(s)/Editor(s)	9. Date
Multiple	March 1999
10. Author's/Editor's Address	**11. Pages**
Multiple	214

12. Distribution Statement There are no restrictions on the distribution of this document. Information about the availability of this and other RTO unclassified publications is given on the back cover.

13. Keywords/Descriptors

Fatigue (materials)
Military aircraft
Corrosion
Transport aircraft
Corrosion fatigue
Nondestructive tests
Management
Service life
Aircraft maintenance
Predictions
Corrosion prevention
Aging (metallurgy)
Structural integrity
Aluminum alloys
Crack propagation
Life cycle costs
Airworthiness
Airframes
NATO forces

14. Abstract

The NATO fleets are aging in both real time and in accrued fatigue damage. Corrosion and fatigue, independently, are high cost maintenance items and both can affect airworthiness. There is a synergistic relationship between these two phenomena. Cost effective and airworthy approaches to design and corrosion prevention must be defined. Work in NATO countries could be accelerated by a sharing of experience.

During the Workshop 22 papers were grouped in four sessions:
Session I: In-service Experience with Corrosion Fatigue
Session II: Simulation/Test Evaluation Programs
Session III: Fatigue Prediction Methodologies in Corrosive Environments
Session IV: Structural Integrity – Corrosion and Fatigue Interactions

NORTH ATLANTIC TREATY ORGANIZATION

RESEARCH AND TECHNOLOGY ORGANIZATION
BP 25 • 7 RUE ANCELLE
F-92201 NEUILLY-SUR-SEINE CEDEX • FRANCE
Télécopie 0(1)55.61.22.99 • Télex 610 176

DIFFUSION DES PUBLICATIONS RTO NON CLASSIFIEES

L'Organisation pour la recherche et la technologie de l'OTAN (RTO), détient un stock limité de certaines de ses publications récentes, ainsi que de celles de l'ancien AGARD (Groupe consultatif pour la recherche et les réalisations aérospatiales de l'OTAN). Celles-ci pourront éventuellement être obtenues sous forme de copie papier. Pour de plus amples renseignements concernant l'achat de ces ouvrages, adressez-vous par lettre ou par télécopie à l'adresse indiquée ci-dessus. Veuillez ne pas téléphoner.

Des exemplaires supplémentaires peuvent parfois être obtenus auprès des centres nationaux de distribution indiqués ci-dessous. Si vous souhaitez recevoir toutes les publications de la RTO, ou simplement celles qui concernent certains Panels, vous pouvez demander d'être inclus sur la liste d'envoi de l'un de ces centres.

Les publications de la RTO et de l'AGARD sont en vente auprès des agences de vente indiquées ci-dessous, sous forme de photocopie ou de microfiche. Certains originaux peuvent également être obtenus auprès de CASI.

CENTRES DE DIFFUSION NATIONAUX

ALLEMAGNE
Fachinformationszentrum Karlsruhe
D-76344 Eggenstein-Leopoldshafen 2

BELGIQUE
Coordinateur RTO - VSL/RTO
Etat-Major de la Force Aérienne
Quartier Reine Elisabeth
Rue d'Evere, B-1140 Bruxelles

CANADA
Directeur - Gestion de l'information
(Recherche et développement) - DRDGI 3
Ministère de la Défense nationale
Ottawa, Ontario K1A 0K2

DANEMARK
Danish Defence Research Establishment
Ryvangs Allé 1
P.O. Box 2715
DK-2100 Copenhagen Ø

ESPAGNE
INTA (RTO/AGARD Publications)
Carretera de Torrejón a Ajalvir, Pk.4
28850 Torrejón de Ardoz - Madrid

ETATS-UNIS
NASA Center for AeroSpace Information (CASI)
Parkway Center, 7121 Standard Drive
Hanover, MD 21076-1320

FRANCE
O.N.E.R.A. (Direction)
29, Avenue de la Division Leclerc
92322 Châtillon Cedex

GRECE
Hellenic Air Force
Air War College
Scientific and Technical Library
Dekelia Air Force Base
Dekelia, Athens TGA 1010

ISLANDE
Director of Aviation
c/o Flugrad
Reykjavik

ITALIE
Aeronautica Militare
Ufficio Stralcio RTO/AGARD
Aeroporto Pratica di Mare
00040 Pomezia (Roma)

LUXEMBOURG
Voir Belgique

NORVEGE
Norwegian Defence Research Establishment
Attn: Biblioteket
P.O. Box 25
N-2007 Kjeller

PAYS-BAS
NDRCC
DGM/DWOO
P.O. Box 20701
2500 ES Den Haag

PORTUGAL
Estado Maior da Força Aérea
SDFA - Centro de Documentação
Alfragide
P-2720 Amadora

ROYAUME-UNI
Defence Research Information Centre
Kentigern House
65 Brown Street
Glasgow G2 8EX

TURQUIE
Millî Savunma Başkanliği (MSB)
ARGE Dairesi Başkanliği (MSB)
06650 Bakanliklar - Ankara

AGENCES DE VENTE

NASA Center for AeroSpace Information (CASI)
Parkway Center
7121 Standard Drive
Hanover, MD 21076-1320
Etats-Unis

The British Library Document Supply Centre
Boston Spa, Wetherby
West Yorkshire LS23 7BQ
Royaume-Uni

Canada Institute for Scientific and Technical Information (CISTI)
National Research Council
Document Delivery,
Montreal Road, Building M-55
Ottawa K1A 0S2
Canada

Les demandes de documents RTO ou AGARD doivent comporter la dénomination "RTO" ou "AGARD" selon le cas, suivie du numéro de série (par exemple AGARD-AG-315). Des informations analogues, telles que le titre et la date de publication sont souhaitables. Des références bibliographiques complètes ainsi que des résumés des publications RTO et AGARD figurent dans les journaux suivants:

Scientific and Technical Aerospace Reports (STAR)
STAR peut être consulté en ligne au localisateur de ressources uniformes (URL) suivant:
http://www.sti.nasa.gov/Pubs/star/Star.html
STAR est édité par CASI dans le cadre du programme NASA d'information scientifique et technique (STI)
STI Program Office, MS 157A
NASA Langley Research Center
Hampton, Virginia 23681-0001
Etats-Unis

Government Reports Announcements & Index (GRA&I)
publié par le National Technical Information Service
Springfield
Virginia 2216
Etats-Unis
(accessible également en mode interactif dans la base de données bibliographiques en ligne du NTIS, et sur CD-ROM)

Imprimé par le Groupe Communication Canada Inc.
(membre de la Corporation St-Joseph)
45, boul. Sacré-Cœur, Hull (Québec), Canada K1A 0S7

NORTH ATLANTIC TREATY ORGANIZATION

RESEARCH AND TECHNOLOGY ORGANIZATION
BP 25 • 7 RUE ANCELLE
F-92201 NEUILLY-SUR-SEINE CEDEX • FRANCE
Telefax 0(1)55.61.22.99 • Telex 610 176

DISTRIBUTION OF UNCLASSIFIED RTO PUBLICATIONS

NATO's Research and Technology Organization (RTO) holds limited quantities of some of its recent publications and those of the former AGARD (Advisory Group for Aerospace Research & Development of NATO), and these may be available for purchase in hard copy form. For more information, write or send a telefax to the address given above. **Please do not telephone.**

Further copies are sometimes available from the National Distribution Centres listed below. If you wish to receive all RTO publications, or just those relating to one or more specific RTO Panels, they may be willing to include you (or your organisation) in their distribution.

RTO and AGARD publications may be purchased from the Sales Agencies listed below, in photocopy or microfiche form. Original copies of some publications may be available from CASI.

NATIONAL DISTRIBUTION CENTRES

BELGIUM
Coordinateur RTO - VSL/RTO
Etat-Major de la Force Aérienne
Quartier Reine Elisabeth
Rue d'Evere, B-1140 Bruxelles

CANADA
Director Research & Development
Information Management - DRDIM 3
Dept of National Defence
Ottawa, Ontario K1A 0K2

DENMARK
Danish Defence Research Establishment
Ryvangs Allé 1
P.O. Box 2715
DK-2100 Copenhagen Ø

FRANCE
O.N.E.R.A. (Direction)
29 Avenue de la Division Leclerc
92322 Châtillon Cedex

GERMANY
Fachinformationszentrum Karlsruhe
D-76344 Eggenstein-Leopoldshafen 2

GREECE
Hellenic Air Force
Air War College
Scientific and Technical Library
Dekelia Air Force Base
Dekelia, Athens TGA 1010

ICELAND
Director of Aviation
c/o Flugrad
Reykjavik

ITALY
Aeronautica Militare
Ufficio Stralcio RTO/AGARD
Aeroporto Pratica di Mare
00040 Pomezia (Roma)

LUXEMBOURG
See Belgium

NETHERLANDS
NDRCC
DGM/DWOO
P.O. Box 20701
2500 ES Den Haag

NORWAY
Norwegian Defence Research Establishment
Attn: Biblioteket
P.O. Box 25
N-2007 Kjeller

PORTUGAL
Estado Maior da Força Aérea
SDFA - Centro de Documentação
Alfragide
P-2720 Amadora

SPAIN
INTA (RTO/AGARD Publications)
Carretera de Torrejón a Ajalvir, Pk.4
28850 Torrejón de Ardoz - Madrid

TURKEY
Millî Savunma Başkanliği (MSB)
ARGE Dairesi Başkanliği (MSB)
06650 Bakanliklar - Ankara

UNITED KINGDOM
Defence Research Information Centre
Kentigern House
65 Brown Street
Glasgow G2 8EX

UNITED STATES
NASA Center for AeroSpace Information (CASI)
Parkway Center, 7121 Standard Drive
Hanover, MD 21076-1320

SALES AGENCIES

NASA Center for AeroSpace Information (CASI)
Parkway Center
7121 Standard Drive
Hanover, MD 21076-1320
United States

The British Library Document Supply Centre
Boston Spa, Wetherby
West Yorkshire LS23 7BQ
United Kingdom

Canada Institute for Scientific and Technical Information (CISTI)
National Research Council
Document Delivery,
Montreal Road, Building M-55
Ottawa K1A 0S2
Canada

Requests for RTO or AGARD documents should include the word 'RTO' or 'AGARD', as appropriate, followed by the serial number (for example AGARD-AG-315). Collateral information such as title and publication date is desirable. Full bibliographical references and abstracts of RTO and AGARD publications are given in the following journals:

Scientific and Technical Aerospace Reports (STAR)
STAR is available on-line at the following uniform resource locator:
http://www.sti.nasa.gov/Pubs/star/Star.html
STAR is published by CASI for the NASA Scientific and Technical Information (STI) Program
STI Program Office, MS 157A
NASA Langley Research Center
Hampton, Virginia 23681-0001
United States

Government Reports Announcements & Index (GRA&I)
published by the National Technical Information Service
Springfield
Virginia 22161
United States
(also available online in the NTIS Bibliographic Database or on CD-ROM)

Printed by Canada Communication Group Inc.
(A St. Joseph Corporation Company)
45 Sacré-Cœur Blvd., Hull (Québec), Canada K1A 0S7

ISBN 92-837-1011-8